Simulating the Effects of Enclosure Retrofits on Post-War High-Rise Apartment Buildings in Cold Climates

by

Matthew Charbonneau

A thesis
presented to the University of Waterloo
in fulfillment of the
thesis requirement for the degree of
Master of Applied Science
in
Civil Engineering

Waterloo, Ontario, Canada, 2011

AUTHOR'S DECLARATION

I hereby declare that I am the sole author of this thesis. This is a true copy of the thesis, including any required final revisions, as accepted by my examiners.

I understand that my thesis may be made electronically available to the public.

Matthew Charbonneau

Abstract

A large portion of the existing building stock in North America is comprised of post-World War II high-rise apartment buildings, particularly in the Greater Golden Horseshoe in Ontario. They are home to a large portion of the Canadian population. These buildings are nearly 50 years old and reaching the end of their useful lifespan. Significant deterioration has lead to life safety concerns, poor standards of living, and aesthetic degradation. They also consume a significant amount of energy resulting in contributing to Canada's high per capita greenhouse gas emissions.

This thesis investigates the impact of various retrofit strategies on the energy consumption, durability, and occupant comfort of the towers. The building enclosure is the primary focus. The impacts were analyzed using three approaches. Whole building energy consumption was simulated by adapting a spreadsheet based *Building Energy and Loads Analysis* (BELA) model, originally intended for office buildings. Heat flow and temperatures across the enclosures were modeled using a two-dimensional finite element model (Therm 5.2). A single, theoretical building dubbed the, "Archetype", was developed to define the characteristics of a "typical" tower using details extracted from four sets of drawings for towers built in Toronto during the late 1960s.

Various quantities and configurations of thermal insulation were added to the Archetype and the resulting effective thermal resistances were modeled. Adding insulation to the interior significantly reduces the effectiveness of any added thermal resistance. Insulating on the exterior allows the insulation around the balconies to reach 80% of its rated value, even without insulating the balconies.

Energy efficiency measures (EEMs) including retrofitting the walls, windows, appliances, or HVAC equipment were simulated and it was found that each on its own did not have a major impact on annual energy consumption. Packages of EEMs were created and simulated. It was found that a basic and high-performance whole building retrofit packages would save approximately 40% and 55% of the annual energy consumption, respectively, based on the Archetype.

An analysis and discussion of the enclosure retrofit impacts on freeze-thaw potential, interior surface and interstitial condensation, occupants' thermal comfort, and passive thermal comfort was completed. An interior versus exterior enclosure retrofit comparison summary illustrated that an exterior enclosure retrofit has significant benefits relative to an interior retrofit including ease of construction, greater durability, and improved comfort. The difference in annual energy reduction between an interior and exterior enclosure retrofit was small.

Acknowledgements

I would like to thank Dr. John Straube for his willingness to share his vast knowledge even beyond the scope of my research. I appreciated his push to help me become a better building engineer and his patience and support to ensure my success.

I would also like to thank my colleagues and friends from the Building Engineering Group; Rob Lepage, Brittany Hanam, Nick Bronsema, Peter Mensinga, and Emily Vance. Their technical help, shared work experiences, and care were greatly appreciated.

Thanks is owed to Building Science Corporation for the building science experience, shared knowledge, and support from Christopher Schumacher, Aaron Grin, Jonathan Smegal, Alex Lukachko, Paul Schumacher, and Ed Reeves.

Thanks are also owed to my always supportive family through all my educational endeavors. Thanks Dad, Mom, Dan, Melinda, Patricia, and Brad. Thanks to all the Charbonneaus and Waddens for the many enjoyable and distracting vacations together.

Finally, thanks to my incredibly supportive Linda… my wife and colleague.

Table of Contents

List of Figures

List of Tables

Chapter 1 - Introduction

1.1 Background

During the post World War II boom, a significant number of concrete framed high-rise apartment towers were built all over North America. Close to 2000 of these towers were built in the Greater Golden Horseshoe (GGH) and over 1000 were built in the City of Toronto. Only New York City has more with approximately 5500. Figure 1-1 illustrates two of these towers seen from Highway 401 in Toronto, Ontario.

Figure 1-1: Post-War Concrete Framed High-Rise Apartment Tower

The towers illustrated in Figure 1-1, along with all the other apartment towers of this era, are approximately 50 years old and reaching the end of their service life. They are showing signs of physical deterioration and need repairs. They also need modernization to improve the tenant's living conditions and to reduce energy use and greenhouse gas production. The current living conditions and state of physical deterioration of these towers along with Canadian greenhouse gas emissions and energy use will be discussed below.

1.1.1 Living Conditions of Tower Tenants

Today these apartments house an increasingly poor population. Figure 1-2 from the *Globe and Mail's* article, "Toronto Increasingly Becoming a City of Vertical Poverty" (Paperny, A., 2011), illustrates the increase in percentage of Toronto high-rise tenants earning less than Statistics Canada's low-income cut-off.

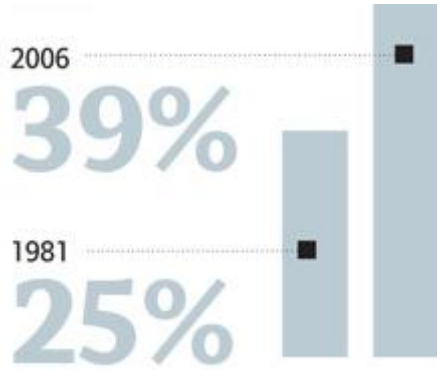

Figure 1-2: Percentage of Toronto High-Rise Tenants Who Earn Less than the Poverty Line

Figure 1-2 illustrates that the average person living in Toronto`s high-rise apartments today have less income than they did in the past. With financially poorer tenants, landlords and property management companies can charge less rent and hence have less money available for capital costs to repair and improve these high-rise apartment towers. This results in continued deterioration and thus poorer living conditions.

Tenants of these apartments are forced to accept poor living conditions. For example, the author of one newspaper article (Melanson, T., 2011) toured a building and apartment unit and described the situation; dead cockroaches and rat holes were found along the hallway walls. The family did not sleep in the bedroom because it was quarantined for a couple months due to mould problems. A sewer pipe had burst above their unit leaking through the drywall into their bedroom and bathroom. The window frames leak enough that during rain showers a bucket is used to collect the penetrating water. The oven is used as a heating source during colder periods when the heat loss is excessive and/or deteriorated heating system can't provide enough comfort.

These conditions described in the above article are a result of significant deterioration that includes corroded piping, failure of the window frame seal, poor thermal insulation, minimal air control, and

failing ventilation systems. Examples of physical deterioration in these towers are discussed in the next section.

1.1.2 Physical Deterioration

Building condition assessments by many different observers of these towers have documented numerous physical deteriorations. These assessments are often completed by visual inspections with findings and recommendations based on observations and measurements. Building condition assessments are often intended as the basis for short-term remedial action and capital expenditure planning. The recommendations of the assessments are usually repairs that require regular annual maintenance. Rarely are recommendations for retrofit made[1]. If significant capital expenditure is recommended for repair, the opportunity for retrofit should be assessed. Examples of common problems include:

- Peeling paint
- Spalling concrete
- Corrosion of reinforcement and balcony guards
- Balcony Failures
- Corrosion of window and door frames
- Efflorescence
- Subflorescence
- Deteriorating flashings
- Deteriorating shelf angles
- Deteriorating plaster ceilings
- Scouring of stone roof
- Staining of brick
- Cracking in balcony soffit
- Deteriorating plumbing riser
- Freeze-thaw

[1] Repair involves restoring the building to its original working order. Retrofit involves improving the building to current or newer working order.

Peeling Paint and Spalling Concrete

Figure 1-3: Peeling Paint and Spalling Concrete on Post-War Apartment Tower (TCHC, 2010)

The exposed paint on the enclosures concrete panel surface illustrated in Figure 1-3 is peeling likely due to exposure to ultra-violet radiation, rain, temperature fluctuations, and trapped moisture. Repairs such as repainting will likely lead to the same problem.

Figure 1-3 also illustrates spalling concrete on the exposed slab edge. The cantilevered reinforced concrete balconies of these towers also have significant spalling and other deterioration problems. Spalling on the top of the balcony surface is illustrated in Figure 1-4.

Figure 1-4: Spalling Concrete on Top Outer Edge of Cantilevered Balcony (CMHC, ND)

Figure 1-4 illustrates concrete spalling on the outer edge of the top side of a cantilevered balcony. Carbonation and chloride diffusion in the reinforced concrete leads to spalling. Carbonation is the process of carbon dioxide in the ambient air penetrating the concrete and reacting with the hydroxides. This process significantly lowers the alkalinity (pH) of the concrete which reduces steel reinforcement protection from corrosion. (Kosmatka et al., 2002) Chloride diffusion is the process of chloride ions, from sodium chloride (salt), penetrating the concrete and reacting with the protective oxide film around the steel reinforcement. This process also reduces the steels protection from corrosion. (Kosmatka et al., 2002) When the steel reinforcement has lost its protective oxide film an electric cell is formed along the steel. The hydroxide ions that are formed combine with the iron from the steel resulting in iron hydroxide. The iron hydroxide combines with oxygen forming iron oxide (rust). This process results in an increase in the steel reinforcement's diameter where sections of iron oxide have built up. This circumferential increase causes tangential stress in the surrounding concrete resulting in cracks. This allows further penetration of chlorides and carbon dioxide, thus accelerating the process. Eventually sections of concrete separate and either fall off or are brushed away by wind or other mechanical processes. The loss of concrete from the section decreases its overall strength which may eventually result in failure.

Corrosion of Reinforcement and Balcony Guards

Figure 1-5 illustrates corrosion around the steel reinforcement and steel guard rail of a balcony.

Figure 1-5: Exposed Steel Reinforcing and Steel Guard Rail in a Concrete Balcony (CMHC, ND)

Figure 1-5 illustrates extensive spalling of the concrete surrounding the steel reinforcement such that it is visible and fully exposed. The corroded steel guard rail is no longer embedded in the concrete, and hence has lost all its structural integrity. The cost to repair this problem is significant, and a complete retrofit should be considered.

Balcony Failures

Figure 1-6 illustrates a balcony failure. This is an extreme result of corrosion over time caused by poor water management.

Figure 1-6: Balcony Failure

Water made its way to the reinforcing steel resulting in corrosion. Cracks in the concrete allowed water to reach the steel, which corroded, expanded, and hence cracked more, allowing more water penetration. The cycle continued until the loads exceeded the capacity leading to the failure. Proper roof, parapet, and/or balcony overcladding would have protected the reinforced concrete from water penetration.

Corrosion of Window and Door Frames

Figure 1-7 illustrates corrosion in the steel window frame of a post-war apartment tower's enclosure entrance.

Figure 1-7: Corrosion of Steel Door and Window Frame of Enclosure Entrance (TCHC, 2010)

Build up of moisture that condensed on the window and frame of this door along with lack of corrosion resistant materials likely lead to this corrosion. Repair is not usually an option and hence replacement is usually necessary. Better thermal performance of the door and glazing would avoid condensation and the resulting damage.

Efflorescence and Subflorescence

Figure 1-8 illustrates efflorescence often seen on the brick surface of the enclosure of the post-war apartment towers.

Figure 1-8: Efflorescence below Windows on Brick Enclosure

The white stains below the windows in Figure 1-8 are likely a result of rain water that has not drained off the edge of the window sills but ran along the underside or condensation of indoor air escaping through leaky windows and frames. The concentration of water runs into the wall or down the enclosures surface soaking into the brick. The drying of the brick initiates efflorescence. Efflorescence is caused by salt residue that is dissolved in liquid water carried within the brick towards the exterior surface where the water evaporates leaving the salt behind. Subflorescence is similar except the salts do not reach the surface. The salts build up just below the surface which can result in spalling of the brick because of pressures that build when salt re-crystallization occurs within pores. A closer view of the salts from efflorescence on the brick surface of one of the towers is illustrated in Figure 1-9.

Figure 1-9: Efflorescence on Brick Surface

Deteriorating Flashing and Shelf Angle

Figure 1-10 illustrates deteriorated flashing and corroded steel shelf angle.

Figure 1-10: Deteriorated Flashing and Steel Shelf Angle (CMHC, 2006)

The deteriorated flashing and corroded steel shelf angle illustrated in Figure 1-10 are a result of poor material choice and inadequate water and vapour control. The vertical load of the brick veneer is no longer taken by the shelf angle and is accumulating on the brick veneer below. This can be detrimental to the structural integrity and it can be especially problematic on these high-rise towers because the greater height has more potential for catastrophic failure. This deterioration can be attributed to a number of reasons. Copper-fabric is sensitive to long-term exposure of moisture and should not have been used as a flashing material. Blocked or an inadequate number of weep holes reduces the ability for this wall to drain. Lack of ventilation holes below the shelf angles reduces the drying potential. Wind and stack effect causing larger pressure differences along with inadequate air barriers result in significant vapour infiltration which condenses on the back side of the brick before running down the brick.

Deteriorating Plaster Ceiling

Figure 1-11 illustrates a deteriorating plaster ceiling in the bathroom of a post-war apartment tower unit.

Figure 1-11: Deteriorating Plaster Ceiling in Bathroom (TCHC, 2010)

The deterioration is likely caused by the repeated wetting from the shower's water vapour condensing on the underside of the ceiling. A properly functioning bathroom exhaust fan that is able to remove air and thus the air's water vapour from the bathroom to the exterior will reduce the bathroom's

interior relative humidity. This will reduce the condensation on the ceiling and thus the problem of premature deterioration of the ceiling plaster.

Scouring of Stone Roof

Figure 1-12 illustrates wind scouring at the corner of the stone roof of a post-war apartment tower.

Figure 1-12: Wind Scouring at Corner of Stone Roof (TCHC, 2010)

The significant wind pressures along the edges of the roofs of these high-rise apartments can cause scouring of stones illustrated in Figure 1-12 exposing the fabric beneath increasing the roofs susceptibility to penetration. A repair would replace the stones and a retrofit may provide scouring protection such as a parapet or patio slabs at the perimeter.

Staining of Brick

Figure 1-13 illustrates rainwater stains at the lower corners of the windows on the exterior of a post-war apartment tower.

Figure 1-13: Rainwater Stains below Window Corners (TCHC, 2010)

The function of window sills and flashings is to encourage water to drain away from the face of the enclosure. The window sills in Figure 1-13 collect water at the corners and drain it along the surface of the enclosure. This results in the dark water marks below the corners of the windows which is unsightly and can cause effloresence or subflorescence. Saturated brick will allow water to penetrate by gravity pressures at poorly bonded brick head joints. Pressure differences across the enclosure can also draw the water into the enclosure and the building's interior resulting in numerous problems. Installing jamb deflectors on the edge of the window sills directs the collected rainwater away from the enclosure.

Cracking in Balcony Soffit

Figure 1-14 illustrates peeling paint and cracking in the soffit of the protruding concrete balconies typical in post-war apartment towers.

Figure 1-14: Peeling Paint and Cracking in Balcony Soffit (TCHC, 2010)

The balcony soffit illustrated in Figure 1-14 can have small gaps between it and the brick facade below. These gaps allow the movement of warm moist interior air to exfiltrate which can then condense on the cooler balcony soffit. The shaded underside of the balcony can stay wet for long periods of time resulting in peeled paint and cracking. A second cause of soffit deterioration is rainwater that runs down the edge of the balcony. It can move along the soffit due to water's surface tension resulting in peeling paint and cracking. This balcony soffit has a keyed edge which breaks the movement of water along the soffit reducing the second cause of soffit wetting.

Deteriorating Plumbing Riser

Figure 1-15 illustrates a deteriorating plumbing riser in one of these towers.

Figure 1-15: Deteriorating Plumbing Riser (TCHC, 2010)

A common problem in the towers is deteriorating plumbing risers illustrated in Figure 1-15 which leak into the adjacent units. Replacing the plumbing risers is a significant renovation and thus any retrofit options should be considered carefully.

The Tower Renewal Guidelines (2009) is a publication that introduces the opportunity of retrofitting post-war apartment towers and their sites in the Greater Toronto Area. It was created by Ted Kesik and Ivan Saleff of Daniels Faculty of Architecture, Landscape, and Design from the University of Toronto with support from the City of Toronto, the Toronto Atmospheric Fund, and Canada Mortgage and Housing Corporation. This document provides a history of the towers, condition assessment, site strategies, retrofit strategies, and cost-benefit analysis.

The condition assessment in the Tower Renewal Guidelines (2009) also describes some of the observed signs of deterioration; the performance problems were noted during field observations. Buildings that had a glazed exterior finish had the glazing pushed off and efflorescence occurring. Failed sealant between the masonry veneer and concrete frame was also a common observation.

Freeze-Thaw

The most significant brick deterioration was found under the window sills and at the slab edges. Inadequate or missing flashings and air leakage can result in a buildup of moisture at these locations. The buildup of moisture is likely to exceed the critical degree of saturation resulting in freeze-thaw spalling as well as deterioration of the mortar joint. Although water within the pores of the masonry expands by 9% during its phase change, the mechanism of freeze-thaw is believed to initiate by the moisture within the solid matrix. Freeze-thaw within the solid matrix of a material is not fully understood, a few of the theories include closed container, ice lensing, hydraulic pressure, and disequilibrium discussed in Mensinga (2009). The moisture content level at which damage is significant in a specific brick or concrete block is known as the critical degree of saturation. An example of freeze-thaw deterioration is illustrated in Figure 1-16.

Figure 1-16: Freeze-Thaw Deterioration

Figure 1-16 illustrates that freeze-thaw can deteriorate the face of the brick completely off. It can cause large vertical cracks which could lead to sections of brick falling off the sides of buildings, which is a life safety concern.

Deterioration at Grade

Another common observation was the deterioration of the concrete and brick where it meets the grade. Where drainage around the building perimeter is not adequate and brick is near the grade, the buildup of snow and rain water can stain the brick, illustrated in Figure 1-17.

Figure 1-17: Brick Staining at Grade

These signs of constant wetting can result in brick deterioration. Brick in contact with the grade can wick water up which can also result in freeze-thaw spalling and efflorescence.

Overall, the concrete frame is structurally adequate in most of these towers apart from the protruding balcony slabs. The non-load bearing masonry veneer is deteriorating much faster. The necessity to repair the masonry veneer provides the opportunity to improve the enclosure and the building as a whole. Retrofitting the enclosure can include the addition of air, vapour, water, and thermal control layers, discussed in Section 5.1, to improve durability and comfort while reducing energy use. The energy used in Canadian apartments is discussed in the following Section.

1.1.3 Canada's Energy Use

Figure 1-18 illustrates energy use in Canada by sector for 2005.

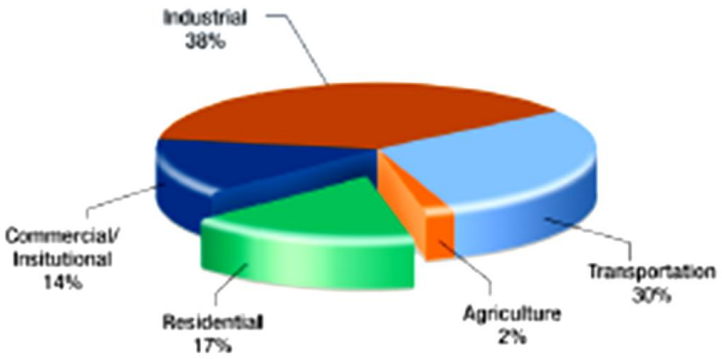

Figure 1-18: Canadian Energy Use in 2005 by Sector (NRCan, 2008)

According to government studies (NRCan, 2008), buildings consumed approximately one third of Canada's energy in 2005. The other two sectors (industrial and transportation) used approximately the same proportion as buildings with 38% and 30% respectively.

1.1.3.1 Canada's Residential Space Heating Trends

A majority of the 31% of energy that buildings consume is for residential buildings. Seventeen percent of all the energy Canada uses goes into its residences. The end-use of Canada's residential energy is illustrated in Figure 1-19.

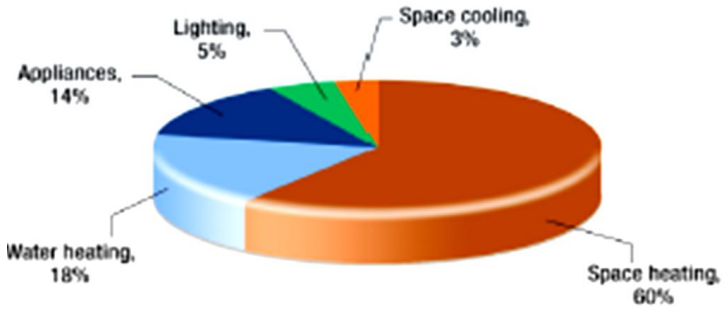

Figure 1-19: Canadian Residential Energy End-Use Percentages in 2005 (NRCan, 2008)

Figure 1-19 illustrates that by far the most significant percentage (60%) goes into heating Canadian residences which means that more than 10% of all of Canada's energy goes directly towards heating its residential buildings. This indicates that a significant percentage of Canada's energy conservation focus should be directed towards heat loss in residential buildings.

Figure 1-20 illustrates the slow decline in energy used to heat residential spaces over the past 20 years for three types of residences.

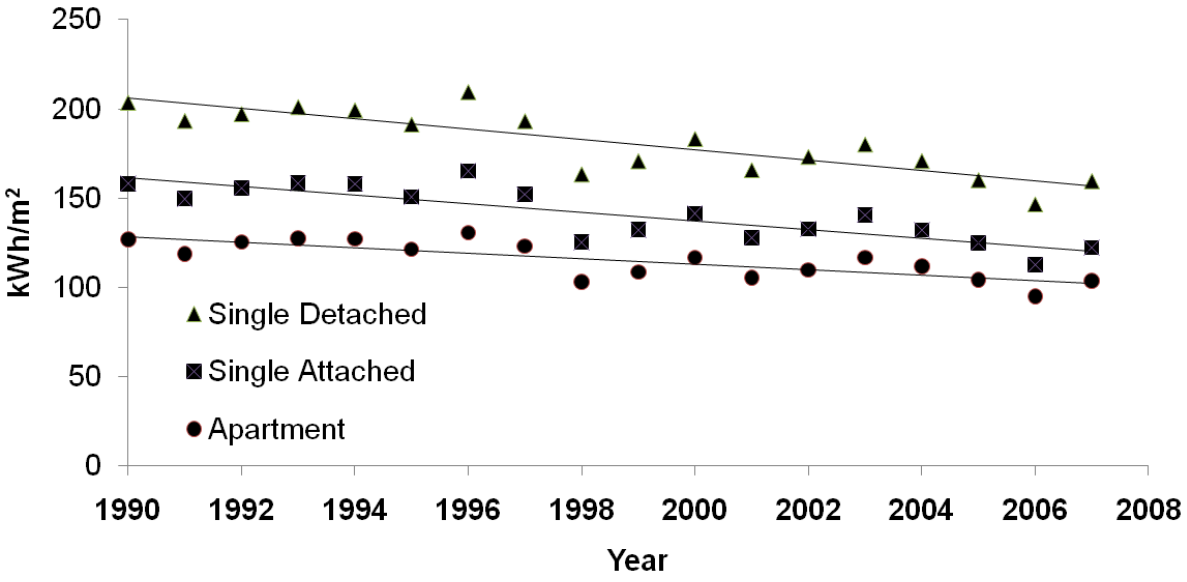

Figure 1-20: Canadian Residential Space Heating Trends

Figure 1-20 illustrates that the average Canadian single detached residence uses a significant amount more energy for space heating than a single attached or apartment residence. However, single family space heating use is decreasing by approximately 2.9kWh/m^2 every year while the average apartment is only decreasing by approximately 1.6kWh/m^2 every year, almost half the rate. This is disconcerting because the ratio of enclosure area to floor area for a single detached residence is approximately 4 times that of the average apartment. Even though this trend will not necessarily continue it does illustrate the opportunity to significantly reduce the space heating energy used by apartments if their enclosures were built to the same standards as single family homes.

Reducing the energy consumption of apartments in Canada contributes to the reduction in Canada's greenhouse gas emissions. The greenhouse gas emitted in Canada and its impact on global warming are discussed in the following section.

1.1.4 Canada's Impact on Global Warming

The concentration of CO_2 in the atmosphere has increased significantly over the last couple centuries. Figure 1-21 illustrates this rapid increase.

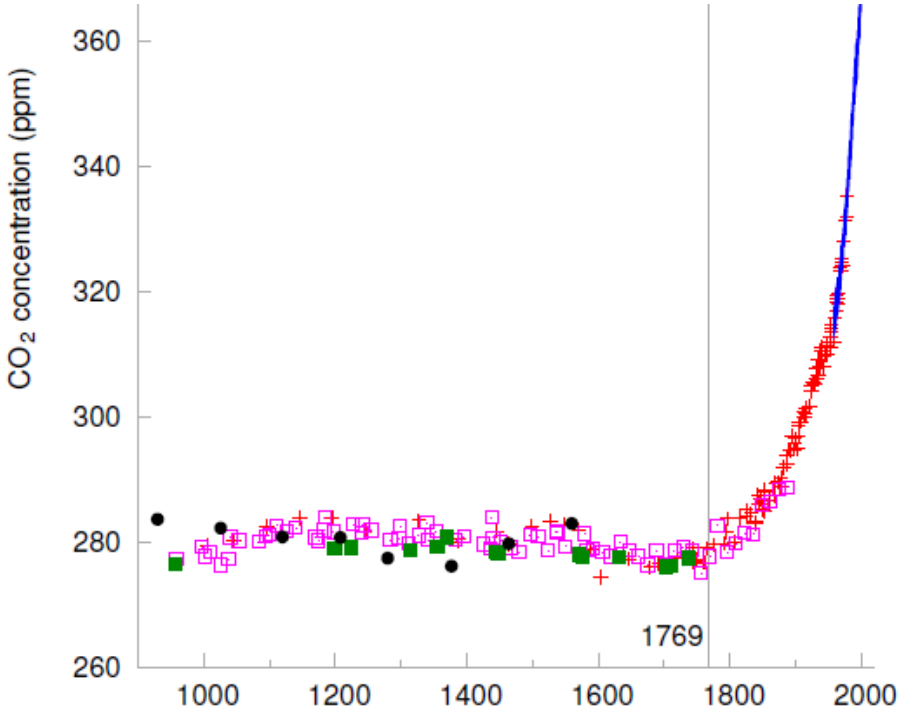

Figure 1-21: Atmosphere CO_2 Concentrations over the Last 1000 Years (MacKay, 2009)

David MacKay singled out the year 1769 because that was the year that James Watt patented his steam engine which was more efficient than the first practical steam engine invented 70 years prior. The burning of fossil fuels emits CO_2 and from this graph appears to have significantly increased the concentration of CO_2 over the past couple hundred years. According to the Intergovernmental Panel on Climate Change (IPCC, 2007) the increase in greenhouse gases from human activity has begun to significantly change the climate. Three indications of climate change are illustrated in Figure 1-22.

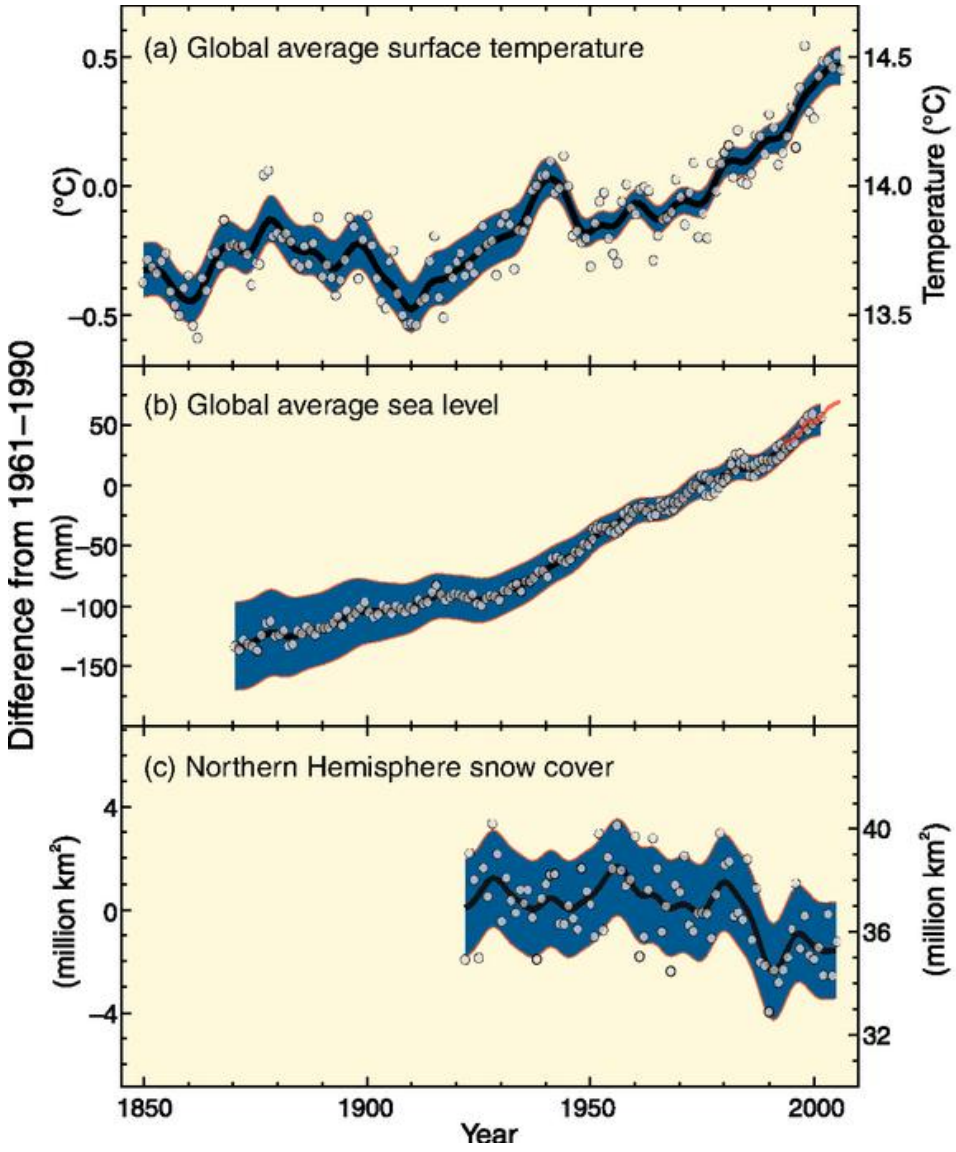

Figure 1-22: Change in Temperature, Sea Level, and Northern Hemisphere Snow Cover (IPCC, 2007)

Figure 1-22 illustrates an increase in the global average surface temperature and sea level and a decrease in the northern hemisphere snow cover. These indications of global warming over the past century align with the increase in CO_2 concentrations over the past couple centuries, previously illustrated in Figure 1-21. The intent of this section isn't to debate global warming but to show that the burning of fossil fuels used for energy consumed by existing buildings connects to it. David MacKay breaks down the greenhouse gas pollution by average person in each country illustrated in Figure 1-23.

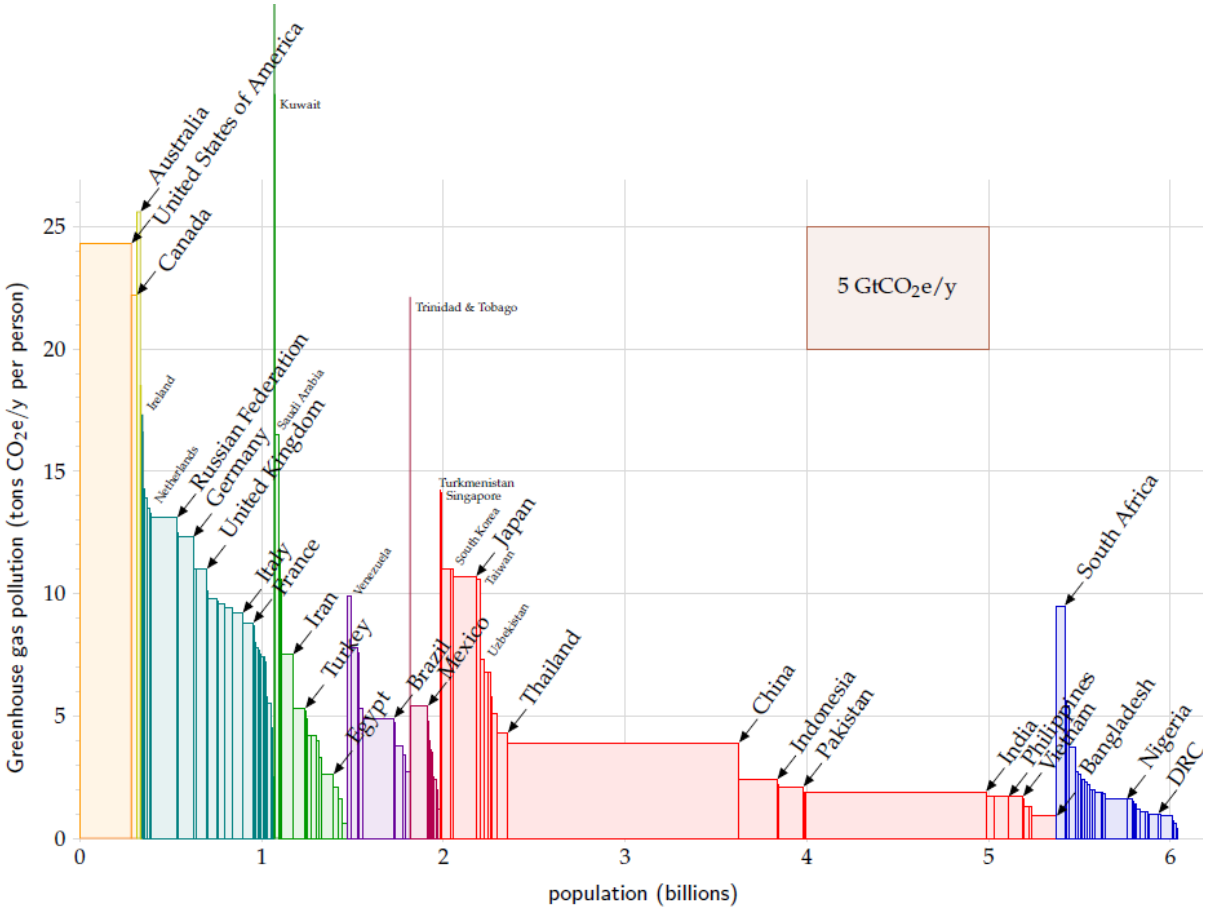

Figure 1-23: Greenhouse Gas Pollution per Average Person of Each Country (MacKay, 2009)

Figure 1-23 illustrates the relative greenhouse gas emissions Canadians emit compared to the rest of the world. United Arab Emirates, Kuwait, Australia, and the United States of America are the only countries who emit more greenhouse gases on a per person basis. The average person in the world only emits approximately 5½ equivalent tons of CO_2 per year, approximately one quarter of the average Canadian. Since greenhouse gas pollution is primarily related to Canada's energy production, it makes not only financial sense to reduce energy use but provides an opportunity to reduce the global warming potential.

1.1.5 The Need for Retrofit

Wikipedia (2011) defines retrofit projects as, "to replace or add equipment to existing power plants to improve their energy efficiency, increase their output and extend their lifespan, while decreasing

emissions." Thus, a building enclosure retrofit could be described as the replacement or addition of enclosure materials to the existing building to improve its energy efficiency, increase the occupants' living conditions and extend the building's service life while decreasing its environment impact.

The need to retrofit the numerous concrete framed high-rise apartment towers in the Greater Toronto Area (GTA) built during the post-war boom (1945-1984) has been identified in many published documents including the *Mayor's Tower Renewal- Opportunities Book* (2008). The Mayor's Tower Renewal was initiated by former Toronto Mayor David Miller to promote the opportunity to retrofit over 1000 towers and their sites in the city of Toronto. *Tower Renewal Guideline- for the Comprehensive Retrofit of Multi-Unit Residential Buildings in Cold Climates* (2009) was developed by Ted Kesik and Ivan Saleff of the University of Toronto to provide overall guidance retrofitting the towers and their sites. Tower Renewal has grown to include cities such as St. Catherines, Brantford, Kitchener, Waterloo, Barrie, and Peterborough as described in the report *Tower Neighbourhood Renewal in the Greater Golden Horseshoe* (2010). This entire tower renewal area is referred to as the Greater Golden Horseshoe (GGH). This report states that there are almost 2000 high-rise (greater than 7 stories) apartment towers in the GGH.

1.2 Objective

The goal of the research reported in this thesis is to provide policy makers, code officials, architects, and building engineers' insight on the effects of various wall enclosure retrofit options for post-war high-rise apartment towers in the context of total building energy use. The three primary effects of the enclosure retrofit options are: (1) the impacts on durability, (2) improved occupant comfort, and (3) the reduction in building energy use and greenhouse gas emissions. Properly designed and executed enclosure retrofits should extend the economic and useful life of this significant building stock.

1.3 Scope

The scope of this thesis is limited to a general investigation of the effects of wall enclosure retrofits. The effects investigated include the impacts on:

- Durability to rain and moisture penetration, condensation potential, and deterioration due to freeze-thaw cracking.
- Occupant comfort based on mean radiant temperature and passive control
- Annual energy consumption and greenhouse gas emissions

A general overall interior versus exterior enclosure retrofit comparison is included. The costs of these retrofits will not be discussed in any detail because costs are highly variable and difficult to ascertain.

1.4 Approach

The thesis begins by describing high-rise apartment towers built during the post-war boom and developing an Archetype building. Energy and air flows through the existing enclosure components are modeled. The miscellaneous electrical loads (MEL) and ventilation conditioning energy are approximated for these towers. The MEL, ventilation, enclosure's thermal resistances, and natural air leakage are incorporated into an open source whole building energy and loads analysis model. The restructured model analyzes the towers existing loads and compares the values to reported measured energy data of existing post-war high-rise apartment towers. Various enclosure retrofit options are described and their heat transfer characteristics and geometries are simulated. The impacts on durability and comfort are discussed based on the results. Energy efficiency measures are described and analyzed to complement the enclosure retrofits. Retrofit packages are created and simulated in the restructured building energy and loads analysis model. The results are compared to illustrate potential overall building retrofit annual energy reductions. Finally, the reduction in greenhouse gas emissions is briefly discussed.

Chapter 2 – Towers

This chapter describes the history and construction technology of the buildings being studied. Ranges of statistics are used to describe these towers.

2.1 History of the Towers

During the 1960s, the demographic bulge known as the 'baby boomers' began to enter the real estate market. Inevitably, there was an increase in demand for residences. Developers, architects, engineers, and contractors began to produce many new, quickly built, and attractive residential units in the form of high-rise apartment towers. These residential apartment towers were commonly situated in park-like settings. The idea of clusters of towers separated by large expanses of green space arguably came from Le Corbusier. His 1922 diagram of *Ville Contemporaine* was a scheme for a large metropolis. A drawing of the view into the Ville Contemporaine is illustrated in Figure 2-1.

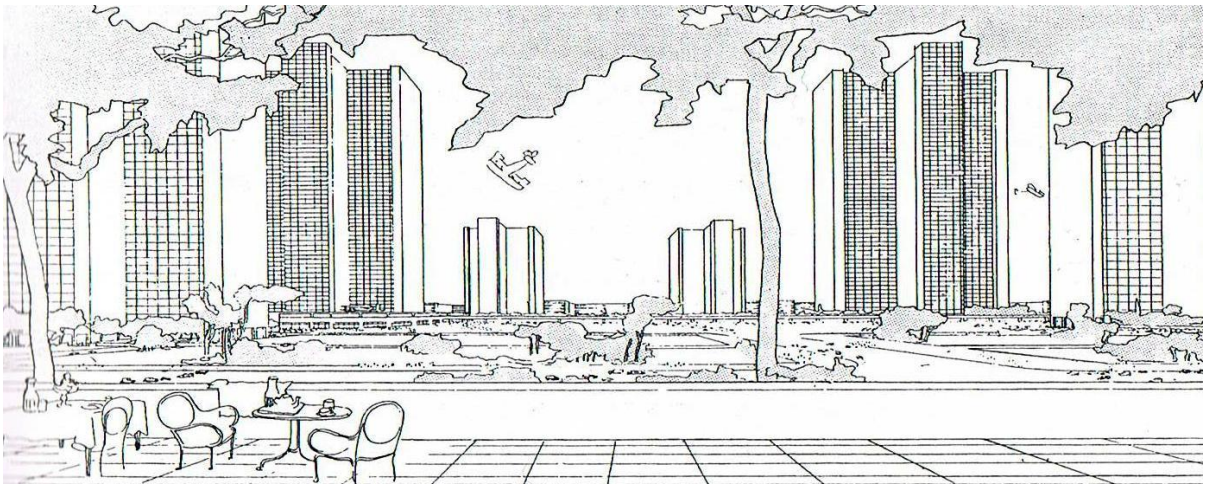

Figure 2-1: Le Corbusier's *Ville Contemporaine* (Blake, P., 1976)

Peter Blake (1976) describes the scheme illustrated in Figure 2-1, "The center of Corbu's (Le Corbusier's) Ville Contemporaine was to be a group of skyscrapers, cruciform in plan, fifty or sixty stories in height, and spaced very far apart to permit the development of generous park spaces between them." The post World War II cluster of apartment towers has this similar scheme and was often referred as 'tower-in-the-park'. The construction of these apartment tower clusters significantly increased the residential housing stock. Figure 2-2 illustrates the significant rise in multi-unit residential building (MURB) construction throughout the 1960's and 1970's.

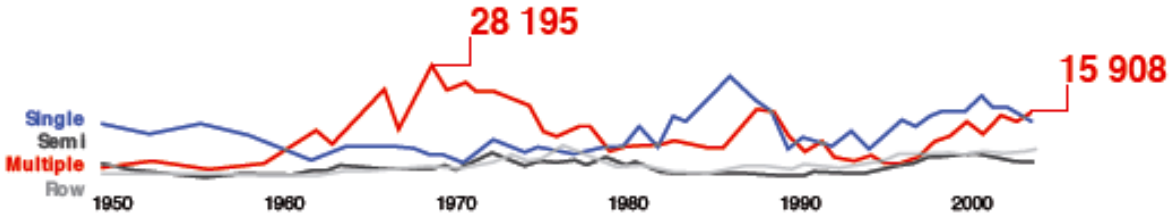

Figure 2-2: Post-War Rise in MURB Construction (Kesik, T. And Saleff, I., 2009)

Figure 2-2 illustrates that in 1968 nearly 30,000 residential units were built, which can be compared to the 16,000 condominium units built in 2005 in the then much more populous GTA (Kesik, T. and Saleff, I., 2009).

2.1.1 Apartment Tower Construction

Figure 2-3 illustrates a common sight throughout the GTA during the 1960's.

Figure 2-3: Tower Construction (Kesik, T. And Saleff, I., 2009)

For most towers the construction of a site-cast reinforced concrete frame was followed by the brick and block exterior walls constructed on top of the outer perimeter of the concrete floor slabs. In the early 1960's, apartment buildings used a hybrid structural system of steel and reinforced concrete. Balconies were not common and single-glazed, steel frame windows were used. During the mid-1960's the implementation of flying forms (see the following figure) shifted the reinforced concrete

frame to the dominant type for both mid-rise and high-rise MURBs. At this time, balconies became much more common. Additional Portland cement was added to the concrete mix so that the strength at which formwork could be removed was reached sooner. The use of flying forms and increased cement content caused the average MURB to go from a range of 6 to 8 storeys to towers ranging from 20 to 30 storeys. Another reason for the increase in these towers was the economical decision to simplify the floor plans and use symmetry. The dimensions were standardized to correspond with Canadian lumber and plywood sizes to minimize cutting and waste.

Figure 2-4: Flying Formwork in Action

Figure 2-4 illustrates a flying form being "flown" from under a newly cast concrete floor slab. This technology allowed the concrete forms to be reused and easily moved between levels making the construction of concrete framed residential towers more efficient.

2.1.2 Planned Communities

Figure 2-5 illustrates a cluster of apartment towers in the City of Toronto.

Figure 2-5: Post-War MURBs in the GTA (Kesik, T. And Saleff, I., 2009)

Figure 2-5 illustrates several of these towers designed around a planned community. These communities provided another option to suburban single family houses sprawling outward. Many included industry, shopping, mixed-housing types, schools, and plenty of green space. The figure also illustrates the similarity in building size and geometry.

2.2 Population of Towers

The report, *Tower Neighbourhood Renewal in the Greater Golden Horseshoe* (2010) describes the quantity, location, and significance of these towers in the Greater Golden Horseshoe (GGH). Nearly 2000 high-rise (greater than 7 storeys) apartment towers were built in the GGH during the post-war boom. (Stewart, G. and Thorne, J., 2010) These towers house approximately 1,000,000 people in the GGH. Figure 2-6 illustrates the percentage of GGH housing stock.

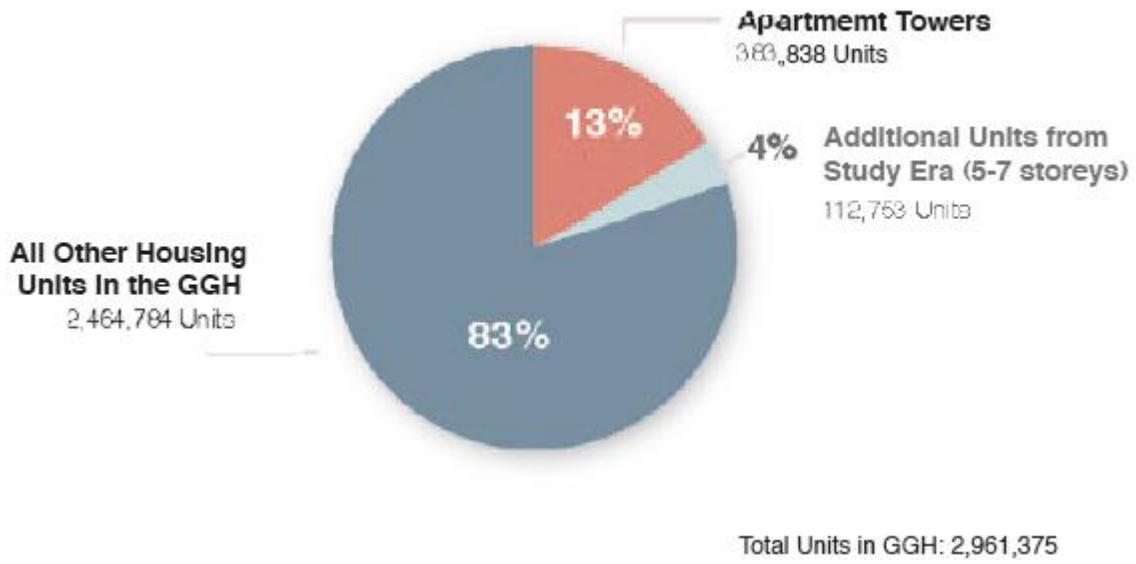

Figure 2-6: Percentage of Apartment Towers in Greater Golden Horseshoe (Stewart, G. and Thorne, J., 2010)

Figure 2-6 illustrates the approximately 380,000 high-rise apartment tower units representing 13% of the nearly 3,000,000 GGH housing units. Statistics Canada considers high-rise as greater than four stories which represent approximately 500,000 high-rise apartment tower units or 17%. Based on Statistics Canada's high-rise criteria, there are more than 3000 high-rise apartment towers in the GGH.

The number of high-rise MURBs built during the post World War II boom is significantly larger than any other period in the history of the GTA. The following figure illustrates the GTA's high-rise MURB construction over the last seven decades.

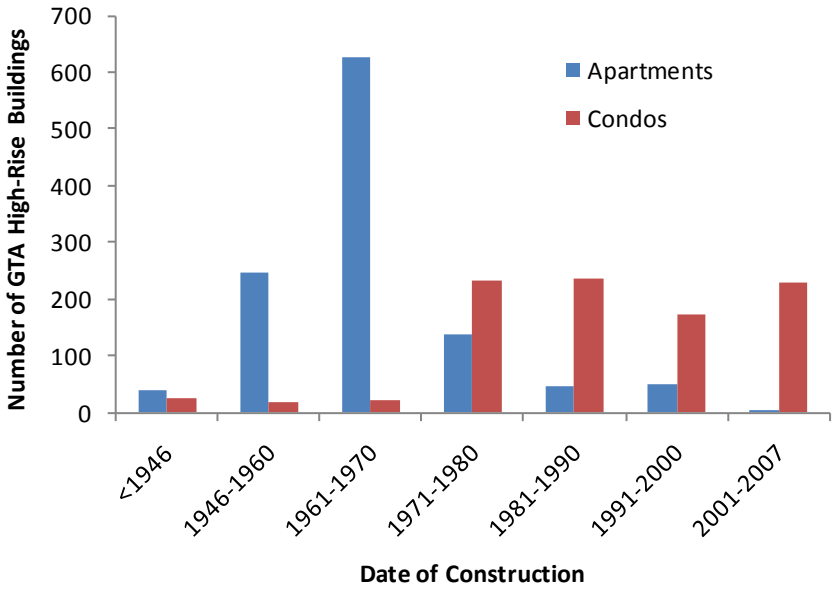

Figure 2-7: GTA High-Rise MURBs Constructed between 1946 and 2007

Figure 2-7 illustrates that over 600 GTA high-rise (defined as greater than 4 stories) apartment towers were constructed during the 1960s. The combination of high-rise apartment towers and condominium towers built during the 1970s is approximately 350 while no other decade exceeds a total of 300 towers.

2.3 Location of Towers

Table 2-1 from the *Tower Neighbourhood Renewal in the Greater Golden Horseshoe* (Stewart, G. and Thorne, J., 2010) illustrates the number of apartment towers from Toronto to the outer ring of the GGH.

Table 2-1: Apartment Tower Location and Stock in GGH

Location	Apartment Towers
Greater Golden Horseshoe	1,925
Greater Toronto and Hamilton Area	1,752
Toronto	1,189
GTHA without Toronto	563
Outer Ring of GGH	173

Table 2-1 illustrates that a majority, approximately two-thirds, of the apartment towers are located in the City of Toronto. Appendix A illustrates a map of the GGH with each county, region, and major city separately labeled with their respective number of towers, tower units, and tower site area.

2.4 Archetype

In this thesis the term "Archetype" will be subsequently used as a general description of the nearly 2000 concrete framed high-rise (greater than 7 storeys) apartment towers in the GGH. Using this single theoretical building has the advantage that it encompasses the common characteristics of the 2000 towers. Using this Archetype simplifies the analysis and takes advantage of average values for the towers' characteristics.

Construction drawings for four different high-rise apartment towers owned and operated by the Toronto Community Housing Corporation (TCHC) were used for most of the geometrical characterizing. The four buildings are defined here as buildings one through four. These buildings were constructed in the GTA in 1967, 1968, 1962, and 1968, respectively. The drawings used for analysis include plans, elevations, sections, exterior wall section details, domestic hot water schematics, ventilation schematics, exhaust fan schedules, supply unit schedules, and pump schedules. Selected drawings are included in Appendix B for buildings 1, 2, 3, and 4 (TCHC, 2010). Buildings 3 and 4 are actually two identical towers connected to form 'V' and 'Z' shaped configurations, respectively. The Archetype was intended to describe a single, rectangular tower, so only the characteristics of one side of buildings 3 and 4 were considered.

The common characteristics that describe the Archetype are the towers' dimensions, number and size of the different unit types, floor area composition, wall types and dimensions, wall composition, roof composition, perimeter composition of the various wall types, window to wall ratio, air leakage parameters, and ventilation system. Some of the common characteristics include a reinforced concrete frame, exposed slab edges, protruding concrete balconies, aluminum window frames, double glazing, brick and block walls, minimal interior insulation, symmetrical rectangular layouts, smaller window to wall ratios, leakier enclosures, and dysfunctional ventilation systems. All these characteristics used to define the Archetype will be described in detail below.

2.4.1 Archetype Dimensions

The construction drawings of the four different apartment towers were reviewed and each building's dimensions were summarized and averaged in Table 2-2.

Table 2-2: Buildings Dimensions

	Stories	Tower Width		Tower Length		Floor to Floor Height		Floor Area per Storey		Total Floor Area		Perimeter	
	#	m	ft	m	ft	m	ft	m^2	Sq ft	m^2	Sq ft	m	ft
Building 1	21	15	49	74	244	2.64	8.67	1,111	11,956	23,326	251,076	179	586
Building 2	12	17	55	79	260	2.63	8.63	1,329	14,300	15,942	171,600	192	630
Building 3	15	15	49	48	156	2.64	8.67	715	7,695	10,724	115,432	125	411
Building 4	29	15	49	64	209	2.64	8.67	951	10,241	27,591	296,989	157	516
Average	19	15	51	66	217	2.64	8.66	1,026	11,048	19,396	208,774	163	536

The four different apartments range from 12 to 29 stories with an average of 19 stories. The Archetype will be assumed to be 20 stories. The average width is 15m and average length is 66m. Since buildings 1 and 2 stand alone and have greater lengths, an average length of 70m for the stand alone Archetype will be used. The floor to floor height is consistently 2.64m (8'-8") which will be used for the Archetype. The average floor area ranges from approximately 11,000m^2 to 28,000m^2 with an average of 20,000m^2 (210,000ft^2). These values include all rooms and corridors within the building enclosure. All buildings have the same basic cross section; a single corridor flanked on both sides by apartment units.

2.4.2 Units in Archetype

Table 2-3 illustrates the quantity of each type of apartment unit in the four TCHC buildings examined. The averages were calculated and used to determine the scheme of apartment types in the Archetype.

Table 2-3: Number of Units in Buildings

	Stories	Bachelor Units	One Bedroom Units	Two Bedroom Units	Three Bedroom Units	Total Units	Typical Units per Storey
	#	#	#	#	#	#	#
Building 1	21	46	64	190	1	301	15
Building 2	12	0	44	92	23	159	14
Building 3	15	39	65	39	8	151	11
Building 4	29	30	173	171	0	374	13
Average	19	29	87	123	8	246	13

The most common unit has two bedrooms with the majority of the other units having one bedroom. Since Buildings 1 and 2 are longer, they have more units per storey, the units in the Archetype will be based on 14 units per storey for the typical floors 2 through 20. The first floor of the towers is different because it contains the lobby and often other building amenities. The first floor configuration also varies considerably. The configuration of units for the Archetype will be the same for all floors and will contain 8 two bedroom units, 4 one bedroom units, and 2 bachelor units. Three bedroom units are uncommon, so they will not be considered in the Archetype.

2.4.3 Archetype Unit Size

Table 2-4 illustrates the size of each type of apartment unit on the typical floors in the four TCHC buildings examined. A weighted average was calculated and used to determine the sizes used for each type of apartment in the Archetype.

Table 2-4: Buildings Unit Sizes

	Bachelor Unit		One Bedroom Unit		Two Bedroom Unit		Three Bedroom Unit	
	ft^2	m^2	ft^2	m^2	ft^2	m^2	ft^2	m^2
Building 1	378	35.1	571	53.0	756	70.2		
Building 2			627	58.2	869	80.7	960	89.2
Building 3	364	33.8	526	48.9	654	60.8		
Building 4	355	33.0	542	50.4	736	68.4		
Weighted Average	370	34.3	558	51.8	779	72.4	960	89.2

The areas illustrated in Table 2-4 are the average finished floor and partition wall areas for each type of apartment unit. The weighted average was based on the number of each type for each building. The average size of the bachelor and one bedroom units do not vary significantly between buildings. The Archetype will use $34m^2$ ($366ft^2$) and $52m^2$ ($560ft^2$) for the bachelor and one bedroom units, respectively. The average size of the two bedroom units in Building 2 are significantly larger than in the other buildings so the Archetype will use a $70m^2$ ($753ft^2$) two bedroom unit.

2.4.4 Archetype Typical Floor Area Composition

Table 2-5 illustrates the percentages of areas including units, corridor, stairwell, elevator, garbage chute, electrical room, ventilation shaft, and all walls on the typical floors in the four TCHC buildings

examined. The average percentage of total floor area was calculated for each type of area to determine the relative sizes of each in the Archetype.

Table 2-5: Typical Floor Area Percentages

	Units	Corridor	Stairwell	Elevator	Other	Walls
Building 1	81%	8%	1.7%	1.4%	0.3%	8%
Building 2	82%	7%	1.6%	0.7%	0.4%	8%
Building 3	74%	10%	2.0%	1.3%	0.7%	16%
Building 4	77%	9%	1.4%	1.8%	0.7%	10%
Average	79%	9%	1.7%	1.3%	0.6%	10%

The other areas are comprised of the garbage chutes, electrical rooms, and ventilation shafts. The percentage of each area is relatively consistent for all four buildings. The percentage of building area designated for the units in the Archetype will be 80% before they are sub-divided into the different types of units. 10% of the Archetype's building area will be designated as common space and will include the corridors, stairwells, elevators, garbage chutes, and electrical rooms. 10% of the Archetype's building area will be designated as walls, both interior and exterior.

2.4.5 Archetype Perimeter Composition and Window to Wall Ratio

The lengths of each of the five previously defined exterior wall types were measured along the perimeter of each of the buildings and the percentage of each relative to the entire perimeter were calculated and provided in the following table. The window to wall ratios (WWR) were also calculated and provided in Table 2-6.

Table 2-6: Building Perimeter Compositions and Window to Wall Ratios

	Wall	Window/Wall	Balcony Wall	Balcony Window	Balcony Door	WWR
Building 1	33%	16%	17%	25%	8%	31%
Building 2	19%	14%	6%	51%	9%	45%
Building 3	58%	23%	6%	0%	12%	23%
Building 4	39%	17%	15%	22%	7%	28%
Average	37%	18%	11%	25%	9%	32%

Buildings 1 and 4 were very close in percentages and also have the composition of exterior walls commonly seen in most of the towers. Weighting these percentages slightly higher, the Archetype perimeter composition is approximately 35% wall, 25% balcony window, 15% window wall, 15% balcony wall, and 10% balcony door. The window to wall ratios ranged from 23% to 45% for these

four buildings. The WWR of 45% for building 2 is atypically high, thus a WWR slightly lower than the 32% average will be used for the Archetype. For simplicity, 30% will be used for the Archetype.

2.4.6 Archetype Wall Types

The opaque wall section of the four buildings consists from interior to exterior of the following:

- Gypsum board or plaster
- One or two inches of EPS insulation or a radiant barrier on airspace
- Sometimes parging or vapour barrier
- Four inch concrete block or backup brick
- Four inch brick facing with no drainage gap

The most common characteristics were used to define the Archetype. The Archetype enclosure can be divided into five different wall sections: two exterior wall sections and three balcony wall sections. All five wall sections are illustrated below.

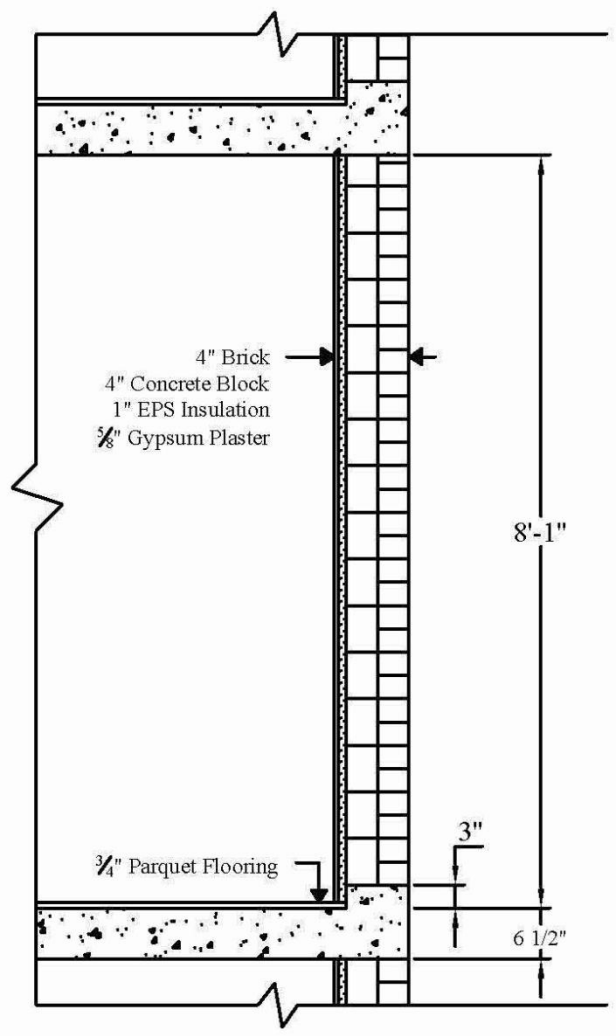

Figure 2-8: Wall Section

Figure 2-8 illustrates the Archetype wall section. It has exposed concrete slab edges with the typical opaque wall section constructed on a 76mm (3") concrete curb on the edge of the concrete slab. The concrete curb and 19mm (¾") thick parquet flooring is the same in all wall sections.

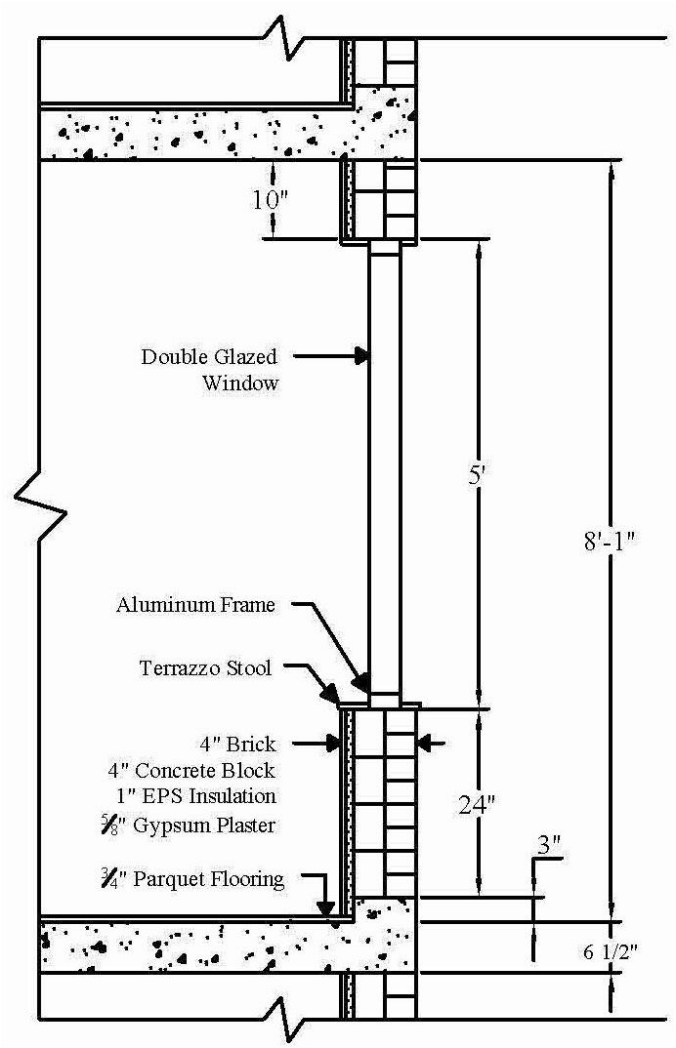

Figure 2-9: Window Wall Section

Figure 2-9 illustrates the Archetype window wall section. It has a 1.53m (5') double-glazed window with an aluminum frame. The window header is 254mm (10") of opaque wall. The interior window sill has a terrazzo stool. There is 610mm (2') of wall below the punched window.

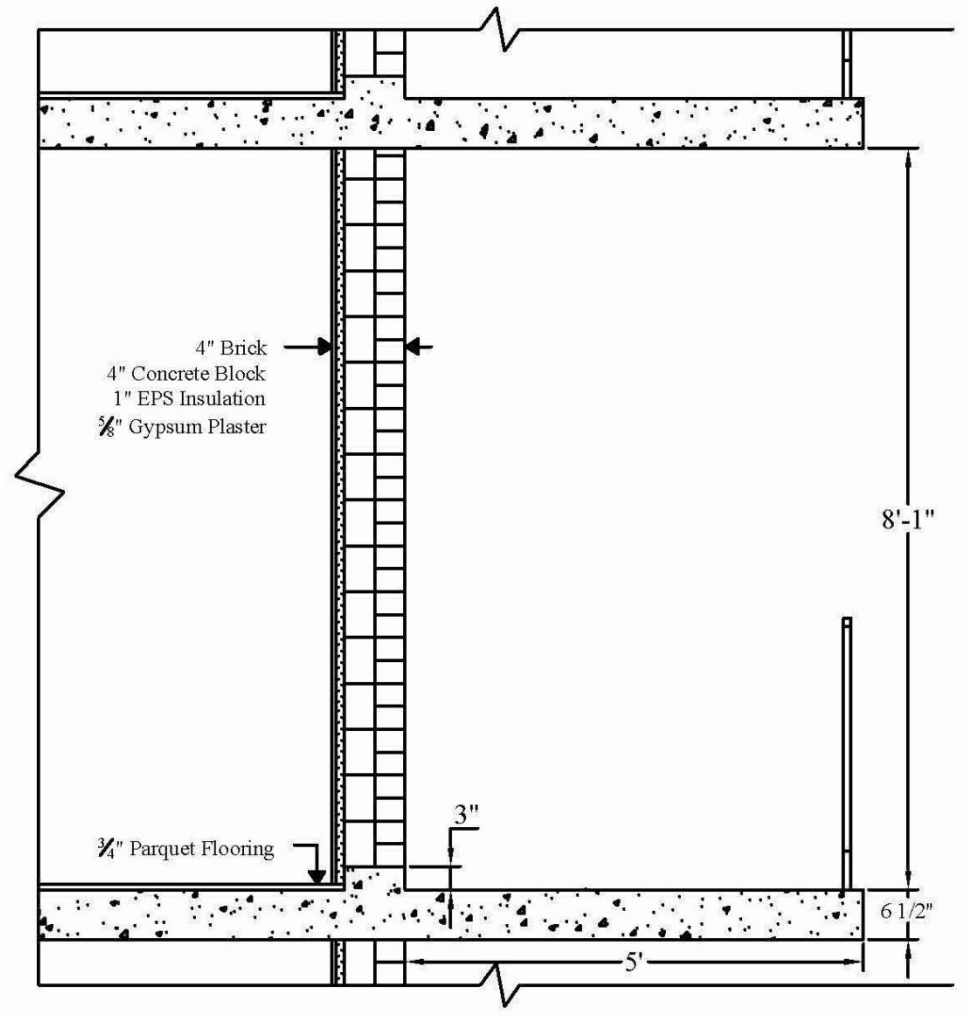

Figure 2-10: Balcony Wall Section

Figure 2-10 illustrates the Archetype balcony wall section. The depths of the balconies vary from approximately 1.12m (3'-8") to over 1.83m (6') with 1.53m (5') being the most common. The protruding concrete slabs are usually tapered on top to drain rainwater away from the enclosure and tapered on the bottom since a thick section is not structurally required towards the end of the slab.

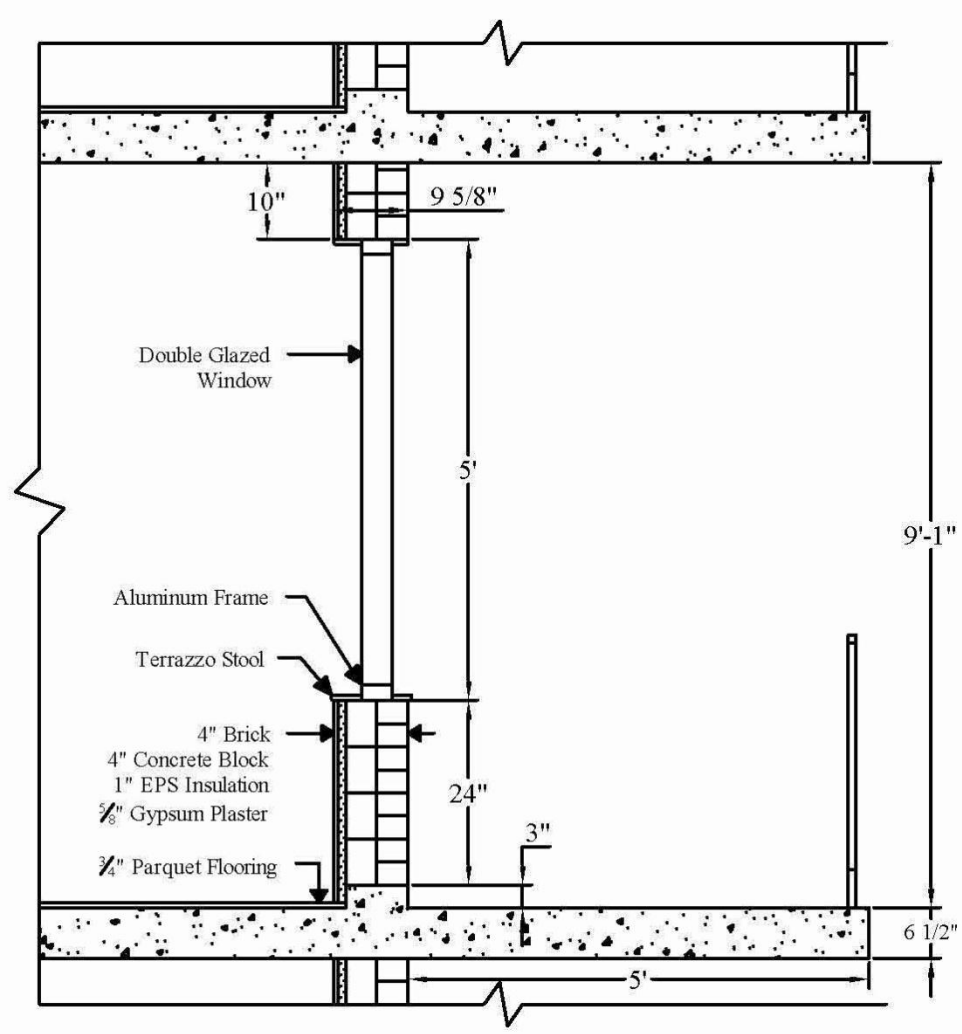

Figure 2-11: Balcony Window Wall Section

Figure 2-11 illustrates the Archetype balcony window wall section. It has the same characteristics as the punched window wall section with the addition of the 1.53m (5') cantilevered concrete balcony.

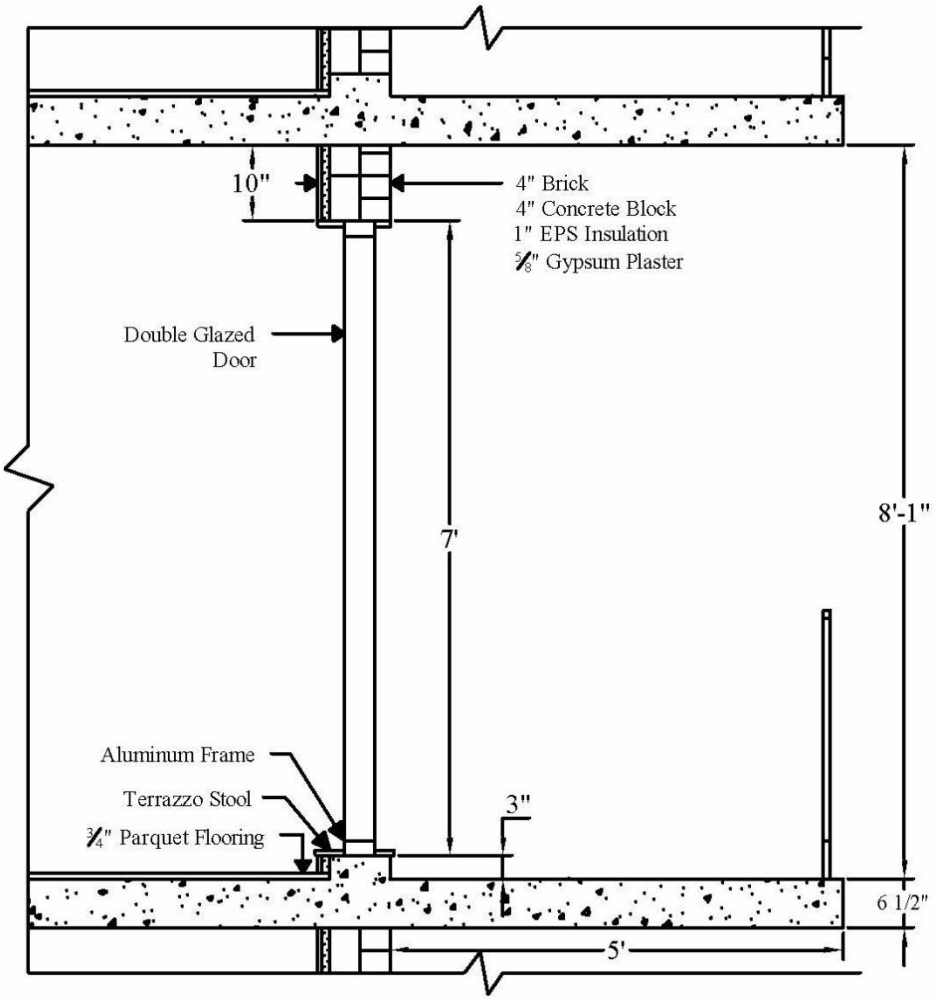

Figure 2-12: Balcony Door Section

Figure 2-12 illustrates the Archetype balcony door section. It has a 2.13m (7') double glazed, aluminum framed balcony door. Since the towers' balcony doors are either sliding or hinged, the Archetype will generalize door as one component and the difference in door width between the sliding and hinged will be accounted for in the perimeter composition. The door has the same header as the window; 254mm (10").

2.4.7 Archetype Enclosure Composition

The enclosure of the Archetype was separated into opaque wall, windows, and roof. The opaque wall and window were analyzed and combined in Section 3.1 using the five wall types previously described.

2.4.7.1 Opaque Wall Composition

The thicknesses and composition of the wall sections for all wall types are identical. They consist of 102mm (4") of brick, 102mm (4") of concrete block, 25mm (1") of extruded polystyrene (EPS) insulation, and 16mm (5/8") of gypsum plaster lath. The thicknesses and thermal conductivities for each of these materials are provided in Table 2-7.

Table 2-7: Existing Opaque Wall Material Characteristics

Material	Thickness (inches)	Thickness (mm)	Conductivity (W/mk)
Gypsum Plaster Lath	5/8	15.9	0.21
EPS Insulation	1	25.4	0.036
Marble	3/4	19.1	1.75
Concrete Block	4	101.6	0.77
Dry Brick	4	101.6	0.53
Wet Brick			0.87
Dry Reinforced Concrete	6 ½	139.7	1.77
Wet Reinforced Concrete			2.0
Parquet Flooring	3/4	19.1	0.13

The thermal conductivity values were calculated as averages from WUFI 4.1, Therm 5.2, and The Engineering Tool Box (2010). According to Suleiman (2006), soft brick's thermal conductivity increases by 65% when saturated with water. Based on this research, a wet brick thermal conductivity of 0.87 W/m·k was calculated. The window stool is typically terrazzo which is pieces of marble molded into one piece. The thermal conductivity of marble is 1.75 W/m·k (Elert G., 2010) and was used for the terrazzo.

2.4.7.2 Archetype Windows

The Archetype's existing windows are double glazed with aluminum frames with no thermal break. The glazing was assumed to be 3.2 mm thick, and the window is operable. The thermal characteristics of the window for the centre of glass, edge of glass, and frame are illustrated in Table 2-8.

Table 2-8: Existing Window Thermal Characteristics

Type	Area	U-Value (w/ films) (W/m^2k)	U-Value (w/o films) (W/m^2k)	R-Value (w/o films) ($hr \cdot ft^2 \cdot °F/btu$)
Double Glazed	Centre of Glass	3.12	6.0	0.94
	Edge of Glass	3.63	8.3	0.68
	Frame	4.62	16.3	0.35

The thermal conductivity values in Table 2-8 were taken from Chapter 15 of the ASHRAE Handbook of Fundamentals (2009). These values include film resistances based on the winter conditions with an outdoor air temperature of -18°C, with 6.7 m/s outdoor air velocity and zero solar flux. Thermal conductivities without films were calculated by subtracting an assumed interior film resistance of 8.3 W/m^2k and exterior film resistance of 29 W/m^2k. Edge of glass effects are assumed to extend over the 63.5 mm band around the perimeter of each glazing unit.

2.4.7.3 Archetype Roof Composition

The roof of the towers is commonly a built up roof illustrated in Table 3-7.

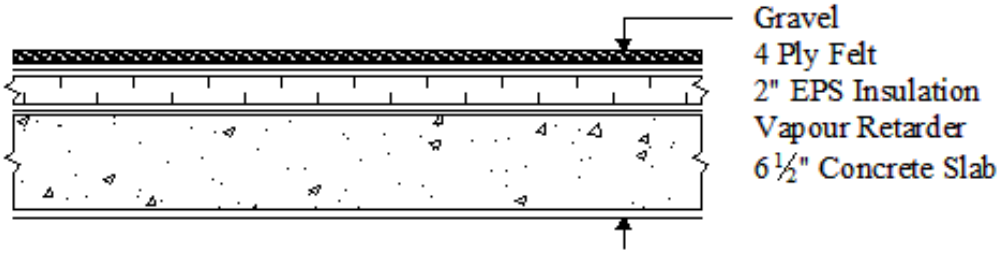

Figure 2-13: Archetype Roof Section

The built up roof is constructed from inside to outside of a 165mm (6 ½") concrete slab, vapour retarder, 51mm (2") of EPS insulation, four ply felt, and gravel. The insulation levels in the roofs vary from 38mm (1½") to 79mm (3 1/8") of insulation, 51mm (2") will be used for the Archetype.

2.4.8 Archetype's Mechanical System and Equipment

The mechanical systems and equipment for the four buildings will be examined and defined for the Archetype based on the average data. The mechanical systems and equipment include the cold water and domestic hot water, the heating, and the ventilation.

2.4.8.1 Cold Water and Domestic Hot Water Systems

All four buildings have a similar cold water (CW) and domestic hot water (DHW) system. The basic flow chart of the CW and DHW system is illustrated in Figure 2-14. The basic system flow chart does not include standby pumps, valves, pressure gauges, temperature gauges, bypass lines, and pressure relief valves.

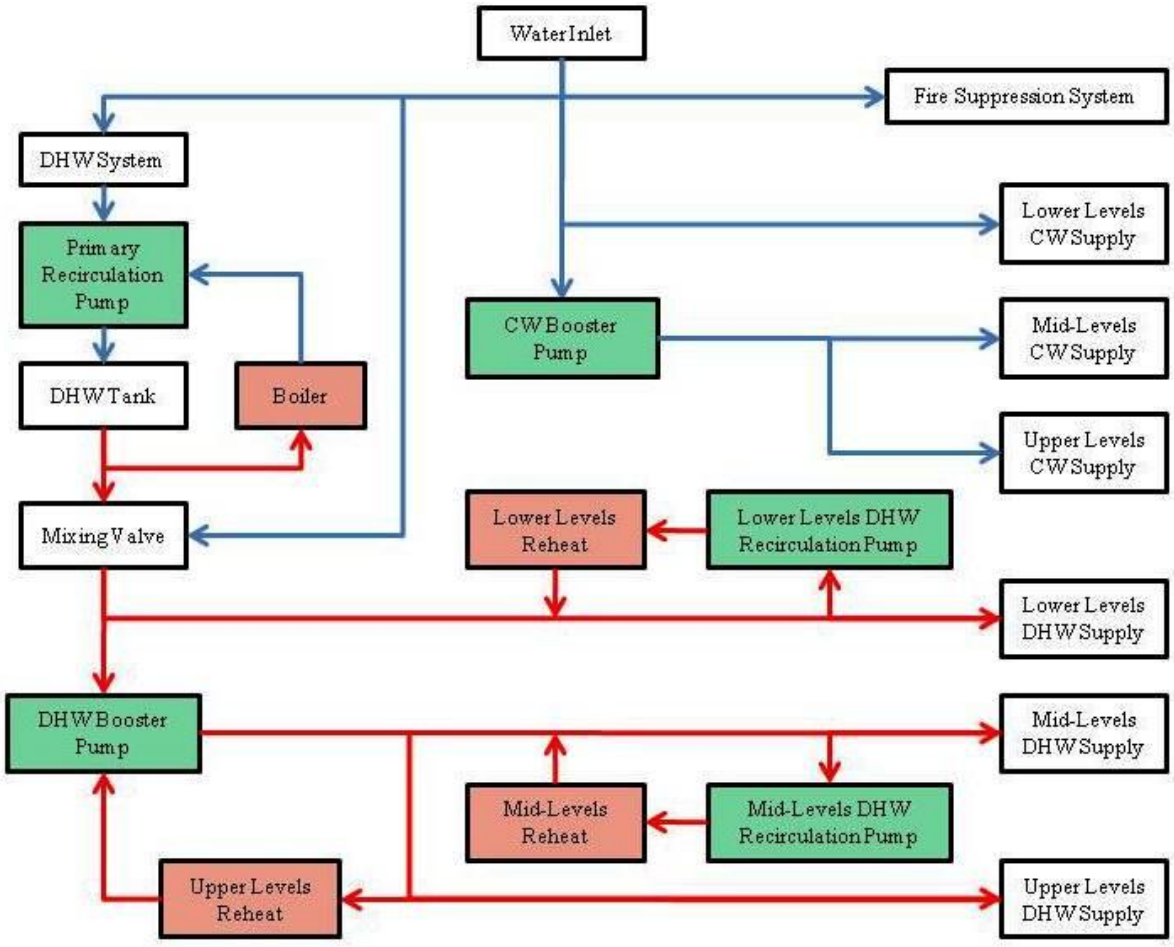

Figure 2-14: Cold Water and Domestic Hot Water Basic System Layout

Figure 2-14 illustrates that the building's water inlet separates and is used for fire suppression, cold water and hot water for the lower levels, mid-levels, and upper levels of the buildings. The cold water and hot water lines are illustrated in blue and red, respectively. The main pumps which require energy are the primary recirculation, CW booster, DHW booster, lower level DHW recirculation, and mid-level recirculation pumps, illustrated in green. The DHW heating units are the boiler and reheat for the lower levels, mid-levels, and upper levels, illustrated in red.

2.4.8.2 Domestic Hot Water Equipment

The equipment used for the DHW system is illustrated in Table 2-9.

Table 2-9: Domestic Hot Water Equipment

	Boiler		CW Booster Pump			DHW Booster Pump			Primary Recirculation Pump		
	Type	Power (kW)	Flow (l/s)	Pressure (kPa)	Power (kW)	Flow (l/s)	Pressure (kPa)	Power (kW)	Flow (l/s)	Pressure (kPa)	Power (kW)
Building 1	Electric	780	12.6	897	22.4	12.6	897	22.4	12.6	60	0.7
Building 2	Gas	373									
Building 3	Oil										
Building 4	Electric	420	14.2	897	22.4	15.8	897	29.8	9.1	135	2.2

Table 2-9 illustrates the capacity specifications for the boiler, CW booster pump, DHW booster pump, and primary recirculation pump for each building. The missing data is due to the unreadable, older drawings.

2.4.8.3 Heating System

The two common forms of heating in the towers are electric baseboard heaters and hydronic convection units. Buildings one and four use electric baseboard heaters along the perimeter. Using electric baseboard heaters is a simple heating approach and will be modeled by the Archetype as one of two heating options. The second heating option the Archetype will model is hydronic convection heating. Buildings two and three use a hydronic convection heating system. They require boilers to heat water along with pumps and piping to distribute the hot water to every convection unit. Buildings two and three use the same general hydronic flow illustrated in Figure 2-15.

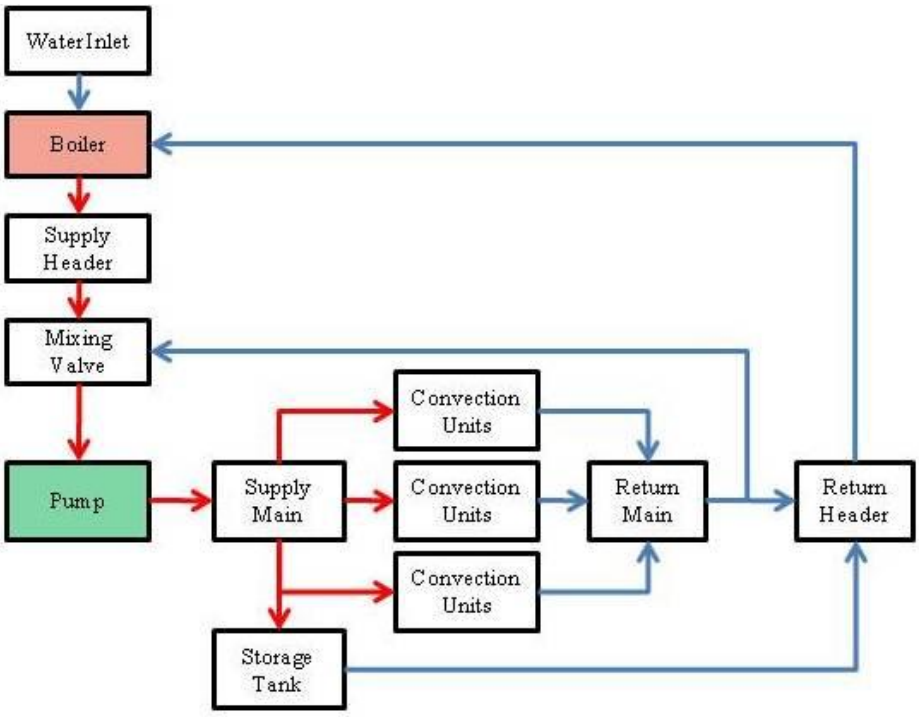

Figure 2-15: Hydronic Heating Flow Chart

Figure 2-15 illustrates the cycling of water which transfers the heat added from the boiler to the convection units. The three convection units represent the many convection units throughout the building.

2.4.8.4 Hydronic Heating Equipment

The specifications for the hydronic heating equipment in Buildings one and two are illustrated in Table 2-10.

Table 2-10: Hydronic Heating Equipment Specifications

	Boiler			Hydronic Circulation Pump		
	Type	Output (kW)	Output (W/m^2)	Flow Capacity (l/s)	Head (m)	Power (kW)
Building 2	Gas	223	14.0	37	13.7	7.5
Building 3	Gas	177	16.5	22	18.3	7.5
Average	Gas		15	30	16	7.5

Table 2-10 illustrates that gas boilers are common for hydronic heating. Buildings two and three have a smaller floor area than the Archetype so the boiler outputs were converted to intensity in W/m^2.

Using the Archetype's floor area of 21,000m^2 and the average boiler output intensity of 15W/m^2 results in a boiler output of 315kW. The Archetype will use an 11°C (20°F) temperature drop and a design heating head of 16m for calculating the hydronic pump demand.

2.4.8.5 Archetype`s Mechanical Ventilation Equipment

The ventilation exhaust and supply fans specifications for all four buildings are illustrated in Table 2-11.

Table 2-11 Mechanical Ventilation Specifications

	Exhaust Fan Capacities			Supply Fan Capacities		
	l/s	kW	W/l/s	l/s	kW	W/l/s
Building 1	7408	7.93	1.07	7434	11.19	1.51
Building 2	9912	3.48	0.35	3398	0.75	0.22
Building 3	10573	4.48	0.42	10384	11.19	1.08
Building 4	10660	12.12	1.14	8489	11.19	1.32
Average	9638	7.00	0.75	7426	8.58	1.03

Table 2-11 illustrates the exhaust fan flow capacity which is the combination of washroom and/or kitchen exhaust fans, electrical room exhaust fans, garbage room exhaust fans, and/or janitors' room exhaust fans. The supply fan flow rate capacities are approximately balanced with the exhaust fan capacities for buildings one and three. Building four's supply capacity is slightly less than the exhaust capacity and building two's supply capacity is approximately one-third the exhaust capacity. The occupants control the exhaust fans on a suite by suite basis and the building owner controls the supply. The occupant controlled exhaust fans run intermittently usually during the use of the shower, toilet, and stove. The building owners usually operate the supply fan continuously or shut it off only during the night, say from 11pm to 5am. Since the exhaust fans operate significantly less than the supply fans and the capacities are similar, theoretically the building is pressurized. This is not always the case because of the addition of stack effect, wind effect, and numerous uncontrolled air leakage paths resulting to a more complex air flow system discussed in Section 3.2.

The exhaust fans' power in Table 2-11 was summed and divided by the total exhaust capacity resulting in average energy consumption per ventilation flow rate. The same approach was used with the supply fans. The average values are 0.75 W/l/s and 1.03 W/l/s for exhaust and supply fans, respectively. The Archetype will use 0.75 W/l/s for the exhaust fans, but a slightly higher value of

1.25 W/l/s for the supply fans in order to discount the unusually low energy consumption rate of building two.

The mechanical ventilation rates for all four buildings are illustrated in the Table 2-12.

Table 2-12: Mechanical Design Ventilation Rates

	Supply Capacity l/s	Maximum Occupancy # of people	Design Ventilation Rate l/s per person	cfm per person
Building 1	7434	618	12	25
Building 2	3398	373	9	19
Building 3	10384	263	39	84
Building 4	8489	777	11	23
Average	7426	508	18	38

Table 2-12 illustrates the maximum occupancy which does not include vacancies and uses these values to calculate the design ventilation rate. The design ventilation rate is based on the supply capacity from the make-up air unit. The four buildings are designed to provide a significant range of ventilation rates with an average of 18 l/s (38 cfm) per person. The Archetype will use a slightly lower value of 15 l/s per person since building three has an unusually large rate. ASHRAE Standard 62.1 (2007) recommends an average minimum ventilation rate of 14 l/s (29 cfm) per person for the four buildings using Equation 1 and dividing it by the maximum occupancy.

$$V_{bz} = \left(R_p \times P_z\right) + (R_a \times A_z) \quad (1)$$

Where V_{bz} = Breathing zone outdoor air flow (l/s)

R_p = Outdoor airflow rate required per person (l/s per person)

P_z = Zone population (# of people)

R_a = Outdoor airflow rate required per unit area (l/s per m^2)

A_z = Zone floor area (m^2)

The breathing zone outdoor air flow is calculated for each zone; bachelor unit, one bedroom unit, two bedroom unit, three bedroom unit, and common areas and then combined. The outdoor airflow rate required per person and per unit area for a residential dwelling unit are 2.5 l/s and 0.3 l/s/m^2. Recommendations at the time were actually lower than the current ASHRAE standard and well lower than the four buildings considered. McGuinness, W. and Stein, B. (1971) recommend an apartment ventilation rate of 12 l/s (25 cfm) per person and a minimum ventilation rate of 6 l/s (13 cfm) per person based on the maximum occupancy numbers for the average of the four buildings.

2.4.9 Summary of Archetype

The characteristics of the Archetype apartment building are presented in Table 2-13 based on the analysis of the four buildings in the previous sections.

Table 2-13: Archetype Characteristic Summary

Stories	20
Width	15 m
Length	70 m
Floor to floor height	2.64 m
Units per storey	14
Two bedroom units per storey	8
One bedroom units per storey	4
Bachelor units per storey	2
Two bedroom finished floor area	70 m^2
One bedroom finished floor area	52 m^2
Bachelor finished floor area	34 m^2
Wall percentage of building perimeter	35%
Balcony window percentage of building perimeter	25%
Window wall percentage of building perimeter	15%
Balcony wall percentage of building perimeter	15%
Balcony door percentage of building perimeter	10%
Window to wall ratio	30%
Hydronic convection heating unit temperature drop	11°C
Hydronic heating pump head	16 m
Ventilation Capacity	15 l/s/person
Exhaust fan power rate	0.75 W/l/s
Supply fan power rate	1.25 W/l/s

The building dimensions presented in Table 2-13 are also illustrated in Figure 2-16 and Figure 2-17 along with other dimensions used for the Archetype to achieve the required building perimeter percentages and window to wall ratio.

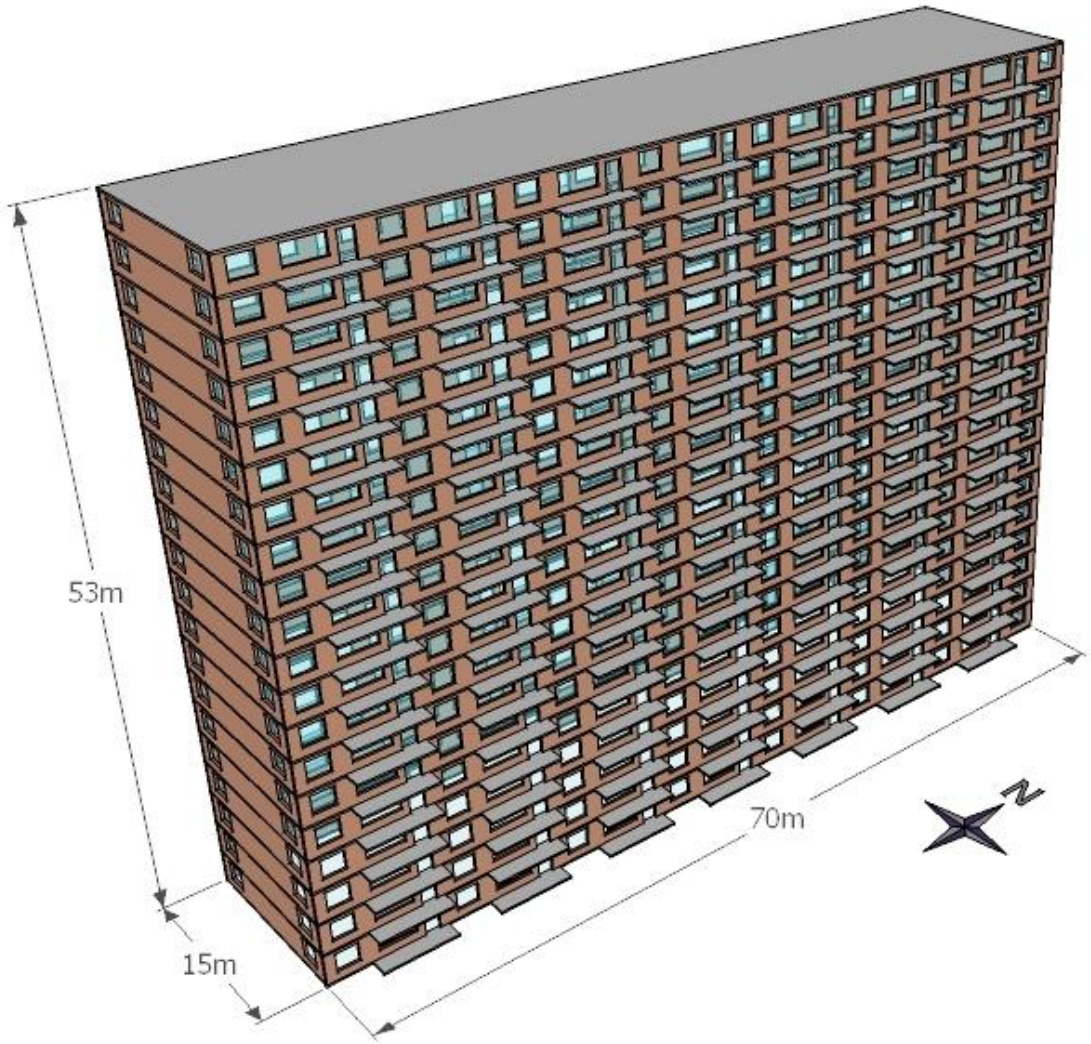

Figure 2-16: Archetype Rendering

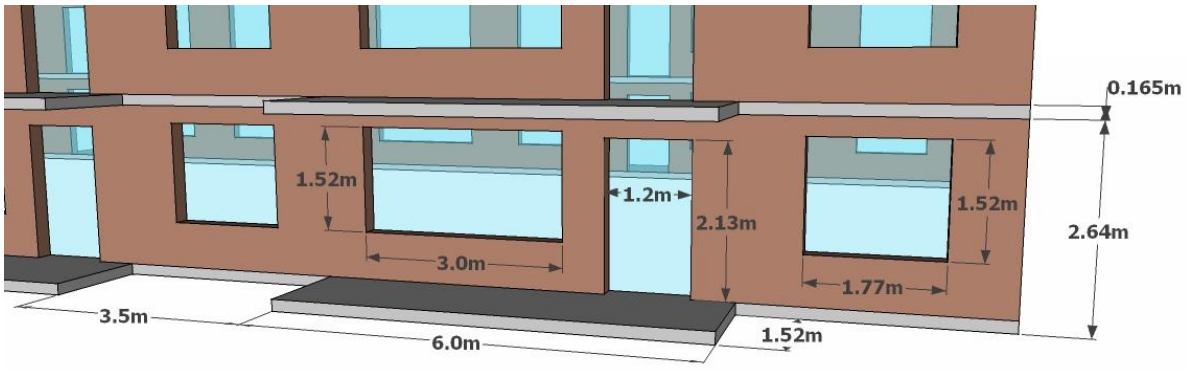

Figure 2-17: Archetype Rendering Close up

The opaque wall section used in the Archetype is illustrated in Figure 2-18.

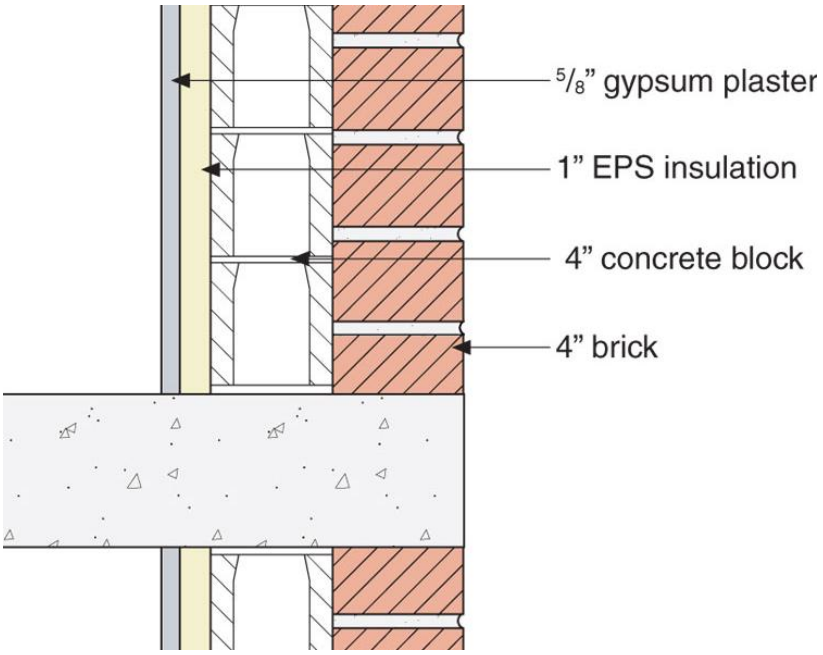

Figure 2-18: Archetype's Opaque Wall Section

The opaque wall section used in the Archetype consists from interior to exterior:

- 16mm (5/8") Gypsum Plaster
- 25mm (1") EPS Insulation
- 102mm (4") Concrete Block
- 102mm (4") Brick (without an air gap)

Chapter 3 – Hygrothermal and Air Leakage Analysis of Towers

Chapter 3 analyzes the heat, air, and moisture on or through the towers' enclosure in order to effectively simulate existing annual energy consumption of towers. Analysis was also completed to identify the existing enclosure conditions of the towers in order to have basis for applying enclosure retrofits and identifying the impacts.

The heat transfer across the enclosure was analyzed using the Archetype's wall sections in a two-dimensional, steady-state heat transfer analysis program. The heat transfer analysis was used to calculate effective thermal resistance values for the Archetype. The heat transfer analysis was also used to calculate interior surface temperatures used for determining condensation potential.

The towers' air leakage was also analyzed. Wind pressures, stack effect, and mechanical ventilation effects on the towers were discussed. The air leakage characteristics of the towers are analyzed and a value for the Archetype was estimated for modeling the Archetype's air leakage. Three infiltration models were analyzed in order to choose an appropriate model for BELA *MURB High-Rise Edition.*

3.1 Heat Transfer Analysis

A significant concern with the towers is the thermal bridging of the concrete floor slabs exposed to the exterior and the protruding concrete floor slabs used for balconies which are very common in the towers. In buildings, thermal bridging occurs where a more conductive material passes through the less conductive materials in an enclosures assembly. Thermal bridging in the towers is evident in the following infrared thermographic images illustrated in Figure 3-2, Figure 3-2, and Figure 3-3. These images were taken during the winter. They illustrate the location and degree of heat loss.

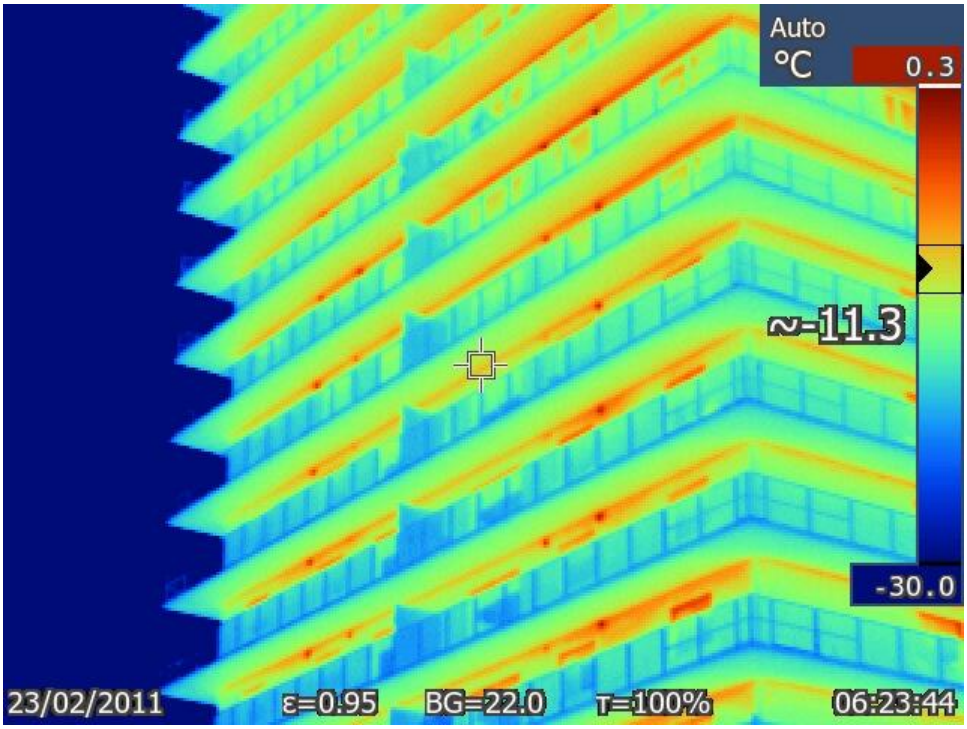

Figure 3-1: Thermographic Image of Protruding Balcony Slabs

Figure 3-1 illustrates a tower with continuous protruding balconies around its perimeter. The warmest surface is indicated in red where the underside of the concrete balcony slab meets the top of the exterior wall surface. Heat loss is significant at this location and gradually decreases towards the outer edge of the balcony.

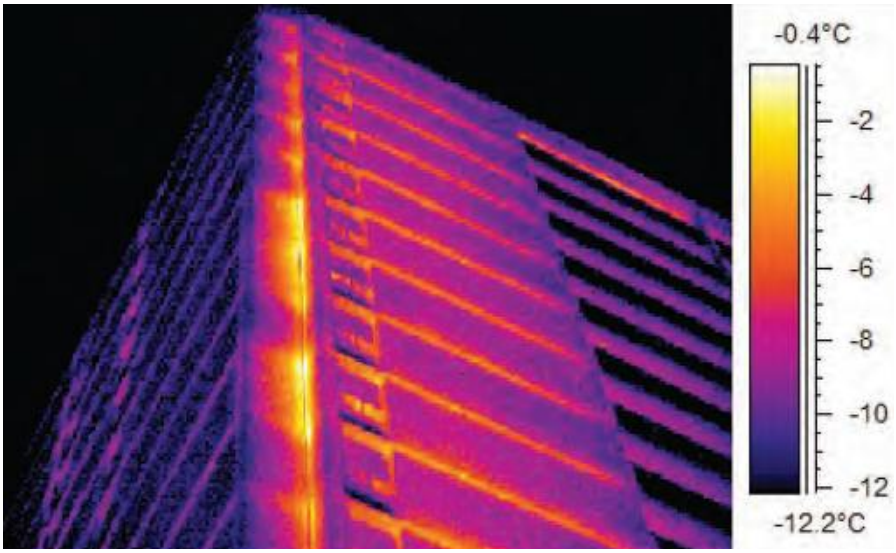

Figure 3-2: Thermographic Image of Penetrating Floor Slabs (Kesik, T. And Saleff, I., 2009)

The orange lines in Figure 3-2 run along the exterior edges of the penetrating concrete floor slabs in this 1960s apartment building. This surface colouring indicates an exterior surface temperature of approximately -4°C while the outdoor temperature is approximately -12°C. This large temperature difference demonstrates a significant amount of heat loss. Figure 3-3 also illustrates the heat loss through the enclosure.

Figure 3-3: Thermographic Image of Windows and Walls Behind Baseboard Heaters (Kesik, T. And Saleff, I., 2009)

The rectangular yellowish white colouring indicates an exterior surface temperature of approximately 7°C when the air temperature is approximately 0°C. These areas of significant heat loss are behind the baseboard heaters which are a common form of heating in these apartment towers. The heat losses out the upper edges of the window are also significant. In order to simulate the heat loss through these thermal bridges, multi-dimensional models must be used.

3.1.1 Therm 5.2

The computer program chosen for analyzing the effective thermal resistances of the opaque wall sections was Therm 5.2 created by Lawrence Berkeley National Laboratory (LBNL, 2003). This program will be used on the wall sections before and after the various enclosure retrofits. This program uses finite element analysis to perform two-dimensional steady-state heat transfer calculations which is ideal for this research application. This program also has the capacity to import basic AutoCAD drawings for easily laying out geometry. It also has the capacity to create materials and change thermal conductivity values. This is ideal because the properties of the materials in the program's library will be adjusted to match the values assumed for the existing materials in the Archetype's enclosure sections. This program also allows the user to adjust the mesh size to provide the necessary precision while minimizing computation time. This is ideal for running many simulations for the various retrofit options. The mesh control parameters in Therm can be adjusted to change the calculation tolerances and mesh size. A Maximum Percent Error Energy Norm parameter of 2% was required to provide consistent results. A Quad Tree Mesh parameter of 9 provided an adequately tight mesh illustrated in Figure 3-4.

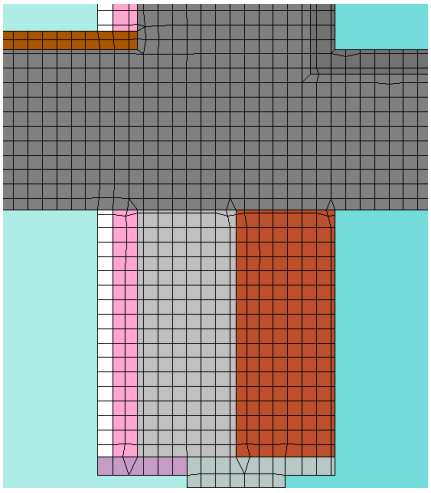

Figure 3-4: Finite Element Mesh

The finite element mesh in Therm is illustrated in Figure 3-4 for the intersection of the Archetype's wall, interior concrete floor slab and exterior concrete slab balcony.

3.1.2 Approach

The sections were drawn in AutoCAD 2007 and imported to Therm. An example of one of the AutoCAD section drawings used in Therm is illustrated in Figure 3-5.

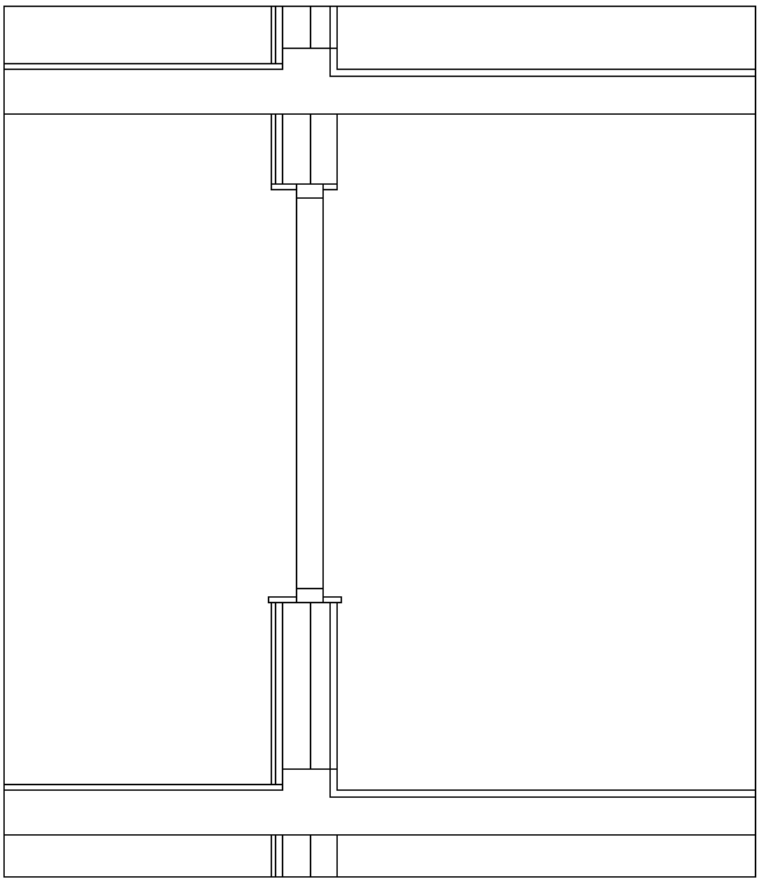

Figure 3-5: AutoCAD Enclosure Section Used in Therm

In order to effectively model the heat loss through the thermal bridging of the concrete floor slab, the enclosure sections were cut 152mm (6") from the top and bottom of the concrete slab. At this point the heat transfer through the wall sections is assumed to be in one dimension so an adiabatic surface edge was used. The exterior boundary condition was set as -20°C with a convection film coefficient of 15W/m^2k to represent a cold winter condition. An exterior radiation enclosure with a temperature of -20°C was created to represent the radiation heat transfer from the building's surroundings. The

convective interior boundary conditions were divided into three sections: ceiling, wall, and floor with convection surface temperatures set as 22°C, 21°C, and 20°C, respectively. The convection film coefficient for all interior surfaces was set to 5W/m^{2}k. An interior radiation enclosure with a temperature of 21°C was created to model the radiation heat transfer from the interior surfaces. The top and bottom of the wall section along with the inside end of the floor slab were set as an adiabatic condition. The temperature distribution through the Archetype's balcony window wall section modeled with these conditions is illustrated in Figure 3-6.

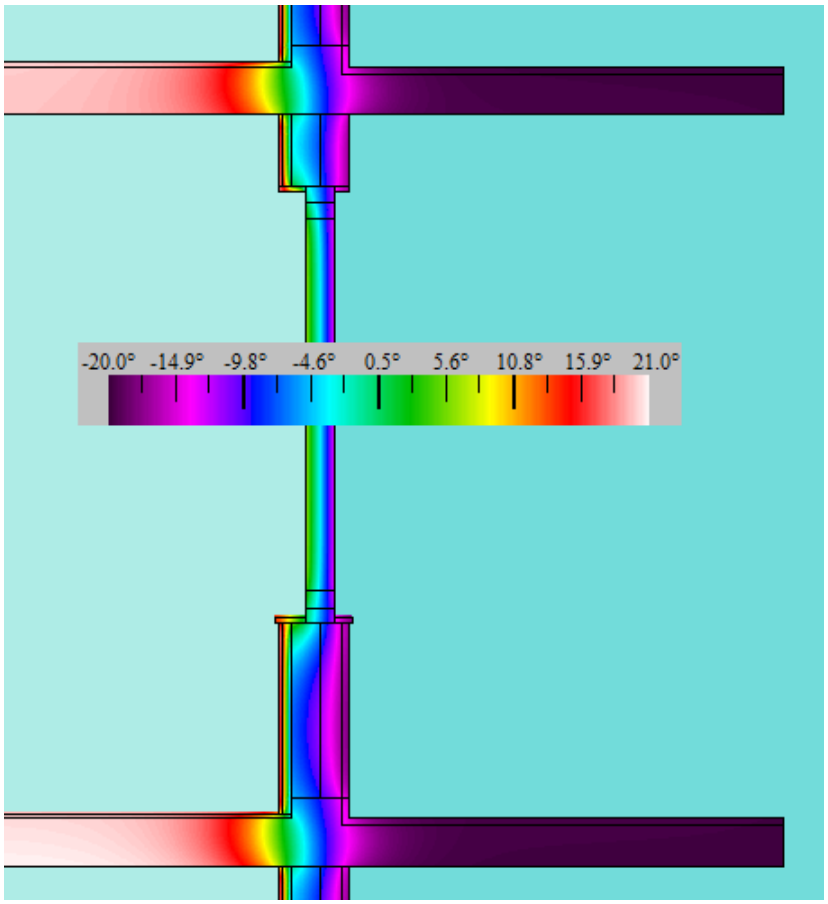

Figure 3-6: Temperature Distribution

The colour legend shown in Figure 3-6 illustrates the distribution of temperatures across the section. The various colours near the interior surface indicate the different interior surface temperatures. The coldest temperatures occur where the window frame meets the terrazzo stool (bottom edge of the window frame). A more detailed cross section was used for the window frame illustrated in Figure 3-7.

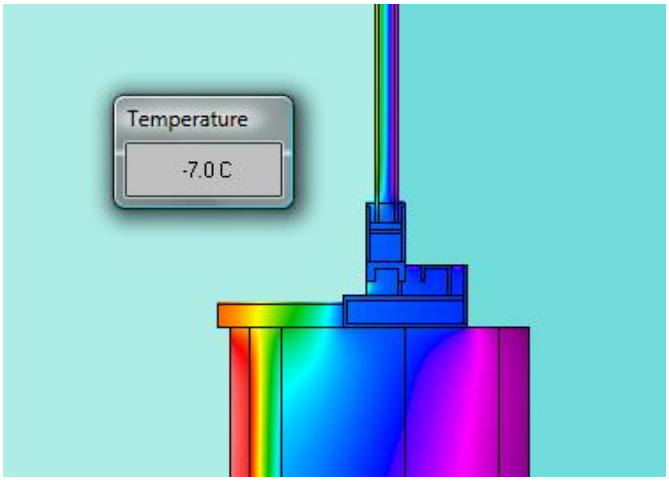

Figure 3-7: Window Frame Temperature Distribution

The temperature of -7°C in Figure 3-7 illustrates the coldest surface temperature which occurs on the interior surface of the aluminum window frame. A more detailed window frame cross section was used to more accurately determine the coldest surface temperatures which were used to determine the condensation potential discussed in Section 3.1.4.

3.1.3 Archetype Enclosure Thermal Resistances

Therm 5.2 was used to simulate the heat transfer across all parts of the above grade enclosure and calculate their thermal resistances. The enclosure sections include the opaque wall sections and windows in the five wall types described in Section 2.4.6. The heat transfer across the roof was also simulated to calculate its thermal resistance.

3.1.3.1 Archetype's Opaque Wall Thermal Resistance

An overall opaque wall thermal resistance was calculated for the Archetype using Table 3-1.

Table 3-1: Archetype Opaque Wall Thermal Resistance

Section	U-Value (W/m^2k)	R-Value (W/m^2k)	R-Value ($hr \cdot ft^2 \cdot °F/btu$)	Opaque Wall Percentage
Wall	1.01	0.99	5.63	51%
Window Wall	1.46	0.68	3.88	9%
Balcony Door	1.82	0.55	3.13	3%
Balcony Wall	1.10	0.91	5.14	22%
Balcony Window	1.35	0.74	4.22	15%
Overall	**1.12**	**0.89**	**5.08**	100%

Table 3-1 illustrates the thermal conductivities calculated for the five different wall types converted to thermal resistances. The thermal resistance of the balcony door section is the lowest because the protruding concrete floor slab accounts for the majority of the opaque wall in that section. The opaque wall percentage is the percentage of overall opaque wall area of each type. They were calculated using the Archetype's perimeter composition previously estimated in Section 2.4.5. The percentages were used to calculate an area weighted average thermal resistance of 0.89 m^2k/W (5.08 $hr \cdot ft^2 \cdot °F/btu$) for the Archetype's overall opaque wall.

3.1.3.2 Archetype's Window Thermal Resistance

An overall window thermal resistance was calculated for the Archetype similarly to the opaque wall using Table 3-2.

Table 3-2: Archetype Window Thermal Resistance

Section	U-Value (W/m^2k)	R-Value ($m^2 \cdot k/W$)	R-Value ($hr \cdot ft^2 \cdot °F/btu$)	Window Percentage
Window Wall	3.10	0.32	1.83	28%
Balcony Door	3.11	0.32	1.83	26%
Balcony Window	3.11	0.32	1.82	46%
Overall	**3.11**	**0.32**	**1.83**	100%

Table 3-2 illustrates that the windows thermal resistances are very similar for all wall sections.

The thermal conductances of the window include centre of glass, edge of glass, and frame. The window characteristics previously assumed in Section 2.4.7.2 were modeled as 102 mm (4 inch) thick layer with the same thermal properties as the window. The window percentages were used to calculate an overall area weighted average window thermal resistance of 0.32 m^2k/W (1.83 $hr \cdot ft^2 \cdot °F/btu$) for the Archetype.

3.1.3.3 Archetype's Roof Thermal Resistance

A thermal conductivity of 0.58 W/m^2·k was calculated using Therm 5.2 for the Archetype's roof section previously described in Section 2.4.7.3. This results in a thermal resistance of approximately 1.73 m^2·k/W (9.8 hr·ft^2·°F/Btu).

3.1.4 Archetype's Condensation Potential

Condensation occurs when a surface is at or below the dew point temperature of the surrounding air. This relationship is best described by the psychometric chart (Figure 3-8).

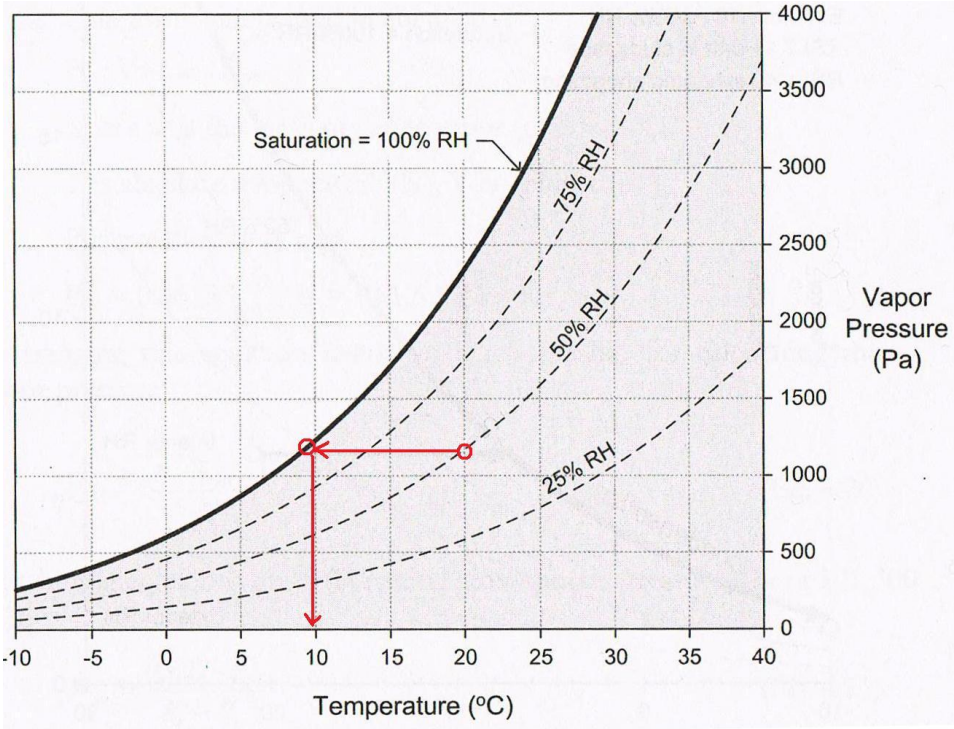

Figure 3-8: Psychrometric Chart (Straube and Burnett, 2005)

As an example, if a building component is surrounded by air that is 20°C with a relative humidity (RH) of 50%, the dew point temperature would be approximately 10°C. As shown on Figure 3-8 this is determined by first finding the intersection of the vertical line corresponding to 20°C and the curved RH line corresponding to 50%. (This shows that the interior air has a vapour pressure of approximately 1200Pa) Second, the intersection of the horizontal vapour pressure and the curved saturation line representing 100% RH represents the dew point. Third, the dew point temperature is the vertical temperature gridline crossing this point. Relating an enclosure's coldest surface

temperatures to the surrounding air's expected temperature and relative humidity provides insight into the potential for surface condensation.

The condensation potential locations that are of concern for the Archetype's wall sections are shown on the balcony window wall section illustrated in Figure 3-9.

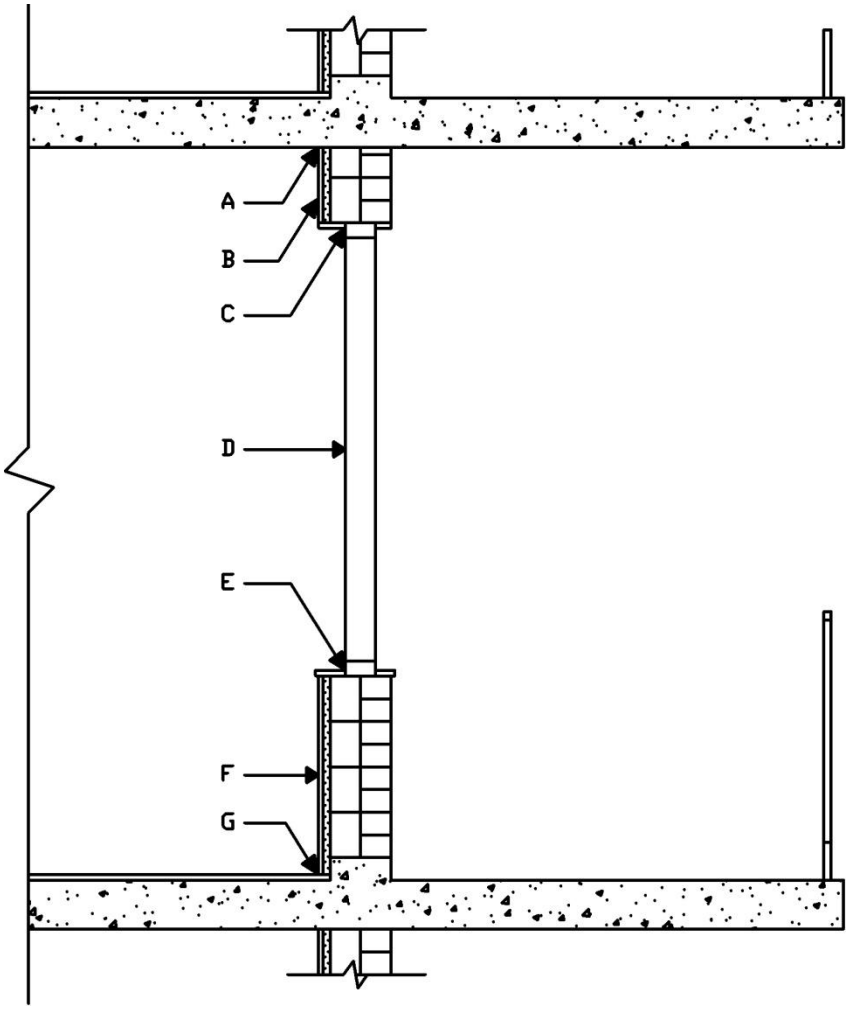

Figure 3-9: Potential Condensation Locations

Points A, C, E, and G are edge locations where the coldest temperatures are likely to be experienced. Points B, D, and F are surface locations where the average temperatures will be determined. Table 3-3 presents all these temperatures for several exterior temperature scenarios for both types of windows common in the towers.

Table 3-3: Condensation Potential

Exterior Temperature (°C)		-20		-10		-5	
Interior Temperature (°C)		21		21		21	
Temperatures (°C) and Relative Humidity (%)	A	7	40%	10	49%	12	56%
	B	17	78%	18	83%	19	88%
	C	-7	15%	0	25%	3	30%
	D	8	43%	11	53%	13	60%
	E	-7	15%	0	25%	3	30%
	F	17	78%	18	83%	19	88%
	G	12	56%	14	64%	15	69%
Lowest Temp (°C) & RH		-7	15%	0	25%	3	30%

The relative humidity (RH) values in Table 3-3 represent the dew points for the interior surface temperatures and interior air temperature. The double glazed, aluminum framed window provides little thermal resistance. The lowest interior surface temperatures occur at C and E which is where the header and sill meet the window frame. Condensation can occur around the window with an indoor RH greater than 15% during the coldest periods (-20°C) and with an indoor RH greater than 25% during the cold periods (-10°C). Since the surface temperatures are below the freezing point of water, frost will form along these surfaces. Fogging of the double glazed window should only occur at approximately 40% RH on the coldest days so long as the double glazed seal is not broken.

The buildup of moisture caused by condensation should be avoided for a number of reasons. Condensation on window glazing reduces the purpose of a window: providing natural light inside and providing occupants' views of the outside. The buildup of moisture can lead to mould growth in many locations either on the enclosures interior surface or interstitially. The buildup of moisture can corrode steel window frames or cause painted surfaces to flake off. Increasing the interior surface temperatures or reducing the interior RH will reduce condensation potential.

The towers lose a significant amount of the interior vapour due to air leakage. The large amount of air leakage keeps the RH during colder periods low which reduces condensation potential. Air leakage should be reduced for a number of reasons including uncomfortable drafts and wasted heating and cooling energy. Reducing the air leakage will increase interior RH, resulting in a greater condensation potential and increased amounts of built up moisture. If retrofitting these towers reduces air leakage, the interior surface temperatures at the condensation surfaces of concern also need to be increased so that the retrofit does not have these negative consequences. The effects of various retrofits on the interior surface temperatures will be discussed in Chapter 5.

3.2 Air Leakage

Air leakage is the uncontrolled movement of air into (infiltration) and out of (exfiltration) the enclosed space of a building. It is important to minimize air leakage to save energy and ensure comfort. However, ventilation must always be provided to ensure healthy indoor air. Modern and efficient buildings strictly control air leakage and provide guaranteed and reliable fresh air. This is described by the mantra, "Build tight, ventilate right".

The driving forces of air leakage are pressure differences caused by wind, stack effect, and mechanical ventilation systems. The amount of air leakage depends on these driving forces and the leakiness of the building enclosure. Wind has a significant impact on the towers because of their height and exposure. Stack effect (buoyancy) also has a significant impact on the towers because of its height but also because of the ability for air to move vertically within the building enclosure. This is modeled with the aid of using the thermal draft coefficient which is described in this chapter. The towers' mechanical ventilation systems do not always have as large an impact on driving air leakage but will be discussed primarily because of their impact on energy and indoor air quality. The towers' enclosure is significantly leaky which allows these driving forces to create significant amounts of air leakage.

3.2.1 Wind Pressures

When the wind hits a building its velocity slows and this is a loss of kinetic energy. The loss of kinetic energy is a gain in potential energy which is in the form of pressures. The pressure acting at any point is affected by the building's height and shape, direction of wind, and surrounding topography. In structural engineering, only the largest wind pressures around a building that occur in extreme wind events are used for structural loading and overestimating is more important than accuracy. In building energy modeling, accuracy is more important and wind pressures are required every hour (assuming an hourly energy model). These pressures are either negative or positive with magnitudes ranging from 4 to 10Pa for sheltered buildings close to the ground and from 10 to 50Pa for taller, unobstructed buildings such as the towers (Straube, 2005). Figure 3-10 illustrates general wind pressures around a tower as a result of a given wind acting at 0° and 45° to the long side of the building.

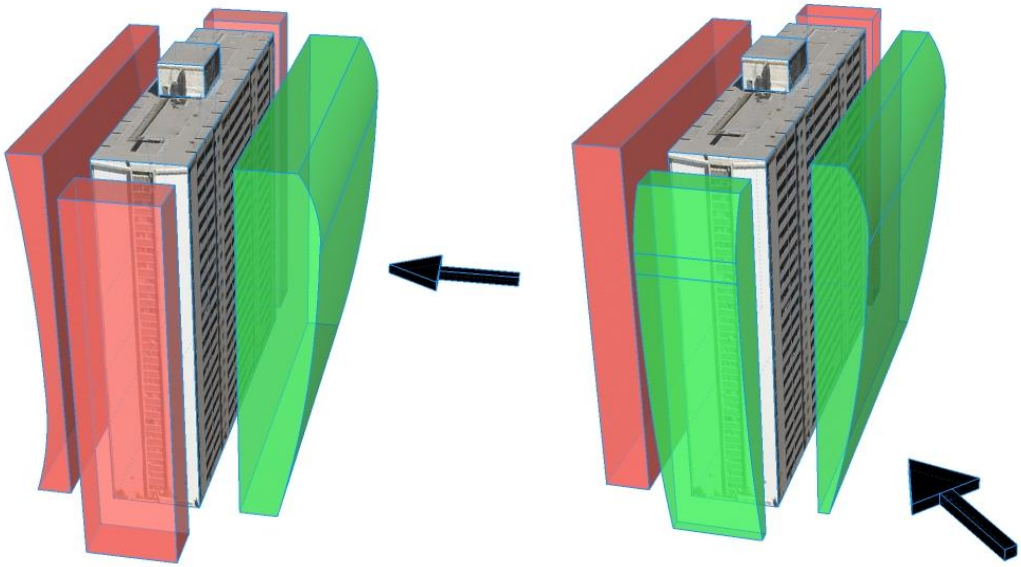

Figure 3-10: Tower Wind Pressures at 0° and 45°

Figure 3-10 illustrates positive pressures in green and negative pressures in red. The largest positive wind pressures occur at approximately four fifths of the height of the building. All other driving forces aside, positive pressures cause infiltration and negative pressures cause exfiltration. Changing wind directions and velocities can lead to fluctuating infiltrations and exfiltrations. Increasing the air tightness of the enclosure can reduce the fluctuating infiltration and exfiltration effects caused by the wind.

3.2.2 Stack Effect

Stack effect involves buoyancy which is the force associated with different fluid densities, warm air and cold air in this case of buildings. Figure 3-11 illustrates the stack effect in the general high-rise shape of the towers.

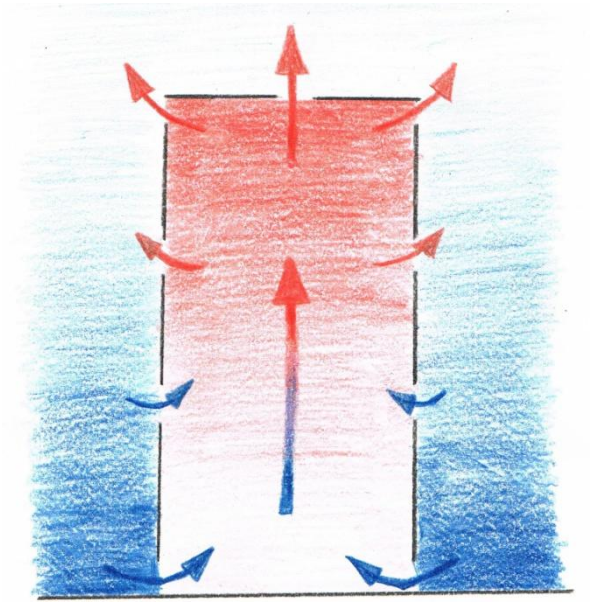

Figure 3-11: Stack Effect

Figure 3-11 represents a heated high-rise apartment tower during a cold period. The blue is cold outdoor air which is denser than the warm indoor air illustrated in red. Buoyancy forces the pocket of warm indoor air upwards while it is surrounded by the cold outdoor air. This creates positive pressures on the inside of the upper portion of the building and negative pressures on the inside of the lower portion of the building. Since the building enclosure is covered in unintentional and intentional openings, the pressures potential energy is converted into kinetic energy or air flows illustrated by arrows in Figure 3-11. The pressure and air flow effect caused by temperature differences and building height is called stack effect. This same process also occurs in chimneys which is why it is also known as chimney effect.

3.2.3 Mechanical Ventilation

A common component in the mechanical ventilation system of the high-rise apartment towers was the corridor pressurization system. This system is illustrated in Figure 3-12.

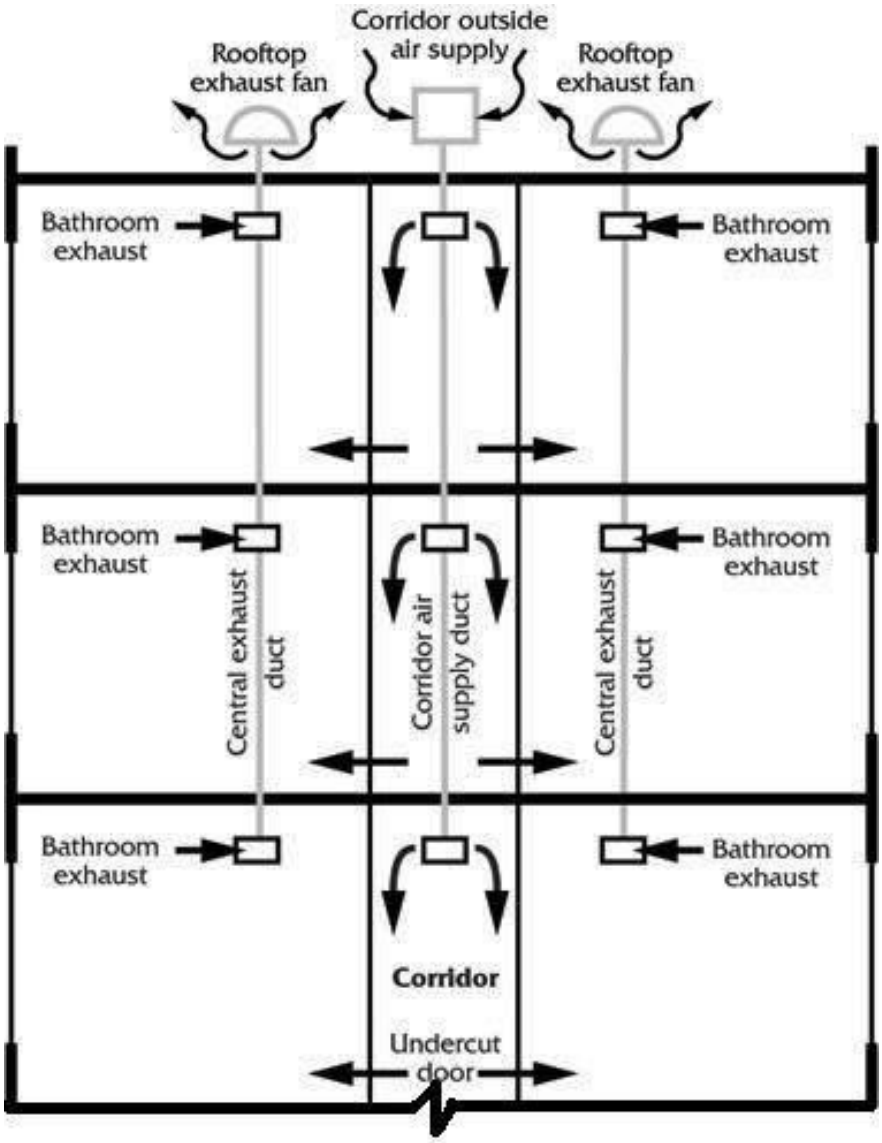

Figure 3-12: Corridor Pressurization System (Lstiburek, 2006)

Figure 3-12 illustrates the outside air entering a corridor outside air supply called a "makeup air handling unit" (MAHU) where the air is conditioned and pressurized with a fan into a vertical shaft extending from the top of the bottom storey of the building. A vent releases air into the corridors at every floor, so that every corridor is supplied or pressurized, with fresh conditioned air. This air is intended to flow under the entry doors of each unit to provide ventilation. Stale air is to be exhausted from the bathrooms. There are two common types of exhaust systems used by the towers. The first system is illustrated in Figure 3-12 where the bathroom exhaust is connected to a central vertical exhaust duct with an additional exhaust fan on the rooftop running constantly. In the second type of

exhaust system, illustrated in Figure 3-13, the bathroom exhaust is connected horizontally to the exterior with no additional fans.

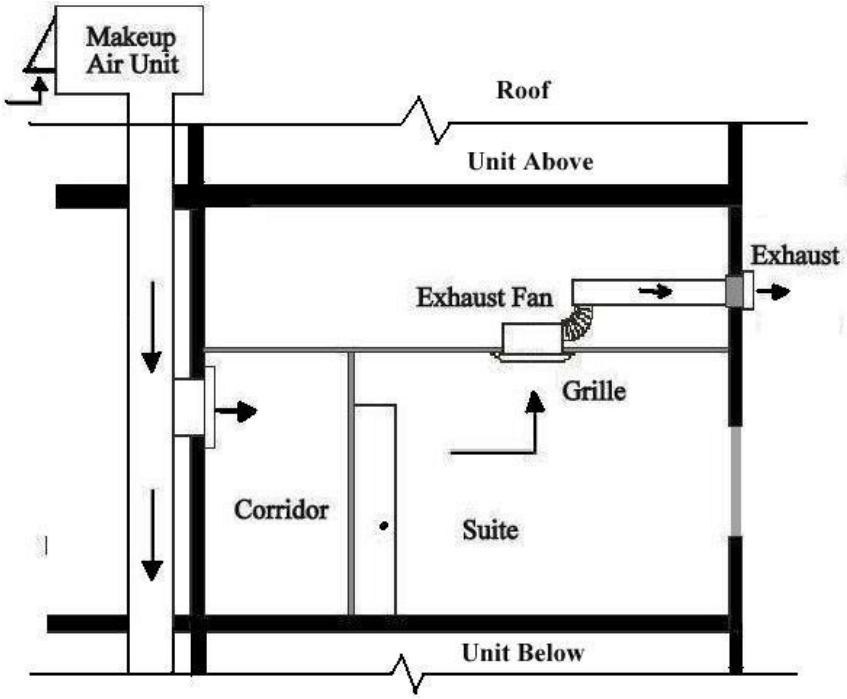

Figure 3-13: Individual Unit Exhaust System (Diamond, R.C. et al, 1999)

Figure 3-13 illustrates the apartment`s bathroom exhaust fan connected to a horizontal duct leading directly to the exterior. It has no additional fans that operate for constant ventilation. The intended ventilation design is for the pressurized central vertical supply shaft to pressurize the corridor which will pressurize the unit such that ventilation air will passively exhaust through the horizontal bathroom exhaust duct. When the bathroom fan operates, a higher rate of exhaust will occur.

The CMHC`s report *Ventilation Systems for Multi-Unit Residential Buildings: Performance Requirements and Alternative Approaches* states, "Research by CMHC and others has shown that conventional corridor air supply and bathroom-kitchen exhaust systems do not, and cannot, ventilate individual apartments." The report goes on to state that these approaches "…consume a significant amount of energy, can be noisy, consume internal floor area and serve as possible conduits for pests and smoke during fire emergencies." (CMHC, 2003)

Figure 3-14 illustrates how a corridor pressurization ventilation system actually functions.

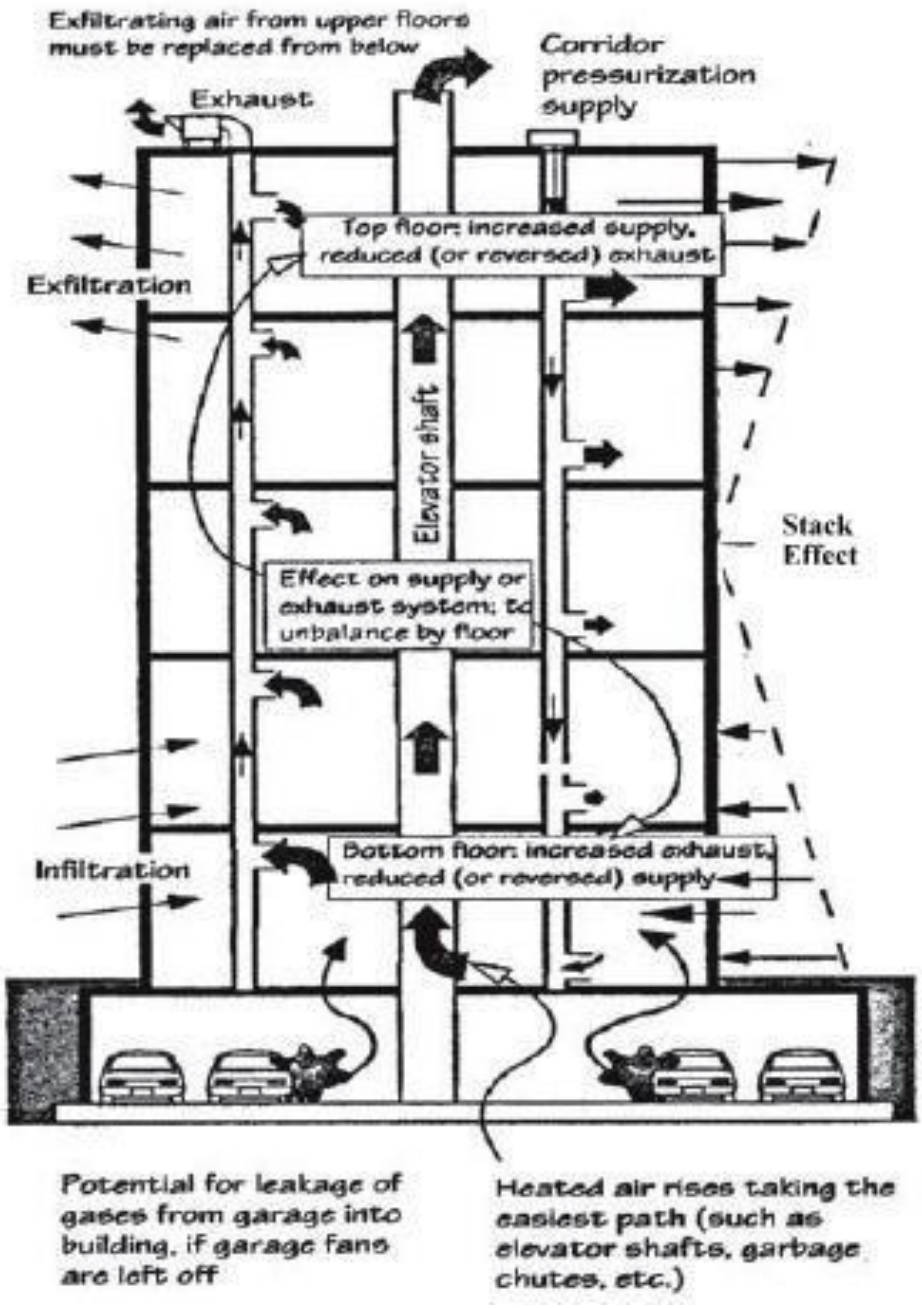

Figure 3-14: Actual Air Flows in Ventilation System (CMHC, 2007)

Figure 3-14 illustrates the influence stack effect has on the air flows in the ventilation system. Stack effect causes the lower units to be negatively pressurized and the upper units to be pressurized. The ventilation air from the roof top corridor pressurization supply often is not delivered to the lower units. Although this was the designed source of ventilation, the actual ventilation comes from air

surrounding the lower parts of the building infiltrating into the lower units. This air often passes by sources of contamination including surrounding garbage dumpsters, underground parking exhaust fumes, smoking sections, and idling delivery vehicles. The building's upper units are often overheated because of the rising warm air. The central exhaust can flow backwards in the upper levels and the individual exhaust can flow backwards in the lower levels because of the stack effect. All of this results in poor indoor air quality (IAQ).

Most of the air that is delivered to the corridors does not flow under the unit entrance doors for two reasons. The first is that many tenants often block the undercut of their entrance door to stop noise and odours entering from the corridor. The second reason is because elevator and other vertical shafts allow large amounts of air to flow more directly upward in the building due to stack effect. The openings in the corridors and pathways are often more conducive for corridor supply air to flow out the elevators and other vertical shafts than through the undercuts of unit entrance doors.

Stack effect also causes the warm air that has gathered moisture from all the units below to be forced out the exterior enclosure. The warm, moist air often reaches surface dew point temperatures within the enclosure resulting in condensation and the buildup of liquid moisture on surfaces below this dew point. This has lead to numerous deterioration problems that focus on the upper sections of the enclosure and is why many towers have been quickly and cheaply over clad along the top only. Figure 3-15 illustrates this common repair with the towers.

Figure 3-15: Common Overcladding around Upper Portion of Tower

Figure 3-15 illustrates the overcladding in red EIFS around the upper five stories of this apartment tower. The overcladding reduces heat loss, reduces air leakage, and prevents further deterioration of the masonry from exfiltration and rain penetration. More common retrofits only apply metal cladding which is about half the cost but has significantly fewer benefits.

3.2.4 Indoor Air Quality of Towers

A Canadian Mortgage Housing Corporation (1991) field investigation survey was conducted on two nearly identical 13 storey towers constructed in 1973 and 1970. The survey measured the air movement and IAQ. The majority of air leakage was through the corridor doors and enclosure walls. The major leakage paths between floors and walls were the service line penetrations. It was also found that only 21 and 25% of the supplied air exhausted through the designated bathroom exhaust vents. The IAQ tests are summarized in Table 3-4.

Table 3-4: Indoor Air Quality Investigation Summary

		Mean Temperature (°C)	Mean Relative Humidity (%)	Mean CO_2 Level (ppm)	Mean CO Level (ppm)	Particulate Concentration ($\mu g/m^3$)
1973 Tower*	Max	29.2	27	660	1.1	456
	Average	27.3	20	434	0.7	94
	Min	25.6	12	220	0.5	31
1970 Tower	Max	28.5	33	960	7.3	32,500
	Average	26.7	25	707	2.7	10,009
	Min	22.3	18	540	0.5	833
Average		27.0	22	571	1.7	5,052
Canadian Exposure Guidelines				1000	11.0	40

*Retrofitted with: exterior thermal fusible membrane, 125mm of exterior semi-rigid fibreglass insulation, aluminum siding, and new PVC windows.

The temperature, relative humidity, carbon dioxide (CO_2) level, carbon monoxide (CO) level, and particulate concentration were measured for seven units in each of the two towers and the results are illustrated in Table 3-4. The maximum, minimum, and averages were calculated for each building along with the overall averages. It was found that the winter air temperatures were set high for comfort, likely because of a low mean radiant temperature. The occupants' complained of a dry environment; the overall average relative humidity was 22%. The mean carbon dioxide levels were all below the recommended 1,000ppm. The mean carbon monoxide levels were all below the recommended 11ppm but one unit reached 7ppm. Particulate concentration is comprised of a variety of substances including cotton, wool, dyes, food particles, hairs, dead skin cells, and decomposed materials. The measured concentrations in both towers were found to exceed the Canadian Exposure Guidelines of $40\mu g/m^3$. The 1970 tower greatly exceeded this value with an average approximately 450 times the suggested maximum. Generally lower CO_2 and CO levels along with significantly lower particulate levels are likely because the 1973 tower's retrofits increased the overall air tightness. Formaldehyde concentrations were also measured for a couple of the units and were found to be well below the level deemed acceptable by workplace health officials.

3.2.5 Archetype Air Leakage Characteristics

A report by the Canadian Mortgage Housing Corporation (CMHC, 1996) summarized the measured exterior wall leakage rates for several buildings. It was found that there was a large variation, ranging from 0.68 to 10.9 $l/s_{*}m^2$ @ 50 Pa. These results included a wide range of enclosure types. An air

leakage rate of 2.15 $l/s*m^2$ @ 50 Pa was reported for a building tested using the whole building method. This building was retrofitted for energy reasons and its air tightness was reduced to 1.76 $l/s*m^2$ @ 50 Pa.

Another Canadian research report (Shaw, C.Y., Gasparetto, S., and Reardon, J.T., 1990) provided measured air leakage results for two buildings constructed in a manner similar to the Archetype. Both were concrete framed, used double wythe brick masonry for infill, and insulated on the inside. The first building is 14 stories and constructed in 1977 while the second building is 17 stories and constructed in 1982. The air leakage test was conducted by depressurizing the entire apartment with a large fan at the ground level to induce a pressure difference across the enclosure. The results of the air leakage measurements in the two high-rise apartment towers are illustrated in Table 3-5.

Table 3-5: 1977 and 1982 High-Rise Apartment Tower's Measured Air Leakage Values

	1977 Apartment Tower	1982 Apartment Tower
Ground Level Pressure Difference	74 Pa	75 Pa
Top Level Pressure Difference	32 Pa	25 Pa
Mean Pressure Difference	53 Pa	50 Pa
Air Leakage at Average Pressure Difference	2.25 $L/s*m^2$	3.39 $L/s*m^2$

Table 3-5 illustrates that the pressure differences decreased higher in the building, this is due to the vertical air flow resistance. The air leakage values of 2.25 and 3.39$L/s\cdot m^2$ correspond to the mean pressure difference of approximately 50 Pa. The overall air leakage values for varying mean pressure differences are presented in Figure 3-16 and Figure 3-17.

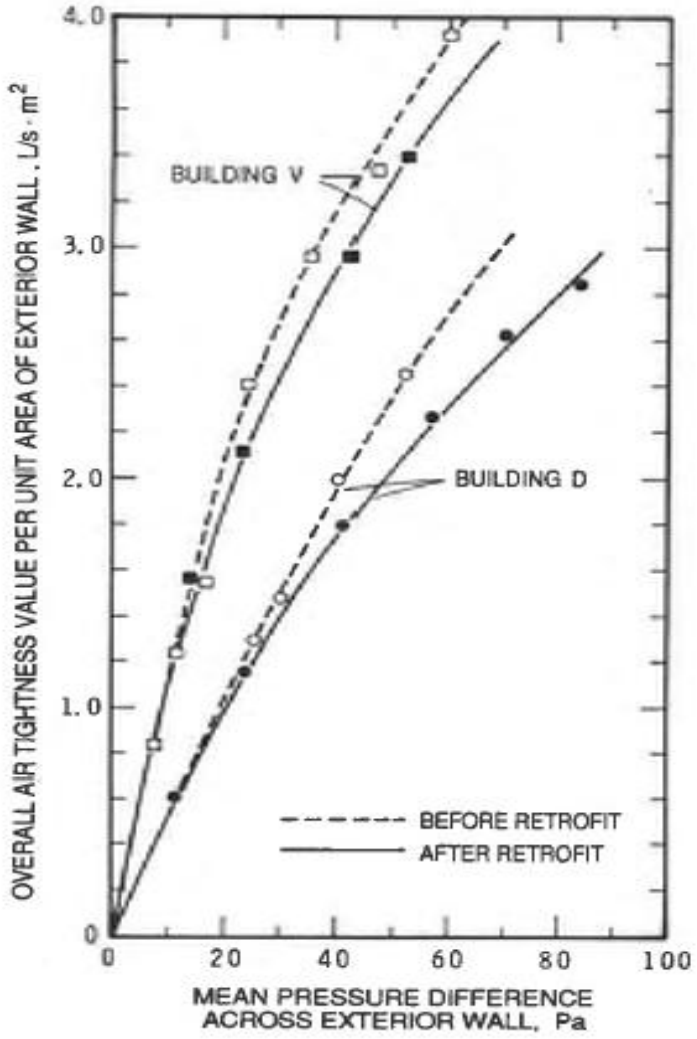

Figure 3-16: 1977 and 1982 Tower's Overall Air Leakage Characteristics

(Shaw, C.Y., Gasparetto, S., and Reardon, J.T., 1990)

Figure 3-16 illustrates the overall air leakage per unit area of exterior wall for both the 1977 14 storey building (D) and 1982 17 storey building (V) before retrofit and after an unknown retrofit.

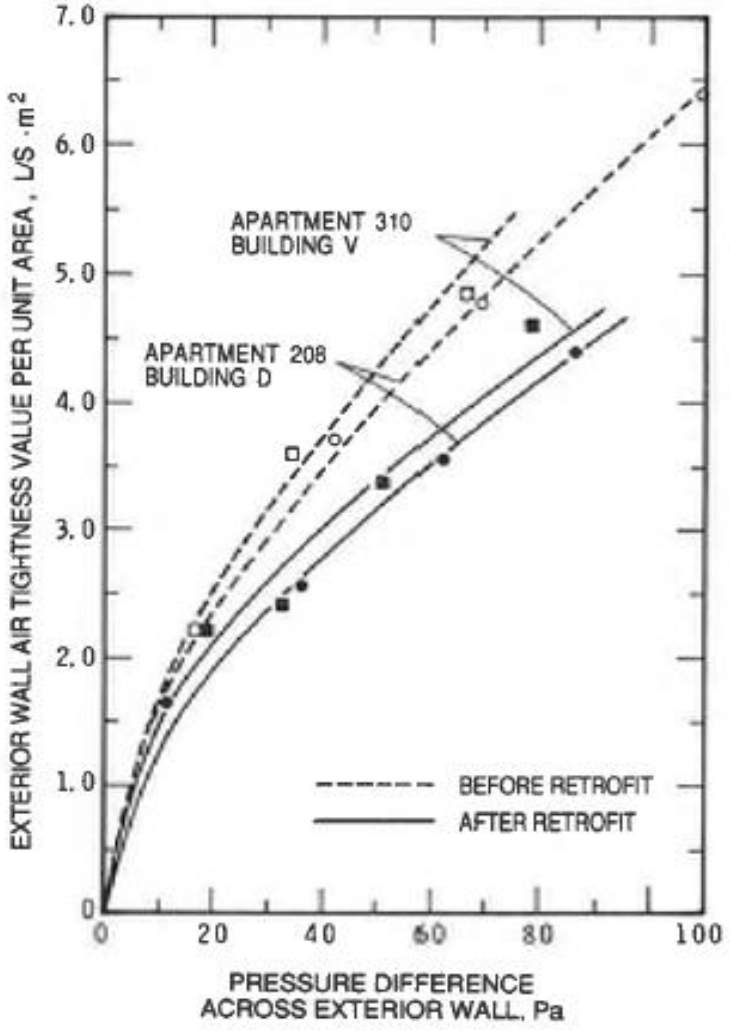

Figure 3-17: 1977 and 1982 Tower's Exterior Wall Air Leakage Characteristics

(Shaw, C.Y., Gasparetto, S., and Reardon, J.T., 1990)

Figure 3-17 illustrates the exterior wall air leakage per unit area of exterior wall for a unit in both the 14 storey (Building D) and 17 storey (Building V) buildings before retrofit and after an unknown retrofit. According to this report, the visual inspection suggests most of the air loss is through the elevator shafts.

A study conducted by the Canada Mortgage and Housing Corporation (CMHC, 1991) measured the overall air leakage in two Montreal apartment buildings. One of the buildings was a 1960 apartment building similar to the towers. It has balconies, two central fuel-fired boilers, hydronic heating to individual units, and original balcony doors and windows. The measured air leakage rates for both the 1991 and 1960 apartment buildings at three different pressure differences are illustrated in Table 3-6.

Table 3-6: 1991 and 1960 Apartment Building's Air Leakage Rates

Pressure Differential	Leakage Rate ($L/s*m^2$)	
	1991 Apartment	1960 Apartment
25 Pa	1.34	2.79
50 Pa	2.20	4.58
75 Pa	3.01	6.12

Table 3-6 illustrates that the apartment constructed in 1960 has approximately twice the air leakage as the 1991 apartment building. Since the enclosure construction of the 1960 building is similar to the towers, its air leakage values were used when setting the values for the Archetype.

Another report by the Canada Mortgage Housing Corporation (CMHC, 2001) summarized air leakage testing results based on a Normalized Leakage Rate at 75 Pa (NLR_{75}). Twelve Canadian MURBs were tested based on air leakage of the whole building with total enclosure area used to calculate a mean NLR_{75} of 3.19 $L/s*m^2$. Three Canadian MURB buildings were tested based on air leakage of the whole building with an alternate enclosure area used to calculate a mean NLR_{75} of 4.00 $L/s*m^2$. Six Canadian MURBs were tested based on individual floors or suites with their corresponding enclosure area used to calculate a mean NLR_{75} of 3.23 $L/s*m^2$. Based on these 19 MURBs, an overall air leakage mean of 3.32 $L/s*m^2$ @ 75Pa. was calculated. This report also concluded that the existing MURB stock in Canada far exceeds (30 to 40 times) the upper limit of what is now considered desirable-established as 0.10 $L/s*m^2$ (for indoor relative humidity levels between 27% and 55%) in the appendices of the 1995 National Building Code.

A study by the Lawrence Berkley National Laboratory (LBNL, 2006) summarized measured data for 25 apartment buildings from different studies. The measured air leakage rates had an average of 4.8 $l/s \cdot m^2$ and a median of 4.0 $l/s \cdot m^2$ at a 50 Pa pressure difference with a standard deviation of 1.7. They estimated that apartment buildings are one and a half to two times leakier than single-family homes.

The American Society of Heating, Refrigerating and Air-Conditioning Engineers (Bohac, D.L. et al., 2007) conducted an air leakage study on various buildings including a 1982 eleven storey brick clad concrete frame building in Minnesota, USA with a corridor supply ventilation system with characteristics similar to the towers. The total air leakage of the individual units was between 177 l/s (376cfm) to 452 l/s (958cfm) with a 50 Pa pressure difference. The median was 214 l/s (454cfm) @ 50 Pa. Approximately 25% of that air leakage is between the adjacent units. Unfortunately the area of exterior wall per individual unit was not provided. Using typical unit dimensions, an approximated

exterior wall leakage rate of 5 l/s∗m^2 @ 50 Pa. was calculated which is in the same order of magnitude as the previous reports.

Based on the limited overall air leakage test data for post-war apartment towers Figure 3-18 was created to determine an appropriate estimate for the Archetype.

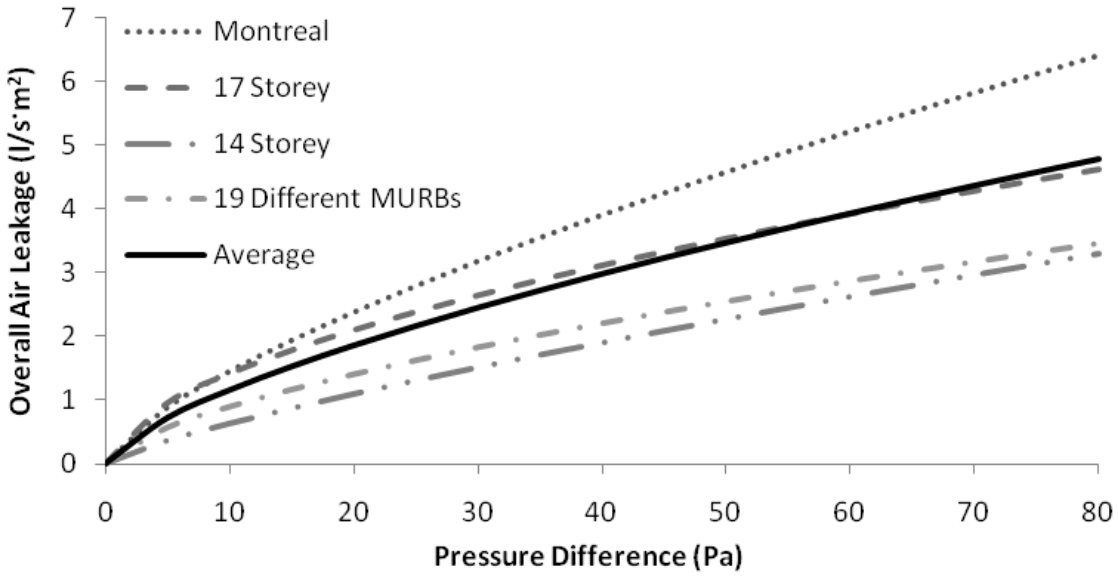

Figure 3-18: Overall Air Leakage Values for Post-War Apartment Buildings

Figure 3-18 was calculated based on data from the four most representative buildings using Equation 2.

$$Q = C \cdot \Delta P^n \quad (2)$$

Where Q is the overall air leakage in l/s∗m^2, C is the flow coefficient, ΔP is the pressure difference across the enclosure, and n is the pressure exponent.

'Montreal' illustrated on Figure 3-18 represents the 1960 apartment building which was classified as a high-rise. '17 Storey' and '14 Storey' represent the 1982 and 1977 apartment buildings, respectively. '19 Different MURBs' represents the average of the various high-rise apartment buildings that the CMHC had overall air leakage test data. The average was calculated based on the average flow coefficient and average pressure exponent and illustrated in Figure 3-18 as a solid line.

The flow rates per unit area of enclosure wall (l/s·m^2) for the Montreal, 17 Storey, and 14 Storey were collected from the data for 25 Pa, 50 Pa, and 75 Pa pressure differences. The flow coefficients and pressure exponents were calculated for all three buildings. The 19 Different MURBs only had data for

an average flow rate at a 75 Pa pressure difference, so the flow coefficient was calculated assuming a pressure exponent of 0.65 which is a common value used for air leakage in buildings. An average flow coefficient of 0.241 $l/s \cdot m^2$ and an average pressure exponent of 0.682 were calculated for the average building. This results in a leakage rate of 4.6 $l/s \cdot m^2$ at 75 Pa which will be used for the Archetype. Using the average pressure exponent of 0.682, the range of air leakage rates would be from 2.9 $l/s \cdot m^2$ to 6.1 $l/s \cdot m^2$ at 75 Pa.

The lack of measured air leakage data for older high-rise apartments is evident. However, based on this limited data, the estimated air leakage parameters can provide for a reasonable estimate of infiltrating air, heating/cooling loads, and whole building energy use.

3.2.6 Air Leakage Models

Since the towers experience a lot of air leakage because of their air leakage characteristics and the significant pressure differences across the enclosure due to stack effect and wind, it is important that the model used to estimate infiltration flow rates accounts for these factors accurately. The air leakage models considered for the towers accounted for stack effect and wind in some form. A comparison of the models was completed to determine which model was best suited for the towers.

Three models were compared for modeling air leakage in the Archetype. The first is AIM-2 by Iain Walker of Lawrence Berkeley National Laboratory (LBL) and David Wilson of the University of Alberta (1998). The second is the LBL model developed in 1980 which was explained and compared to measured data by M.H. Sherman and M.P. Modera (1986). The third is C.Y. Shaw and G.T. Tamura's model for tall buildings (1977). The models will be referred to, respectively, as AIM-2, LBL, and Shaw and Tamura models in this thesis. The equations for these models were set up in Microsoft Excel then inputs were entered and the results analyzed and compared.

The LBL model considers the leakage of the enclosure to act like a perfect orifice since its only input for air leakage is an equivalent leakage area. Shaw and Tamura and AIM-2 models are derived from a power law pressure-flow relationship which has been proven to be more accurate than an orifice flow assumption (Walker, I.S. and Wilson, D.J., 1998). This relationship was given in Equation 2.

All three models separate natural infiltration into the two driving forces, wind and stack effect, and then combine them uniquely. The pressure-flow relationships are calculated for both wind and stack effect with corresponding wind and stack factors. These factors account for each model's various

considerations. The formulation of each models infiltration rates for both wind and stack effect are described below.

3.2.6.1 Modeling Wind Effect

The air flow rates across the enclosure due to wind depend on the angle and velocity of the approaching wind. It causes various pressure differences around the enclosure; negative pressure differences pull air from inside to outside the building and positive pressure differences cause the reverse. All three models are derived from Equation 3 to convert wind velocity to pressure differences.

$$\Delta P_w = \frac{\rho \cdot V^2}{2} \tag{3}$$

Where ΔP_w is the pressure difference due to wind effects, ρ is air density, and V is wind velocity.

3.2.6.2 Modeling Stack Effect

The infiltration rates across the enclosure due to stack depend on the difference of inside temperature to outside temperature, gravity, air density, and building height. AIM-2 and LBL models use Equation 4 which is based on buoyancy to estimate the pressure differences.

$$\Delta P_s = \rho g h \left(\frac{\Delta T}{T_{in}}\right) \tag{4}$$

Where ΔPs is the pressure difference due to stack effects, ρ is air density, g is gravity, h is building height, ΔT is the temperature difference between inside and outside, and Tin is the temperature inside. Shaw and Tamura's model uses the same equation except the gravity term is replaced by $0.52/T_o$, where T_o is the outside temperature.

3.2.6.3 Infiltration Model Comparison

Each of the three models account for a different mix of variables. Table 3-7 summarizes some the more significant factors for each model.

Table 3-7: Model Comparisons

Consideration	AIM-2	Shaw and Tamura	LBL
Building Height	Yes	Yes	Yes
Meteorological Station Height	Yes	Yes	Yes
Local and Meteorological Station Terrain	Yes	No	Yes
Flue	Yes	No	No
Thermal Draft	No	Yes	No
Fixed Neutral Pressure Plane	Yes	Yes	Yes
Wind Angle	No	Yes	No

The three models combine air flow rate due to stack and wind differently. The LBL model combines the two using a simple squared sum given by Equation 5.

$$Q = \sqrt{Q_w^2 + Q_s^2} \tag{5}$$

The AIM-2 model is similar to the LBL model except it uses a power law flow exponent relationship. It is given in Equation 6.

$$Q = \left[Q_w^{1/n} + Q_s^{1/n} - 0.33(Q_w \cdot Q_s)^{1/2n}\right]^n \tag{6}$$

Q_w and Q_s in Equations 5 and 6 represent air flow rate due to wind and stack, respectively.

The Shaw and Tamura model uses an empirical approach based on redefining the wind and stack air flow rates as a larger and a smaller flow. It is given in Equation 7.

$$Q = Q_{larger} + 0.24\left(\frac{Q_{smaller}^{3.3}}{Q_{larger}^{2.3}}\right) \tag{7}$$

Q_{larger} and $Q_{smaller}$ in Equation 7 are the respective larger and smaller values of Q_w and Q_s.

The three models were set up in Microsoft Excel and the natural infiltration was calculated for each model every hour of a representative year for the Archetype. The infiltration rates calculated were converted to air changes per hour (ACH) and the number of hours in a year for different ACH values were graphed and illustrated in Figure 3-19.

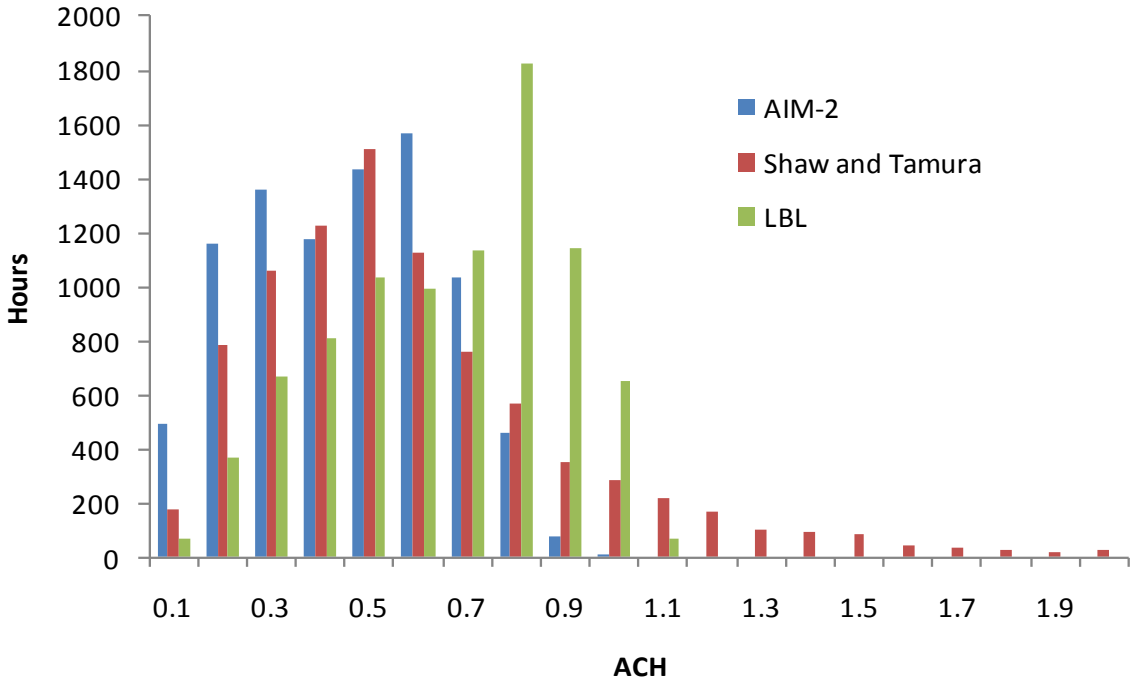

Figure 3-19: Natural ACH for Various Models over One Year

Figure 3-19 illustrates the differences in the estimated ACH for each model. The LBL model shows significantly more hours at higher rates than the other models. The Shaw and Tamura model has a wider spread with very few hours. The average and maximum ACH values were calculated for comparison between models. The results are illustrated in Table 3-8.

Table 3-8: Average and Maximum Natural ACH for Various Models

	LBL	Shaw and Tamura	AIM-2
Average ACH	0.60	0.55	0.40
Maximum ACH	1.1	4.0	0.9

The average values for all models are within 20% of 0.5 ACH under natural conditions without mechanical ventilation. The maximum values indicate that the Shaw and Tamura model estimates can have significantly larger ACH; approximately 4 times that of the other models. This is because during windier conditions, the Shaw and Tamura model estimates significantly larger infiltration rates. Since this model was the only one developed for high-rise buildings, it is the only model that captures the larger wind impacts on infiltration rates of high-rise buildings. During the hours with significant interior and exterior temperature differences, when stack effect is more prevalent, all three models estimate similar infiltration rates.

Overall, the results indicate a large variation between estimated maximum natural air leakage rates but relatively little difference between averages. The larger maximum values the Shaw and Tamura model estimated likely indicate that the AIM-2 and LBL models cannot accurately estimate the worst case natural air leakage rate for certain circumstances. As expected the ventilation provided by natural infiltration is highly variable but often sufficient in a leaky building such as the Archetype.

3.2.6.4 Effect of Open Windows on Air Leakage Models

These estimates have significant limitations that include window operation. The air leakage characteristics that these results are based on assume all windows are closed. Proskiw and Phillips (2006) studied the impact of window operation on a seventeen storey 1970s apartment in Winnipeg, Manitoba, Canada (referred to as Building #2 in their study). Their results, shown in Table 3-9 provide significant insight to the effect of window openings on natural infiltration.

Table 3-9: Impact of Window Operation on NLR_{75} for Building #2 (Proskiw, G. and Phillips, B., 2006)

Outdoor Temperature (°C)	Percent Open Window Area	Increase in NLR_{75} [2] ($l/s \cdot m^2$)
20	8.8%	39.4
4	7.0%	31.3
-25	2.3%	10.3
Typical Range of NLR_{75} Values for Canadian MURB's		1.18 to 6.37

Table 3-9 illustrates that for a summer, spring/fall, and winter day 9, 7, and 2% of windows were open, respectively. It was also noted that even during a cold winter night of -40°C some windows were seen open. The significance shown in the table is that increases in overall leakage rate were calculated as approximately 2, 6, and 8 times that of a building with closed windows, depending on season. Based on the insight from this study, the air leakage was increased for all models based on Table 3-10.

[2] NLR_{75} stands for Normalized Leakage Rate at 75 Pa of pressure difference.

Table 3-10: Seasonally Adjusted Overall Average Flow Coefficients

	From	To	Overall Air Leakage Rate at 75 Pa per m^2 of Wall	Increase by Factor	Adjusted Overall Air Leakage Rate at 75 Pa per m^2 of Wall
Winter	December	February	4.6 l/s	2	9.2 l/s
Spring	March	May	4.6 l/s	6	27.6 l/s
Summer	June	August	4.6 l/s	8	36.8 l/s
Fall	September	November	4.6 l/s	6	27.6 l/s

The results after adjusting for approximate increases in overall average flow coefficients due to window operation for each model are presented in Figure 3-20.

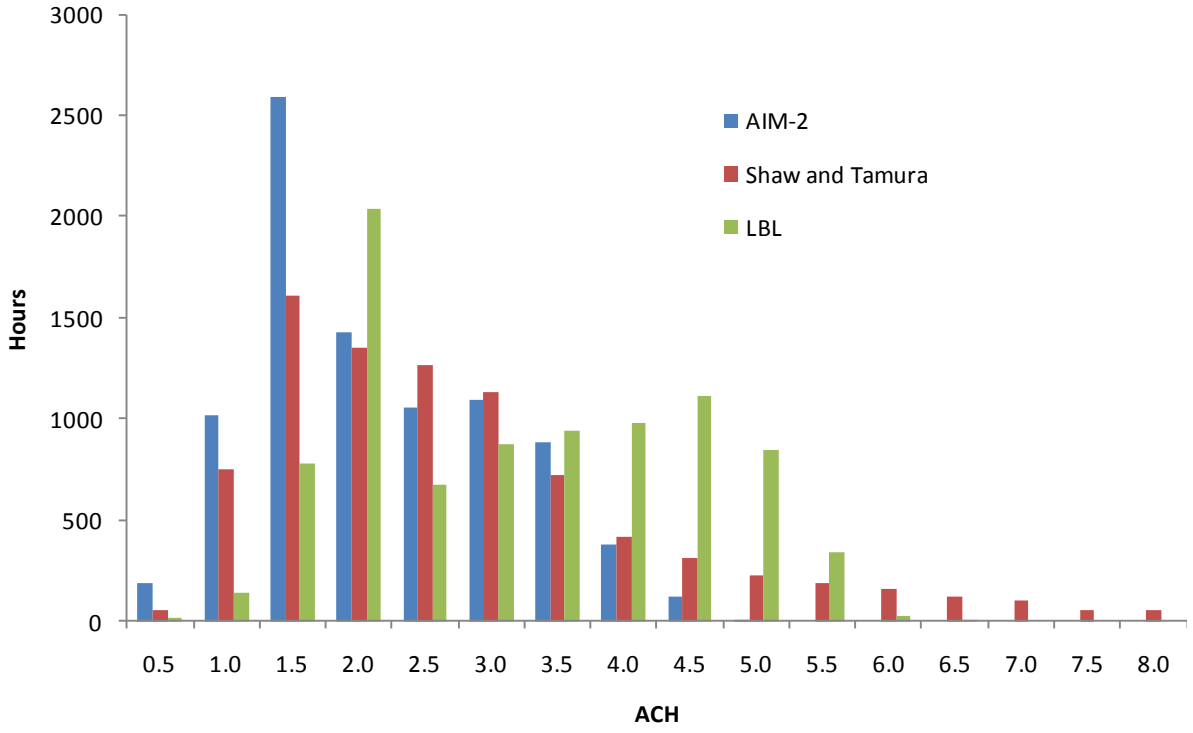

Figure 3-20: Window Adjusted Natural ACH for Various Models over One Year

Figure 3-20 illustrates that the Shaw and Tamura model continues to estimate larger ACH under certain circumstances and it also keeps a consistent shape unlike AIM-2 and LBL models. The adjusted average ACH and maximum ACH for the models are illustrated in Table 3-11.

Table 3-11: Adjusted Average and Maximum Natural ACH for Various Models

	LBL	Shaw and Tamura	AIM-2
Average ACH	3.0	2.7	1.9
Maximum ACH	6.0	24.2	4.9

Table 3-11 illustrates that the average estimated natural air leakage with window openings approximated ranges from approximately two to three ACH. This table also illustrates that the Shaw and Tamura model will estimate the worst case natural air leakage to approximately four times that of the other models. The adjusted average and maximum natural ACH values over the course of the year increased to approximately six times the original ACH when window openings were considered and estimated within the calculations.

3.3 Heat, Air, and Moisture Analysis Summary

It is evident from thermographic images illustrated in Figure 3-1 through Figure 3-3 that significant heat is lost from the enclosure of the towers and hence they have poor thermal control. Two-dimensional, steady-state heat transfer analysis was completed on all five wall sections and combined using a weighted area average. The overall enclosure thermal resistances used for the Archetype are illustrated in Table 3-12.

Table 3-12: Archetype's Enclosure Thermal Resistances

Enclosure	U-Value (W/m^2k)	R-Value (m^2k/W)	R-Value ($hr \cdot ft^2 \cdot °F/btu$)
Opaque Wall	1.12	0.89	5.08
Window	3.11	0.32	1.83
Roof	0.60	1.68	9.53

Table 3-12 illustrates the three main enclosures and their thermal resistances in metric and imperial units. These values were used in simulating the Archetype's annual energy consumption. They were the basis for which retrofits were applied and modeled. The interior surface temperatures of the balcony window wall section were modeled for various exterior temperatures and the potential for frost and condensation was analyzed. There is significant condensation potential on the towers aluminum frames. The interior surface temperatures and dewpoint RH values for the Archetype presented in Table 3-3 were used to compare with the retrofit values presented in Chapter 5.

Previous studies of the towers' air leakage characteristics were researched and a value of 4.6 $l/s/m^2$ at 75 Pa for the Archetype was assumed based on the limited findings. A range from 2.9 to 6.1 $l/s \cdot m^2$ at

75 Pa was estimated. An analysis of three air leakage models was completed and the Shaw and Tamura model was chosen for the Archetype. It was chosen because it accounts for thermal draft which is a significant factor in high-rise MURBs relative to townhouses and single-family houses. The Shaw and Tamura model also accounts for wind angle which is provided in a representative year's weather file and can decrease estimated infiltration rates by as much as one half. The results of comparing the models also indicated that the Shaw and Tamura model was the only one to capture the higher infiltration rates. It was also the only model intended for high-rise buildings. The effects of open windows on air leakage models was analyzed and found that it can affect the air leakage estimates, however considering open windows would be too complex for the model and was not accounted for BELA *MURB High-Rise Editions.*

Chapter 4– Energy Modeling High-Rise MURBs

The purpose of modeling the energy consumption of the towers is to determine the effects of retrofits on its energy use. This is achieved by simulating the energy use before and after retrofit adjustments and comparing the differences in consumption.

In order to effectively model the energy use of high-rise MURBs a significant amount of information is needed. This information includes weather data, enclosure thermal characteristics, an air leakage model, heat transfer physics, a domestic hot water use schedule, the number and size of different units, energy consumption of miscellaneous electrical loads, an understanding of the ventilation system, and heating or cooling efficiencies. Most of this information is available from previous research, architectural drawings, or separate calculations.

Annual energy consumption of high-rise MURBs varies from under 100kWh/m^2 to over 500kWh/m^2. The annual energy consumption of the towers is expected to be in the higher half of the range, estimated around 350kWh/m^2.

4.1 Building Energy and Loads Analysis (BELA)

The energy model chosen to simulate the Archetype's energy demands (loads) was Building Energy and Loads Analysis (BELA). BELA is a Microsoft Excel spreadsheet based program developed by Brittany Hanam (2010). This single zone building energy modeling program has a transparent, open architecture that allows it to be adapted to specific building modeling applications. The existing structure of the model is illustrated in Figure 4-1.

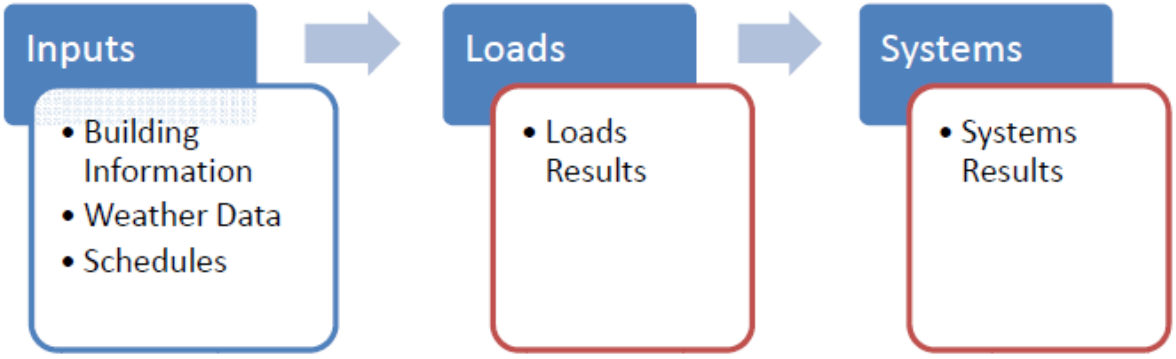

Figure 4-1: BELA Model Structure (Hanam, 2010)

Figure 4-1 illustrates that the model has three general steps: inputs, loads, and systems. In the first step, inputs, the characteristics of the building are entered along with the boundary conditions such as hourly weather for a typical meteorological year, schedules defining when equipment is operated, and occupancy occurs.

In the second step, loads, the amount of heating and cooling required is calculated based on the inputs. BELA's load calculation includes solar radiation on vertical building enclosure surfaces, but is limited to walls facing the four cardinal directions. BELA assumes the interior temperatures vary over the year in the form of a sine curve with the summer and winter indoor temperature set points being the maximum and minimum of the curve, respectively. The load calculations also include interior relative humidity, conduction through the four cardinal walls, roof, foundation, windows, and doors, solar heat gain, infiltration, and internal gains. The rate of sensible heat loss and gain along with the latent loading rate are calculated and combined for an overall rate of heating or cooling every hour. The rate of heating and cooling for ventilation is calculated every hour separately. The total heating, cooling, and net loads are calculated and presented in kilowatt hours for each month and the year.

The final step, systems, defines the heating and cooling systems and calculates the energy use. A separate sheet is used to customize each type of heating and cooling system. Each system's parameters are defined and the energy use every hour is calculated based on the hourly loads from the previous step. The system results summarizes the energy used by space distribution, heating, and cooling, ventilation distribution, heating, and cooling, lights, and plug loads for each month and the year in kilowatt hours per square metre of floor space for each system. The space conditioning systems are also compared and the total predicted building energy consumption for each system is totaled.

BELA was chosen to model the Archetype's energy and loads primarily because of its simplicity and adaptability. The Archetype is a high-rise MURB and needs to be modeled as such. In order to obtain accurate energy and load results all major factors that influence energy use in this unique set of buildings needs to be accounted in the model; this includes stack effect, wind effects, domestic hot water, and miscellaneous electrical loads for a combination of units. BELA is mostly based on fundamental physics not empirical correlations which makes it easier to add the energy influencing factors specific for high-rise MURBs. Another reason for selecting BELA was because it decouples loads from mechanical design which mirrors the normal process of design. To be useful and accurate

for assessing the impact of enclosure retrofits, an extension and customization of BELA was implemented. This is called BELA *MURB High-Rise Edition* and is described below.

4.1.1 BELA Inputs

BELA was originally used to simulate a single zone office. The following inputs are based on but not limited to the energy influencing factors required for an office. The inputs section of BELA starts with a general information section which remains the same for most building energy models. The next section is the enclosure inputs including a single air leakage parameter, enclosure thermal resistance values, solar heat gain coefficients, and solar absorptance values. The final section is the internal gains inputs which include lights, plug loads, and occupant loads. Internal gains will be significantly different for the MURB edition since MURBs internal gains are based on the number and type of unit. BELA's inputs section is illustrated in Appendix B.

4.1.2 BELA Schedules

BELA has another sheet for schedules that allows the user to enter daily and weekly schedules for lighting, plug loads, and occupancy in terms of percentage of full operation. These are illustrated in Appendix C. Office building schedules are different and more predictable than residential schedules so this section will be significantly adjusted. The weekly schedule is less significant in residential energy use and may not be used.

4.1.3 BELA Weather Data

BELA uses hourly weather data for a single year; two types of files are the Canadian Weather for Energy Calculations (CWEC) and the Typical Meteorological Year (TMY). The office-based BELA uses the CWEC file for Toronto International Airport. The information in these files includes dry bulb temperature, dew point temperature, relative humidity, atmospheric pressure, global horizontal radiation, wind direction, and wind speed. The global horizontal radiation is converted to vertical radiation for the four cardinal directions based on an Excel function developed by Nick Bronsema (2009). No changes were necessary.

4.1.4 BELA Load Calculations

Only a few changes were made in the load calculation methodology. Weather parameters were calculated based on the weather input data using psychrometric equations. The saturated vapour pressure, vapour pressure, air density, vapour density, total air density, and mass concentration of

vapour in air were all calculated and used as the boundary conditions in BELA. An average convection coefficient of 17 W/m^{2}k was used in BELA even though it was understood that in reality surface film coefficients vary with wind speed, solar radiation, and surface roughness. (Hanam, 2010) The surface temperatures and conduction heat transfer rates were calculated for each hour for the four cardinal walls, roof, foundation, doors, and windows. The thermal mass was calculated by using a weighting factor method on the conduction, solar heat gain, occupancy, equipment, and lighting. Since BELA was originally used for a lightweight office building the weighting factors are for lightweight enclosures and only consider the previous hour. Weighting factors generated by eQuest (Hanam, 2010) were used and illustrated in Table 4-1.

Table 4-1: Weighting Factors for Thermally Lighweight Construction (Hanam, 2010)

Loads	**V_0**	**V_1**	**W_1**
Conduction	0.94386	0.05354	0.0026
Solar Heat Gain	0.85703	0.14037	0.0026
People & Equipment	0.94386	0.05354	0.0026
General Lighting	0.91567	0.08173	0.0026
Task Lighting	0.91027	0.08713	0.0026

Table 4-1 illustrates weighting factors used with the current and previous hour's instantaneous gains/losses. The weighting factor relationship is presented in Equation 8 from Chapter 19 of the Handbook of Fundamentals (ASHRAE, 2009).

$$Q_\theta = V_0 q_\theta + V_1 q_{\theta-1} - W_1 Q_{\theta-1} \quad (8)$$

Where q_θ = Instantaneous heat gains or losses at hour θ

$q_{\theta-1}$ = Instantaneous heat gains or losses at hour θ-1

Q_θ = Heating or cooling load at hour θ

$Q_{\theta-1}$ = Heating or cooling load at hour θ-1

V_o, V_1, and W_1 = Weighting factors

For thermally massive buildings the weighting factor method uses different factors and considers the previous two hours. The load calculations in BELA also calculate the solar heat gain, infiltration, and internal gains for people, lighting, and plug loads. The loads are combined such that a total heating load and total cooling load is produced.

4.1.5 BELA Ventilation

Ventilation calculations in BELA for the office building used both a required rate per person and per floor area along with a minimum rate and it was assumed that the ventilation system would meet these requirements. The use of energy recovery ventilators (ERV) and heat recovery ventilators (HRV) were assumed. Parameters for a single fan with a maximum flow capacity and maximum power along with fan and motor efficiencies were used to calculate fan energy based on either an on/off or variable speed design. Significant changes were made.

4.1.6 BELA Load Results

The load results in BELA are presented in three tables: heating, cooling, and net loads, for every month and yearly total. The office-based BELA divided heating loads into conduction, infiltration, and ventilation. The cooling loads were divided into conduction, infiltration, window solar heat gain, occupants, lights, plug loads, and ventilation. BELA produces five plots illustrating January heating loads, August cooling loads, monthly load intensity, net monthly load intensity, and total annual loads. Examples of office-based BELA load result plots are presented in Appendix D.

4.1.7 BELA System Results

One advantage of BELA is its ability to be as detailed with the system design and control as desired and to create as many different system designs as required. The office-based BELA included two systems for heating and cooling: radiant panels and fan coil units, and included details such as heating and cooling design flows and head losses. Two examples of office related system inputs are presented in Appendix E. BELA's system results are presented in a table for each system comprised of monthly energy consumption in kWh/m^2 for each energy source. The energy sources used in the office based BELA are: space distribution, space heating, space cooling, ventilation distribution, ventilation heating, ventilation cooling, lights, and plug loads. Another table compares the systems by illustrating the yearly energy consumption for each energy source along a comparison of total yearly energy consumption. The system results are also presented in charts. The office based BELA uses five charts for the two systems it compares (radiant versus fan coil): radiant energy density, fan coil energy density, energy source pie charts for radiant and fan coil, and a systems comparison. These five plots are illustrated in Appendix F.

4.2 BELA *MURB High-Rise Edition*

Changes needed to be made to BELA because the original version was intended for new office buildings. High-rise MURBs energy consumption is affected in several different ways including: a significant increase in hot water use, the operation is dependent on units, different operation schedules, often a different type of enclosure, and the ventilation and space conditioning systems are usually quite different.

The BELA *MURB High-Rise Edition* has seven significant changes listed below.

1. Exterior Convection Coefficient and Thermal Mass in Section 4.2.1.
2. MURB Units and Occupancy in Section 4.2.2.
3. Domestic Hot Water in Section 4.2.3.
4. Miscellaneous Electrical Loads in Section 4.2.4.
5. Air Leakage in Section 4.2.5.
6. Ventilation in Section 4.2.6.
7. Space Conditioning in Section 4.2.7.

The first significant change is actually two smaller changes; the exterior convection coefficient and thermal mass. Since high-rise buildings are more susceptible to wind it was decided to make the convection coefficient depend on wind speed. Thermally massive construction was incorporated along with a parameter capable of adjusting the degree of thermal mass. This was chosen because BELA *MURB High-Rise Edition* was intended to be used with thermally massive Archetype-type MURBs.

The second change was incorporating the many individual apartment suites and a common area for calculating internal gains. Since MURBs are defined by the number and type of units, it was important to differentiate among them. Occupancy was also defined by the number and type of units and the daily schedule for occupancy was adjusted.

The third change was incorporating domestic hot water (DHW) which is a significant part of the total energy use in MURBs; both the latent and sensible DHW loads in each type of unit were considered. The daily schedules were also adjusted to be used with DHW calculations.

The fourth change was transforming plug loads and lighting loads into miscellaneous electrical loads and specifying each major electrical load typical in a MURB for each type of unit. The daily schedule was changed to generalize usage of all MEL. The weekly schedules were not used.

The fifth change was incorporating a more detailed analysis of infiltration by including the effects of both stack effect and wind. Stack effect and wind are significant factors in high-rise buildings.

The sixth change was creating a new ventilation model to account for the operation of bathroom exhaust fans, kitchen exhaust fans, electrical room exhaust fans, garbage room exhaust fans, make up air units, and system ventilation inefficiencies.

The seventh change was creating a basic system for calculating energy consumption of space heating, space cooling, ventilation heating, ventilation cooling, ventilation distribution, and DHW heating. Each of these seven changes is described in detail below.

A significant reference used in the development of BELA *MURB High-Rise Edition* was the *Building America House Simulation Protocol* by Robert Hendron and Cheryn Engebrecht of the National Renewable Energy Laboratory (2010). It was developed specifically to support inputs for hourly building energy simulation tools, which is the intent of BELA. This reference was useful for a number of reasons; it considers pre-retrofit specifications for simulating existing homes which is the same intention for the Archetype's energy use. This document provides simulation data for MURBs which is less common than data for single family homes. This document covers a lot of the requirements of BELA including electricity loads for each appliance on a number of bedrooms basis, both sensible and latent heat gains, DHW usage based on number of bedrooms for each end use, an equation for water main temperature, and an equation for occupancy based on number of bedrooms for multi-family dwellings. It also includes hourly schedules which are useful in BELA.

4.2.1 Exterior Convection Coefficient and Thermal Mass

The exterior convection coefficient was calculated based on an empirical correlation with wind speed presented in Equation 9 (LBL, 1982).

$$h_c = 0.0378V_w^2 + 4.687V_w + 12.49 \quad (9)$$

Where h_c = surface film coefficient, W/m^2°C

V_w = wind speed, m/s

The coefficients in Equation 9 are for brick and rough plaster (LBL, 1982). This equation is used in DOE-2 calculations. The yearly average convection coefficient based on a typical meteorological year for Toronto International airport was found to be 33 W/m^2°C.

The original BELA used the weighting factor method to account for thermal mass. This method was also used for the MURB high-rise edition except it was extended to consider thermally massive construction more typical of the Archetype style buildings. The effects of thermal mass for thermally massive construction are calculated by considering the instantaneous gains or losses from the previous two hours. The heating or cooling load is calculated using Equation 10 from Chapter 19 of the Handbook of Fundamentals (ASHRAE, 2009).

$$Q_\theta = V_0 q_\theta + V_1 q_{\theta-1} + V_2 q_{\theta-2} - W_1 Q_{\theta-1} - W_2 Q_{\theta-2} \quad (10)$$

Where q_θ = Instantaneous heat gains or losses at hour θ

$q_{\theta-1}$ = Instantaneous heat gains or losses at hour θ-1

$q_{\theta-2}$ = Instantaneous heat gains or losses at hour θ-2

Q_θ = Heating or cooling load at hour θ

$Q_{\theta-1}$ = Heating or cooling load at hour θ-1

$Q_{\theta-2}$ = Heating or cooling load at hour θ-2

V_o, V_1, V_2, W_1, and W_2 = Weighting factors from Table 4-2

Table 4-2: Weighting Factors for Thermally Massive Construction (Hanam, 2010)

Loads	V_0	V_1	V_2	W_1	W_2
Conduction	0.63352	0.76520	0.16675	1.26391	0.30311
Solar Heat Gain	0.30443	0.40111	0.10411	1.51970	0.52895
People & Equipment	0.58050	0.69305	0.14702	1.26391	0.30311
General Lighting	0.59848	0.71752	0.15371	1.26391	0.30311
Task Lighting	0.59848	0.71752	0.15371	1.26391	0.30311

Table 4-2 illustrates the empirical coefficients used to manipulate loads to account for thermal mass effects in thermally massive construction. The parameter "percentage of heavy construction" in the MURB *High-Rise Edition* allows the user to enter 100% if the building is thermally massive and 0%

if the building is lightweight. The user can also enter a percentage in between and the model will linearly interpolate between the two approaches to account for varying levels of thermal mass.

4.2.2 MURB Units and Occupancy

A new section of inputs was added to describe the number and size of units as well as the occupancy and common area per floor. A screen shot of these inputs is illustrated in Figure 4-2.

Units, Common Areas, and Occupants per Floor					
3 Bedroom Units	0		Occupants per 3 Bedroom Unit	3.05	
Finished Floor Area/Unit	89	m^2	Occupants per 2 Bedroom Unit	2.22	
2 Bedroom Units	8		Occupants per 1 Bedroom Unit	1.40	
Finished Floor Area/Unit	70	m^2	Occupants per Bachelor Unit	0.90	
1 Bedroom Units	4		Occupants	25.16	
Finished Floor Area/Unit	52	m^2			
Bachelor Units	2		Total Units	14	
Finished Floor Area/Unit	34	m^2	Total Bedrooms	20	
Occupancy Percentage	90%		Approx. FFA of Units	836	m^2
Common Area	105	m^2	Approx. FFA	941	m^2

Figure 4-2: BELA *MURB High-Rise Edition* Inputs for Units

Figure 4-2 illustrates the input cells highlighted in yellow. They include the number of bachelor, one, two, and three bedroom units per floor. The corresponding finished floor areas per unit are also entered. The input for occupancy percentage allows the user to account for vacancies and different types of occupancy. The common area input accounts for hallways, electrical rooms, stairwells, and garbage rooms. This model considers all floors to be the same; in reality the first floor and penthouse are usually different. These two floors represent a small portion of a high-rise MURB and generally are not dramatically different in terms of energy consumption than a typical floor. Therefore, this should not make a significant difference on the whole building's energy consumption; however the user of the model should be aware of this.

The highlighted blue cells in Figure 4-2 are calculated values based on the inputs. They consist of occupants per unit type. These values are calculated based on Equation 11 of Hendron and Engebrecht (2010).

$$N_{occ} = 0.92 \times N_{br} + 0.63 \quad (11)$$

Where N_{occ} = Number of occupants

N_{br} = Number of bedrooms

Equation 11 was used for modeling number of occupants in a multi-family dwelling during non-vacation periods. A bachelor unit was assumed to have one occupant. The numbers of occupants illustrated in blue have also been multiplied by the occupancy percentage. The occupants' cell presents the number of occupants per floor. The approximate finished floor area (FFA) of the units per floor and entire floor are also calculated. The wall area percentage is calculated based on the building width and length inputs to ensure that the FFA inputs make sense; a reasonable wall area percentage for a building like the Archetype is approximately 10%.

The daily occupancy schedule used for MURBs is illustrated in Figure 4-3

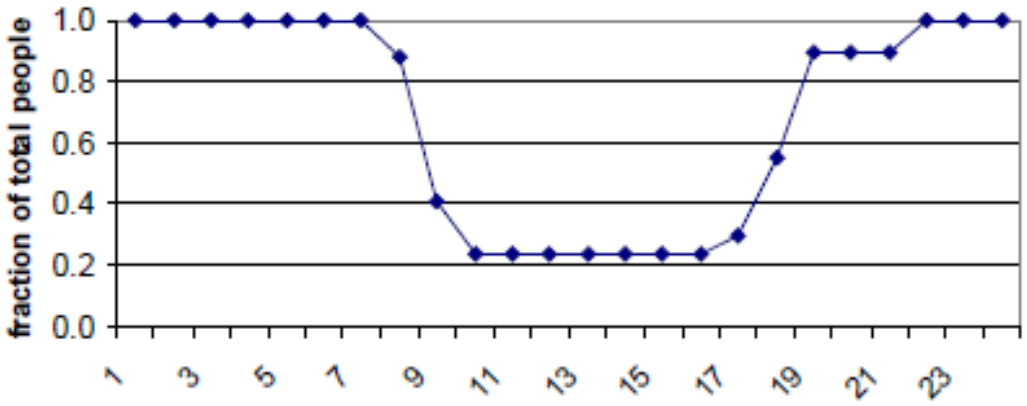

Figure 4-3: Daily Occupancy Schedule (Hendron, R. And Engebrecht, C., 2010)

Figure 4-3 illustrates that from the hours of 10pm through 7am 100% of the occupancy is modeled as being in the building. During the hours of 10am through 4pm approximately 77% of the occupancy is vacant. Overall 16.5 hours/day/person are spent in the building. These values are generalized for all day types and family types. The values from this chart have been approximated and entered into the daily occupancy schedule. The peak residential internal gains from occupancy are 64.5 watts per person of sensible heat and 48.1 watts per person of latent load (Hendron, R. and Engebrecht, C., 2010).

4.2.3 Domestic Hot Water

The DHW usages per capita for each of the primary DHW household uses are illustrated in Table 4-3.

Table 4-3: Per Capita Hot Water Use (DeOreo, W. and Mayer, P., 1999)

Category	Per Capita Hot Water Use (l/day)
Bath	15.9
Clothes Washer	14.8
Dishwasher	3.4
Faucet	32.6
Leak	4.5
Shower	23.8
Toilet	0.0
Other	0.04
Total	95.0

Table 4-3 illustrates the hot water use for seven significant household water use categories. The data is based on 10 households over 14 days with an average number of residents of 2.6. BELA *MURB High-Rise Edition* uses these values in calculating the DHW used by each type of unit based on the assumed number of occupants. The DHW calculations for each type of unit in BELA *MURB High-Rise Edition* are illustrated in Figure 4-4.

	Bachelor Unit	1 Bedroom Unit	2 Bedroom Unit	3 Bedroom Unit
Loads	l/day/unit	l/day/unit	l/day/unit	l/day/unit
Bath	15.4	23.9	38.1	52.3
Clothes Washers	14.4	22.3	35.5	48.7
Dishwashers	3.3	5.1	8.1	11.2
Faucet	31.6	49.0	78.1	107.2
Leak	4.4	6.8	10.8	14.8
Shower	23.1	35.8	57.0	78.3
Other	0.0	0.1	0.1	0.1
TOTAL	92	143	228	313

Figure 4-4: BELA *MURB High-Rise Edition* DHW Calculations

Figure 4-4 is a screen shot illustrating the total DHW consumption in l/day/unit for each type of unit. Each of the primary DHW uses is shown in its own row. The amount of DHW use was calculated on a per capita basis and thus different for each unit type. The total DHW use was calculated by

multiplying each unit total by the number of that specific unit type in the building being simulated and combining them which results in a total building DHW usage in l/day.

4.2.3.1 DHW Heating Load

The total building's DHW use in l/day illustrated in Figure 4-4 was used to calculate the energy required to heat the DHW:

$$Q_{DHW,Heat} = \frac{Q_{DHW} \times C_p \times \rho \times (T_{tank} - T_{inlet})}{3600 \times 1000 \times \eta} \quad (11)$$

Where $Q_{DHW,Heat}$ = Energy required to heat the DHW in kW/hr

Q_{DHW} = DHW flow rate in l/hr

C_p = Specific heat capacity of water in J/kg·k

ρ = Density of water in kg/l

T_{tank} = Temperature of DHW tank in k

T_{inlet} = Temperature of inlet water in k

η = DHW heating efficiency in %

This equation was developed from first principles. The 3600 value converts seconds into hours and the 1000 converts J/s into kW. 4200 J/kg·k and 0.997 kg/l were used for the specific heat capacity and density of water, respectively. The DHW tank temperature is an input; 60°C is a common temperature. The water inlet temperature was calculated using Equation 12 (Hendron, R. and Engebrecht, C., 2010).

$$T_{inlet} = (T_{avg} + \text{Offset}) + \text{Ratio} \times \left(\frac{T_{max}}{2}\right) \sin[0.986 \times (\text{Day\#} - 15 - \text{Lag}) - 90] \quad (12)$$

Where T_{inlet} = Inlet temperature to DHW tank (°F)

T_{avg} = Annual average ambient air temperature (°F)

Offset = 6°F

Ratio = $0.4+0.01(T_{avg}-44)$

T_{max} = Maximum difference between monthly average ambient temperature (°F)

(eg. $T_{avg,July} - T_{avg,January}$)

0.986 = Degrees per day (360°/365days)

Day# = Day of the year (1 to 365)

Lag = 35-1.0(T_{avg}-44)

Equation 12 estimates the inlet temperature by using the average ambient air temperature over the year, coldest month (January), and warmest month (July). The values are then distributed over the year using a sine wave. The DHW heating efficiency parameter is used to account for the overall efficiency of the DHW heating system; 70% is a common efficiency but this can be changed in BELA. The DHW flow rate in Equation 11 was calculated by multiplying the total building's DHW use in l/day by the hourly percentage of DHW in the daily schedule section.

The hourly percentage of daily DHW use was obtained from Figure 4-5 and Figure 4-6.

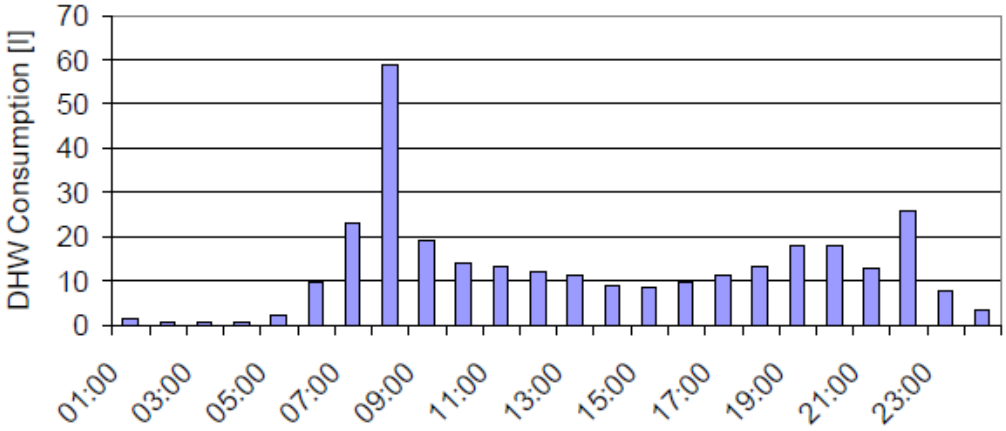

Figure 4-5: Average Daily DHW Consumption for Canada in litres per hour (Knight, I. et al., 2007)

Figure 4-5 illustrates the average DHW consumption for an average Canadian household over an average day. The hourly values were approximated from the chart and used to calculate the percentage of daily DHW consumption every hour.

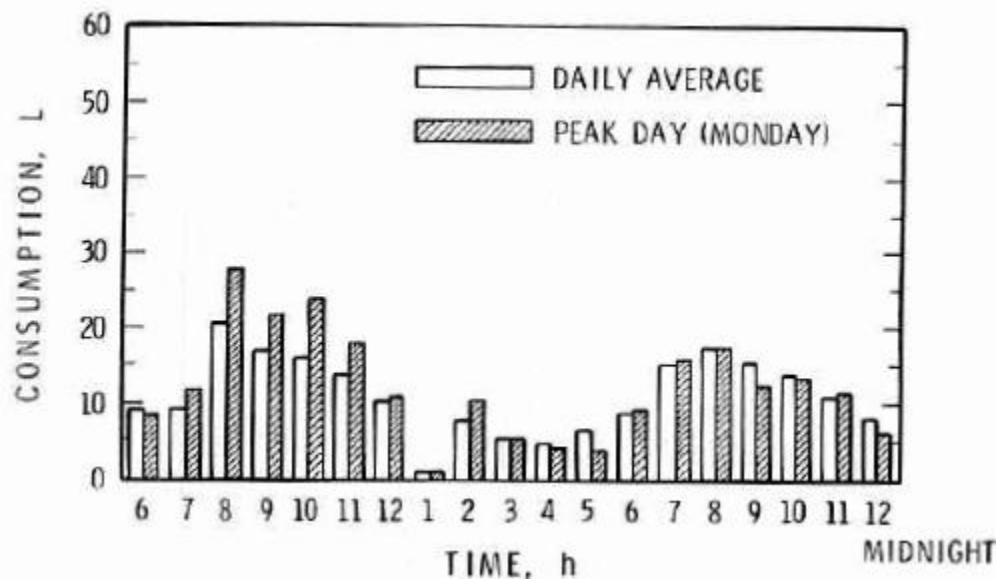

Figure 4-6: Average Hot Water Consumption "CEA Typical" Household (Barakat, S., 1984)

Figure 4-6 illustrates the average DHW consumption in a Canadian Electrical Association (CEA) typical household. The data was obtained from a survey for the CEA. The daily average hourly values were approximated from the chart and used to calculate the percentage of daily DHW consumption every hour.

The hourly percentages of daily DHW usage for the two sources are plotted along with the average of the two in Figure 4-7.

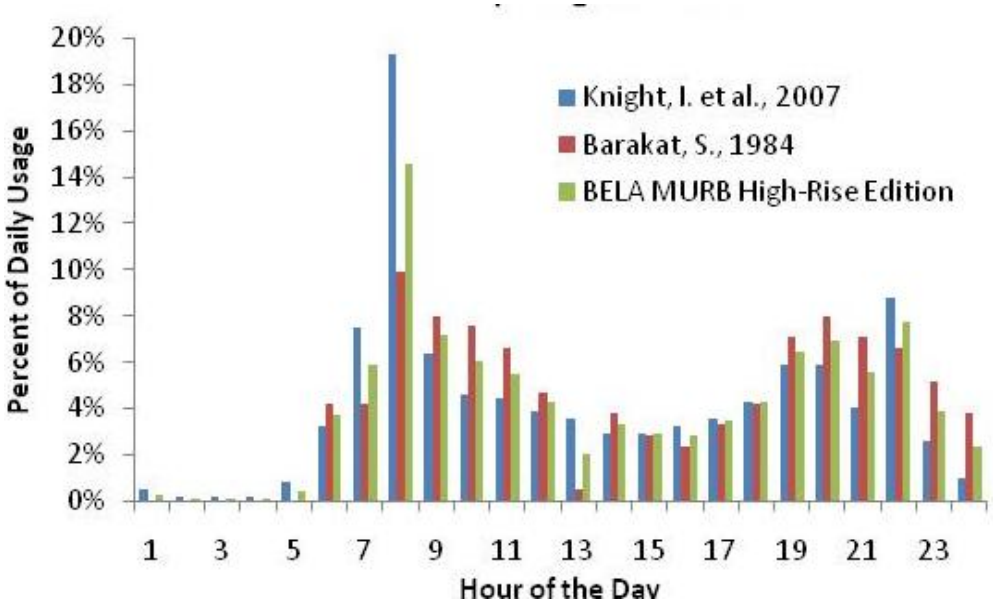

Figure 4-7: Domestic Hot Water Consumption

Figure 4-7 illustrates that the peak hourly DHW use occurs at 8am and varies between 10% and 20% for the two sources. The study by Knight (2007) indicates a more abrupt use of DHW compared to the study by Barakat (1984). In reality, the hourly DHW use can vary dramatically. The distribution of DHW use throughout the day is less important than the accurate quantity of DHW use in terms of whole building energy modeling. The average of the two sources was used for the DHW hourly schedule in BELA *MURB High-Rise Edition.*

4.2.3.2 Internal Gains from Domestic Hot Water

The use of DHW creates both a sensible and latent heat gain in buildings. The sensible heat gain from typical water consumption in a household is minimal. According to Barakat (1984), "In most cases these gains can be neglected, particularly in locations where the average cold water supply temperature is low (less than about 10°C), which is typical of most locations in Canada and northern United States." Barakat measured the water inlet temperature, hot water tank temperature, and drain temperature in an experimental household. The data was used with Equation 13 from Barakat (1984) to calculate the net heat gain from water usage. Although the experimental household was a single family home with two-stories, three bedrooms, and a full basement, the percentage of sensible heat gain data was assumed to be similar to MURBs. The services considered in the experiment were: bathroom sink, kitchen sink, shower, bath, toilet, dishwasher, and washing machine.

$$Q_f = \rho \cdot C_p \cdot [(V_h \cdot T_h + V_c \cdot T_c) - (V_h + V_c) \cdot T_d] \quad (13)$$

Where Q_f = Net heat gain

ρ = Water density

C_p = Specific heat capacity of water

V_h = Volume of DHW

T_h = Temperature of DHW in tank

V_c = Volume of cold water

T_c = Temperature of cold water

T_d = Temperature of drain water

The results Barakat obtained from the experiment using Equation 13 are summarized in Table 4-4.

Table 4-4: Net Heat Gain from Water Use (Barakat, S., 1984)

Use Profile	Hot Water Consumption, l/day	Hot Water Energy Content, MJ	Net Heat Gain, MJ	Percentage Gain, %
Spring (T_c = 3°C)				
Light	235	59.0	-1.0	-1.7%
Heavy	332	83.2	0.4	0.5%
Very Heavy	535	134.2	6.6	4.9%
CEA	196	48.8	-3.4	-6.9%
Fall (T_c = 13°C)				
Light	208	41.6	2.6	6.1%
Heavy	303	63.4	4.9	7.7%
Very Heavy	492	102.8	10.2	9.9%
CEA	196	41.0	1.2	2.9%

Table 4-4 illustrates the energy used to heat the specific volume of DHW in the experimental household for four levels of DHW users. The light, heavy, and very heavy water users use an average of approximately 220, 320, and 510 l/day of DHW, respectively. Barakat also found that heat losses also occurred because of the cold toilet water gaining heat before being flushed. Under certain circumstances the heat gains were overcome by these heat losses illustrated by negative net heat gains and negative percentage gains in Table 4-4. This table also illustrates the significance of the season;

during the colder ground temperatures the percentage gain is smaller than during the warmer ground temperatures. The average percentage gain for the light, heavy, and very heavy water users during the coldest inlet water temperature of 3°C is approximately 1%. During the warmest inlet water temperature of 13°C the average is approximately 8%. The percentage of sensible heat gain was linearly interpolated between 1% and 8% based on the cold water inlet temperature. The monthly ground temperature four metres below grade was used as the cold water inlet temperature previously assumed in Equation 12.

The latent load calculations are illustrated in Table 4-5 (Hendron, R. and Engebrecht, C., 2010).

Table 4-5: Latent Load Calculations

Latent Source	**(Hendron, R. and Engebrecht, C., 2010)**	**BELA Formula (kWh/day)**
Shower	$703 + 235 \times N_{br}$ (Btu/day)	$0.206 + 0.069 \times N_{br}$
Sinks	$140 + 47 \times N_{br}$ (Btu/day)	$0.041 + 0.014 \times N_{br}$
Dishwasher	$0.15(87.6 + 29.2 \times N_{br})$ (kWh/yr)	$0.036 + 0.012 \times N_{br}$
Electric Range	$0.30(250 + 83 \times N_{br})$ (kWh/yr)	$0.205 + 0.068 \times N_{br}$
Other	$0.16(1703 + 266 \times N_{br} + 0.454 \times FFA)$ (kWh/yr)	$0.747 + 0.117 \times N_{br} + 0.0002 \times FFA$

Table 4-5 illustrates the four major sources of DHW latent load plus an 'other' source accounting for all minor sources. The Building America House Simulation Protocols (Hendron, R. and Engebrecht, C., 2010) provides various formulas for the different latent sources. These formulas were adjusted to produce a load in kilowatt hours per day. The calculations are based on the number of bedrooms so each type of unit was calculated separately. The BELA *MURB High-Rise Edition* DHW latent load outputs are illustrated in Figure 4-8.

	Bachelor Unit	1 Bedroom Unit	2 Bedroom Unit	3 Bedroom Unit
Loads	kWh/day/unit	kWh/day/unit	kWh/day/unit	kWh/day/unit
Shower	0.21	0.28	0.34	0.41
Sinks	0.04	0.06	0.07	0.08
Dishwasher	0.04	0.05	0.06	0.07
Electric Range	0.21	0.27	0.34	0.41
Other	0.82	0.98	1.01	1.29
TOTAL	1.3	1.6	1.8	2.3

Figure 4-8: BELA *MURB High-Rise Edition* DHW Latent Load Calculations

Figure 4-8 illustrates a range of daily DHW latent loads from 1.3 to 2.3 kWh for the different unit types. The DHW schedule previously created for DHW heating load was also used to convert the total building's DHW latent load to kilowatts for every hour of the day.

4.2.4 Miscellaneous Electrical Loads

The values for the miscellaneous electrical loads from BELA *MURB High-Rise Edition* are illustrated in Figure 4-9.

	Sensible Fraction	Bachelor Unit	1 Bedroom Unit	2 Bedroom Unit	3 Bedroom Unit	Common Area per Storey
Loads		kWh/yr/unit	kWh/yr/unit	kWh/yr/unit	kWh/yr/unit	kWh/yr/storey
Refridgerators	1	558	558	558	558	0
Clothes Washers	0.8	54	54	54	54	0
Clothes Dryers	0.15	951	951	951	951	0
Dishwashers	0.6	82	82	82	82	0
Ranges	0.4	697	697	697	697	0
Lighting	1	680	1040	1400	1780	2100
Other	0.734	1869	2223	2577	2936	285
TOTAL		4891	5605	6319	7058	2385

Figure 4-9: BELA *MURB High-Rise Edition* Miscellaneous Electrical Load Calculations

Figure 4-9 illustrates the five primary appliance electrical loads in MURBs along with lighting and other sources. The sensible load fractions used to convert the MEL energy to sensible loads are also illustrated in this figure (Hendron, R. and Engebrecht, C., 2010). The latent loads from all these sources are accounted for within the DHW calculations described in Section 4.2.3.2.

4.2.4.1 Appliances

It is assumed that all four types of units have one refrigerator, clothes washer, clothes dryer, dishwasher, and range. The annual energy use of each of the five major appliances was taken from the 2008 Canadian stock of electric appliances in the *Residential Appliance Unit Energy Consumption* (NRCan, 2011).

4.2.4.2 Lighting

There is a significant difference in energy of various types of lighting technologies from incandescent to compact fluorescent. According to the *Comprehensive Energy Use Database*, (NRCan, 2011) apartment buildings in 2008 used 7.8 petajoules of energy for lighting and comprised 355 million m^2 of floor space resulting in a lighting intensity of approximately 6.1 kWh/year/m^2. According to Annex 42 of the International Energy Agency (Knight, I., 2007) the average Canadian household uses 14.4 kWh/year/m^2. Using T12 fixtures in the common areas and incandescent fixtures in the suites results in a lighting capacity of approximately 10.1 W/m^2 (Enermodal, 2005). If the common area lighting operates continuously and the units' lighting operates 5.6 hours per day according to ASHRAE 90.1 reported by Enermodal (2005), the overall lighting intensity would be approximately 27.5 kWh/year/m^2. The average of 6.1, 14.4, and 27.5 kWh/year/m^2 is 16 kWh/year/m^2 which was used for modeling the Archetype. This is an input and hence can be changed if more information is available.

4.2.4.3 Other Electrical Loads

Other electrical loads include all minor appliances including televisions, laptops, alarm clocks, and coffee makers. Since these electrical loads are more likely to stay current, they were estimated based on current data. Equation 14 was used to estimate the other loads within each of the unit types (Hendron, R. And Engebrecht, C., 2010).

$$1703 + 266 \times N_{br} + 0.454 \times FFA \quad (14)$$

Where N_{br} = Number of bedrooms

FFA = Finished floor area (ft^2)

The elevator's electrical load is also considered in other electrical loads under the common area in Figure 4-9. An elevator uses approximately 1900 kWh/year (Hendron, R. And Engebrecht, C., 2010). The elevator load was calculated by multiplying the number of elevators input by 1900 kWh/year and dividing out the number of stories to produce an electrical load in kWh/year/storey. The sensible load

from the elevator was assumed to be negligible since the location of the elevator motor usually provides little effect on the internal heat gain. This should be refined in future work as elevator usage will depend on the size of each floor as well as the number of floors.

4.2.4.4 Miscellaneous Electrical Loads Schedule

The daily schedule for the MEL was calculated based on Figure 4-10.

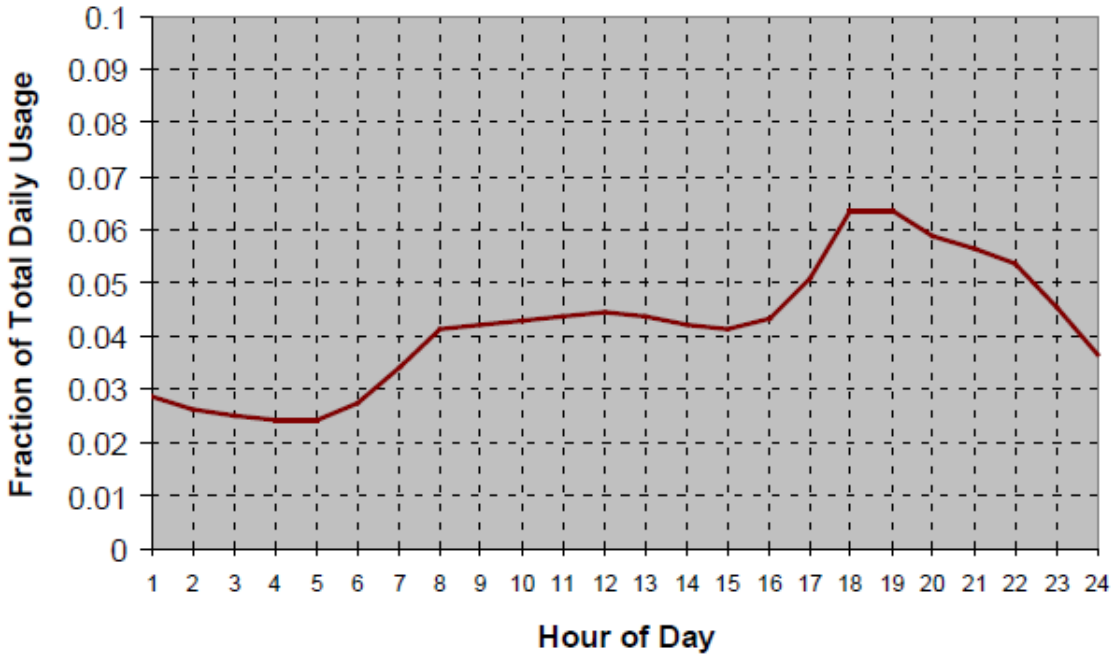

Figure 4-10: Miscellaneous Electrical Loads Daily Usage (Hendron, R. And Engebrecht, C., 2010)

The fractions at each hour were estimated from Figure 4-10 and used in the schedule for MEL in BELA *MURB High-Rise Edition*. The fractions are based on total daily usage which was previously calculated.

4.2.5 Air Leakage Model

The expanded air leakage model in BELA *MURB High-Rise Edition* requires more inputs because the type of building is different. High-rise MURBs are more affected by stack effect and wind pressures. These inputs are illustrated in Figure 4-11.

AIR LEAKAGE CHARACTERISTICS		
Overall Average Flow Coefficient (OAFC)	0.241	l/s-Pa^n-m2 wall
Overall Average Pressure Exponent	0.682	
Pressure Difference Coefficient (Windward)	0.96	
Gradient Height of Meteorological Station	173	m
Anemometer height of Meteorol. Station	30	m
Gradient Height of Building Site	173	m
Thermal Draft Coefficient	0.63	
Normalized Neutral Pressure Plane	0.7	

Figure 4-11: BELA *MURB High-Rise Edition* Air Leakage Characteristics Inputs

Figure 4-11 illustrates the two primary building air leakage characteristics: Overall Average Flow Coefficient in l/s·Pa^n per m^2 of enclosure wall and Overall Average Pressure Exponent. These two values, 0.241 l/s·Pa^n·m^2 and 0.682 were approximated for the Archetype in Section 3.2.5. The windward mean pressure difference coefficient of 0.96 is for wind acting normal to the long wall. (Shaw, C. and Tamura, G., 1977) All other wind angles are accounted for using empirical factors described in Section 4.2.5.1. The gradient height of the meteorological station, anemometer height of meteorological station, and gradient height of building site are inputs used to adjust the weather file's wind speeds to wind speeds around the building.

The thermal draft coefficient (TDC) accounts for the vertical air flow reduction where one indicates the complete freedom for air to move vertically. A TDC range of 0.63 to 0.82 was measured for three high-rise commercial buildings ranging from 17 to 44 stories (Tamura, G. and Wilson, A., 1967). Since residential buildings generally have more restriction to vertical air movement than commercial buildings, the 0.63 value was used. Figure 4-11 list a value of 0.7 for the normalized neutral pressure plane (NPP). Stack effect in buildings causes pressure differences across the enclosure to increase or decrease approximately linearly from top to bottom. The NPP location is the height at which that pressure difference becomes zero. The normalized NPP is the NPP location divided by the building height. A normalized NPP of 0.7 was used based on Proskiw and Phillips research (2006). These inputs are used for either the infiltration calculations based on wind effect or stack effect.

4.2.5.1 Implementing Wind Effect Infiltration

The infiltration rate due to wind effect in BELA *High-Rise Edition* was calculated using Equation 15. (Shaw, C. and Tamura, G., 1977)

$$Q_w = C \times A \times {\Delta P_w}^n \times \alpha_w \quad (15)$$

Where Q_w = infiltration rate due to wind (m^3/s)

C = overall average flow coefficient ($m^3/s/Pa^n/m^2$)

A = area of enclosure wall (m^2)

ΔP_w = pressure difference across the enclosure due to wind (Pa)

n = overall average pressure exponent

α_w = wind angle correction factor

The pressure difference across the enclosure due to wind was calculated using Equation 16. This equation was created using the formulas in Shaw and Tamura's report (1977).

$$\Delta P_w = \tfrac{1}{2} \times \rho_{tot} \times C'_{pm} \times {v_w}^2 \times \left(\frac{G_s}{Z_s}\right)^{2/7} \times \left(\frac{H}{G}\right)^{2/3} \quad (16)$$

Where ρ_{tot} = total of the air density and vapour density (kg/m^3)

C'_{pm} = mean pressure difference coefficient

v_w = wind speed at anemometer height (m/s)

G_s = gradient height of the meteorological station (m)

Z_s = anemometer height at the meteorological station (m)

H = height of building (m)

G = gradient height at the building site (m)

The wind angle correction factor was estimated from Figure 4-12 (Shaw, C. and Tamura, G., 1977).

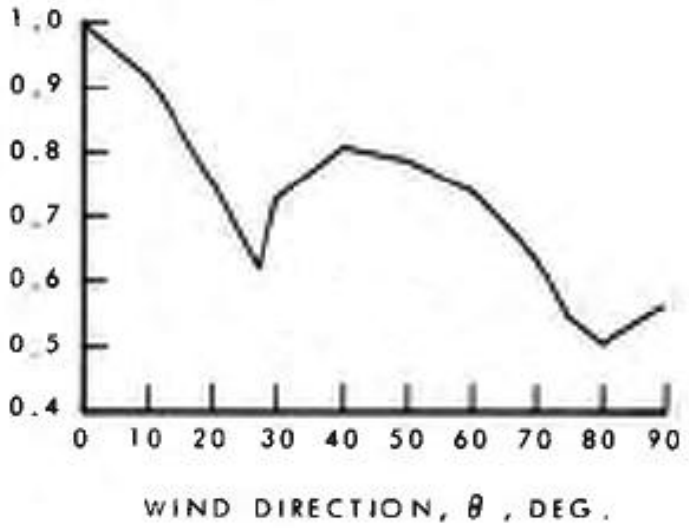

Figure 4-12: Correction Factor of Air Infiltration Rates Due to Wind Approaching at Various Directions (Shaw, C. and Tamura, G., 1977)

Figure 4-12 illustrates that when the wind is acting perpendicular to the long side of the building, theta equal to zero, the correction factor is one which causes the largest wind induced infiltration. The other angles of approaching wind produce different pressures resulting in lower rates of infiltration. This chart was created using a wind tunnel and a scaled rectangular building model with a length to width ratio of 2:1. The Archetype has a length to width ratio of approximately 5:1. Shaw and Tamura tested 1:1, 1.5:1, and 2:1, the differences between the last two are less than the differences between the first two. Since this was the case, correction factor differences between 2:1 and 5:1 ratios was assumed to be small. The correction factor was estimated from Figure 4-12 for every 10 degrees of wind direction. The hourly wind directions provided by the weather files are from 0 to 360 degrees, so they were converted to approaching angles of 0 degrees for wind perpendicular to the long side up to 90 degrees for wind parallel to the long side of the building. The approaching angles were also divided into ten degree increments to match up with the ten degree increments estimated from Figure 4-12.

4.2.5.2 Implementing Stack Effect Infiltration

The infiltration rate due to stack effect in BELA *High-Rise Edition* was calculated using Equation 17. (Shaw, C. and Tamura, G., 1977)

$$Q_s = C \times S \times \left[0.0342 \times \gamma \times p_{atm} \times \left(\frac{\Delta T}{T_i \times T_o}\right)\right]^n \times \left(\frac{\beta \times H}{n+1}\right)^{n+1} \quad (17)$$

Where Q_s = infiltration rate due to stack effect (m^3/s)

C = overall average flow coefficient ($m^3/s/Pa^n/m^2$)

S = perimeter of building (m)

γ = thermal draft coefficient

p_{atm} = atmospheric pressure (Pa)

ΔT = indoor to outdoor temperature difference (K)

T_i = indoor temperature (K)

T_o = outdoor temperature (K)

n = overall average pressure exponent

β = thermal draft coefficient

H = building height (m)

The infiltration rates due to stack effect and wind effect are calculated and combined every hour. Equation 6 previously described in Section 3.2.6.3 was used to combine them.

4.2.6 Ventilation System

The ventilation system for BELA *MURB High-Rise Edition* considers a corridor pressurization system. The ventilation system could have either a central exhaust or individual exhaust illustrated in Figure 4-13 and Figure 4-14, respectively. This is the most common method of ventilating MURBs even today.

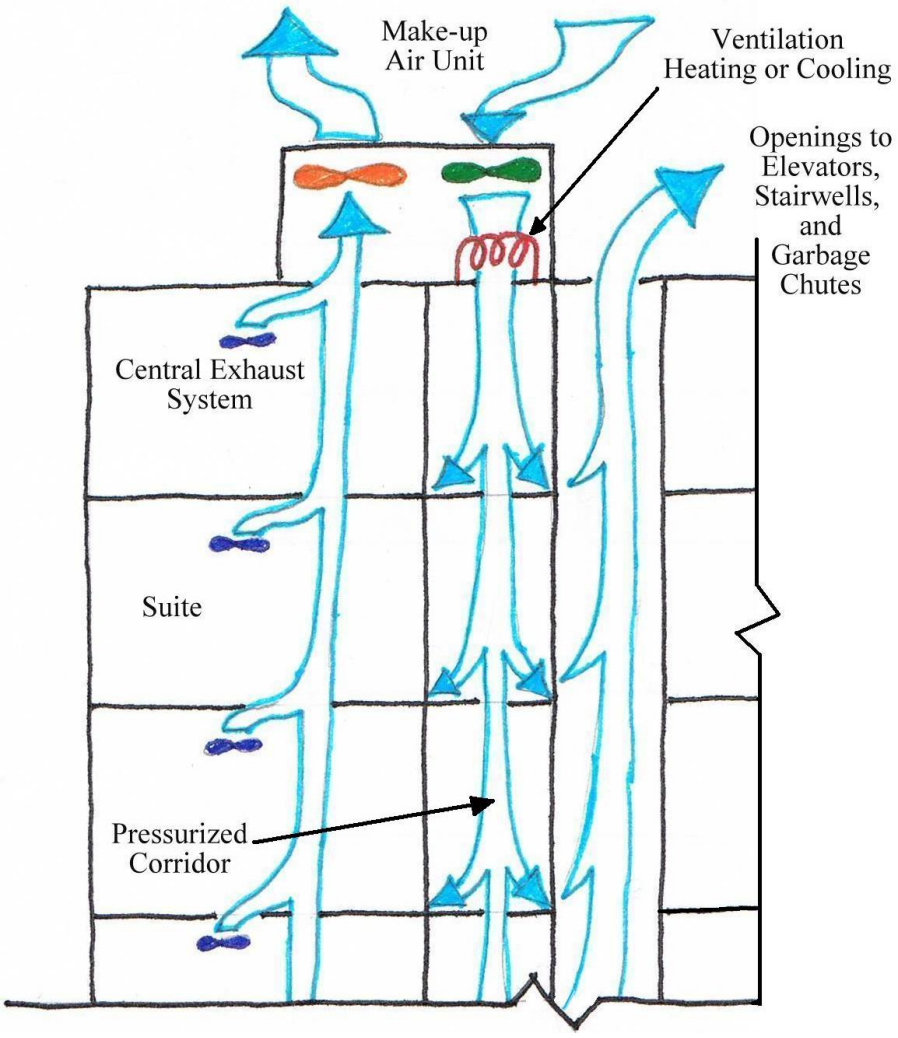

Figure 4-13: BELA *MURB High-Rise Edition* Central Exhaust Ventilation Flow Chart

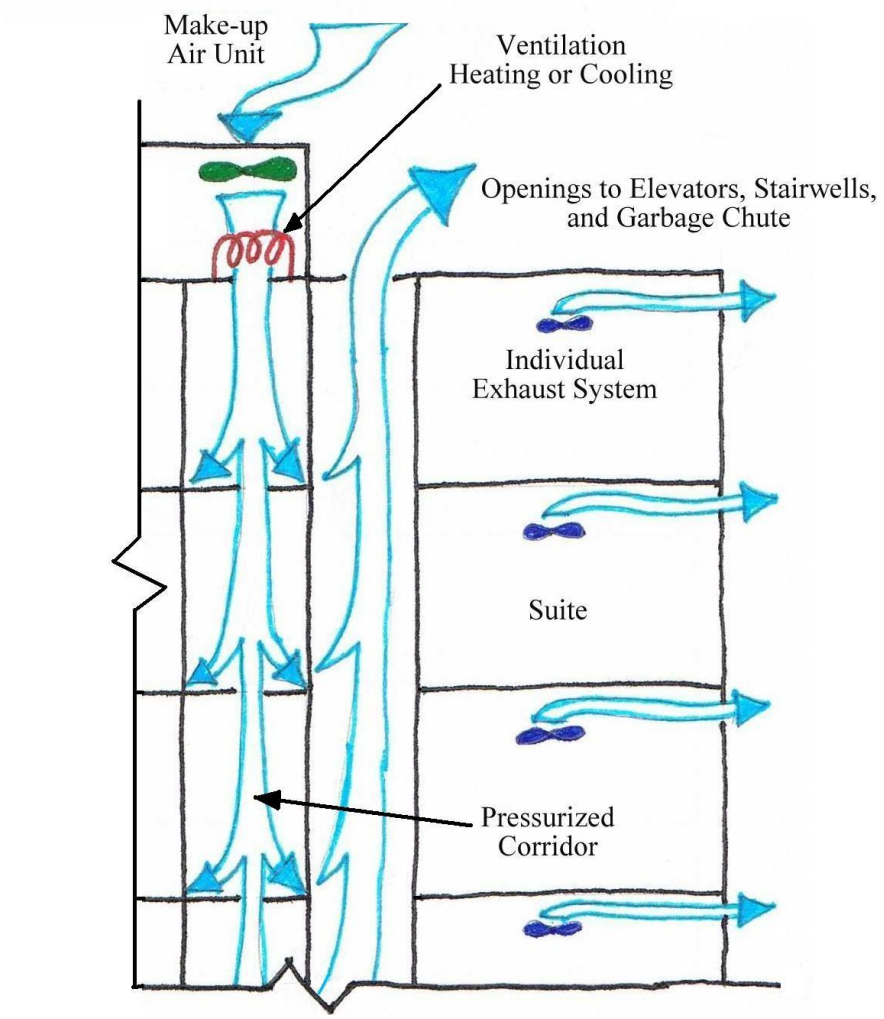

Figure 4-14: BELA *MURB High-Rise Edition* Individual Exhaust Ventilation Flow Chart

Figure 4-13 and Figure 4-14 illustrate the ventilation air flow systems and all there components. A make up air unit has a fan (illustrated in green) that forces ventilation air through a heating and/or cooling system (illustrated in red) before being distributed to all the corridors in the building. The pressurized corridor's air is driven to a number of locations by the pressure differences and openings to each of the locations including: suites, elevators, stairwells, and garbage chute. The operation of the bathroom and kitchen fans (illustrated in dark blue) depressurizes the unit drawing ventilation air into the unit. The operation of the garbage chute and electrical room fans function the same way. The operation of a central exhaust fan (illustrated in orange) in Figure 4-13 can provide a continuous depressurization in the units, garbage chute and electrical rooms to drive the ventilation process. The loss of ventilation air through the elevator shaft and stairwells short circuits the ventilation system

causing the actual ventilation to be far less than the design ventilation. However, the energy in supplying, heating, and cooling that lost air is still consumed and accounted for in the model.

Energy is consumed by ventilation in the form of heating and cooling of the air, and the energy to operate the supply and exhaust fans.

The heating, cooling, and supply distribution loads specifically require the calculation of the make-up air flow capacity. BELA *MURB High-Rise Edition* assumes the exhaust capacity is the same as the supply capacity since this is true for most towers and hence the Archetype so the exhaust distribution load also uses the make-up air flow capacity. The model calculates the make-up air flow capacity by multiplying the design ventilation rate in units of l/s per person by the maximum occupancy of the building.

The ventilation heating and cooling loads were calculated based on the original BELA calculations (Hanam, 2010). The make-up air flow capacity was multiplied by the make-up air units operating schedule and used to calculate the sensible load and latent load. The sensible load and latent load were multiplied by the heat recovery ventilator (HRV) and enthalpy recovery ventilator (ERV) efficiencies, respectively. They were then used to calculate the ventilation heating and cooling loads.

The ventilation supply and exhaust distribution loads were calculated using Equation 18. All fans are assumed to operate as either fully on or off. The operation of the make-up air supply fan and exhaust fans are governed by their respective schedules.

$$\epsilon_{fan} = q \times \omega \tag{18}$$

Where ϵ_{fan} = Fan load (kW)

q = Air flow (l/s)

ω = Maximum design fan power rating (kW/l/s)

The air flow was calculated by multiplying the make-up air flow capacity by the make-up air unit fan or the exhaust fans schedules. The maximum design fan power ratings are different for the make-up air unit and the exhaust fans.

The inputs used to model the Archetype's ventilation loads in BELA *MURB High-Rise Edition* are illustrated in Figure 4-15.

VENTILATION CAPACITY INPUTS			EXHAUST FAN INPUTS		
Design Supply Capacity	15	l/s/person	Max Design Fan Power Rating	0.75	W/l/s
Total Design Supply Capacity	8388	l/s	MAKE-UP AIR UNIT (MUAU) INPUTS		
			HRV Efficiency	0%	
			ERV Efficiency	0%	
			Max Design Fan Power Rating	1.25	W/l/s

Figure 4-15: BELA *MURB High-Rise Edition* Ventilation Inputs

Figure 4-15 illustrates the inputs for ventilation supply capacity, maximum fan power ratings, and recovery ventilator efficiencies. Most towers and hence the archetype do not have either an HRV or ERV. In order to model this, the HRV and ERV efficiencies were set to zero. An HRV or ERV would be ideal for the towers with central exhaust since they are usually in the same mechanical penthouse as the make-up air unit. HRV and ERV systems would require a major retrofit for the towers that exhaust out of each suite.

4.2.7 Space Conditioning Analysis

In order to calculate overall energy consumption for the building, the heating and cooling system must be considered. Since the intent of BELA *MURB High-Rise Edition* is not for the design or analysis of the mechanical systems, a general approach was used to consider the heating and cooling systems. The inputs for the systems are illustrated in Figure 4-16.

ELECTRIC BASEBOARD HEATING, WINDOW A/C COOLING, AND GAS BOILER DHW HEATING				
Unit Heating Efficiency	100%	MUAU Heating Efficiency	70%	
Unit Window A/C COP	3	MUAU A/C COP	3.5	
Percentage of Units with Window A/C	50%	DHW Heating Efficiency	70%	

Figure 4-16: BELA *MURB High-Rise Edition* System Inputs

Figure 4-16 illustrates the inputs for efficiencies (or coefficients of performance (COP)) for electric baseboard heating, window air conditioner (A/C) cooling, and gas boiler for DHW heating. These are very commonly used systems and hence are the systems assumed in the Archetype. The percentage of units with window A/C accounts for the fact that many unit owners choose not to install cooling.

The energy demands are separated into: space heating, space cooling, ventilation distribution, ventilation heating, ventilation cooling, miscellaneous electrical loads, and domestic hot water. The space heating is calculated by dividing the space heating load by the unit heating efficiency. Electric baseboard heating is 100% efficient because all the electricity put through the heating coils enters the

unit as heat. The space cooling demand is calculated by dividing the space cooling load by the unit window A/C COP and multiplying by the percentage of units with window A/C. Three is a reasonable COP for modern window A/C units and 50% was chosen as a mid-range estimate (the percentage of units with window A/C varies significantly). The sensible load fraction of the window A/C units was not considered. The ventilation distribution energy demand was described previously in Section 4.2.6. The ventilation heating demand was calculated by dividing the ventilation heating load by the make-up air unit heating efficiency. A gas furnace with an efficiency of 70% was chosen as a reasonable estimate for the Archetype. The ventilation cooling demand was calculated by dividing the ventilation cooling load by the make-up air unit A/C COP. A COP of 3.5 was assumed since a large centralized A/C unit or cooling tower would likely be more efficient than the window A/C units. The MEL energy demand was calculated by multiplying the MEL energy previously calculated in Section 4.2.4 by the MEL schedule previously described in Section 4.2.4.4. The DHW energy demand was previously calculated in Section 4.2.3.1 using the DHW heating efficiency of 70% which is reasonable for a centralized gas boiler. The total energy demand was calculated by combining all seven energy demands. All of these energy demands for the Archetype are presented in Section 4.3.1.

4.3 Simulated Energy Use of the Archetype

Using the BELA *MURB High Edition* developed, and the assumptions described for the hydronically- and electrically-heated Archetypes, the energy usages were calculated. The results are presented below and analyzed.

4.3.1 Simulated Annual Energy Consumption of the Archetype

The monthly energy density for the hydronically- and electrically-heated Archetypes for all the demands and the totals are illustrated in Figure 4-17 and Figure 4-18.

HYDRONIC RADIATOR HEATING & WINDOW A/C COOLING with MUAU VENTILATION {kWh/m^2}													
	Jan.	Feb.	Mar.	Apr.	May	June	July	Aug.	Sept.	Oct.	Nov.	Dec.	TOTAL
Space Distribution	0.1	0.1	0.1	0.1	0.0	0.0	0.0	0.0	0.0	0.0	0.1	0.1	1
Space Heating	28.0	27.7	24.3	13.6	6.4	2.2	0.9	0.9	3.0	9.0	15.8	26.4	158
Space Cooling	0.2	0.2	0.2	0.3	0.5	0.9	1.1	1.1	0.7	0.3	0.2	0.2	6
Vent. Distribution	0.4	0.4	0.4	0.4	0.4	0.4	0.4	0.4	0.4	0.4	0.4	0.4	5
Vent. Heating	10.1	9.3	8.5	5.9	3.6	1.6	0.8	1.0	2.5	4.9	6.6	8.9	64
Vent. Cooling	0.0	0.0	0.0	0.0	0.0	0.1	0.1	0.1	0.0	0.0	0.0	0.0	0
MEL	6.6	5.9	6.6	6.4	6.6	6.4	6.6	6.6	6.4	6.6	6.4	6.6	78
DHW	6.8	6.3	6.9	6.4	6.3	5.7	5.7	5.5	5.4	5.9	6.0	6.5	73
TOTAL	52	50	47	33	24	17	16	16	18	27	35	49	385

Figure 4-17: Monthly Energy Intensity Demands for the Hydronically-Heated Archetype

ELECTRIC BASEBOARD HEATING & WINDOW A/C COOLING with MUAU VENTILATION {kWh/m^2}													
	Jan.	Feb.	Mar.	Apr.	May	June	July	Aug.	Sept.	Oct.	Nov.	Dec.	TOTAL
Space Heating	22.4	22.2	19.4	10.9	5.1	1.8	0.7	0.8	2.4	7.2	12.6	21.1	127
Space Cooling	0.2	0.2	0.2	0.3	0.5	0.9	1.1	1.1	0.7	0.3	0.2	0.2	6
Vent. Distribution	0.4	0.4	0.4	0.4	0.4	0.4	0.4	0.4	0.4	0.4	0.4	0.4	5
Vent. Heating	10.1	9.3	8.5	5.9	3.6	1.6	0.8	1.0	2.5	4.9	6.6	8.9	64
Vent. Cooling	0.0	0.0	0.0	0.0	0.0	0.1	0.1	0.1	0.0	0.0	0.0	0.0	0
MEL	6.6	5.9	6.6	6.4	6.6	6.4	6.6	6.6	6.4	6.6	6.4	6.6	78
DHW	6.8	6.3	6.9	6.4	6.3	5.7	5.7	5.5	5.4	5.9	6.0	6.5	73
TOTAL	47	44	42	30	23	17	15	16	18	25	32	44	353

Figure 4-18: Monthly Energy Intensity Demands for the Electrically-Heated Archetype

Figure 4-17 and Figure 4-18 illustrate a total estimated energy intensity of approximately 390kWh/m^2 and 350kWh/m^2 for the hydronically- and electrically-heated Archetypes, respectively. The most significant demand is space heating with 161 and 129kWh/m^2 for the hydronically- and electrically-heated Archetypes, respectively. BELA *MURB High-Rise Edition* also outputs the monthly energy density in the form of bar graphs illustrated in Figure 4-19 and Figure 4-20.

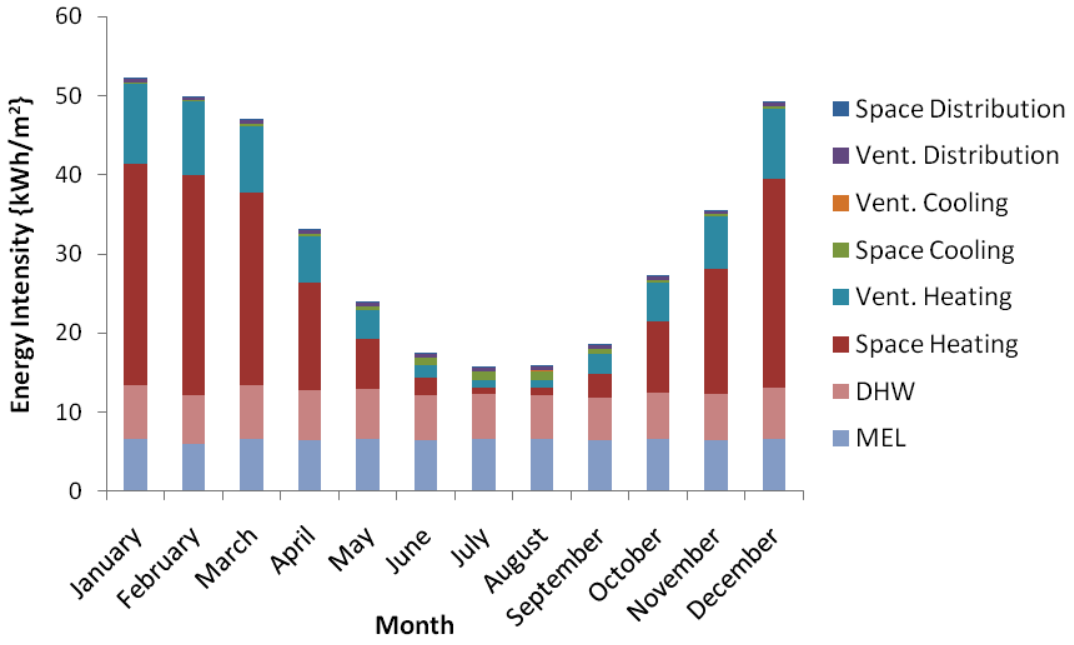

Figure 4-19: Monthly Energy Density Bar Graph for the Hydronically-Heated Archetype

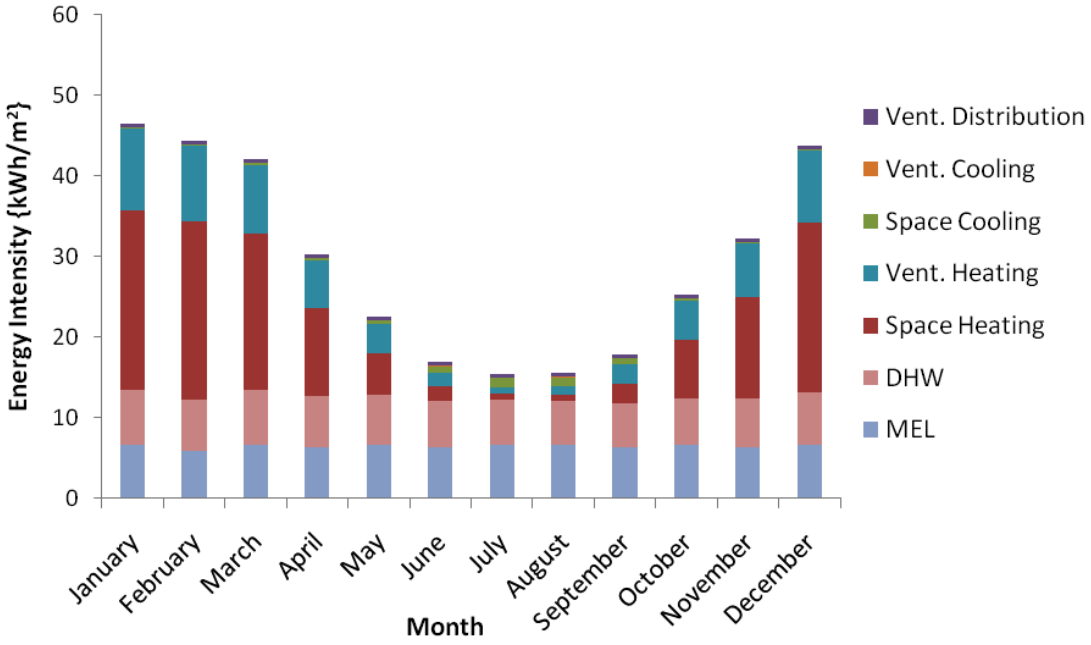

Figure 4-20: Monthly Energy Density Bar Graph for the Electrically-Heated Archetype

Figure 4-19 and Figure 4-20 illustrate the seasonal change in energy intensity demand. January consumes the most energy with an intensity of 53 and 47kWh/m^2 for the hydronically- and

electrically-heated Archetypes, respectively. The January energy intensities are more than three times July and August indicating the significant heating load during colder months. The DHW and MEL demands remain consistent throughout the year. The space heating and ventilation heating demands are significant and seasonally influenced. These demands are also presented in percentage form illustrated in Figure 4-21 and Figure 4-22.

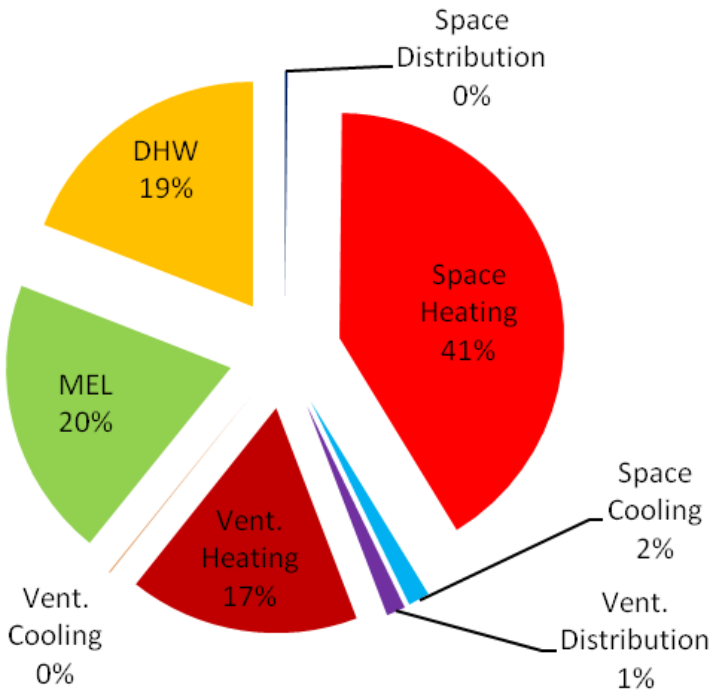

Figure 4-21: Energy Demand Percentages for the Hydronically-Heated Archetype

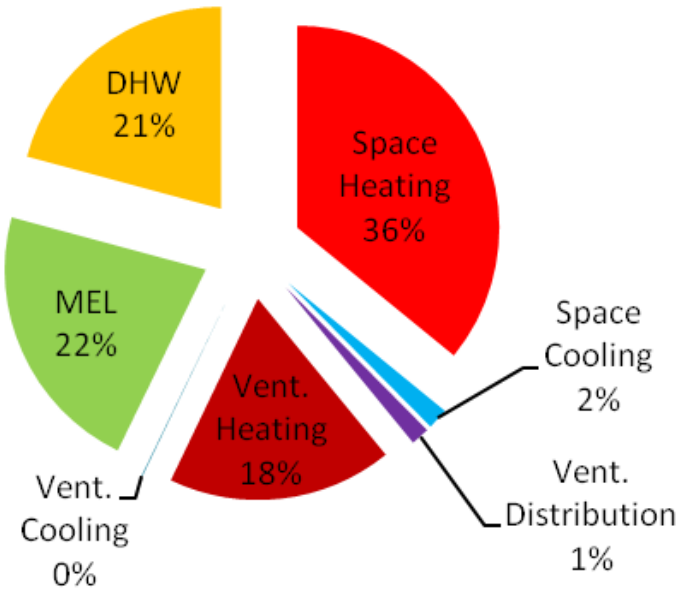

Figure 4-22: Energy Demand Percentages for the Electrically-Heated Archetype

Figure 4-21 and Figure 4-22 illustrate that space and ventilation heating accounts for approximately 60% of the overall annual energy demand for both the hydronically- and electrically-heated Archetypes. DHW and MEL each account for approximately 20% of the annual energy demand. The space cooling and ventilation distribution energy demands are relatively small. The ventilation cooling and space distribution energy demands are almost negligible.

4.3.2 Comparison to Measured Average Annual Energy Consumption of Towers

Natural gas and electricity consumption data were recorded from 34 MURBs mostly from the GTA. The 34 MURBs were separated into four different classifications illustrated in Table 4-6.

Table 4-6: Annual Energy Consumption of Four Types of Apartment Towers (CMHC, 2005)

Group	**1**	**2**	**3**	**4**
Central A/C	No	Yes	No	No
Heating Source	Electric	Natural Gas	Natural Gas	Natural Gas
In-suite electricity included	Yes	Yes	Yes	No
Sample Size	3	17	6	8
Annual Natural Gas Consumption ($ekWh/m^2$)	135	290	315	350
Annual Electricity Consumption (kWh/m^2)	205	115	110	30
Total Annual Energy Consumption ($ekWh/m^2$)	340	405	425	380

Table 4-6 illustrates that group one is the most common to the modeled electrically-heated Archetype. Group one has no central A/C, electric baseboard heating, and in-suite electricity or MEL is included. This set of three buildings has an average annual energy consumption of 340 $ekWh/m^2$ which is close to the 350 kWh/m^2 estimated for the Archetype. The remaining 31 buildings are heated by central gas fired boilers connected to in-suite baseboard convectors or fan-coils (i.e. similar to the hydronically-heated Archetype). Their measured consumption ranged from 281 to 581 $ekWh/m^2$ with an average of approximately 400 $ekWh/m^2$ which is close to the 390 kWh/m^2 calculated for the hydronically-heated Archetype by BELA. All the buildings domestic hot water was heated by centralized gas-fired boilers similar to the modeled Archetypes. Overall, it was found that for the gas heated buildings, approximately half of the annual average energy went to space heating, and a quarter went to both electricity and domestic hot water results similar to the modeled Archetypes. (CMHC, 2005)

The Canada Mortgage and Housing Corporation's HiSTAR database contains 81 MURBs with their physical and operational characteristics and recorded energy consumption. 46 of these buildings were built during the 1970s. The average annual utility energy for 22 Ontario MURBs between 10,000 and 20,000 m^2 (the modeled Archetypes have approximately 20,000 m^2) is 310 $ekWh/m^2$ (Enermodal, 2005). Twenty-six buildings built between the years 1961 and 1980 were monitored for average annual energy consumption. These buildings were found to use 317 $ekWh/m^2$ (CMHC, 2001). According to page 107 of the Tower Renewal Guidelines the average 1960`s and 1970`s high-rise apartment in a Toronto climate uses approximately 322.5 $ekWh/m^2$ (Kesik and Saleff, 2009). The annual energy consumption averages reported by these three studies combine for an average annual energy consumption of approximately 317 $ekWh/m^2$. This is approximately 15% less than the

modeled Archetypes; however the characteristics of the Archetype were generally chosen to have slightly more energy consuming characteristics.

Overall, the reported existing annual energy uses of the towers were close to the simulated annual energy use of the Archetype. Thus, the inputs for the Archetype characteristics were assumed to satisfactorily represent the towers. The BELA *MURB High-Rise Edition* model was also assumed to satisfactorily simulate the towers. Based on these results, confidence is attained in simulating and analyzing pre- and post-retrofit effects on energy consumption as discussed in the following chapter.

4.3.3 Archetype Loads Analysis

According to the results of Section 4.3.1, space and ventilation heating comprise approximately 60% of the annual energy demand while cooling comprises less than 2%. An analysis of the heating loads during the coldest month was completed because of the significant heating energy consumption. The Archetype's January heating loads are illustrated in Figure 4-23.

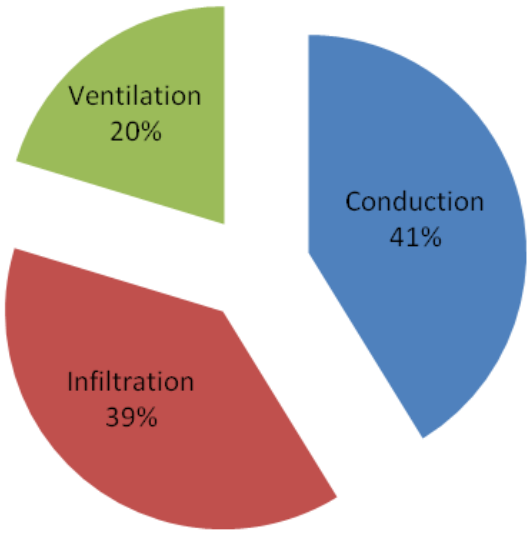

Figure 4-23: Archetype's January Heating Loads

Figure 4-23 illustrates that the cold weather heating loads are approximately split 1:2:2 for ventilation, infiltration, and conduction. Reducing ventilation or recovering ventilation heat, air tightening the enclosure, and insulating are apparent solutions to significantly reducing the heating load of the towers. The Archetype's monthly load density is illustrated in Figure 4-24.

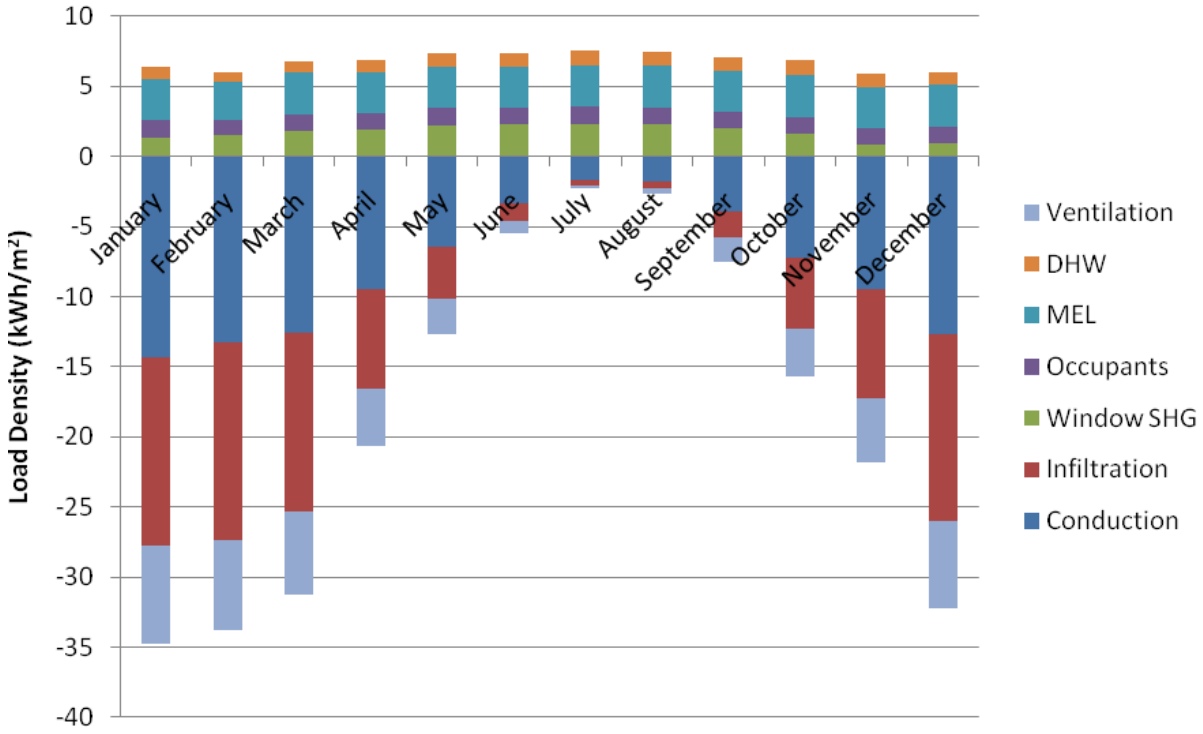

Figure 4-24: Archetype's Monthly Load Intensity

Figure 4-24 illustrates a consistent heat gain of approximately 7kWh/m^2 comprised of DHW, MEL, occupants, and solar heat gain through windows. The heat loss is significantly seasonal with a range from approximately 2kWh/m^2 during the summer to over 30kWh/m^2 during the winter.

Chapter 5 – Energy and Durability Impacts of Tower Retrofits

This chapter discusses the primary effects of retrofitting the enclosure of the towers. The effects analyzed, simulated, and/or discussed include:

- Air, vapour, heat, and moisture control
- Enclosure retrofit details such as material options
- Effective thermal resistances for various enclosure retrofit options
- Energy efficiency measures to compliment the enclosure retrofits
- Durability impacts including interstitial and surface condensation potential
- Comfort impacts such as mean radiant temperature and passive control
- Interior versus exterior enclosure retrofit comparison
- Potential annual energy reduction
- General impact on the reduction of greenhouse gas emissions

The Archetype, Therm, and BELA *MURB High-Rise Edition* described in the previous chapters were used in the majority of the simulated effects of the enclosure retrofits. This chapter will first describe the functions of the enclosure and then proceed to investigate retrofitting impacts.

5.1 Function of the Enclosure

The enclosure separates the interior from the exterior and provides the finished look of a building. Since the enclosure is more often seen than the superstructure, owners, occupants, and the public put more emphasize on the visual appeal of the enclosure. Aside from appearance, the enclosures operation influences comfort, energy efficiency, durability, and occupant satisfaction. Three sub-categories of the enclosures physical separation requirement are:

1. Support – The enclosure must accommodate the structural loads imposed on it from wind, gravity, snow, etc. and transfer them to the superstructure.
2. Control – The enclosure must block or regulate the flow of mass and energy between interior and exterior including rain, vapour, heat, sound, etc.

3. Finish – The enclosures interior and exterior surfaces must interface with the interior and exterior environments in order to meet the requirements of aesthetics, abuse, ease of cleaning, etc.

The enclosure can also be used as a distribution channel for distributing services such as cables, ducts, piping, etc. The support and control layers are required to be continuous and present everywhere. The lack of continuity is the cause of the vast majority of enclosure performance problems.

The support function is critical because without it, all the other functions would be useless. Assuming it is functioning adequately, the next most important function is control. The most common required enclosure control functions include rain, air, heat, vapour, fire, sound, light, insects, particulates, and access. All of these control functions must be continuous throughout the building enclosure in order to physically perform. In terms of durability, the order of importance is generally considered to be: rain control, airflow control, thermal control, and vapour control.

The finish function which does not have to be continuous is often referred to as cladding or interior finishes even though cladding sometimes includes control functions. Although support and finish functions are referenced throughout this thesis, the primary focus of the analysis of enclosure retrofits on the towers is the control function. As such, the following section will discuss the control functions and the layers relating to the towers enclosure in more detail.

5.1.1 Enclosure Control Layers

As previously discussed, the control layer must control water, air, heat, and vapour. A conceptual building enclosure with its control function divided into its four primary layers is presented in Figure 5-1.

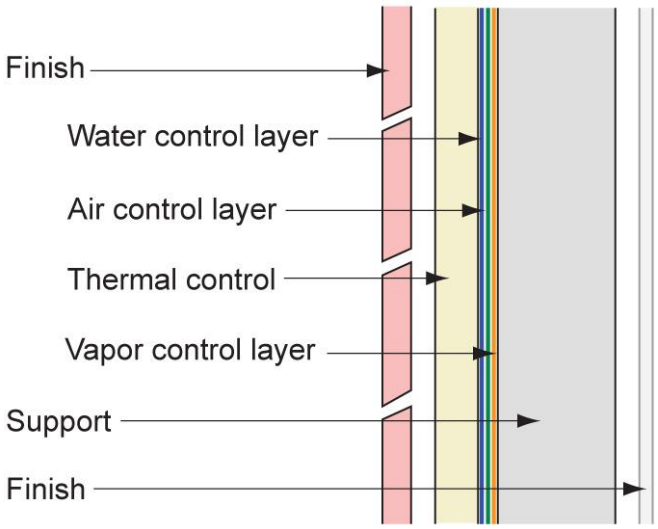

Figure 5-1: Conceptual Building Enclosure with its Functional Layers

In addition to functioning as a finish, the exterior finish layer can provide sun protection to the underlying layers and contributes to rain and fire control. Figure 5-1 illustrates the exterior finish layer not in direct contact with the layers behind it allowing it to also provide a ventilated air gap for drying. This successful design approach, developed and popularized by Canadian researchers (Hutcheon, N., 1964), also provides a continuous thermal control layer on the exterior side of the continuous water, air, and vapour control layers resulting in a durable and high performance cold climate enclosure. The existing control layers for the towers are generalized for the Archetype and illustrated in Figure 5-2.

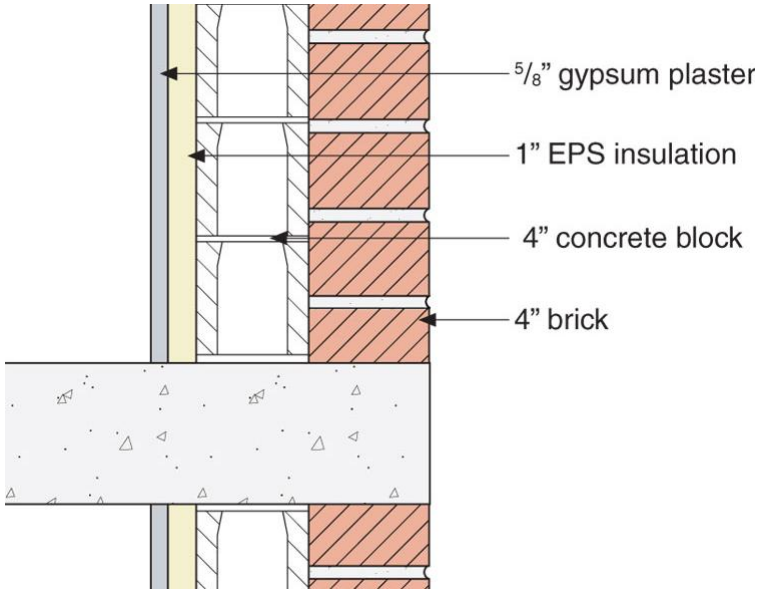

Figure 5-2: Archetype Section Detail

The Archetype, like almost all of the towers, has poorly defined and discontinuous air, rain, water, and thermal control layers. The four inch brick-facing and masonry block functions as part of a mass rain control system and is relied upon to control water, air, and vapour. In some cases parging on the interior acted as the air control layer. The one inch of interior insulation controls heat. The mass storage system is less successful than a drained system because the storage capacity can often be overwhelmed, leading to leaks, and moisture absorbed in the masonry can lead to freeze thaw damage. The towers interior insulation adds to this problem by keeping the masonry colder. The effects on durability will be discussed in Section 5.6. The concrete block also provides lateral support to transfer wind loads to the primary structure.

Two general approaches that can be used to provide dedicated control layers to the towers' enclosure are from the interior or exterior of the existing enclosure. A general interior enclosure retrofit is illustrated in Figure 5-3.

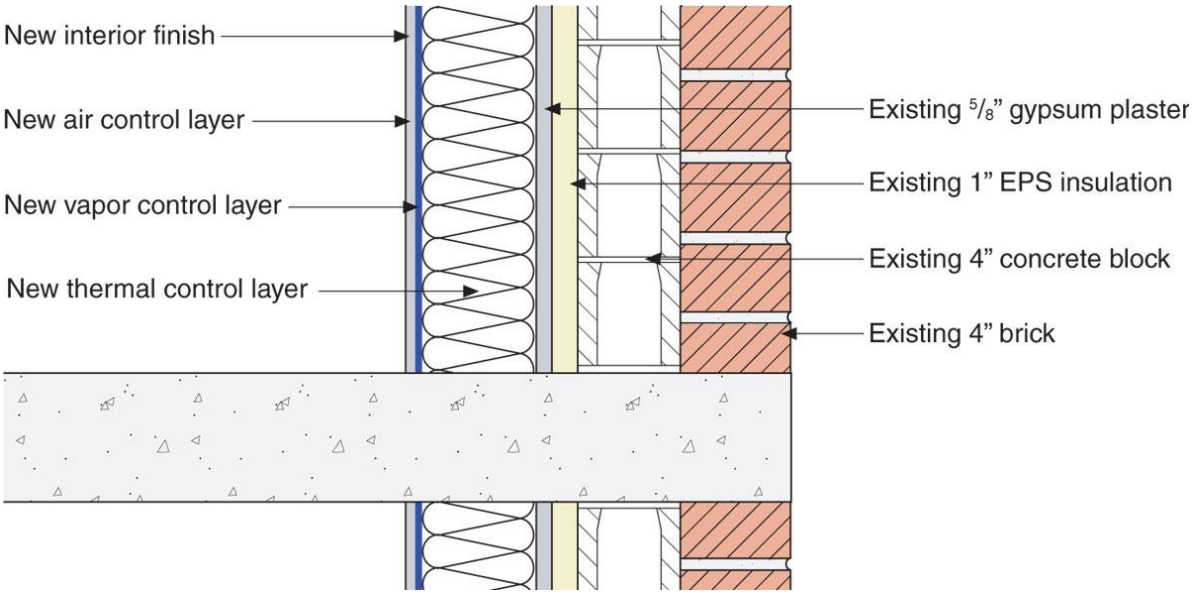

Figure 5-3: Interior Enclosure Retrofit

Figure 5-3 illustrates the addition of insulation on the inside of the existing gypsum plaster to provide the desired level of thermal resistance. The addition of an air control and a vapour control layer on the inside of the new insulation results in these control layers functioning more effectively on the correct side of the thermal control layer. The air, vapour, and thermal layers still remain discontinuous. Also, the rain control still functions as a mass system. The existing brick and block would continue to function as the lateral support.

A general exterior enclosure retrofit is illustrated in Figure 5-4.

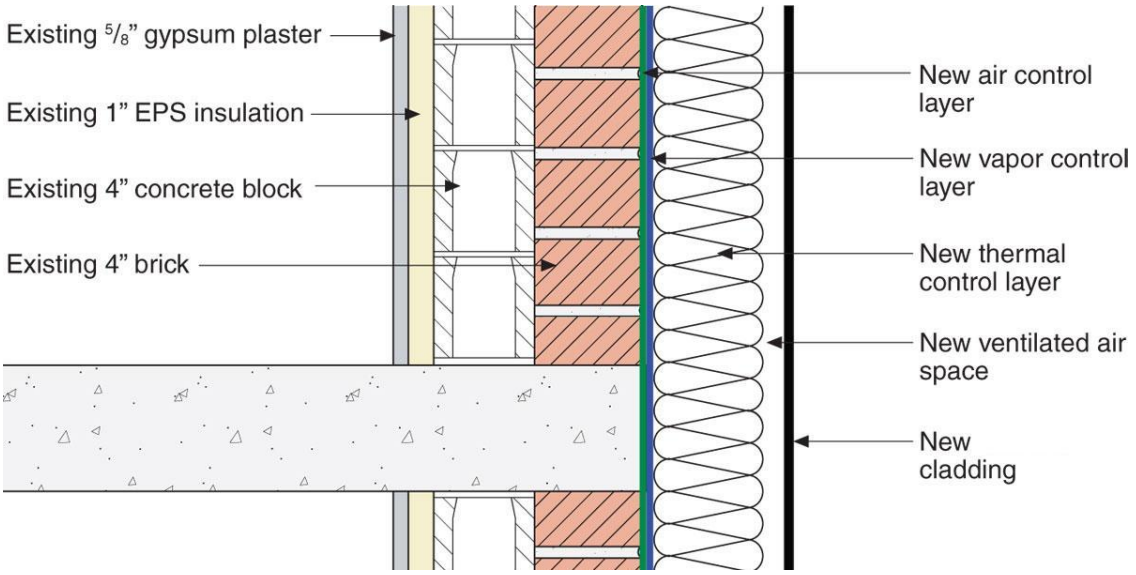

Figure 5-4: Exterior Enclosure Retrofit

Figure 5-4 illustrates the addition of continuous air, moisture, and vapour control layers on the exterior of the existing brick face. The addition of continuous insulation on the exterior of the air, moisture, and vapour control layers results in the layers functioning more effectively in the correct order. The addition of a drainage plane and drainage gap and exterior finish layer over a ventilated air space converts the existing mass system to a drained and ventilated system.

The air and water control layer installed on the exterior can be continuous resulting in a more air and water tight assembly. The vapour and moisture control layer installed on the exterior and the addition of the rainscreen protects the brick, block, and concrete slab edge from moisture and associated damages and unsightly efflorescence. The function of the brick and block would be reduced to just lateral support. The thermal control layer installed on the exterior can also be continuous eliminating thermal bridging through the concrete slab. The exterior thermal control layer reduces the temperatures that the brick and concrete experiences which can eliminate the potential for freeze-thaw damage to occur. The additional exterior thermal control layer improves the overall thermal resistance of the enclosure effectively. The new cladding provides the opportunity for new exterior finish possibilities. The exterior enclosure retrofit reduces the significance of the interior insulation and thus the existing interior finish and insulation could be removed if desired.

5.1.2 Enclosure Retrofit Details

Both the interior and exterior enclosure retrofit approaches are quite flexible. Many different materials can be used to meet the architectural, budget, and performance needs of a range of projects. For example, the following materials that could be used for the air control layer for interior or exterior retrofit options include:

- Liquid-applied polymeric or asphalt-based membranes (also water and vapour)
- Closed cell spray foams (also vapour and thermal)
- Some open-cell spray foam (also thermal)
- Taped and sealed polyethylene-fiber or spun-bonded polyolefin membranes (also rain)
- Self-adhered membranes (also vapour and rain)

Material choices for the vapour control layer for interior or exterior retrofit could include:

- Foil-face materials
- Polyethylene facers
- Closed cell spray foams
- Some open-cell spray foams

Material choices for the thermal control layer for the interior of exterior retrofit could include:

- Extruded polystyrene (XPS)
- Expanded polystyrene (EPS)
- Open- or closed-cell spray foams
- Rockwool
- Polyisocyanurate (PIC)

Since the materials used for the interior retrofit do not have to withstand exterior weather conditions, there are more options available. Some additional material choices for the interior retrofit could include:

- Taped and sealed gypsum board (air control)

- Taped and sealed Polyethylene sheets (air and vapour control)
- Vapour retarding paint (vapour control)
- Fibreglass batt (thermal control)
- Blown-in cellulose or fibreglass (thermal control)

The exterior retrofit option requires a new cladding. A lightweight cladding would generally be desirable to reduce the loads on the existing structure, simplify and lighten the new connection of the cladding back to the existing wall, and for ease of installation. The cladding should ideally be impact resistant especially near grade. The cladding must also meet code requirements for combustibility and flame spread. Some material choices include:

- Galvanized steel sheet
- Aluminum sheet
- Fibre-cement board
- High pressure laminates
- Glass
- Thin brick or stone faced sheets
- Polycarbonate

An important consideration in the cladding design is to ensure continuity of the control layers where the structural connection between the cladding and support is made. The attachment mechanisms for the cladding must meet the following requirements:

- Strength to support insulation and all cladding loads
- Minimal cross sectional area or low thermal conductivity to avoid thermal bridging
- Moisture and temperature resistant material
- Preferably simple and quick installation

5.2 Effective Thermal Resistances

The configuration of insulation applied to an enclosure can have different impacts on the effective thermal resistance. Effective thermal resistance is defined as the area of enclosure divided by the heat flow for a unit temperature difference. This definition means that all two and three dimensional geometrical effects are considered. However, air leakage and thermal mass, while sometimes important, are not considered in this thesis.

Since the protruding concrete balcony slabs are significant thermal bridges, the different configurations are primarily focused around them.

First an analysis on the effects of various existing towers balcony geometries was completed. Heat transfer modeling using Therm 5.2 was completed on balconies ranging from 1.12m (3'-4") to 2.29m (7'-6") in extension length with slab thickness ranging from 165mm (6 1/2") to 203mm (8"). The range of effective thermal resistances due to varying geometry were 5%, 6%, and 8% for no overcladding, 76mm (3") of continuous exterior XPS insulation around the balcony and walls, and 76mm (3") of exterior XPS insulation over just the walls, respectively. The results indicated that the largest range in thermal resistance based on various towers balcony geometries was approximately 8% or about half an R-Value. The results are illustrated in Appendix D. Since the effect of balcony geometry was relatively insignificant, the rest of the modeling was based on the Archetype's 1.52m (5') balcony extension with 165mm (6 ½") thick concrete slab.

Four different configurations of insulating the Archetype`s enclosure were analyzed. The percentage of each wall section present in the Archetype (see Chapter 2) was assumed when calculated. Effective thermal resistance was then calculated by area weighting the results of the two dimensional Therm analysis as described in Section 3.1. The effective thermal resistances were calculated for the addition of 0.88 (R5), 1.76 (R10), and 3.52 $m^2 \cdot k/W$ (R20) to the existing wall sections for the four different configurations.

5.2.1 Retrofit 1

The first configuration was insulated on the interior and designated as Retrofit 1 illustrated in Figure 5-5 through Figure 5-9 for all five wall conditions. The new insulation is illustrated in magenta.

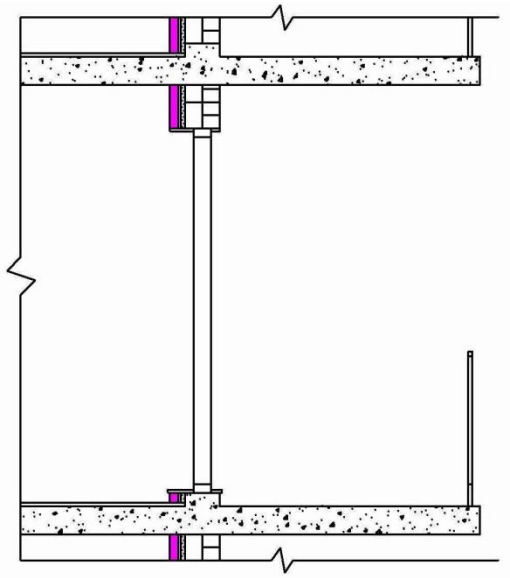

Figure 5-5: Balcony Door Retrofit 1

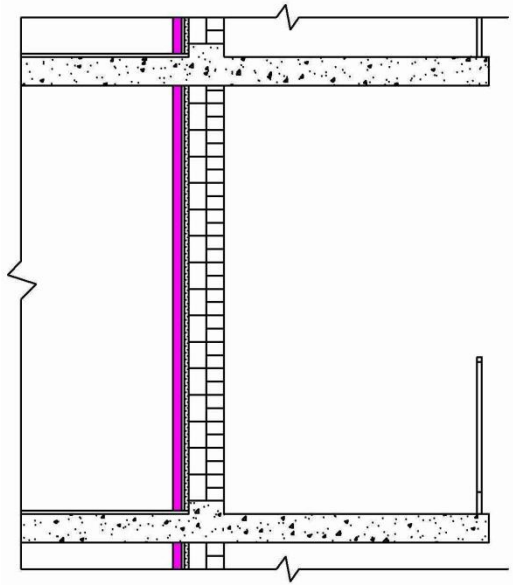

Figure 5-6: Balcony Wall Retrofit 1

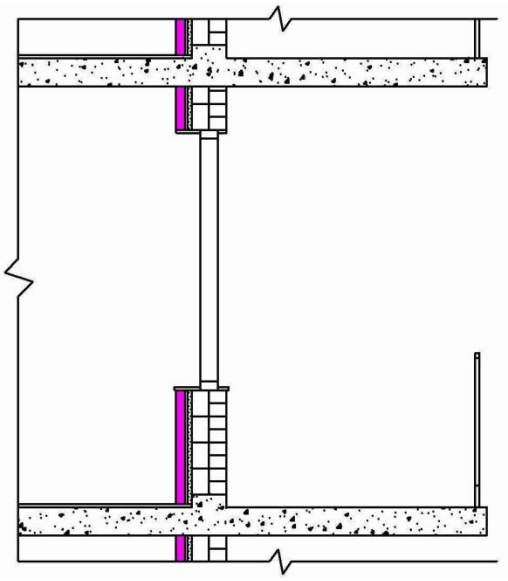

Figure 5-7: Balcony Window Wall Retrofit 1

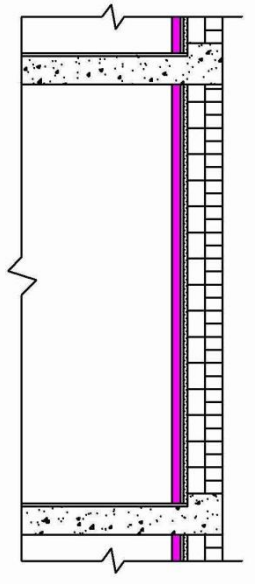

Figure 5-8: Wall Retrofit 1

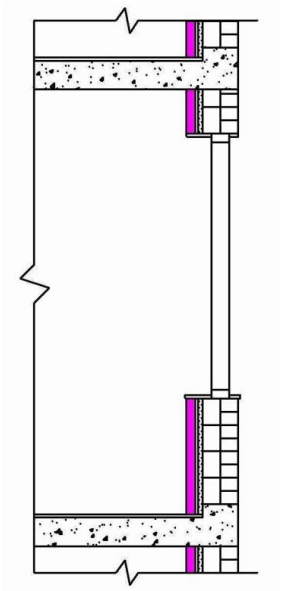

Figure 5-9: Window Wall Retrofit 1

The opaque wall thermal resistances for the five enclosure conditions for Retrofit 1 were calculated and summarized in Table 5-1.

Table 5-1: Effective Thermal Resistances of Opaque Wall Sections for Retrofit 1

Opaque Wall Sections	Additional R5		Additional R10		Additional R20	
	($m^2 \cdot k/W$)	($hr \cdot ft^2 \cdot °F/btu$)	($m^2 \cdot k/W$)	($hr \cdot ft^2 \cdot °F/btu$)	($m^2 \cdot k/W$)	($hr \cdot ft^2 \cdot °F/btu$)
Wall	1.44	8.2	1.72	9.8	2.09	11.9
Window Wall	0.81	4.6	0.85	4.8	0.89	5.1
Balcony Door	0.44	2.5	0.44	2.5	0.45	2.5
Balcony Wall	1.44	8.2	1.73	9.8	2.08	11.8
Balcony Window Wall	0.84	4.8	0.89	5.1	0.93	5.3
Overall	**1.26**	**7.2**	**1.48**	**8.4**	**1.76**	**10.0**

5.2.2 Retrofit 2

The second configuration was insulated on the exterior and designated as Retrofit 2 illustrated in Figure 5-10 through Figure 5-14 for all five wall conditions. The new insulation is also illustrated in magenta.

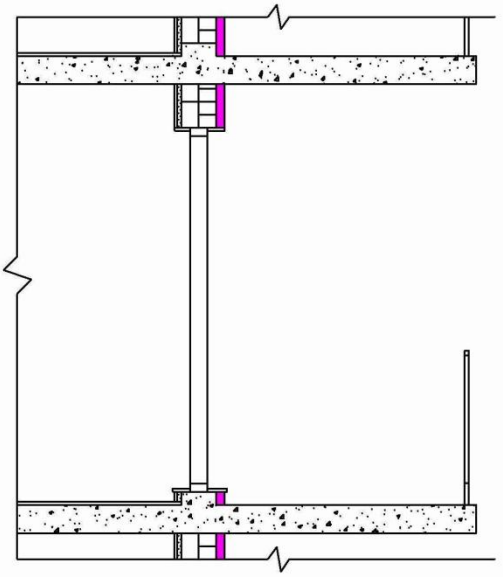

Figure 5-10: Balcony Door Retrofit 2

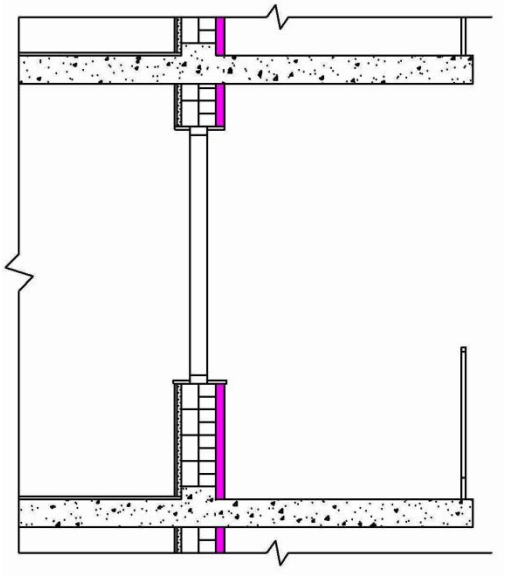

Figure 5-12: Balcony Window Wall Retrofit 2

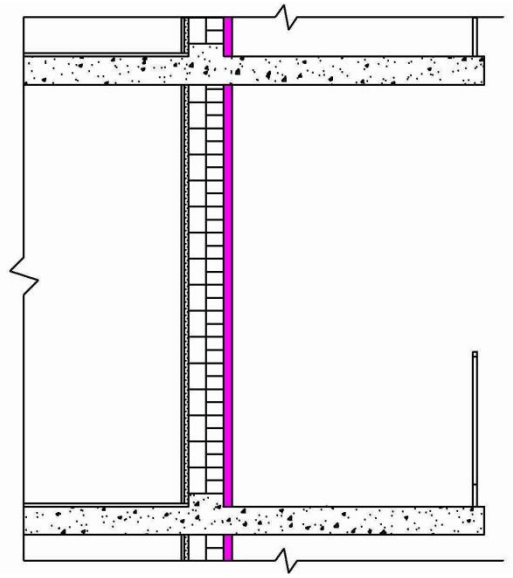

Figure 5-11: Balcony Wall Retrofit 2

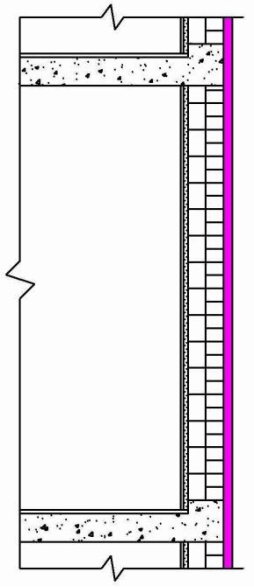

Figure 5-13: Wall Retrofit 2

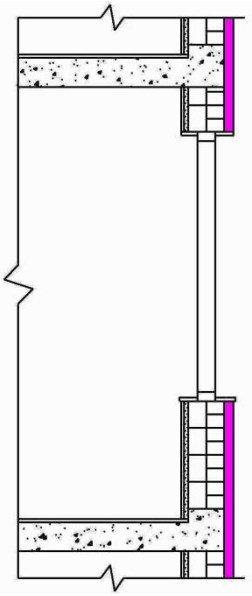

Figure 5-14: Window Wall Retrofit 2

The opaque wall thermal resistances for the five enclosure conditions for Retrofit 2 were calculated and summarized in Table 5-2.

Table 5-2: Effective Thermal Resistances of Opaque Wall Sections for Retrofit 2

Opaque Wall Sections	R5 Retrofit		R10 Retrofit		R20 Retrofit	
	($m^2 \cdot k/W$)	($hr \cdot ft^2 \cdot °F/btu$)	($m^2 \cdot k/W$)	($hr \cdot ft^2 \cdot °F/btu$)	($m^2 \cdot k/W$)	($hr \cdot ft^2 \cdot °F/btu$)
Wall	1.96	11.1	2.86	16.3	4.68	26.5
Window Wall	1.87	10.6	2.99	17.0	5.24	29.7
Balcony Door	0.56	3.2	0.58	3.3	0.59	3.4
Balcony Wall	1.32	7.5	1.55	8.8	1.81	10.3
Balcony Window Wall	0.93	5.3	1.01	5.8	1.08	6.1
Overall	**1.61**	**9.2**	**2.24**	**12.7**	**3.43**	**19.5**

5.2.3 Retrofit 3

The third configuration was also insulated on the exterior with the addition of insulation on the underside of the balconies and designated as Retrofit 3. The wall and window wall sections are the same as Retrofit 2 illustrated in Figure 5-13 and Figure 5-14. The balcony sections for Retrofit 3 are illustrated in Figure 5-15 through Figure 5-17. The new insulation is also illustrated in magenta.

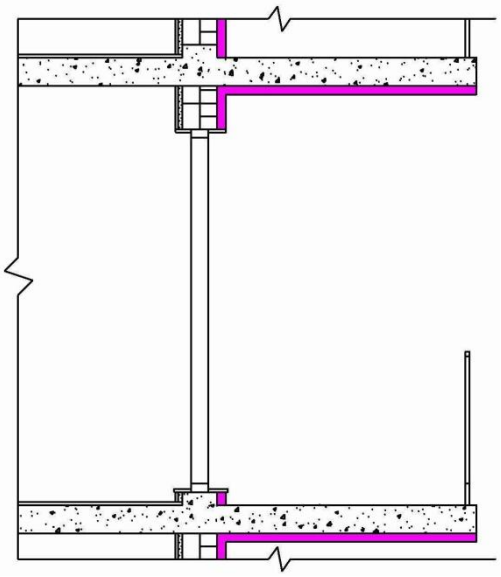

Figure 5-15: Balcony Door Retrofit 3

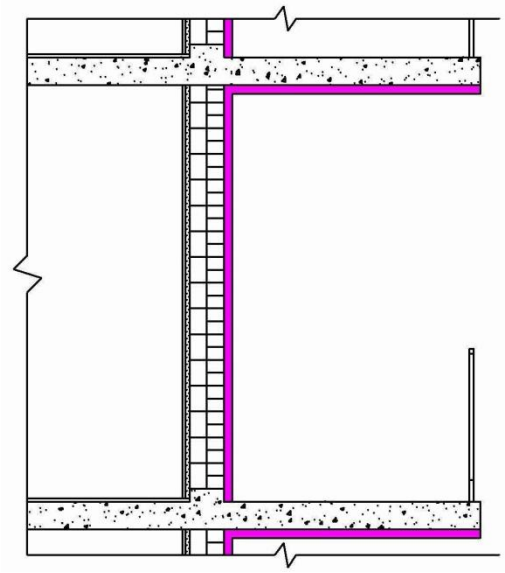

Figure 5-16: Balcony Wall Retrofit 3

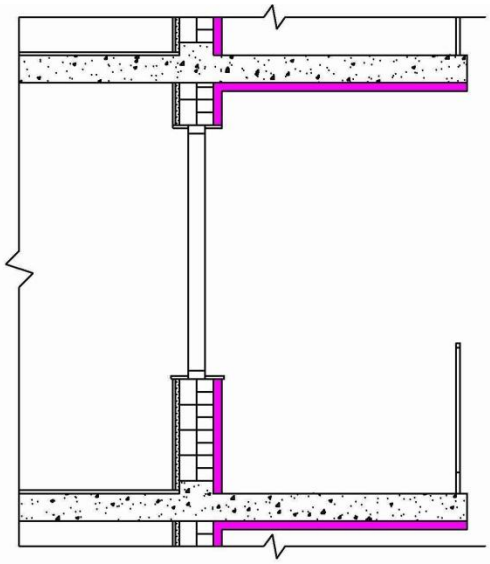

Figure 5-17: Balcony Window Wall Retrofit 3

The opaque wall thermal resistances for the five enclosure conditions for Retrofit 3 were calculated and summarized in Table 5-3. The values for the wall and window wall are the same as in Retrofit 2.

Table 5-3: Effective Thermal Resistances of Opaque Wall Sections for Retrofit 3

Opaque Wall Sections	R5 Retrofit		R10 Retrofit		R20 Retrofit	
	(m^2·k/W)	(hr·ft^2·°F/btu)	(m^2·k/W)	(hr·ft^2·°F/btu)	(m^2·k/W)	(hr·ft^2·°F/btu)
Wall	1.96	11.1	2.86	16.3	4.68	26.5
Window Wall	1.87	10.6	2.99	17.0	5.24	29.7
Balcony Door	0.60	3.4	0.62	3.5	0.64	3.6
Balcony Wall	1.32	7.5	1.56	8.9	2.37	13.4
Balcony Window Wall	0.96	5.4	1.06	6.0	1.14	6.4
Overall	**1.62**	**9.2**	**2.25**	**12.8**	**3.57**	**20.2**

5.2.4 Retrofit 4

The fourth configuration was also insulated on the exterior with the addition of insulation all around the balconies. This was designated as Retrofit 4. The wall and window wall sections are the same as Retrofit 2 illustrated in Figure 5-13 and Figure 5-14. The balcony sections for Retrofit 4 are illustrated in Figure 5-18 through Figure 5-20. The new insulation is also illustrated in magenta.

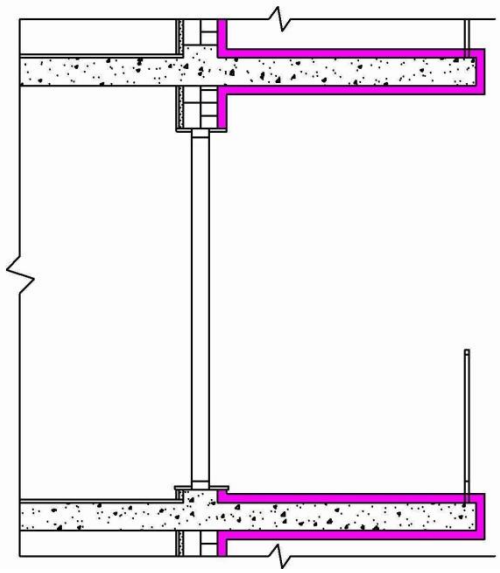

Figure 5-18: Balcony Door Retrofit 4

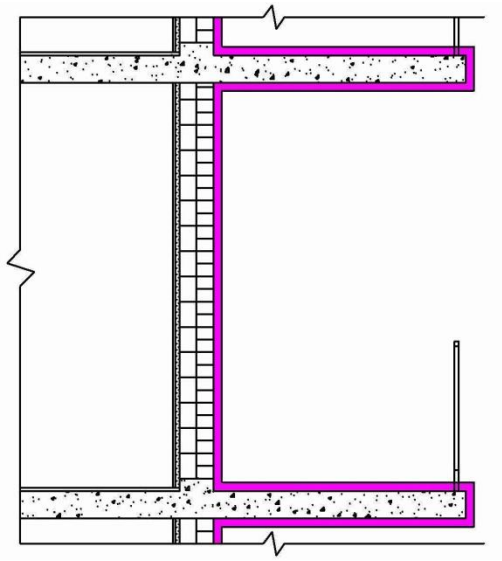

Figure 5-19: Balcony Wall Retrofit 4

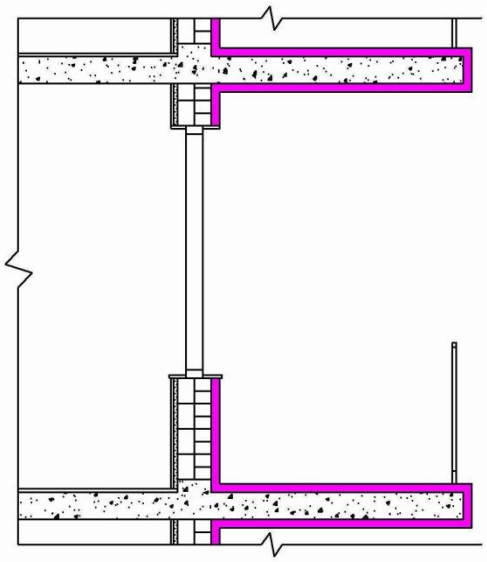

Figure 5-20: Balcony Window Wall Retrofit 4

The opaque wall thermal resistances for the five enclosure conditions for Retrofit 4 were calculated and summarized in Table 5-4. The values for the wall and window wall are the same as in Retrofit 2.

Table 5-4: Effective Thermal Resistances of Opaque Wall Sections for Retrofit 4

Opaque Wall Sections	R5 Retrofit		R10 Retrofit		R20 Retrofit	
	($m^2 \cdot k/W$)	($hr \cdot ft^2 \cdot °F/btu$)	($m^2 \cdot k/W$)	($hr \cdot ft^2 \cdot °F/btu$)	($m^2 \cdot k/W$)	($hr \cdot ft^2 \cdot °F/btu$)
Wall	1.96	11.1	2.86	16.3	4.68	26.5
Window Wall	1.87	10.6	2.99	17.0	5.24	29.7
Balcony Door	1.05	6.0	1.35	7.7	1.78	10.1
Balcony Wall	1.70	9.7	2.28	13.0	3.29	18.7
Balcony Window Wall	1.40	8.0	1.86	10.6	2.55	14.5
Overall	**1.78**	**10.1**	**2.55**	**14.5**	**4.02**	**22.8**

5.2.5 Summary of Effective Thermal Resistances

The effective thermal resistances for all four retrofits are presented in Table 5-6, for exterior insulation values of R5, R10, and R20. Approximate insulation thicknesses to achieve these three thermal resistance values are illustrated in Table 5-5 for three levels of typical insulation materials.

Table 5-5: Approximate Thicknesses of Insulation

	R4/inch Rockwool/Expanded Polystyrene	**R5/inch** Extruded Polystyrene	**R6/inch** Polyisocyanurate/Closed -Cell Spray Foam
R5	1 1/4"	1"	5/6"
R10	2 1/2"	2"	1 2/3"
R20	5"	4"	3 1/3"

Table 5-6: Effective Thermal Resistances

Archetype	m^2k/W	0.89			
	$hr{\cdot}ft^{2}{\cdot}°F/btu$	**5.1**			
		Retrofit 1 Interior	**Retrofit 2** Exterior (No Balconies)	**Retrofit 3** Exterior (Underside of Balconies)	**Retrofit 4** Exterior (Around Balconies)
Additional R5	m^2k/W	1.26	1.61	1.62	1.78
	$hr{\cdot}ft^{2}{\cdot}°F/btu$	**7.2**	**9.2**	**9.2**	**10.1**
	Effective R-Value Added	2.1	4.1	4.1	5.0
Additional R10	m^2k/W	1.48	2.24	2.25	2.55
	$hr{\cdot}ft^{2}{\cdot}°F/btu$	**8.4**	**12.7**	**12.8**	**14.5**
	Effective R-Value Added	3.3	7.6	7.7	9.4
Additional R20	m^2k/W	1.76	3.43	3.57	4.02
	$hr{\cdot}ft^{2}{\cdot}°F/btu$	**10.0**	**19.5**	**20.3**	**22.8**
	Effective R-Value Added	4.9	14.4	15.2	17.7

Table 5-6 illustrates that insulating the interior significantly reduces the effective thermal resistance added. The addition of R20 insulation to the interior results in an overall increase of approximately R5. The more insulation added the less effective that insulation becomes. Overall, adding interior insulation is approximately 25 to 40% effective. Adding insulation to the exterior walls only is approximately 75% to 80% effective; continuing the insulation along the underside of the balconies adds little value. Adding exterior insulation to the exterior walls and the around the protruding concrete balcony slab is approximately 90 to 100% effective.

5.3 Energy Efficiency Measures

Energy efficiency measures (EEMs) are individual ways to reduce energy. The general categories of EEMs for the towers include the heating, ventilation, and air conditioning (HVAC) equipment, walls,

roof, windows, lights, appliances, and DHW usage. Each of these were described and analyzed on the Archetype.

5.3.1 Window Retrofit

A window retrofit is common and often effective in a number of ways. It can reduce air infiltration which leads to less uncomfortable drafts and reduced energy consumption, better insulation value and the resulting warmer surface temperatures reduce condensation potential. Three potential window retrofit options and their characteristics are illustrated in Table 5-7.

Table 5-7: Window Retrofit Characteristics

	Glazing Separation	Gap Fill	Number of Panes	Low-E Coating	Frame
Archetype	6.4mm	Air	2	None	Aluminum, no thermal break
Retrofit 1	12.7mm	Air	2	Yes (0.2)	Vinyl/Wood
Retrofit 2	12.7mm	Argon	2	Yes (0.1)	Vinyl/Fibreglass
Retrofit 3	12.7mm	Argon	3	Yes(0.1)	Vinyl/Fibreglass

The Archetype was assumed to have the lowest performance double-glazed, aluminum-framed window and it was used as the base case for comparison. Retrofit 1 reduces the solar heat gain with a modest low emissivity (low-e) coating and reduces the significant thermal bridging at the frame with vinyl or wood replacing the non-thermally broken aluminum. Retrofit 2 assumes best-in-class double-glazed window performance and Retrofit 3 is a high-performance triple-glazed window. The effects on overall window thermal resistance and the solar heat gain coefficients (SHGC) are illustrated in Table 5-8.

Table 5-8: Window Retrofit Scenarios

	Overall Window R-Value			SHGC
	($m^2 \cdot k/W$)	($hr \cdot ft^2 \cdot °F/btu$)	Improvement to Archetype	
Archetype	0.32	1.83		0.69
Retrofit 1	0.49	2.81	54%	0.55
Retrofit 2	0.63	3.59	96%	0.51
Retrofit 3	1.10	6.25	242%	0.34

Table 5-8 illustrates that each of the three window retrofits increases the overall window thermal resistance (including surface films) by approximately 50%, 100%, and 250%, respectively.

5.3.2 Wall and Roof Retrofit

Five of the wall retrofits analyzed in Section 5.2 were selected as retrofit EEMs. The retrofits' effective thermal resistance percentage improvements compared to the Archetype were also calculated. The selected sections and percentage improvements are illustrated in Table 5-9.

Table 5-9: Opaque Wall Retrofit Scenarios

	Overall Opaque Wall R-Value		
	(m^2·k/W)	(hr·ft^2·°F/btu)	Improvement of Archetype
Archetype	0.89	5.1	
Retrofit 1 – R10	1.48	8.4	66%
Retrofit 1 – R20	1.76	10.0	98%
Retrofit 2 – R10	2.24	12.7	152%
Retrofit 2 – R20	3.43	19.5	285%
Retrofit 4 – R20	4.02	22.8	352%

Table 5-9 illustrates that the interior retrofit improvements are approximately 70% and 100% for an additional 1.76 (R10) and 3.52 m^2·k/W (R20), respectively. An overcladding to the exterior walls results in approximately 150% and nearly 300% for the same respective insulation levels. Complete overcladding including around the balconies with 3.52 m^2·k/W (R20) results in approximately 350% improvement to the Archetype's wall thermal resistance.

Three roof retrofits were analyzed. Retrofits 1, 2, and 3 represent additional overcladding insulation of 1.76 (R10), 3.52 (R20), and 7.04 m^2·k/W (R40), respectively. The thermal resistances and percentage improvement to the Archetype are illustrated in Table 5-10.

Table 5-10: Roof Retrofit Scenarios

	Overall Roof R-Value		
	(m^2·k/W)	(hr·ft^2·°F/btu)	Improvement to Archetype
Archetype	1.67	9.5	
Retrofit 1	3.47	19.7	106%
Retrofit 2	5.25	29.8	213%
Retrofit 3	8.82	50.1	425%

Table 5-10 illustrates that retrofits 1, 2, and 3 improve the Archetype's roof thermal resistance by approximately 100%, 200%, and 425%, respectively.

5.3.3 HVAC Retrofit

Replacing the older, less efficient HVAC equipment can be a quick and simple retrofit. It generally has little effect on the occupants, can happen quickly, and can often reduce maintenance of older, malfunctioning equipment. The efficiencies assumed for the Archetype along with two HVAC retrofit packages are illustrated in Table 5-11.

Table 5-11: HVAC Retrofit Packages

	Archetype Efficiencies	Retrofit 1 Efficiencies	Retrofit 2 Efficiencies
HRV	0%	55%	80%
Hydronic Boiler	80%	92%	95%
Window A/C COP	3	3.2	3.5
MUAU Heating	70%	84%	95%
MUAU Cooling COP	3.5	4	4.5
DHW Boiler	70%	82%	97%

A heat recovery ventilator (HRV) is generally not installed in the towers. Window A/C technology has generally not achieved coefficient of performance (COP) beyond 3.5. Centralized cooling units are able to achieve COPs of 4 and 4.5 for a good and best performing unit, respectively. The highest performing non-condensing furnace is approximately 84% and a realistic high performing condensing furnace achieves an efficiency of approximately 95%. The same is true for boilers with approximately 82% and 97% efficiencies for non-condensing and condensing, respectively.

5.3.4 Appliance and Lighting Retrofit

Two appliance retrofit scenarios are illustrated in Table 5-12.

Table 5-12: Appliance Retrofit Unit Energy Consumption

	Archetype (kWh/yr)	Retrofit 1 (kWh/yr)	Retrofit 2 (kWh/yr)
Refrigerator	558	457	350
Clothes Washer*	54	21	15
Clothes Dryer	951	916	850
Dishwasher*	82	53	40
Range	697	522	400
Total	2342	1969	1655

*Does not include hot water heating energy

Retrofit 1 illustrated in Table 5-12 was based on new 2008 Energy Star appliance replacements. Retrofit 2 was based on high performance appliance replacements.

Two lighting retrofit scenarios are illustrated in Table 5-13.

Table 5-13: Lighting Retrofit Values

	Archetype	Retrofit 1	Retrofit 2
Lighting (kWh/m^2/yr)	16	11	9
Equivalent Continuous Lighting (W/m^2)	1.8	1.3	1.0

Lighting retrofit 1, illustrated in Table 5-13, was calculated from Equation 19. (Hendron, R. and Engebrecht, C, 2010)

$$Interior\ Lighting = FFA \times 5.832 + 334 \quad (19)$$

Where Interior Lighting is yearly energy consumption calculated in kWh/yr and FFA is finished floor area calculated in m^2. Retrofit 2 was assumed for a high-performance lighting upgrade that would include light emitting diodes (LED).

5.3.5 Air Leakage Reduction Consequences

Since the window, wall, and roof retrofits presented in Sections 5.3.1 and 5.3.2 would likely result in reduced air leakage, various air leakage reductions need to be considered with these three EEMs. Four air leakage scenarios and their associated percent reduction relative to the Archetype are illustrated in Table 5-14.

Table 5-14: Air Leakage Reduction Scenarios

	Air Leakage Rate ($l/s \cdot m^2$ @ 75 Pa)	Percentage in Air Leakage Reduction relative to Archetype
Archetype	4.58	
Scenario 1	4.12	10%
Scenario 2	3.66	20%
Scenario 3	3.21	30%
Scenario 4	2.75	40%

Table 5-14 illustrates scenarios 1 through 4 correspond to 10%, 20%, 30%, and 40% air leakage reductions, respectively. The range of air leakage rates for these scenarios is from 4.12 to 2.75 $l/s \cdot m^2$ at a 75Pa pressure difference.

Reducing the air leakage can have significant energy saving benefits illustrated in Table 5-17. If air leakage provides the ventilation to a unit then significantly reducing air leakage can result in insufficient ventilation. Insufficient ventilation can result in health consequences that are termed "sick building syndrome". Sick building syndrome was first defined in the late 1970's following reduced ventilation requirements for buildings intended to save energy. Far too often the result was sick occupants. Since the enclosure of the towers is approximately one and a half to two times as leaky as single-family homes (see Section 3.2.5) reducing the air leakage by up to 40% is unlikely to cause sick building syndrome. However, access to ventilation air either through the original design described in Section 3.2.3, an opened window, or a retrofitted ventilation system needs to be ensured when air tightening.

5.3.6 Reduced Domestic Hot Water Usage

The most common and effective way to reduce DHW is to replace faucets and showerheads with low flow fixtures. Reducing the DHW consumption results in reduced DHW heating loads. Two faucet and showerhead retrofit scenarios are illustrated in Table 5-15.

Table 5-15: Faucet and Showerhead Retrofit

	Faucets (l/day/person)	Showerheads (l/day/person)	Reduction relative to Archetype
Archetype	32.6	23.8	
Retrofit 1	22.8	16.7	30%
Retrofit 2	16.3	11.9	50%

Table 5-15 illustrates that retrofit 1 and 2 were assumed to reduce the hot water consumption by 30% and 50%, respectively. The resulting faucet hot water consumption for the retrofits was approximately 23 and 16 l/day per person. The resulting range of showerhead hot water consumption for the retrofits was approximately 17 and 12 l/day per person, respectively.

5.3.7 Energy Efficiency Measures Summary

All of the EEMs described from Section 5.3.1 through 5.3.6 are summarized in Table 5-16.

Table 5-16: Energy Efficiency Measures Description Summary

		Description
Windows	Retrofit 1	Basic double glazed replacement
	Retrofit 2	High performance double glazed replacement
	Retrofit 3	High performance triple glazed replacement
Walls	Retrofit 1 (R10)	Additional R10 interior insulation
	Retrofit 1 (R20)	Additional R20 interior insulation
	Retrofit 2 (R10)	Additional R10 exterior wall insulation
	Retrofit 2 (R20)	Additional R20 exterior wall insulation
	Retrofit 4 (R20)	Additional R20 exterior wall and complete balcony insulation
Roof	Retrofit 1	Additional R10 exterior insulation
	Retrofit 2	Additional R20 exterior insulation
	Retrofit 3	Additional R40 exterior insulation
HVAC	Retrofit 1	Non-condensing boilers and furnace replacement. Basic HRV, window A/C, and central A/C.
	Retrofit 2	Condensing boilers and furnace replacement. High performance HRV, window A/C, and central A/C.
Appliances	Retrofit 1	Basic refrigerator, washer, dryer, dishwasher, and range upgrade.
	Retrofit 2	High performance refrigerator, washer, dryer, dishwasher, and range upgrade.
Lighting	Retrofit 1	Basic CFL upgrade
	Retrofit 2	High performance LED upgrade
Air Leakage	Retrofit 1	10% Air leakage reduction
	Retrofit 2	20% Air leakage reduction
	Retrofit 3	30% Air leakage reduction
	Retrofit 4	40% Air leakage reduction
DHW	Retrofit 1	30% reduction in showerhead and faucet flow
	Retrofit 2	50% reduction in showerhead and faucet flow

The EEMs illustrated in Table 5-16 were modeled in BELA *MURB High-Rise Edition*. The energy consumed, energy saved relative to the hydronically-heated Archetype, and corresponding percent reduction for each of the EEMs are illustrated in Table 5-17. The results relative to the electrically-heated Archetype are illustrated in Appendix E.

Table 5-17: Energy Efficiency Measures Results

		Energy Consumed kWh/yr/m^2	Energy Saved kWh/yr/m^2	Percent Reduction
Archetype		**384**		
Windows	Retrofit 1	368	16	4.3%
	Retrofit 2	362	22	6.1%
	Retrofit 3	355	29	8.2%
Walls	Retrofit 1 (R10)	371	13	3.5%
	Retrofit 1 (R20)	368	16	4.3%
	Retrofit 2 (R10)	364	20	5.5%
	Retrofit 2 (R20)	359	25	7.0%
	Retrofit 4 (R20)	358	26	7.3%
Roof	Retrofit 1	383	1	0.3%
	Retrofit 2	382	2	0.5%
	Retrofit 3	381.6	2.4	0.6%
HVAC	Retrofit 1	313	71	22.7%
	Retrofit 2	283	101	35.7%
Appliances	Retrofit 1	381	3	0.8%
	Retrofit 2	378	6	1.6%
Lighting	Retrofit 1	382	2	0.5%
	Retrofit 2	381	3	0.8%
Air Leakage	Retrofit 1	374	10	2.7%
	Retrofit 2	364	20	5.5%
	Retrofit 3	355	29	8.2%
	Retrofit 4	345	39	11.3%
DHW	Retrofit 1	371	13	3.5%
	Retrofit 2	363	21	5.8%

Based on the results illustrated in Table 5-17, retrofitting individual parts of the towers cannot significantly reduce the annual energy consumption. Individual retrofits may have significant effects on comfort, maintenance, durability, or aesthetics, but alone have little effect on energy. If there is an intention to reduce the high annual energy consumption of the towers, a whole building retrofit approach is required. Retrofit packages were created, simulated, and the results were discussed in Section 5.4.

5.4 Energy Efficiency Measure Retrofit Packages

Three retrofit packages were created based on Section 5.3. The first package is an interior enclosure retrofit with moderate upgrades and was designated as Package A. The second package is an exterior enclosure retrofit with moderate upgrades designated as Package B. The third package is a high-

performance upgrade designated as Package C. The three packages and the selection of EEMs based on Table 5-16 are summarized in Table 5-18.

Table 5-18: Retrofit Package Summary

EEM	Package A	Package B	Package C
Windows	Retrofit 2	Retrofit 2	Retrofit 3
Walls	Retrofit 1 – R20	Retrofit 2 – R20	Retrofit 4 – R20
Roof	Retrofit 2	Retrofit 2	Retrofit 3
HVAC	Retrofit 1	Retrofit 1	Retrofit 2
Appliances	Retrofit 1	Retrofit 1	Retrofit 2
Lighting	Retrofit 1	Retrofit 1	Retrofit 2
Air Leakage	Retrofit 2	Retrofit 3	Retrofit 4
DHW	Retrofit 1	Retrofit 1	Retrofit 2

Table 5-18 illustrates that Package A and B are very similar with modest retrofit options. The only differences are the walls and air leakage. Interior R20 insulation and a corresponding 20% air leakage reduction were assumed for Package A. Exterior R20 insulation on the opaque wall sections only and a corresponding 30% air leakage reduction was assumed for Package B.

Package C has exterior R20 insulation on the opaque wall sections including around the balconies and a corresponding 40% air leakage reduction along with all the other high performance retrofit options. Package C was intended to illustrate the highest performing level of retrofit with current technologies.

5.4.1 Annual Energy Consumption

The annual energy consumptions for the Packages were simulated in BELA *MURB High-Rise Edition* on the hydronically-heated Archetype and the results are presented below. The packages were also simulated on the electrically-heated Archetype and the results were provided in Appendix F.

Retrofit Package A, B, and C simulated annual energy distribution and savings relative to the Archetype are illustrated in Figure 5-21 through Figure 5-23, respectively.

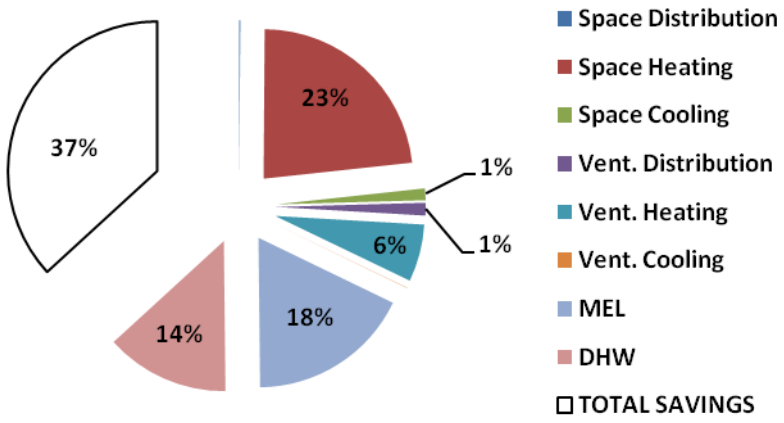

Figure 5-21: Annual Energy Distribution and Savings of Retrofit Package A on the Archetype

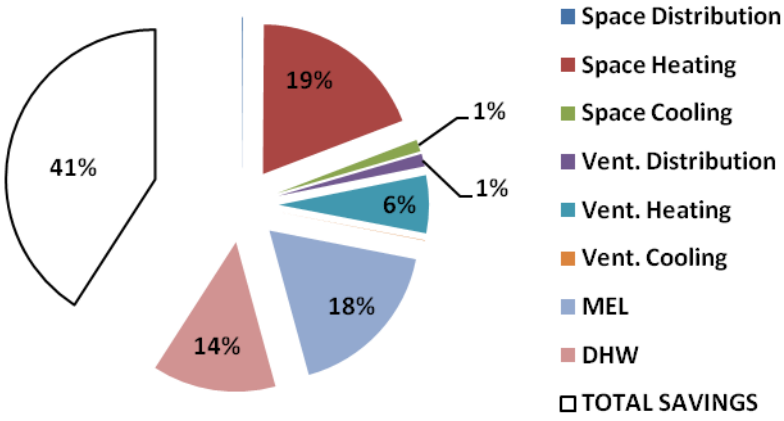

Figure 5-22: Annual Energy Distribution and Savings of Retrofit Package B on the Archetype

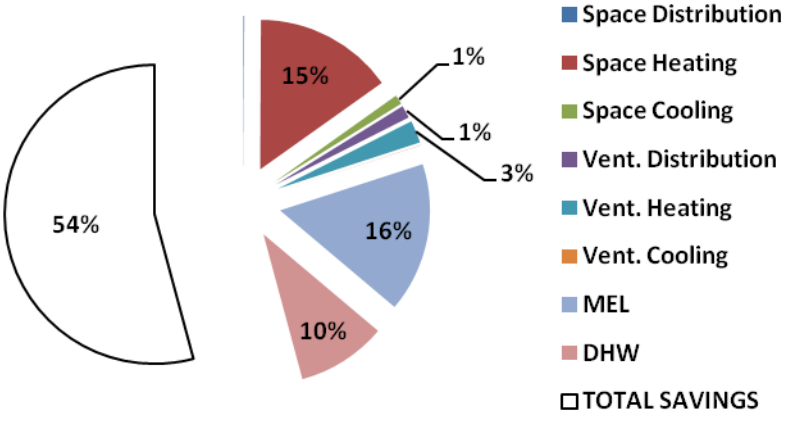

Figure 5-23: Annual Energy Distribution and Savings of Retrofit Package C on the Archetype

Figure 5-21 and Figure 5-22 illustrate that Package A and B each reduces the Archetype's annual energy consumption by approximately 40% with Package B saving 4% more. Package B reduces the space heating demand to approximately the same demand as the MEL. Package C presented in Figure 5-23 illustrates that the largest reduction in annual energy consumption of the Archetype is over 50%.

A comparison of all three packages, a new MURB, and a low-energy MURB are presented in Figure 5-24.

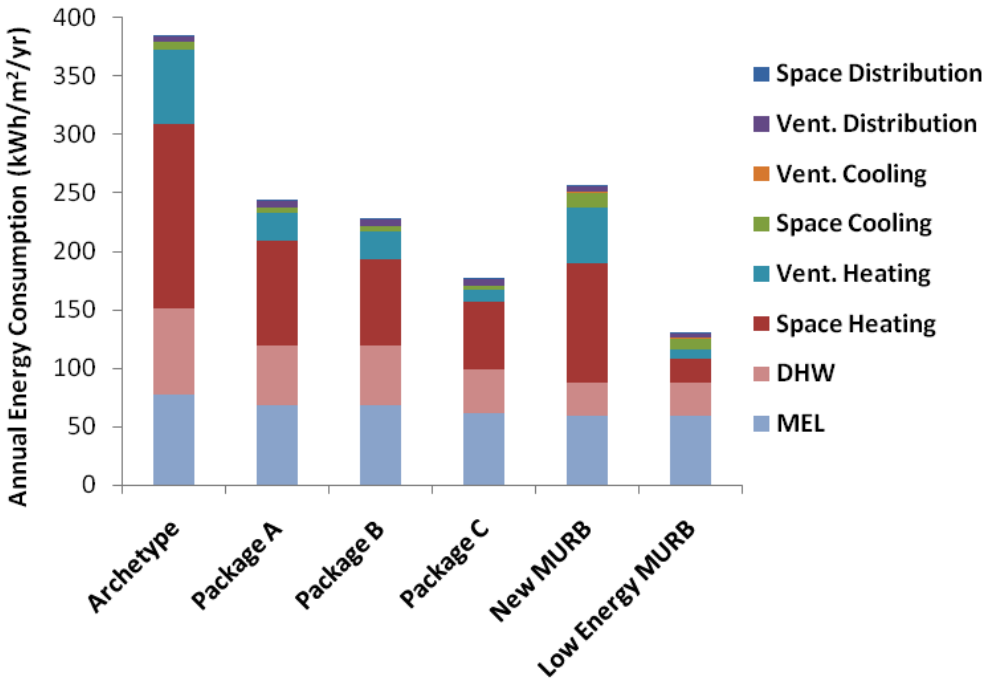

Figure 5-24: Retrofit Package Comparison Relative to the Archetype

Figure 5-24 illustrates Packages A, B, and C reduce the annual energy consumption to approximately 240, 230, and 180 kWh/m^2, respectively. Therefore, an interior retrofit (Package A) reduces the annual energy consumption of the Archetype by almost the same amount as the exterior retrofit (Package B). Although there may only be a small savings in annual energy consumption for an exterior enclosure retrofit, the numerous non-energy-related benefits and consequences must be considered when comparing an exterior and interior enclosure retrofit, as illustrated in Table 5-22. All three retrofit packages can reduce the annual energy consumption below a typical new MURB. The high-performance retrofit package cannot surpass the annual energy consumption of a new low-energy MURB.

5.4.2 Peak Energy Consumption

The reduction in peak energy consumption is also important, particularly for power plants. The peak electricity consumptions for the retrofit packages on the electrically-heated Archetype are illustrated in Figure 5-25.

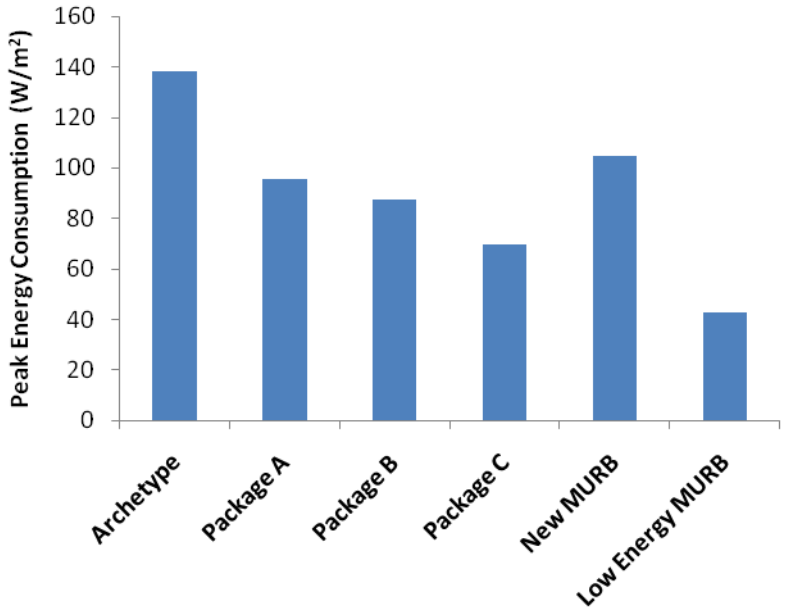

Figure 5-25: Peak Energy Consumption for the Electrically-Heated Archetype

The Archetype has a peak electricity consumption of approximately 140 W/m^2, this occurs in January during the cold conditions of winter. Retrofit Packages A and B reduce the peak electricity consumption by approximately one-third and Package C reduces the peak by approximately half.

The peak gas and electricity consumptions for the retrofit packages on the hydronically-heated Archetype are illustrated in Figure 5-26.

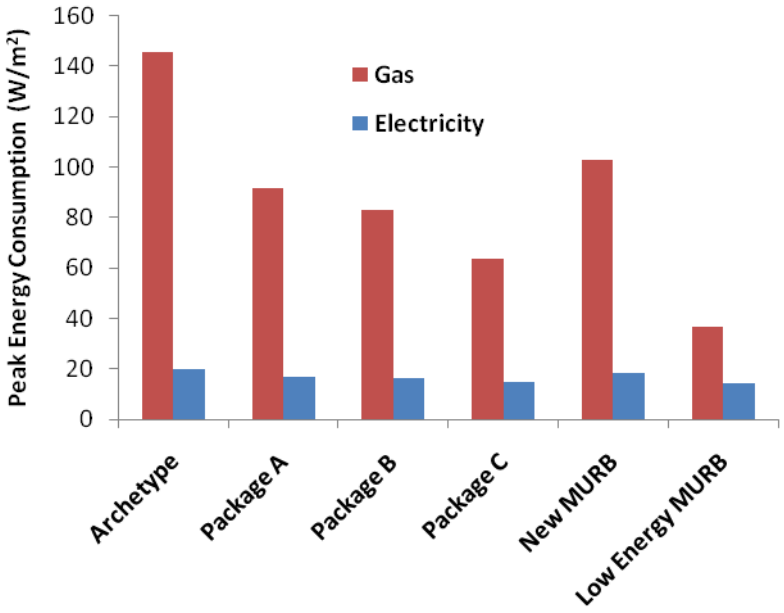

Figure 5-26: Peak Energy Consumption for the Hydronically-Heated Archetype

The peak electricity consumption for the hydronically-heated Archetype is approximately 80% less than the electrically-heated Archetype and occurs in August during the warm conditions of summer. Applying the retrofit packages to the hydronically-heated Archetype has little effect on the peak electricity consumption. The peak natural gas consumption has approximately the same rate of energy consumption as the electricity consumption in the electrically-heated Archetype.

5.5 Impact and Shift in Reduced Greenhouse Gas Emissions

The energy saved by retrofitting the towers with a retrofit package similar to those described above will reduce the amount of energy used by around 40-55%. Any reduction in energy use results in a reduced amount of greenhouse gases (GHG) emitted in the production of that energy.

According to Stewart and Thorne (2010), there are approximately 500,000 units in the 3000 over-four-storey towers in the GGH. Based on simulating the 280 units in the 20 storey Archetype, the average unit uses approximately 27,700 kWh per year of energy. Therefore the 3000 towers consume approximately 13.85 TWh per year (500,000 units times 27,700 kWh/yr) of energy. This is site energy and is divided primarily between electricity and natural gas with corresponding greenhouse gas emissions. If the 3000 towers reduced their annual energy consumption by 40% (Package A) the GGH would save approximately 5,540 GWh per year of equivalent site energy. In terms of understanding this quantity of energy, 1000 two megawatt wind towers (each assumed to produce

5,300 MWh per year assuming a 30% capacity factor) produce nearly the equivalent in electrical energy.

The energy use and GHG emissions of transportation represents a significant portion of Canada's usage and emissions. Improving the living conditions of these urban apartment towers will improve perceptions of urban living. This can lead to a shift in percentage of Canadians living in suburban areas to urban areas which would likely reduce the average commute and general travel by car. This same shift is also likely to decrease the number of trips by cars and increase the number of public transportation trips. Public transportation trips use significantly less energy per capita and emit significantly less GHG than car travel. An increase in the demand for public transportation would likely increase the incentive to construct more public transportation systems thus increasing the shift from car travel to lower energy using and GHG emitting public transportation.

5.6 Durability

5.6.1 Wall Section Temperature Profiles

The temperatures across the Archetype's existing wall section were calculated for two winter conditions and presented in Figure 5-27.

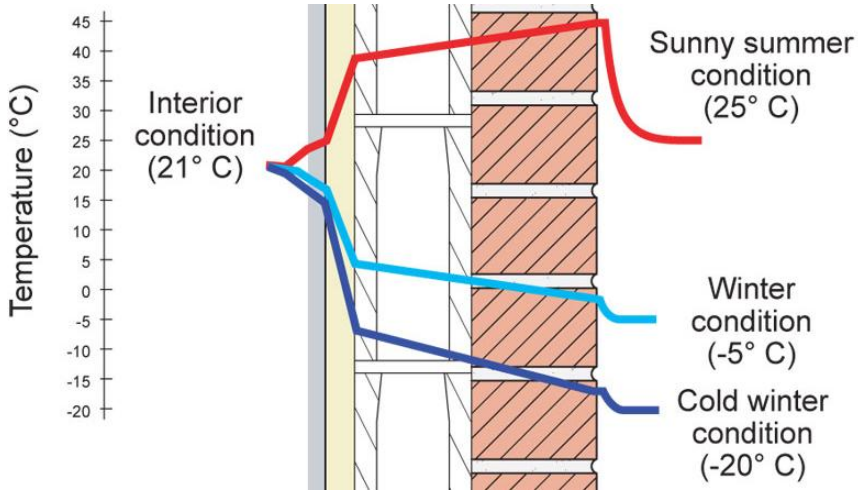

Figure 5-27: Existing Wall Section Winter Temperature Profiles

Figure 5-27 illustrates that during an average winter and cold winter condition the brick experiences temperatures below zero. With the warmer temperatures in the summer or periods of direct solar radiation, the concrete block and brick experiences freeze-thaw temperature swings. When the brick

retains water during freeze-thaw temperature swings the potential for freeze-thaw deterioration is significant. The interior surface of the concrete block experiences temperatures of approximately 2°C to -8°C during typical winter temperatures of -5°C to -20°C. Condensation will form on the concrete block if air with an RH greater than 28% reaches that surface during a typical winter day (-5°C). Frost will form on the concrete block if air with an RH greater than 13% reaches that surface during a typical cold winter day (-20°C).

The temperatures across the wall section with an interior R10 retrofit were calculated for the same two winter conditions and presented in Figure 5-28.

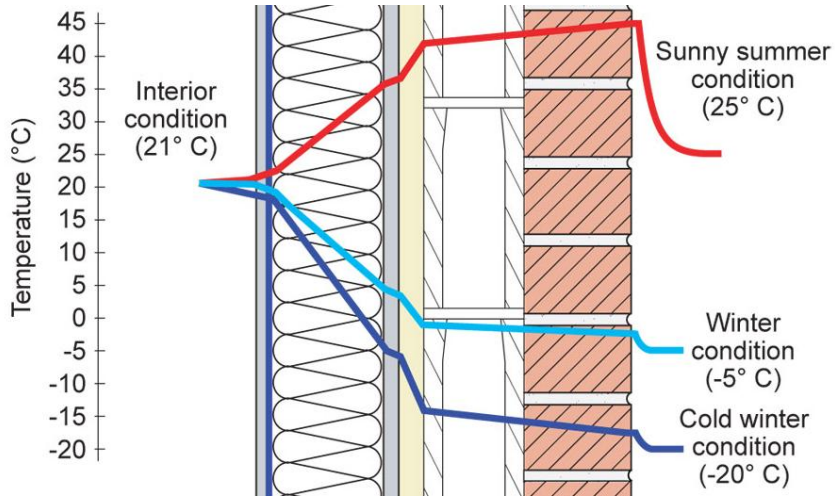

Figure 5-28: Interior R10 Retrofit Wall Section Winter Temperature Profiles

Figure 5-28 illustrates that applying insulation to the interior decreases the temperatures experienced by the concrete block and brick during the winter. Frost can accumulate during a typical winter day (-5°C) on the interior side of the concrete block if interior air with an RH greater than 21% passes around the discontinuous air control layer.

The temperatures across the wall section with an exterior R10 retrofit were calculated for the same two winter conditions and presented in Figure 5-29.

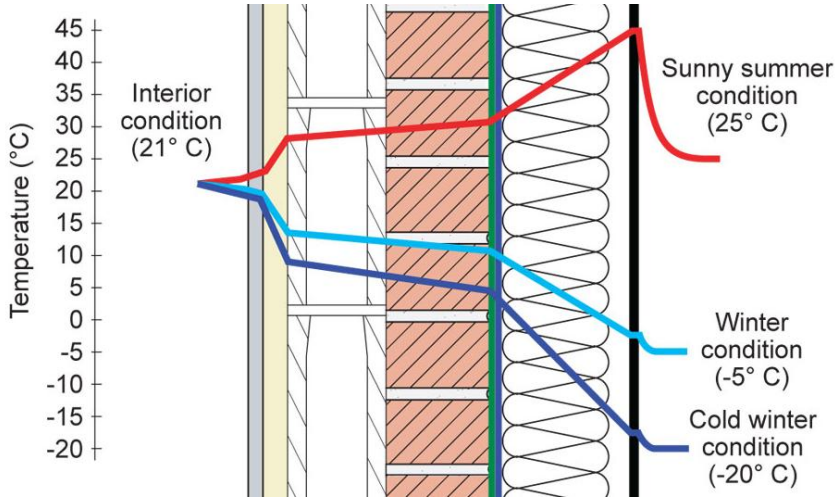

Figure 5-29: Exterior R10 Retrofit Wall Section Winter Temperature Profiles

Figure 5-29 illustrates that applying the insulation to the exterior of the brick decreases the range of temperatures the brick and concrete block experiences. An exterior R10 retrofit ensures the brick does not experience temperatures below approximately 5°C. This would protect the brick from potential freeze-thaw deterioration. The interior concrete block surface would remain above approximately 9°C, eliminating frost potential and limiting condensation to occur only when the interior air has an RH greater than approximately 50%.

5.6.2 Surface Condensation Potential

Insulating the towers enclosure has the potential to reduce surface temperatures which reduces the potential for interior surface condensation. An analysis of the interior surface temperatures for the four enclosure retrofits on the balcony window wall section was completed using Therm. The approach was the same as described in Section 3.1.2. The potential condensation locations have the same designations, illustrated in Figure 3-9, previously used for the Archetype in Section 3.1.4. Window Retrofit 2 (high performance double-glazed) and R10 insulation were used with all four enclosure retrofits. The effectiveness of reducing the potential surface condensation for the retrofits is illustrated in Table 5-19.

Table 5-19: Retrofit Condensation Potential

	Archetype		Retrofit 1		Retrofit 2		Retrofit 3		Retrofit 4	
A	7°C	40%	7°C	40%	10°C	49%	11°C	53%	14°C	64%
B	17°C	78%	19°C	88%	18°C	83%	18°C	83%	19°C	88%
C	-7°C	15%	6°C	38%	9°C	46%	9°C	46%	10°C	49%
D	8°C	43%	14°C	64%	14°C	64%	14°C	64%	15°C	69%
E	-7°C	15%	6°C	38%	11°C	53%	11°C	53%	12°C	56%
F	17°C	78%	19°C	88%	19°C	88%	19°C	88%	19°C	88%
G	12°C	56%	12°C	56%	14°C	64%	14°C	64%	17°C	78%
Lowest	0°C	25%	6°C	38%	9°C	46%	9°C	46%	10°C	49%

Table 5-19 illustrates that all four retrofits increase the lowest interior surface temperature from -7°C to at least 6°C. This is primarily because of the window frame improvement. The Archetype has a poorly performing aluminum window frame and the enclosure retrofits include a high performance frame with the window retrofit used. This reduces the largest potential for interior surface condensation in the Archetype.

The second largest interior surface condensation potential occurs where the concrete slab ceiling meets the top of the interior finish (A). This edge could experience condensation if the interior air's RH is greater than 40%. The interior retrofit (1) does not significantly increase this surface temperature. The exterior wall retrofit increases the surface temperature such that the interior RH would have to exceed 50% for condensation to occur here. Adding insulating all around the balconies increases the surface temperature such that the interior RH would have to exceed 60% for condensation to occur here.

5.7 Thermal Comfort

5.7.1 Operative Temperature

The thermal comfort of an occupant is dependent on three factors: dry bulb air temperature, humidity, and mean radiant temperature (MRT). The HVAC equipment primarily controls the first two factors and the enclosure primarily controls the MRT. The MRT is basically the area weighted average temperature of all the objects surrounding the occupant. The view angles of the surrounding surfaces are used to calculate the MRT. The view angles for an occupant standing one metre from the balcony window wall enclosure section are illustrated in Figure 5-30. The interior floor, wall, and ceiling were assumed to have surface temperatures of 20, 21, and 22°C, respectively.

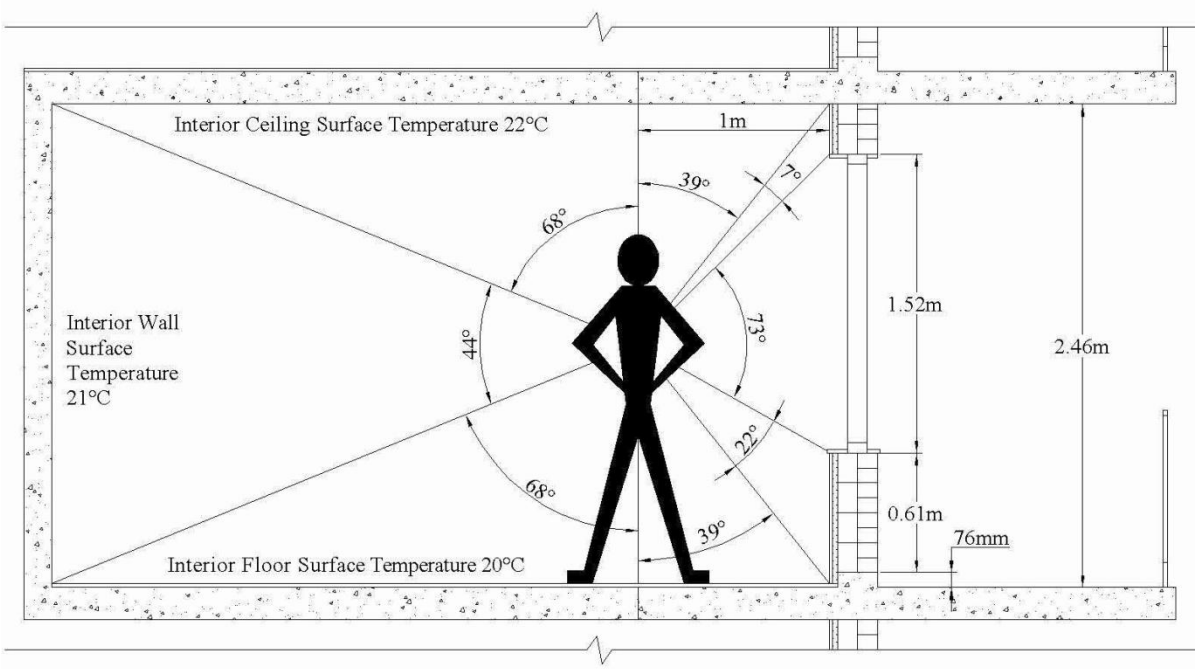

Figure 5-30: Mean Radiant Temperature View Angles

Figure 5-30 illustrates that standing near the exterior wall; approximately half of the occupant's MRT is affected by the enclosure. The 1.52m (5') window accounts for a significant percentage of that. On the interior side of the occupant the slightly warmer ceiling and slightly cooler floor average out to the interior wall's surface temperatures because their respective view angles are the same.

If the temperature and humidity are at comfortable levels, but the surrounding wall surfaces are cold, the occupant will feel cold on account of the radiant heat loss to the wall. The operative temperature can provide a measure of the comfort of an occupant in a building's space. It is calculated by taking the weighted average of the MRT and the ambient air temperature using the linear radiative and convective heat transfer coefficients, respectively. ASHRAE (2009) calculates the operative temperature using Equation 20.

$$t_o = \frac{h_r \bar{t_r} + h_c t_a}{h_r + h_c} \quad (20)$$

Where t_o = operative temperature, (°C)

h_r = linear radiative heat transfer coefficient, W/(m^2·K)

h_c = convective heat transfer coefficient, W/(m^2·K)

t_r = mean radiant temperature, (°C)

t_a = ambient air temperature, (°C)

For calm indoor conditions, h_r and h_c are approximately equal, which simplifies the calculation of the operative temperature to the average of the MRT and ambient air temperature. The simplified, linear form for calculating MRT according to ASHRAE (2009) is illustrated in Equation 21.

$$\bar{t_r} = t_1 F_{p-1} + t_2 F_{p-2} + \cdots + t_N F_{p-N} \quad (21)$$

Where t_r = mean radiant temperature, (°C)

t_n = surface temperature of surface n, (°C)

$F_{p\text{-}n}$ = angle factor between a person and surface n.

The surface temperatures were obtained from the same Therm model used to calculate the condensation potential in Section 5.6.2. The angle factors were calculated based on Figure 5-30.

The Archetype, enclosure Retrofit 2, and enclosure Retrofit 4 were modeled. The retrofits include Window Retrofit 2 (high-performance double-glazed). The enclosure sections were modeled with an exterior temperature of -20°C and additional retrofit insulation equivalent to R10. The surface temperatures, calculated MRT, and calculated operative temperature are illustrated in Table 5-20 and Table 5-21 for the balcony window wall section and balcony wall section, respectively.

Table 5-20: MRT and Operative Temperatures for the Balcony Window Wall Section

		Archetype	Retrofit 2	Retrofit 4
	View Angle	Temp. (°C)	Temp. (°C)	Temp. (°C)
Ceiling*	39°	16.9	17.8	19.0
Headwall	7°	17	18	19
Window	73°	7.8	14.4	14.6
Kneewall	22°	17.4	18.5	19.2
Floor*	39°	17.8	18.3	19.3
Reverse	180°	21	21	21
MRT		17.2	18.8	19.2
Operative		**19.1**	**19.9**	**20.1**

***Average within 1m of wall**

Table 5-21: MRT and Operative Temperatures for the Balcony Wall Section

		Archetype	Retrofit 2	Retrofit 4
	View Angle	Temp. (°C)	Temp. (°C)	Temp. (°C)
Ceiling*	39°	17.3	18.4	19.6
Wall	102°	17.3	19.2	19.6
Floor*	39°	18	18.6	19.6
Reverse	180°	21	21	21
MRT		19.2	19.9	20.3
Operative		**20.1**	**20.5**	**20.7**

***Average within 1m of wall**

Table 5-20 illustrates that the window replacement approximately doubles its surface temperature which significantly contributes to the nearly one degree improvement in operative temperature for Retrofit 2. Both tables illustrate that choosing to insulate around the balconies (Retrofit 4 versus Retrofit 2) improves the operative temperature by approximately 1%.

5.7.2 Passive Comfort during Electrical or Mechanical Failures

During cold periods, the poor enclosure thermal resistance of the towers results in many poor performance issues previously described. These problems assumed a functioning heating system. If the heating equipment fails during cold periods the poor thermal resistance puts the towers at another disadvantage, a lack of passive comfort.

During the winter of 2011 a power outage at a Toronto apartment tower forced approximately 1000 occupants to seek warmer shelter (Globe and Mail, 2011). If the towers enclosure had more thermal resistance, the rate of heat loss would be reduced and the internal gains from occupants, thermal mass, and maybe candles could have possibly maintained a temperature comfortable enough for the occupants to remain in the towers until the heating equipment was fixed.

5.8 Interior versus Exterior Enclosure Retrofit Comparison

One of the main differences between the enclosure retrofits is the interior option (Retrofit 1) versus the exterior option (Retrofits 2, 3, and 4). The differences are summarized in Table 5-22 for a number of criteria and include criteria previously discussed throughout Chapter 5.

Table 5-22: General Interior versus Exterior Retrofit Comparison

Criteria	Interior Retrofit	Exterior Retrofit
Control Layers (Section 5.1.1)	Discontinuous	**Continuous**
Rainscreen Opportunity	No	**Yes**
Moisture Tolerant Materials (Section 5.1.2)	**Not required**	Required
Effective Thermal Resistance (Section 5.2.5)	Significant reduction in effective value	**2 to 4 times more effective than interior**
Annual Energy Consumption (Section 5.3.7)	Uses more energy	**Saves approximately 10 kWh/m^2/year or 3% more than interior**
Brick Durability (Section 5.6.1)	Less durable	**Significantly more durable**
Condensation Potential (Section 5.6.2)	Potential improvement	**Significantly Improved**
Aesthetics (Curb Appeal)	No opportunity for improvement	**Opportunity for improvement**
Economies of scale	Good	**Better**
Construction interference to occupants	Significant	**Minimal**
Construction displacement of tenants	Yes	**No**
Construction scaffolding required	**No**	Yes
Construction weather sensitive	**No**	Yes
Finished Floor Area	Reduced	**Unaffected or potentially increased**

Table 5-22 illustrates a significant overall advantage for the exterior retrofit. The small number of disadvantages includes the constructions sensitivity to weather, the requirement for scaffolding, and exterior insulation materials can't be susceptible to weather.

5.9 Summary

Retrofitting the enclosure can provide better definition and performance of air, vapour, heat, and moisture control. Choosing a rainscreen exterior enclosure retrofit can result in a significantly more durable wall, extending the buildings expected useful life by protecting the masonry and concrete structure. Insulating on the interior can significantly reduce the effective thermal resistance. Insulating around the balconies adds only minimal effective thermal resistance. Reducing the conductive heat loss through the enclosure by overcladding the towers is not likely to reduce the annual energy consumption beyond 8%, but the resulting reduction in air leakage could be upwards of 10%. A packaged retrofit of the towers is significantly more effective in reducing annual energy consumption. A 40% reduction in annual energy consumption is very reasonable and a 60% reduction

could be approached with the latest technologies, excluding any on-site power generation. The benefits of exterior enclosure retrofits are significant in many other ways including: improved occupant comfort, reduced interstitial and surface condensation potential, minimal disruption, and opportunities for improved aesthetics.

Chapter 6 – Conclusions and Recommendations

6.1 Conclusions

Studies have shown that there are a large number of post-World War II high-rise apartment towers in North America and especially in parts of Canada. The Greater Golden Horseshoe, in Ontario, has approximately 3000 greater than four stories that are home to approximately 1,000,000 people. Significant deterioration exists in these towers including life safety concerns that need to be addressed immediately. The deterioration presents two main options: demolish and construct a new building or retrofit. A retrofit can extend the lifespan of the towers, improve comfort, improve durability, reduce energy and associated greenhouse gas emissions. Residential space heating accounts for a significant percentage of Canada's energy use. The space heating reduction rate for apartments is less than that of single family detached and attached residences. The significant number of towers that require retrofits presents an opportunity to also reduce apartment space heating loads at a rate similar to the other residential types.

These towers usually have fourteen units per storey comprised of mostly two bedroom units, followed by one bedroom, then bachelor units. The average sizes of these units are approximately $70m^2$ ($750ft^2$), $50m^2$ ($550ft^2$), and $35m^2$ ($375ft^2$), respectively. Half of the average tower's perimeter consists of a balcony wall section, although this varies significantly. They have approximately 30% window to wall ratio and the typical rectangular plan dimension are 15m (50ft) wide by 70m (230ft) long. The towers floor to floor height is consistently 2.64m (8'-8"). The windows are generally double-glazed with aluminum frames. The opaque wall and roof sections have effective thermal resistance of approximately $0.9W/m^2{\cdot}k$ (R5) and $1.7W/m^2{\cdot}k$ (R10), respectively. The towers air leakage varies significantly around $4.6l/s{\cdot}m^2$ at 75Pa and their height and lack of compartmentalization makes them susceptible to significant stack effect and wind pressures.

The predicted annual energy consumption of the towers is approximately $390kWh/m^2$ and $350kWh/m^2$ for the hydronically- and electrically-heated variants. This can of course vary significantly. The energy consumption is approximately divided into: 40% space heating, 20% ventilation heating, 20% domestic hot water use, and 20% electrical loads such as appliances and lighting. The space cooling, hydronic space heating distribution, and ventilation cooling and distribution energy are a small contribution to overall energy use. The winter space heating loads are comprised of approximately 40% conduction, 40% infiltration, and 20% ventilation.

Because of thermal bridging, adding insulation to the enclosure results in an additional effective thermal resistance less than the amount added. Insulating the interior of the enclosure walls is 25 to 40% effective. Insulating only the vertical parts of exterior walls is 75 to 80% effective; continuing this insulation along the underside of the protruding concrete balcony slab has little effect. Insulating the exterior including around the tops and bottoms of balconies allows the overall insulation value to reach 90 to 100% of its rated thermal resistance.

Individual Energy Efficiency Measures (EEMs) have little effect on the overall annual energy consumption of the average tower, however a tower that has a specific unusual deficiency could significantly reduce its annual energy consumption for an EEM that addresses the lacking condition. The estimated total annual energy reductions on the average tower for the following EEMs are:

- 20-40% for HVAC equipment replacement
- 4-8% for replacing windows (excludes air leakage reduction)
- 4-8% for insulating the enclosure walls (excludes air leakage reduction)
- 5-10% for air sealing/air leakage reduction consequences (varies significantly)
- 3-6% for installing low flow fixtures
- 1-2% for improving appliances
- 1% for retrofitting lighting with energy efficient bulbs

As only 60% of the pre-retrofit energy consumption is heating and cooling retrofits of enclosures and mechanical systems can only reduce total energy consumption by about 40%. Appliances, lighting, and DHW must be part of any more aggressive reduction strategies. A retrofit package using a number of mid-range EEMs could save approximately 40% for both interior and the slightly better performing exterior option. A retrofit package using high performance EEMs could save the annual energy consumption of the average tower by more than 50%. If an existing tower consumes significantly more energy for certain purpose, targeted EEMs could result in larger savings.

Enclosure retrofits have many more significant benefits, especially exterior enclosure retrofits. The interior retrofit and existing condition allow the brick to experience an annual 60°C temperature range and cold weather temperatures well below freezing. An exterior 1.76W/m^2·k (R10) retrofit can reduce the annual range of temperatures experienced by the brick to 35°C and maintain the bricks

temperature over 5°C, eliminating the potential for freeze-thaw deterioration. With the addition of a high performance double-glazed, fiberglass-framed window replacement, the maximum interior relative humidity can increase from 25% to 50% before the potential of surface condensation. This retrofit can also improve the occupant's thermal comfort by increasing the operative temperature by one degree Celsius. Adding thermal insulation also increases the passive thermal control; providing occupants adequate thermal comfort during a mechanical heating failure.

The benefits of an exterior enclosure retrofit that cannot be achieved by an interior enclosure retrofit include providing continuous control layers to manage water, vapour, air, and heat effectively, improving rain water management, eliminating the risk of freeze-thaw, improvement of aesthetics or curb appeal, avoidance of tenant displacement, and maintenance of the finished floor area. The exterior enclosure retrofit reduces heat loss, annual energy consumption, condensation potential, and occupant interference more than an interior retrofit. The limited disadvantages include required construction scaffolding, weather sensitive construction, and the need for moisture tolerant insulation materials.

6.2 Recommendations

Since the feasibility of the retrofit options depends on current economics, a cost estimate should be completed for implementing the retrofit packages on the buildings under consideration. Cost estimates for the buildings under consideration for all the retrofit packages would provide decision makers with the means to determine the most energy savings for a given expenditure. This could then be compared to other policy decisions such as implementing stricter codes for new buildings, subsidizing renewable energy, or supporting programs to retrofit existing buildings.

More testing of overall air leakage characteristics in the towers would provide more confidence in the average overall air leakage characteristics. More accurate air leakage values would add to the accuracy in estimating the effects of existing air leakage and associated retrofits.

The adaptation of BELA to be used for simulating conditions within an individual unit could be useful in determining the comfort of an occupant within a suite. It could also be used to estimate energy consumption for a single suite.

Monitoring actual energy usage of retrofitted towers would determine the amount that BELA *MURB High-Rise Edition* under or overestimates the energy consumption. Measured energy usage results would also confirm the impact of retrofitting other towers.

References

ASHRAE, *Standard 62.1: Ventilation for Acceptable Indoor Air Quality.* Atlanta: American Society of Heating, Refrigerating, and Air Conditioning Engineers, Inc., 2007.

ASHRAE, *ASHRAE Handbook – Fundamentals.* Atlanta: American Society of Heating, Refrigerating, and Air Conditioning Engineers, Inc., 2009.

Barakat, S., *Net Energy Contribution of Domestic Water Use to House Heating Requirements*, Division of Building Research, National Research Council of Canada, Ottawa, March 1984.

Blake, P., *The Master Builders: Le Corbusier, Mies Van Der Rohe, Frank Lloyd Wright*, Norton & Company, New York, 1976

Bohac, D.L., Fitzgerald, J.E., and Grimsrud, D., Hewett, M.J., "Measured Change in Multifamily Unit Air Leakage and Airflow Due to Air Sealing and Ventilation Treatments". *American Society of Heating, Refrigerating and Air-Conditioning Engineers*, 2007.

Bronsema, N. *Solar Equations.* University of Waterloo, Waterloo ON, 2009.

CMHC, *Air Tightness, Air Movement and Indoor Air Quality in British Columbia High-Rise Apartment Buildings*, Technical Series 90-232, Canada Mortgage and Housing Corporation, Ottawa ON, 1990.

CMHC, *Air Tightness, Air Movement and Indoor Air Quality in Quebec High-Rise Apartment Buildings*, Technical Series 91-205, Canada Mortgage and Housing Corporation, Ottawa ON, 1991.

CMHC, *Air Tightness, Air Movement, and Indoor Air Quality in High Rise Buildings*, Technical Series 96-220, Canada Mortgage and Housing Corporation, Ottawa ON, 1996.

CMHC, *Air Leakage Characteristics, Test Methods and Specifications for Large Buildings*, Technical Series 01-123, Canada Mortgage and Housing Corporation, Ottawa ON, 2001 (revised 2007).

CMHC, *Analysis of the Annual Energy and Water Consumption of Apartment Buildings in the CMHC HiSTAR Database*, Technical Series 01-142, Canada Mortgage and Housing Corporation, Ottawa ON, 2001

CMHC, *Ventilation Systems for Multi-Unit Residential Buildings: Performance Requirements and Alternative Approaches,* Technical Series 03-121, Canada Mortgage and Housing Corporation, Ottawa ON, 2003.

CMHC, *Energy and Water Consumption Load Profiles in Multi-Unit Residential Buildings*, Technical Series 05-119, Canada Mortgage and Housing Corporation, Ottawa ON, December 2005.

CMHC, *Brick Cladding Repairs – Ottawa, Ontario*, Better Buildings – Case Study Number 61, Canada Mortgage and Housing Corporation, Ottawa ON, September 2006.

CMHC, *Air Leakage Control Manual for Existing Multi-Unit Residential Buildings*, Canada Mortgage and Housing Corporation, Ottawa ON, December 2007.

CMHC, *Repair of Deteriorated Balcony Slabs*. Better Buildings - Case Study Number 11, Canada Mortgage and Housing Corporation, Ottawa ON, No Date.

DeOreo, W. and Mayer, P., *The End Uses of Hot Water in Single Family Homes from Flow Trace Analysis,* Aquacraft Incorporated, Water Engineering and Management, 1999

Diamond, R.C., Feustel, H.E., and Matson, N.E. *Energy-Efficient Ventilation for Apartment Buildings* U.S. Department of Energy Rebuild America Guide, 1999

Elert G., The Physics HyperTextbook, http://physics.info/conduction/, October 24, 2010

Enermodal, *Monitored Performance of an Innovative Multi-Unit Residential Building*, Enermodal Engineering Limited, Kitchener ON, September 2002

Enermodal, *Green House Gas Emission Reduction Potential within the Multi-Unit Residential Buildings of the HiSTAR Database*, Enermodal Engineering Limited, Kitchener ON, March 2005

The Engineering Tool Box, http://www.engineeringtoolbox.com/thermal-conductivity-d_429.html, October 17, 2010.

Globe and Mail, "Power outage forces about 1,000 out of Toronto apartment building overnight", article 1878153, January 20, 2011.

Hanam, B., *Development of an Open Source Hourly Building Energy Modeling Software Tool* (Master's thesis). University of Waterloo, Waterloo ON, 2010.

Hendron, R. And Engebrecht, C., *Building America House Simulation Protocol*, National Renewable Energy Laboratory, Building America United States Department of Energy, September 2010.

Hutcheon, N., *Principles Applied to an Insulated Masonry Wall.* Canadian Building Digest 50, National Research Council Canada, February 1964.

IPCC, *Climate Change 2007: Synthesis Report*. Intergovernmental Panel on Climate Change, Valencia, Spain, November 2007.

Kesik, T. And Saleff, I., *Tower Renewal Guidelines: For the Comprehensive Retrofit of Multi-Unit Residential Buildings in Cold Climates*, Daniels Faculty of Architecture, Landscape, and Design, University of Toronto, 2009.

Knight, I., Kreutzer, N., Manning, M., Swinton, M., And Ribberink, H., *European and Canadian non-HVAC Electric and DHW Load Profiles for Use in Simulating the Performance of Residential Cogeneration Systems,* Annex 42 of the International Energy Agency Energy Conservation in Buildings and Community Systems Program, May 2007.

Kosmatka, Steven H.; Kerkhoff, Beatrix; Panarese, William C.; MacLeod, Norman F.; and McGrath, Richard J., *Design and Control of Concrete Mixtures*, EB101, 7th Edition, Cement Association of Canada, Ottawa, Ontario, Canada, 2002, 368 pages.

LBNL, THERM Finite Element Simulator Version 5.2, Regents of the University of California, Lawrence Berkley National Laboratories, 2003.

LBNL, *Indoor-Outdoor Air Leakage of Apartments and Commercial Buildings,* PIER Final Project Report, CEC-500-2006-111, Lawrence Berkley National Laboratories, December 2006.

LBNL, *Energy-Efficient Ventilation for Apartment Buildings*, Rebuild America, U.S. Department of Energy, Lawrence Berkley National Laboratories, No Date.

Lstiburek, J., *Pressures in Buildings*. Building Science Digest 109, Building Science Press, BuildingScience.com, October 25, 2006.

Mackay, D., *Sustainable Energy – without the hot air*, UIT Cambridge Ltd., England, 2009

Melanson, T., "Portrait of a beleaguered tenant", *Globe and Mail*, January, 12, 2011

Mensinga, P., *Determining the Critical Degree of Saturation of Brick Using Frost Dilatometry* (Master's thesis). University of Waterloo, Waterloo ON, 2009.

McGuinness, W. and Stein, B., *Mechanical and Electrical Equipment for Buildings 5th Edition*, 1971.

NRCan, *Energy Efficiency Trends in Canada 1990 to 2005*, Natural Resources Canada, Her Majesty the Queen in Right of Canada, 2008.

NRCan, *Residential Appliance Unit Energy Consumption (UEC)*, http://oee.nrcan.gc.ca/corporate/statistics/neud/dpa/tableshandbook2/res_00_16_e_4.cfm?attr=0 Natural Resources Canada, March 28, 2011.

NRCan, *Comprehensive Energy Use Database,* Table 46, http://oee.nrcan.gc.ca/corporate/statistics/neud/dpa/trends_res_ca.cfm, Natural Resources Canada, March 28, 2011.

Paperny, A., "Toronto increasingly becoming a city of vertical poverty", *Globe and Mail*, January 12, 2011.

Proskiw, G. and Phillips, B., *Characterizing Air Pressure/Air Movement Patterns in Multi-Unit Residential Buildings*, prepared for Canadian Mortgage and Housing Corporation, 2006.

RDH, *Energy Consumption and Conservation in Mid and High Rise Residential Buildings in British Columbia Report #1: Energy Consumption and Trends*, RDH Building Engineering Ltd., Vancouver BC, February 10, 2009.

Shaw, C.Y., Gasparetto, S., and Reardon, J.T., "Methods for Measuring Air Leakage in High-Rise Apartments," *Air Change Rate and Airtightness in Buildings, ASTM STP 1067*, M. H. Sherman, Ed., American Society for Testing and Materials, Philadelphia, 1990, pp. 222-230.

Shaw, C. and Tamura, G., "The Calculation of Air Infiltration Rates Caused By Wind and Stack Action for Tall Buildings". *ASHRAE Transactions,* Volume 83, Part 2, 1977, pp. 145-158.

Sherman, M.H. and Modera, M.P., "Comparison of Measured and Predicted Infiltration Using the LBL Infiltration Model," *Measured Air Leakage of Buildings, ASTM STP 904,* H.R. Trechsel and P.L. Lagus, Eds., American Society for Testing and Materials, Philadelphia, 1986, pp. 325-347.

Stewart, G. and Thorne, J., *Tower Neighbourhood Renewal in the Greater Golden Horseshoe – An Analysis of High-Rise Apartment Tower Neighbourhoods Developed in the Post-War Boom (1945-1984),* E.R.A. Architects, planningAlliance, and the Cities Centre at the University of Toronto, November 2010.

Straube, J. and Burnett, E., *Building Science for Building Enclosures*. Building Science Press, Westford MA, 2005

Suleiman, B., *Thermal Conductivity of Saturated Samples Using the Hot-Disk Technique.* University of Sharjah, UAE, Proceedings of the 4th WSEAS International Conference, Elounda, Greece, August 21-23, 2006.

Tamura, G. and Wilson, A., "Pressure Differences Caused By Chimney Effect in Three Buildings". *ASHRAE Transactions*, Volume 73, Part 2, 1967

TCHC, Personal Communication with Colin Shane, Byrne Engineering Inc., Burlington, Ontario, February 12, 2010

Waide, P., *High-Rise Refurbishment, The energy-efficient upgrade of multi-story residences in the European Union*, International Energy Agency, November 2006

Wikipedia, http://en.wikipedia.org/wiki/Retrofitting/, Retrofitting, March 7, 2011

*Appendix A - Inventory and Location of Apartment Towers in the GGH (*Stewart, G. and Thorne, J., 2010*)*

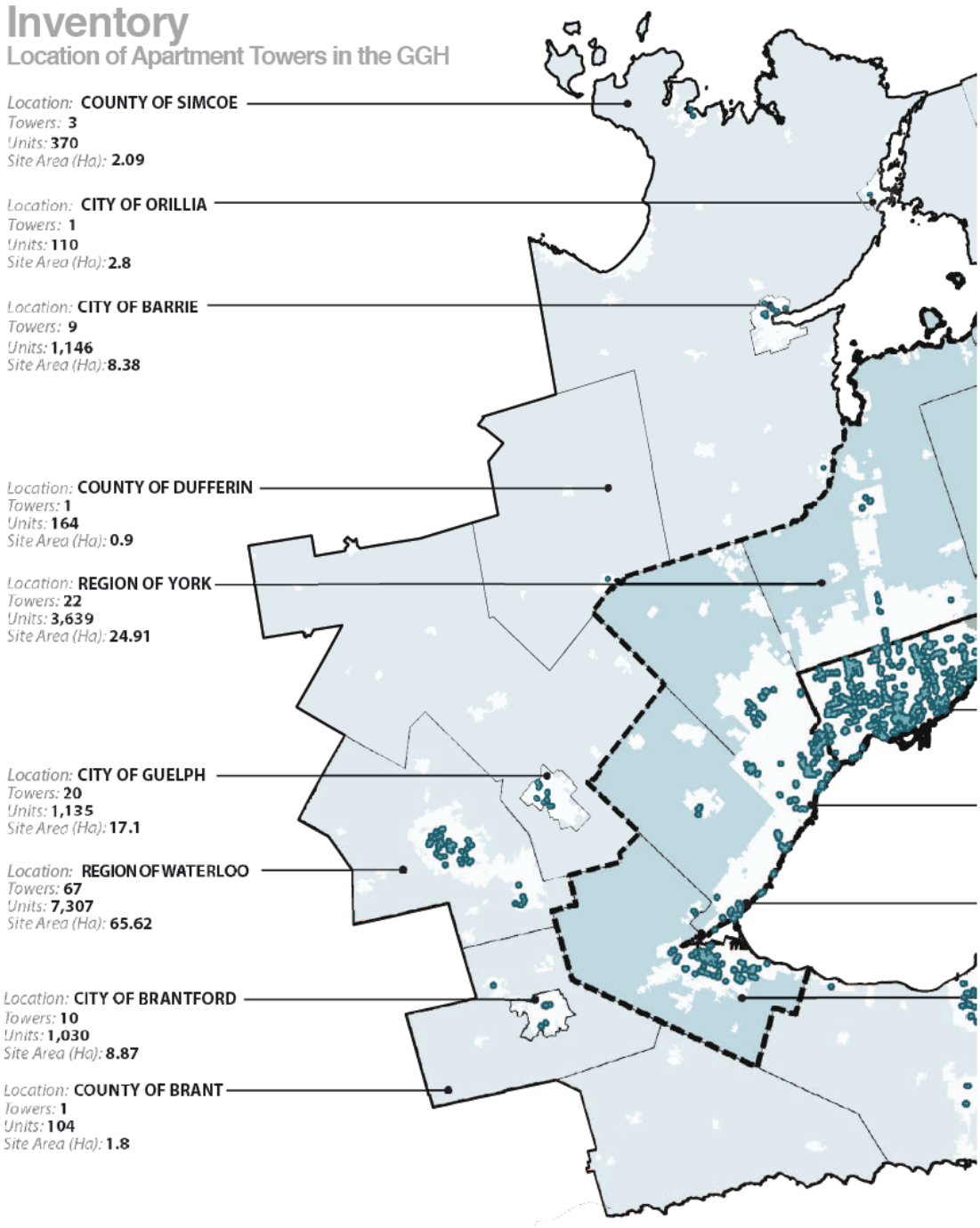

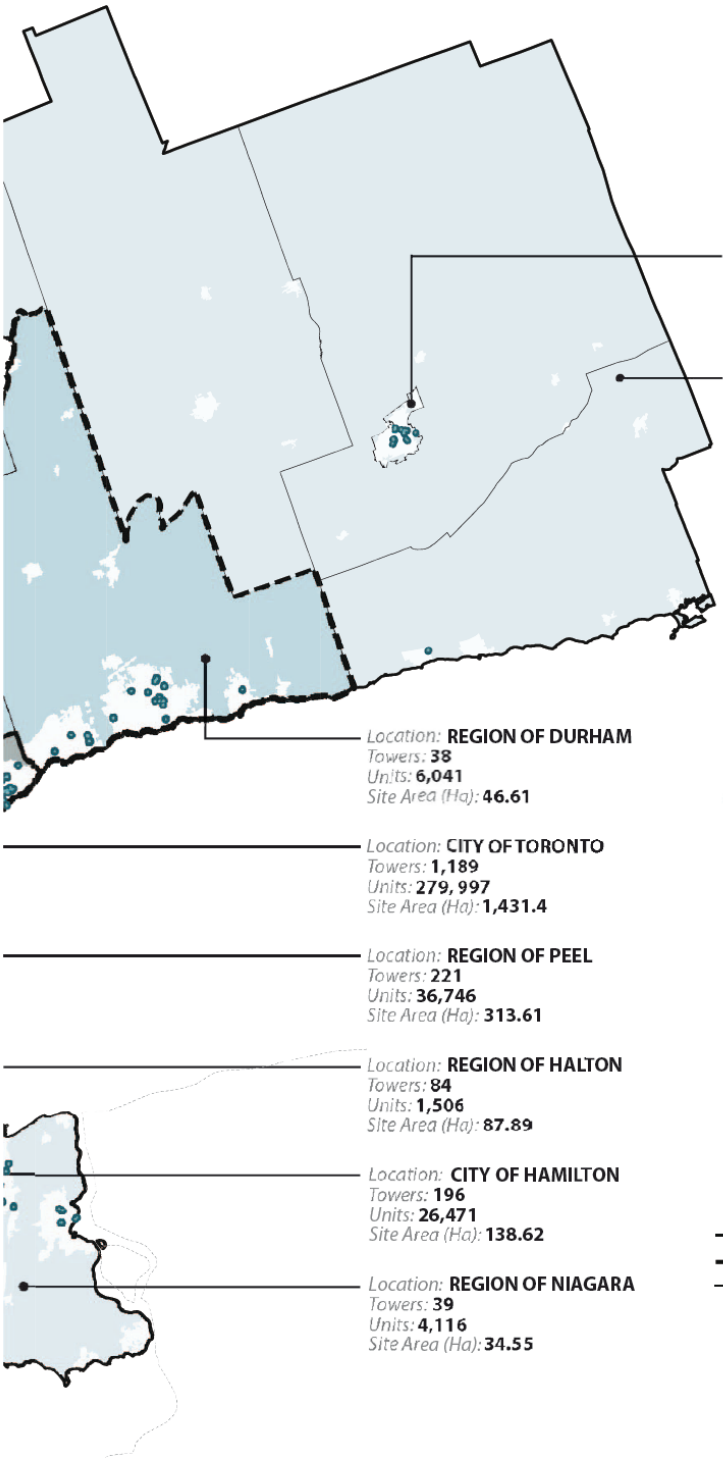

Location: **CITY OF PETERBOROUGH**
Towers: **22**
Units: **2,058**
Site Area (Ha): **19.5**

Location: **COUNTY OF NORTHUMBERLAND**
Towers: **2**
Units: **1,294**
Site Area (Ha): **4.23**

Location: **REGION OF DURHAM**
Towers: **38**
Units: **6,041**
Site Area (Ha): **46.61**

Location: **CITY OF TORONTO**
Towers: **1,189**
Units: **279, 997**
Site Area (Ha): **1,431.4**

Location: **REGION OF PEEL**
Towers: **221**
Units: **36,746**
Site Area (Ha): **313.61**

Location: **REGION OF HALTON**
Towers: **84**
Units: **1,506**
Site Area (Ha): **87.89**

Location: **CITY OF HAMILTON**
Towers: **196**
Units: **26,471**
Site Area (Ha): **138.62**

Location: **REGION OF NIAGARA**
Towers: **39**
Units: **4,116**
Site Area (Ha): **34.55**

Apartment Towers in the Greater Golden Horseshoe:

Greater Golden Horseshoe (GGH):
Towers: **1,925**
Units: **383,838**
Site Area (Ha): **2,209.1**

Greater Toronto and Hamilton Area (GTHA):
Towers: **1,752**
Units: **364,518**
Site Area (Ha): **2,043.2**

GTHA without Toronto:
Towers: **563**
Units: **84,521**
Site Area (Ha): **611.8**

Toronto:
Towers: **1,189**
Units: **279,997**
Site Area (Ha): **1,431.4**

The Outer Ring of the GGH:
Towers: **173**
Units: **19,320**
Site Area (Ha): **165. 9**

Legend

- **Apartment Towers (Not to Scale)**
- **Delineated built up areas**
- **Greater Golden Horseshoe (GGH)**
- **Greater Toronto and Hamilton Area (GTHA)**
- **Boundary of upper and single-tier municipalities**
- **Outer Ring of the GGH**
- **GTHA without Toronto**
- **Toronto**

Base layers for this map, as well as designated Greenbelt Areas and Urban Growth Centre Locations provided by the Ministry of Infrastructure and the Ministry of Municipal Affairs and Housing of the Ontario government.

Appendix B – Building Drawings (TCHC, 2010)

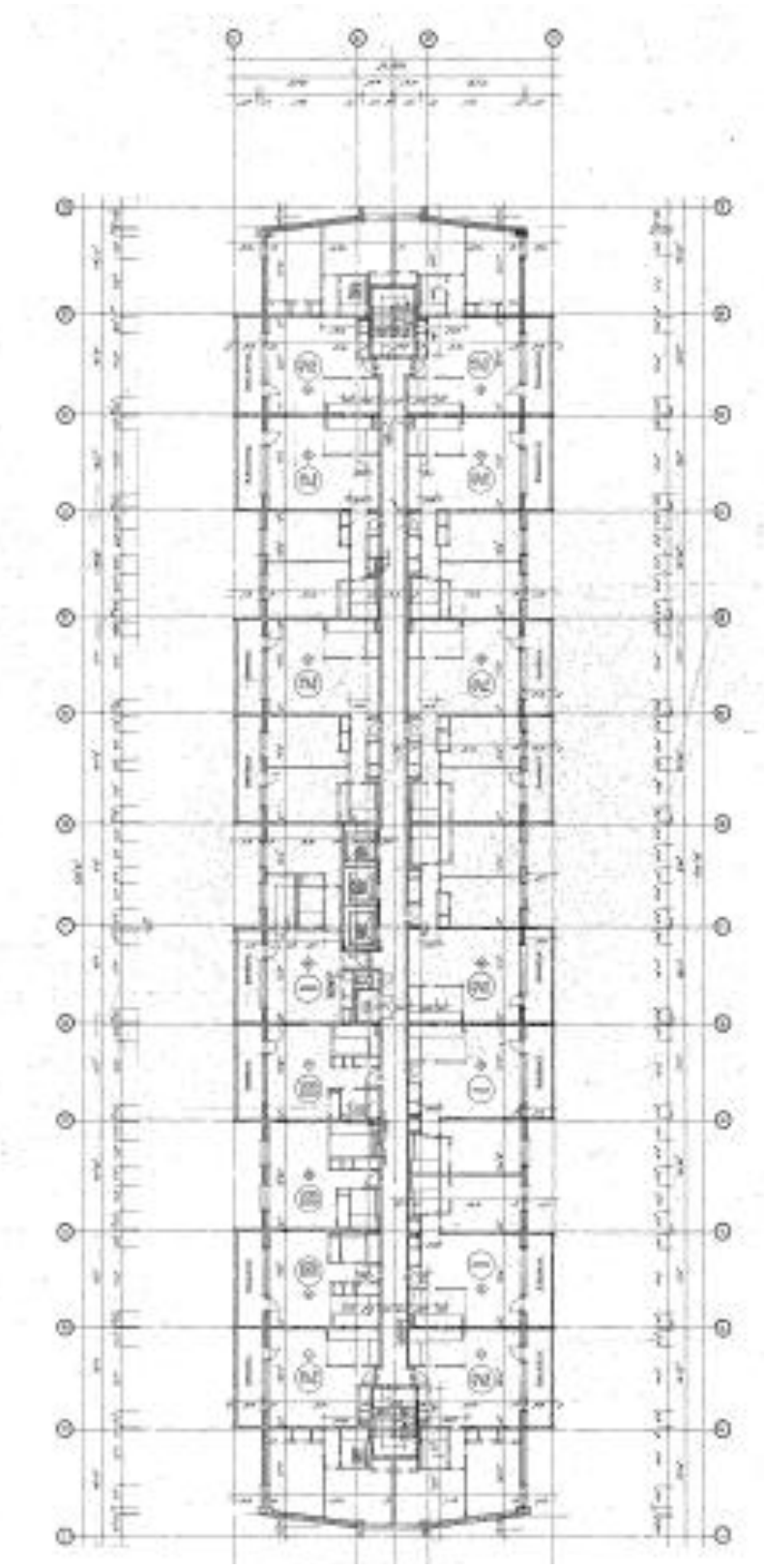

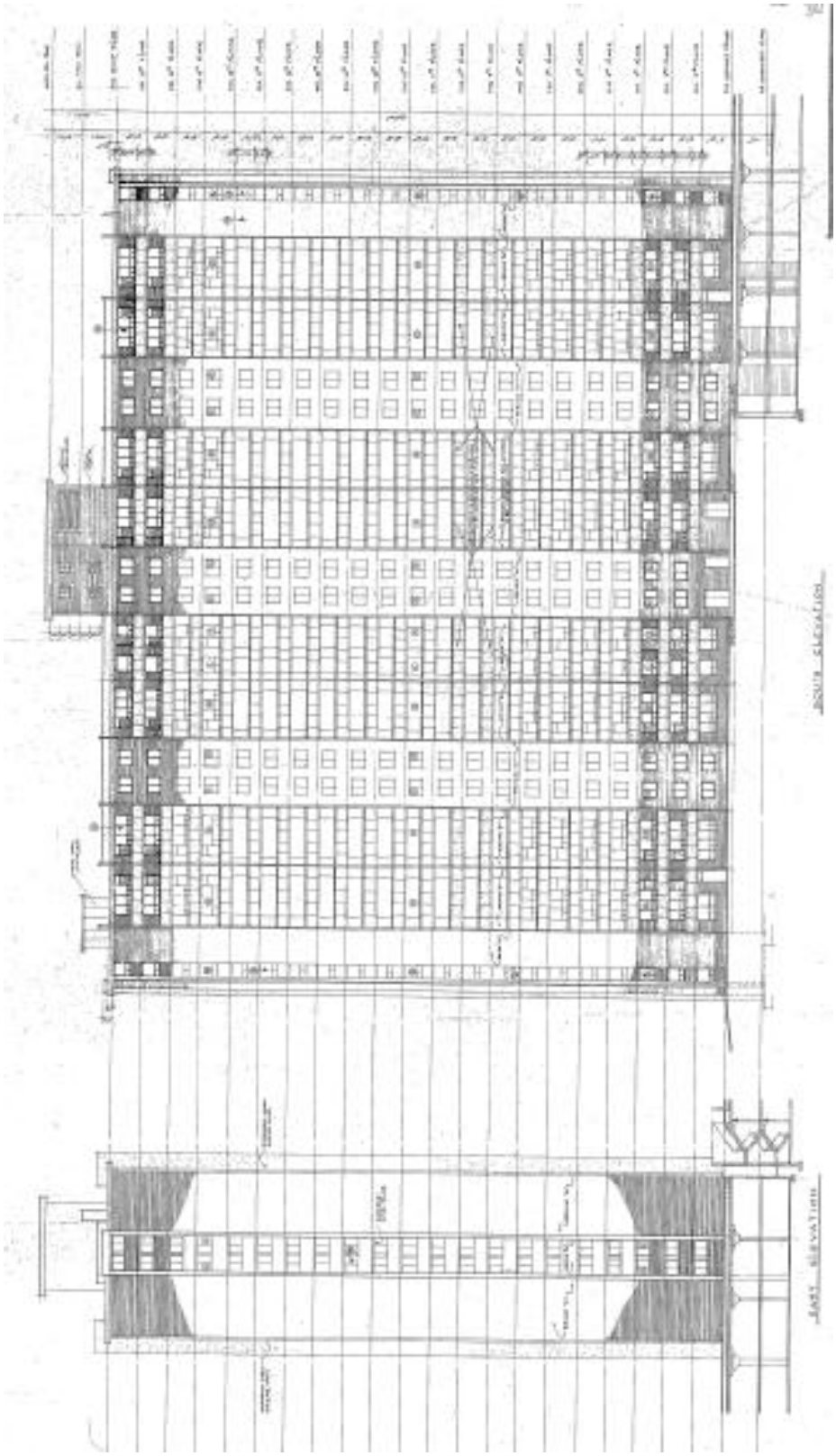

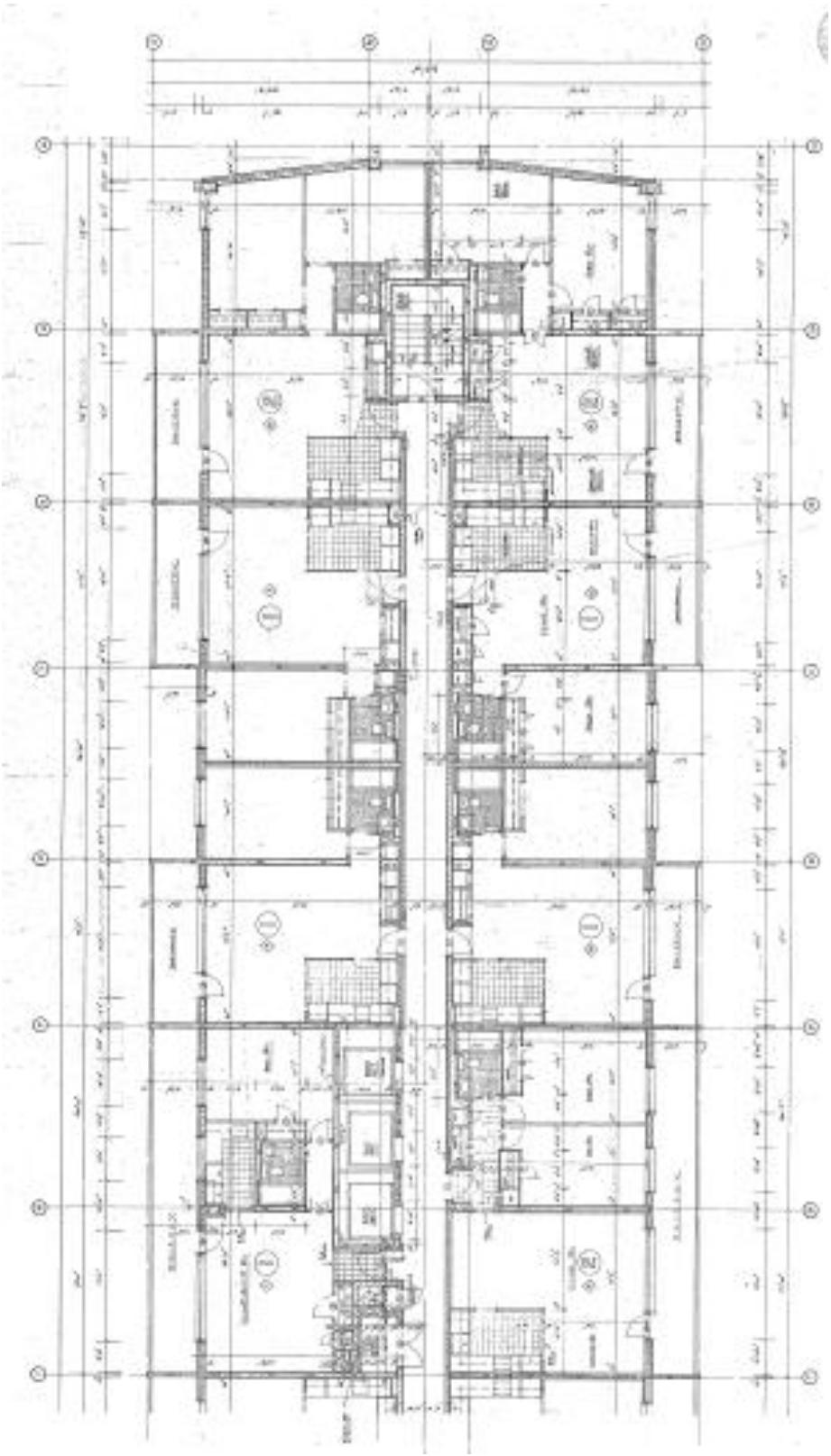

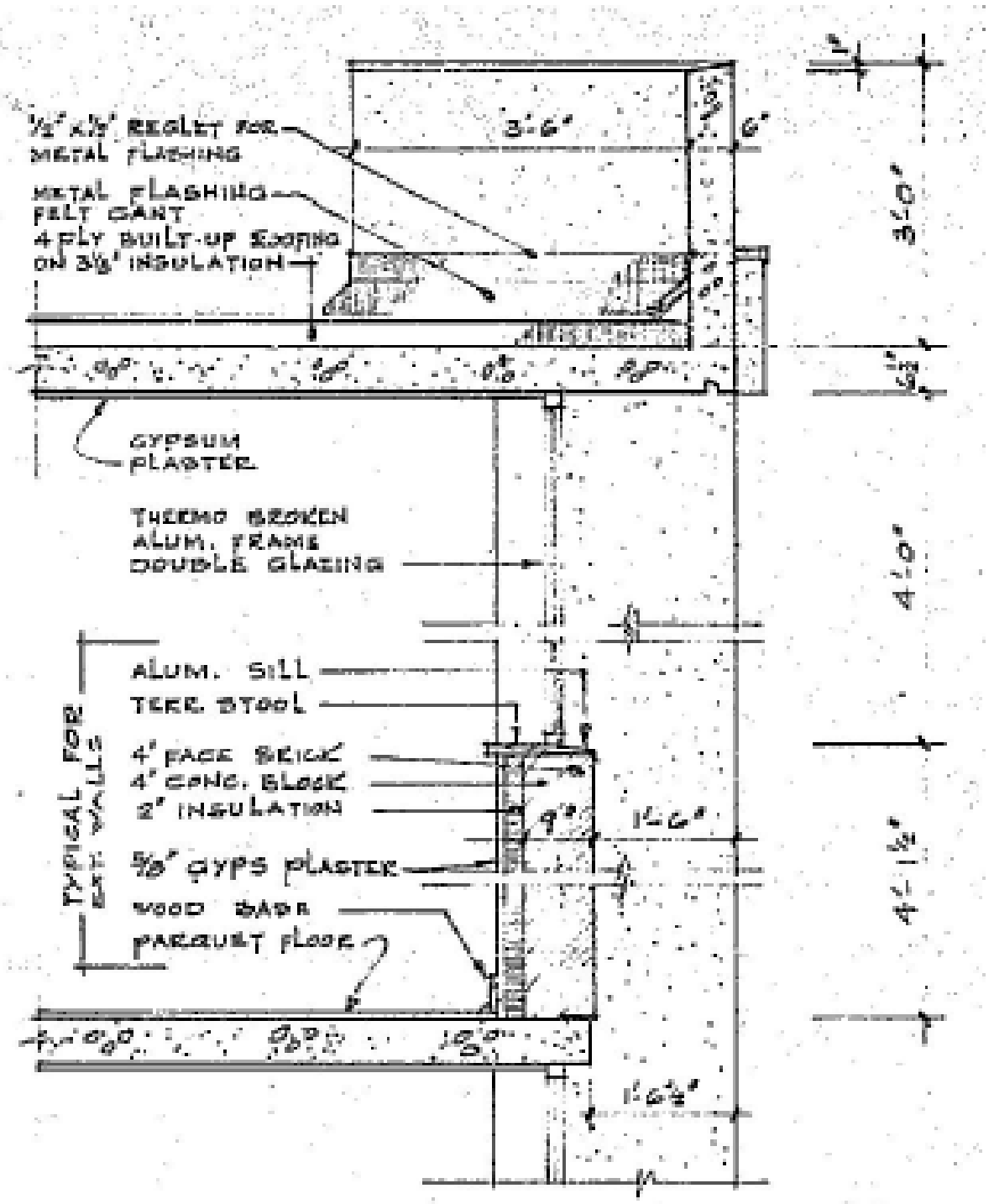

SECTION 6/9

SCALE ½"=1'-0"

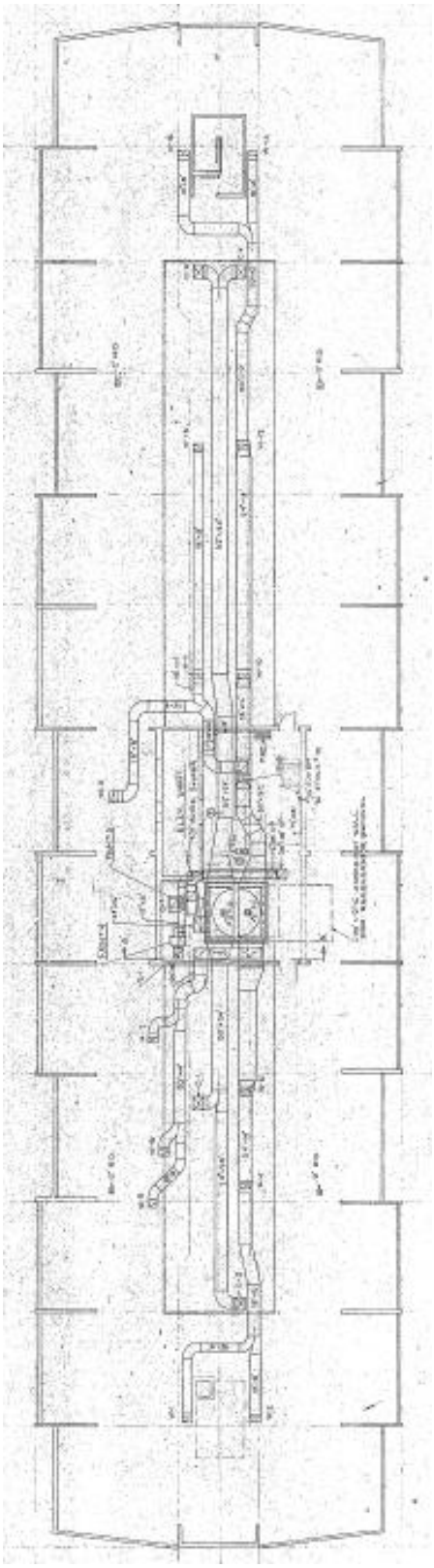

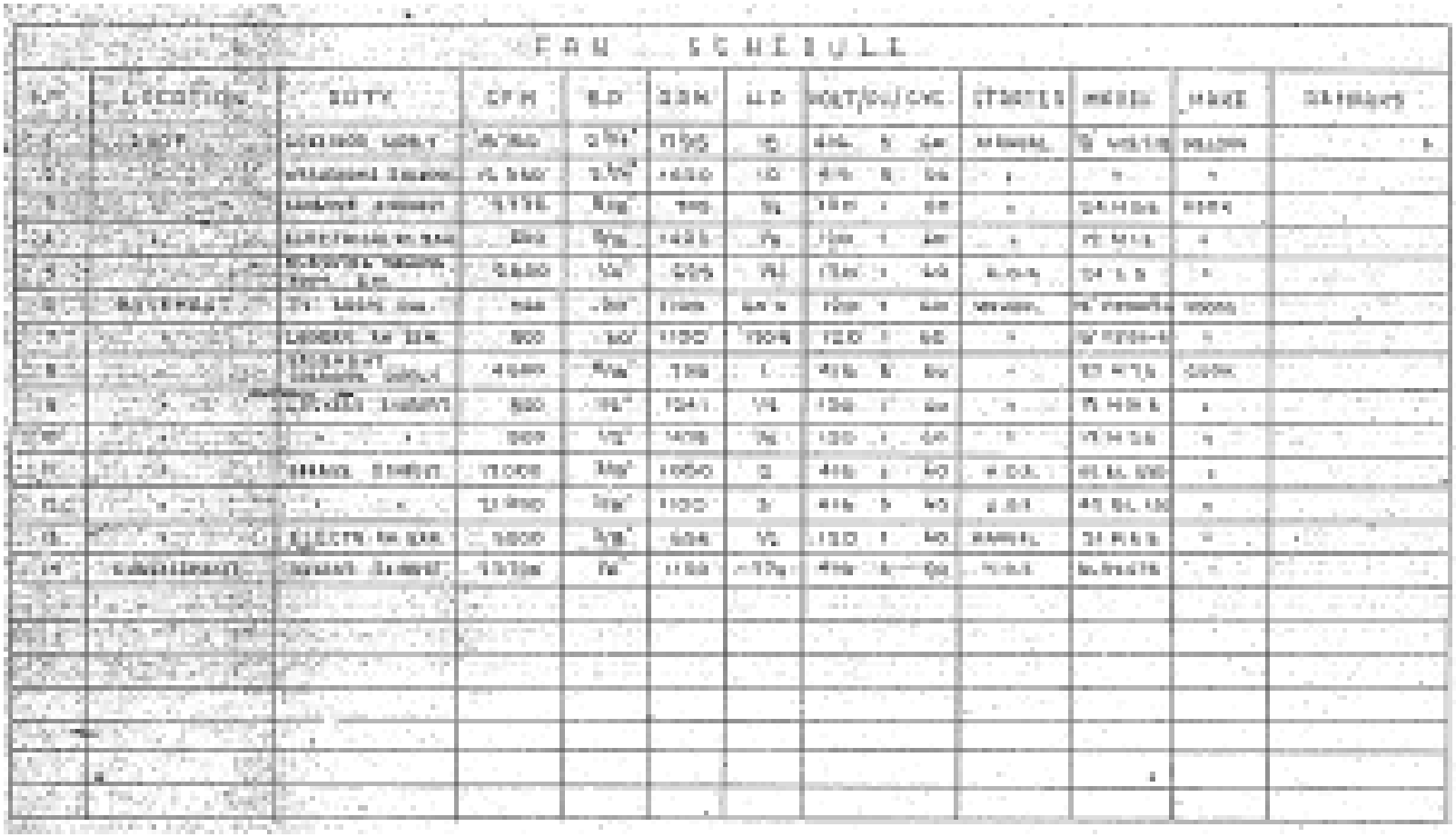

FARM SCHEDULE

NO.	LOCATION	DUTY	GPM	H.P.	RPM	H.P.	VOLT/PH/CYC.	STARTER	MODEL	MAKE	REMARKS
1	[illegible]	[illegible]	[illegible]	[illegible]	[illegible]	[illegible]	[illegible]	[illegible]	[illegible]	[illegible]	[illegible]
2	[illegible]	[illegible]	[illegible]	[illegible]	[illegible]	[illegible]	[illegible]	[illegible]	[illegible]	[illegible]	[illegible]
3	[illegible]	[illegible]	[illegible]	[illegible]	[illegible]	[illegible]	[illegible]	[illegible]	[illegible]	[illegible]	[illegible]
4	[illegible]	[illegible]	[illegible]	[illegible]	[illegible]	[illegible]	[illegible]	[illegible]	[illegible]	[illegible]	[illegible]
5	[illegible]	[illegible]	[illegible]	[illegible]	[illegible]	[illegible]	[illegible]	[illegible]	[illegible]	[illegible]	[illegible]
6	[illegible]	[illegible]	[illegible]	[illegible]	[illegible]	[illegible]	[illegible]	[illegible]	[illegible]	[illegible]	[illegible]
7	[illegible]	[illegible]	[illegible]	[illegible]	[illegible]	[illegible]	[illegible]	[illegible]	[illegible]	[illegible]	[illegible]
8	[illegible]	[illegible]	[illegible]	[illegible]	[illegible]	[illegible]	[illegible]	[illegible]	[illegible]	[illegible]	[illegible]
9	[illegible]	[illegible]	[illegible]	[illegible]	[illegible]	[illegible]	[illegible]	[illegible]	[illegible]	[illegible]	[illegible]
10	[illegible]	[illegible]	[illegible]	[illegible]	[illegible]	[illegible]	[illegible]	[illegible]	[illegible]	[illegible]	[illegible]
11	[illegible]	[illegible]	[illegible]	[illegible]	[illegible]	[illegible]	[illegible]	[illegible]	[illegible]	[illegible]	[illegible]
12	[illegible]	[illegible]	[illegible]	[illegible]	[illegible]	[illegible]	[illegible]	[illegible]	[illegible]	[illegible]	[illegible]
13	[illegible]	[illegible]	[illegible]	[illegible]	[illegible]	[illegible]	[illegible]	[illegible]	[illegible]	[illegible]	[illegible]
14	[illegible]	[illegible]	[illegible]	[illegible]	[illegible]	[illegible]	[illegible]	[illegible]	[illegible]	[illegible]	[illegible]

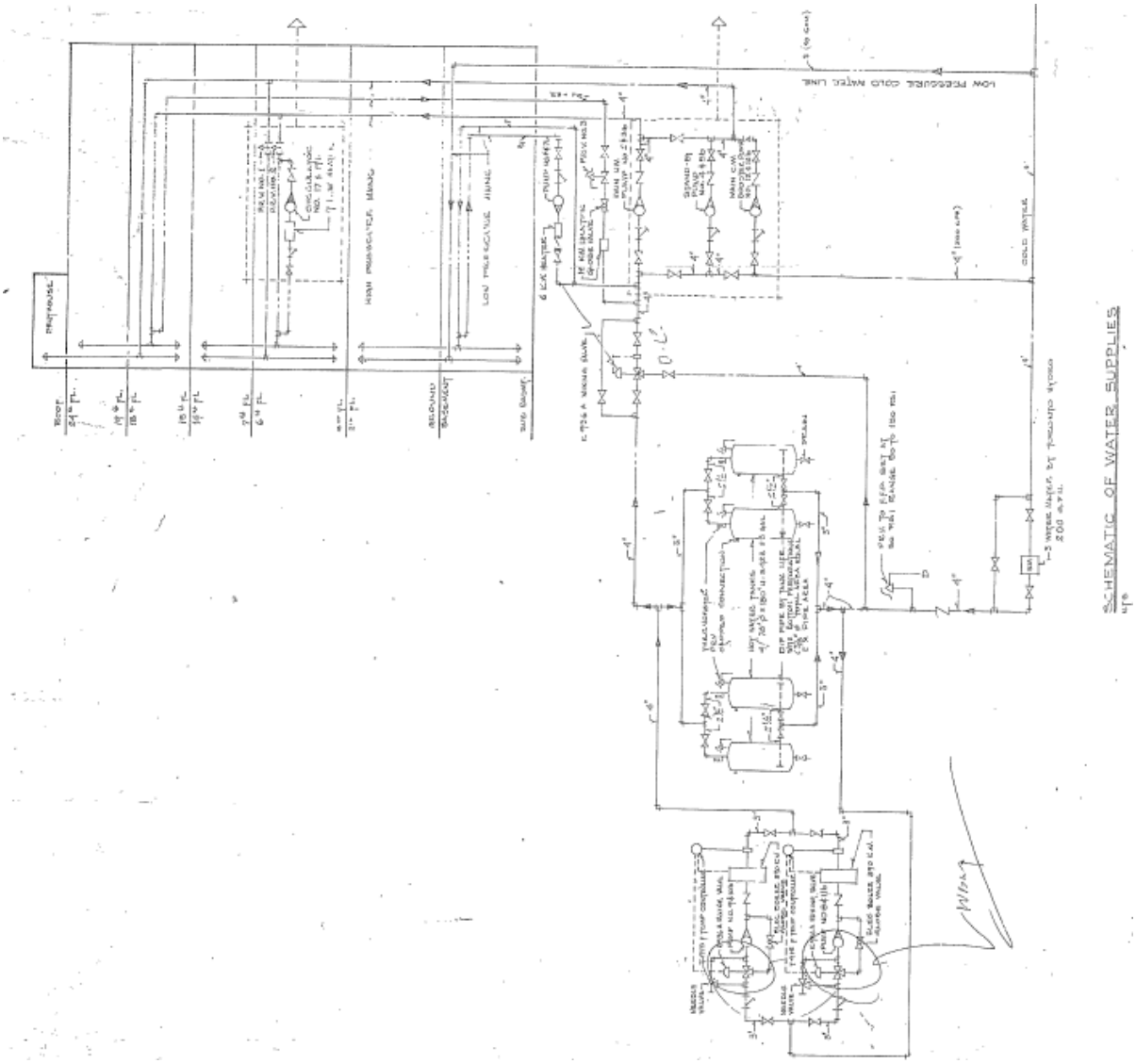
SCHEMATIC OF WATER SUPPLIES

FAN SCHEDULE

No	LOCATION	DUTY	CFM	S.P.	R.P.M.	H.P.	VOLT/PH/CYC	STARTER	MAKE
1, 2b	PENTHOUSE BLDG. A & B	CORRIDOR SUPPLY	17780	2½"	1271	15	416 3 60	MANUAL	AMERICAN STAND SIZE 2420
3, 4b	" "	WASHROOM EXHAUST	13180 12470 b	2½	856	10	416 3 60	"	AMERICAN STAND SIZE 2418
5 6b	"	GARBAGE RM EXH.	2700	5/8	1250	¾	416 3 60	H.O.A	BARRY BLOWER 165 BVB
7, 8b	"	ELECTR RM EXH.	810	5/8"	1200	⅛	120 1 60	H.O.A	BARRY BLOWER 123 BVB
9	BASEMENT GARAGE BLDG A	GARAGE EXH.	22 500	3/8"	587	5	416 3 60		CHELSEA IND 60A
10	SUB-BASMT UNIT BLDG 'A'	" "	20000	3/8"	367	5	416 3 60		"
11	BASEMENT BDG 'A'	LOCKERS EXH.	1100	.75	1056	⅛	120 1 60		CHELSEA UXF 10 BA
12&13b	"	" "	450	.75	1800	⅙	120 1 60		" UXF 5 BA
13	BASEMENT BLDG 'A'	MAIN ELECTR RM EXHAUST	2000	¼"	791	½	120 1 60		BARRY BLOWER 203 BVB
15, 16b	"	H.W. STORAGE TANK RM EXH.	3400	5/8"	719	¾	416 3 60		"
17	BASMT GARAGE	LAUNDRY RM EXH	1400	3/8"	1500	⅓	120 1 60		BARRY BLOWER 155 BVB
18	LOCKER	PLANT RM EXH.	400	5/8"	1152	⅛	120 1 60		CHELSEA UXF 5 BA
19, 20b	ELEVAT MACH ROOM	ELEVATOR MACH RM EXHAUST	2600	25	716	¼	120 1 60		" IND 24 CA
21	BASEMENT BLDG 'A'	BASEMENT CORRIDOR SUPPLY	4160	1"	740	1	416 3 60	H.O.A.	BARRY BLOWER 245 BVB
22	BASEMENT BLDG. 'A'	LOCKER EXHAUST	200	3/8"	1750	⅛	120 1 60	MANUAL	CHELSEA UDF 5 BA.
23b	BASEMENT (N) LOCKERS	LOCKER EXHAUST	260	½"	980	⅙	120 1 60	MANUAL	CHELSEA UXF 5 BA
25b	BASMT. BLDG 'B' H.W. ROOM	GYM EXHAUST	1000	¾"	1373	¼	120 1 60	MANUAL	CHELSEA 122 BVB
26b	BASMT. BLDG 'B' GARAGE WALL	RECREATION RM. EXHAUST	1450	5/8"	1050	⅓	120 1 60	MANUAL	CHELSEA 150 BVB
27b	BASMT BLDG 'B' GARAGE WALL	CHANGE RM. EXHAUST	700	3/4"	1384	⅙	120 1 60	H.O.A	CHELSEA 120 B.V.B.
28b	POOL EQPT. ROOM	POOL SUPPLY FAN	6900	1¼"	675	2	416 3 60	H.O.A	CHELSEA 300 BVB
29b	BASEMENT GARAGE	LAUNDRY ROOM EXHAUST	900	5/8"	1250	⅛	120 1 60	H.O.A	CHELSEA 113 BVB
30b	H.W. STORAGE RM	GYM SUPPLY FAN	1000	1¼"	1630	⅓	120 1 60	H.O.A	CHELSEA 122 BVB
31b	H.W. STORAGE RM	CORRIDOOR SUPPLY FAN (SUMMER)	3400	1¼"	900	1	416 3 60	H.O.A.	CHELSEA 232 BVB
32b & 37b	BASMT. GARAGE SUB BASMT. GARAGE	GARAGE EXHAUST	38000	3/8"	322	5	416 3 60	H.O.A.	CHELSEA IND 72 PA
33b	POOL EQPT RM.	POOL EXHAUST FAN	6000	1¼"	661	2	416 3 60	H.O.A.	CHELSEA 300 BVB
34b	SUB BASMT (N) LOCKER RM	LOCKER EXHAUST	700	¾"	883	⅛	120 1 60	MANUAL	CHELSEA UXF 10 BA
35b	SUB BASMT (S) LOCKER RM	LOCKER EXHAUST	400	¾"	1230	⅛	120 1 60	MANUAL	CHELSEA UXF 5 BA
36b	SUB BASMT GEN. STORAGE RM	LOCKER EXHAUST	100	½"	1750	⅛	120 1 60	MANUAL	CHELSEA UDF 5 BA
38b	GROUND FL. STORAGE UNIT	RECREATION RM SUPPLY FAN	1450	1¼"	1300	½	120 1 60	H.O.A.	CHELSEA 150 BVB
39b	BASMT GARAGE BLDG 'B'	ELECTR. RM EXHAUST	2000	¾	1750	¾	416 3 60	MANUAL	CHELSEA PLEX 24 H.A.
40b	BASMT STORAGE BLDG 'B'	STORAGE EXHAUST	150			.15 AMP	120 1 60	"	PAGCO 698

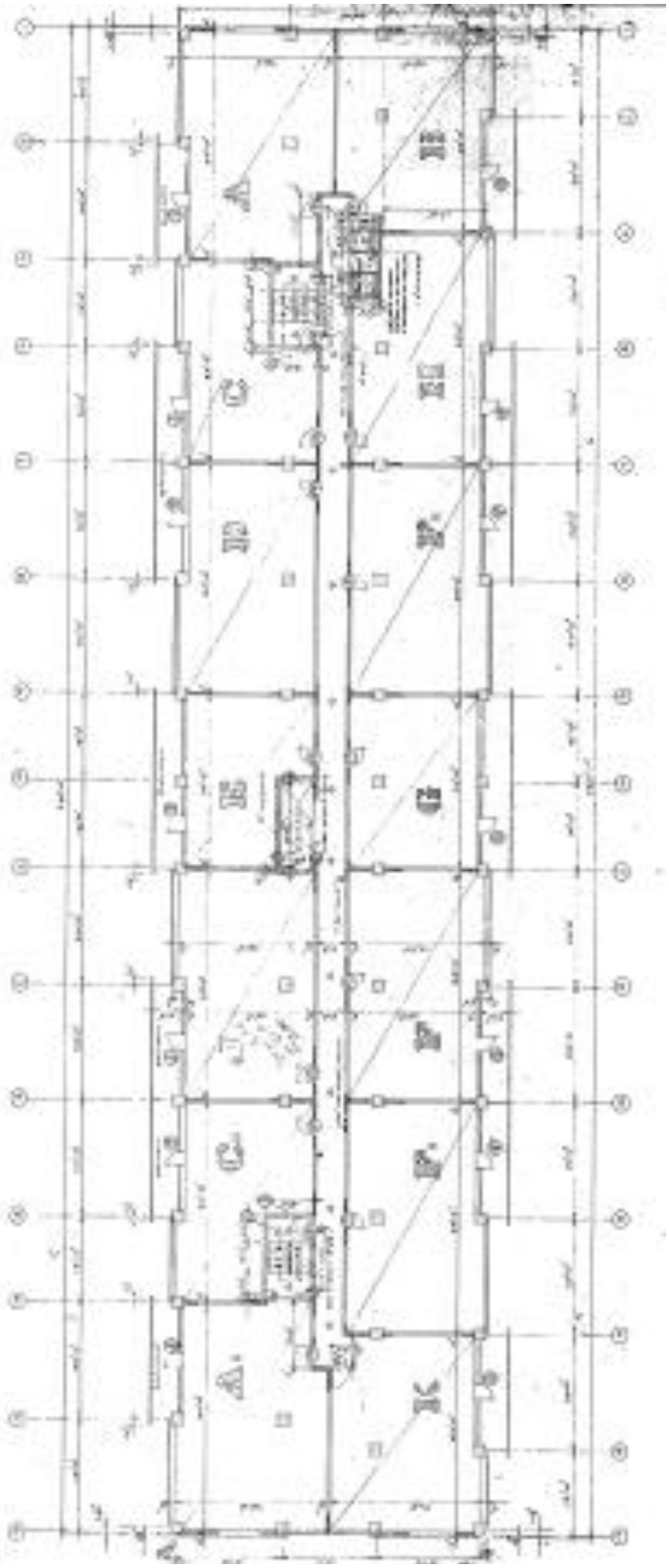

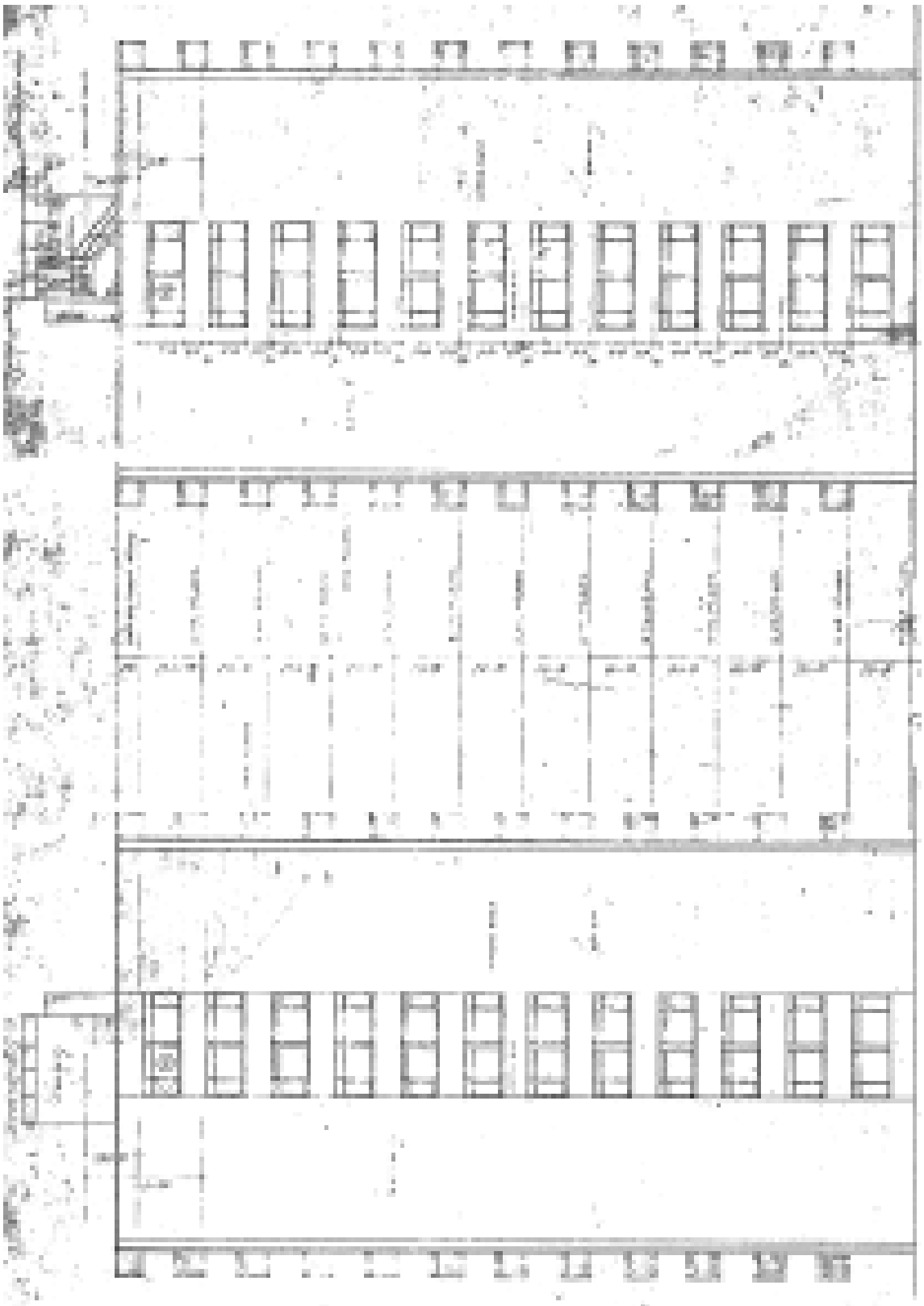

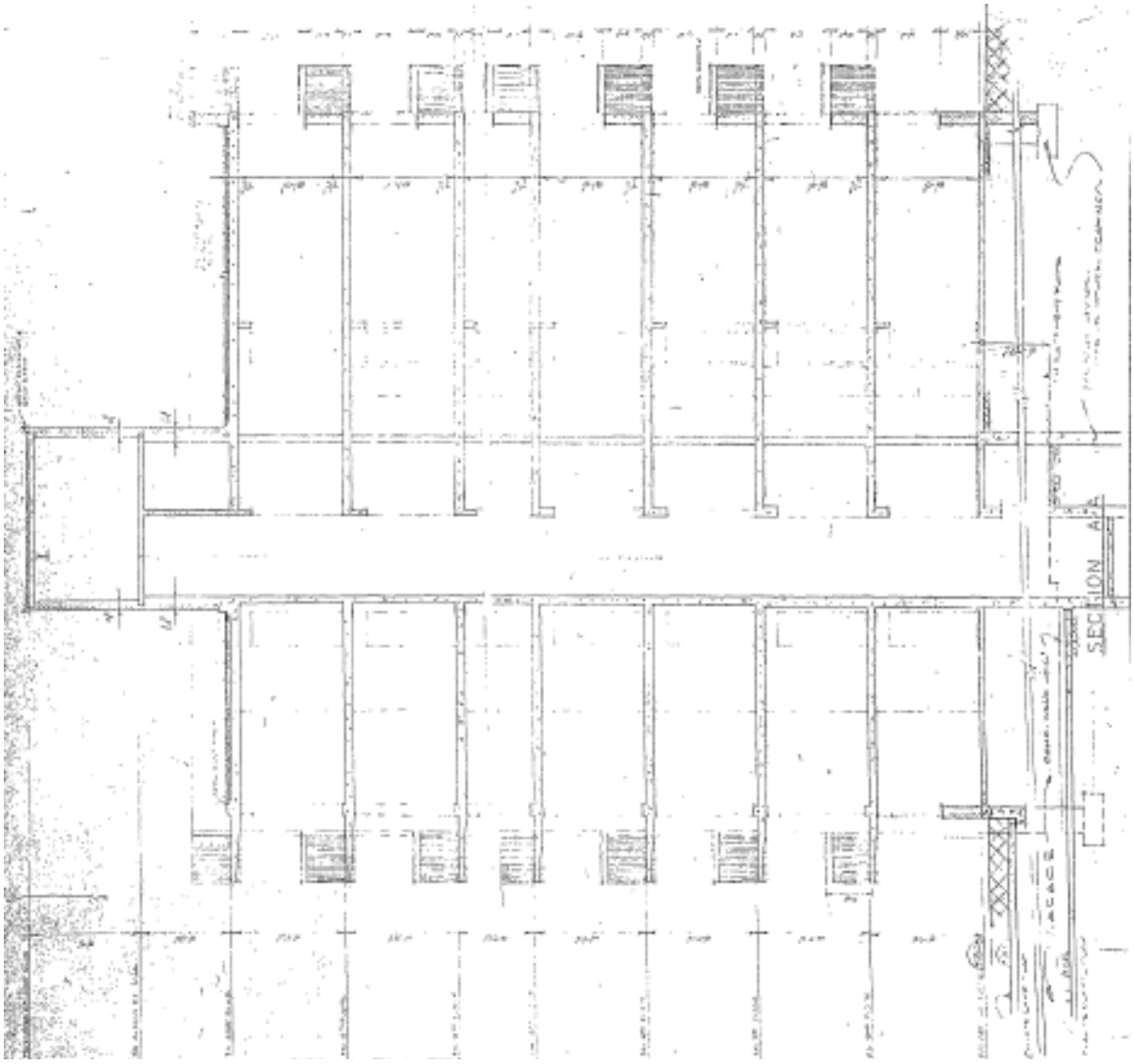
SECTION A-A

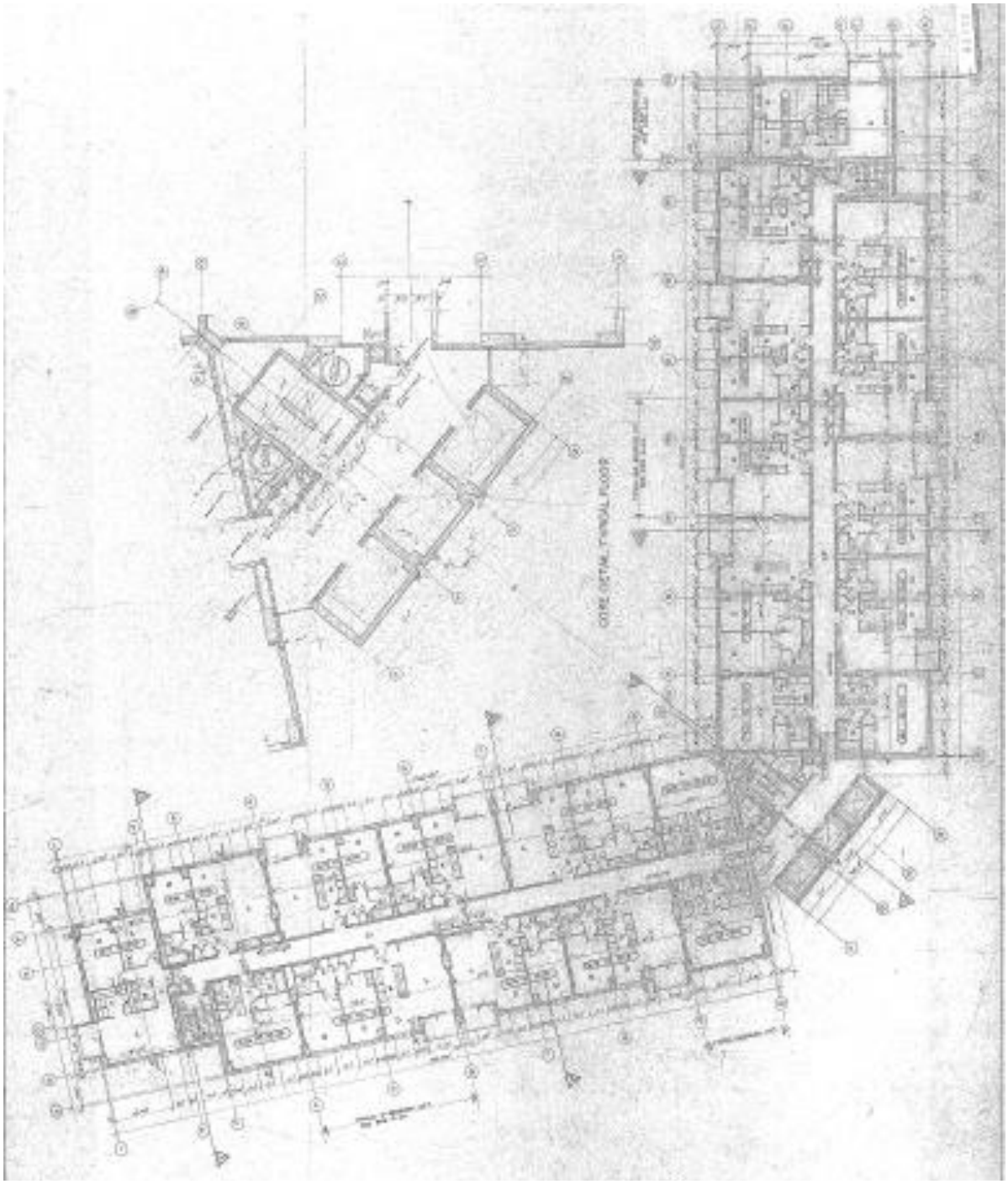

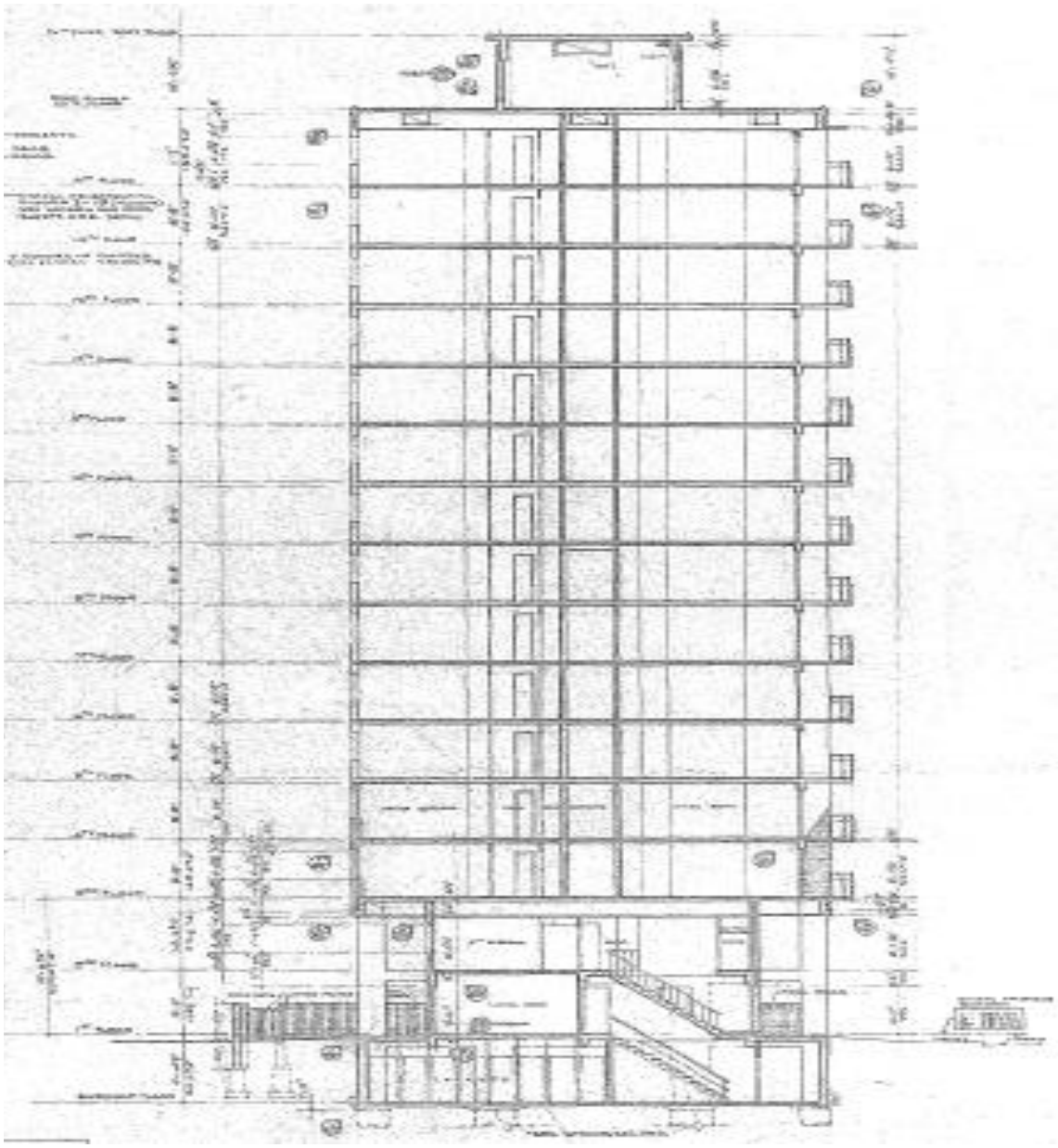

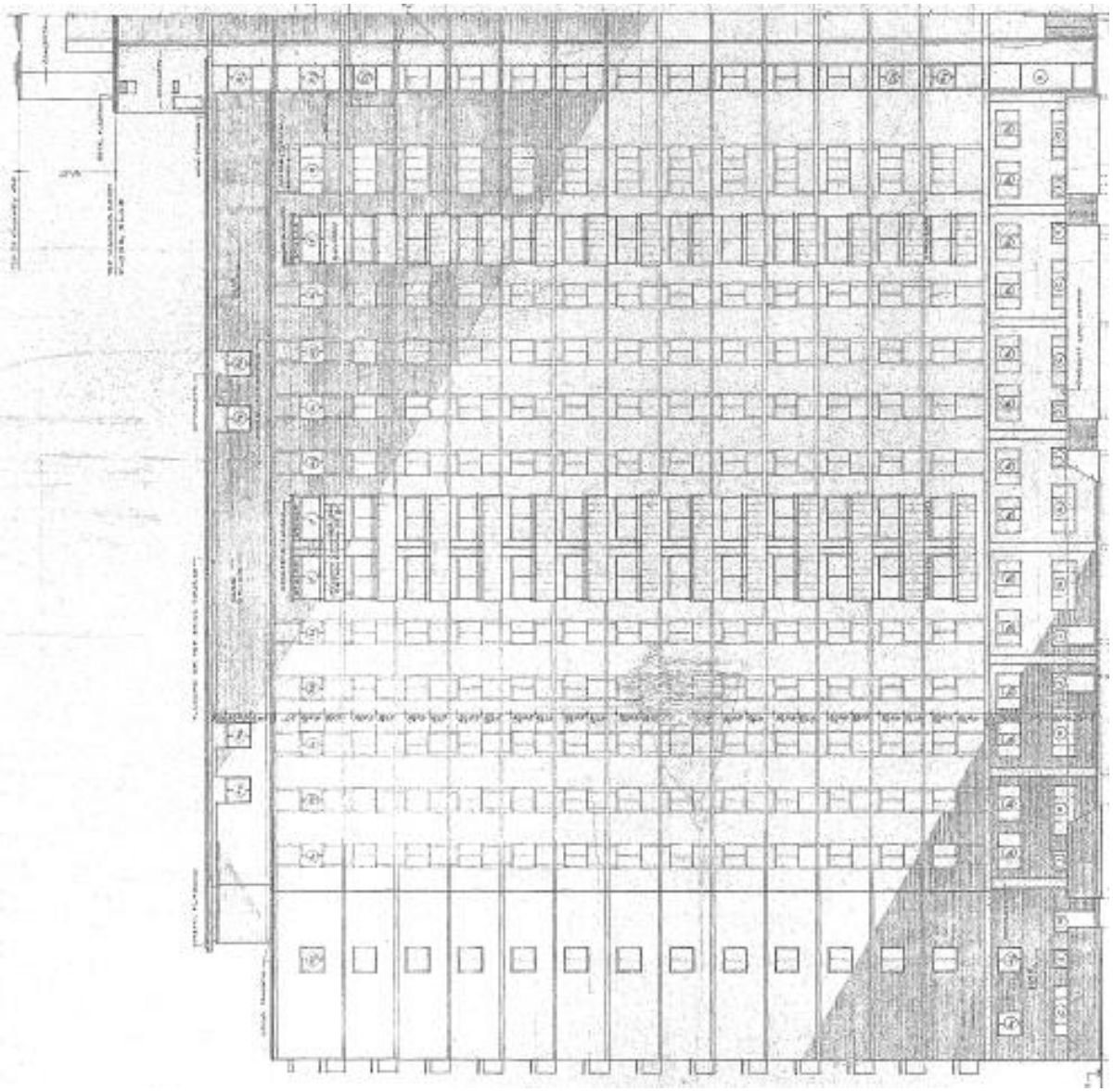

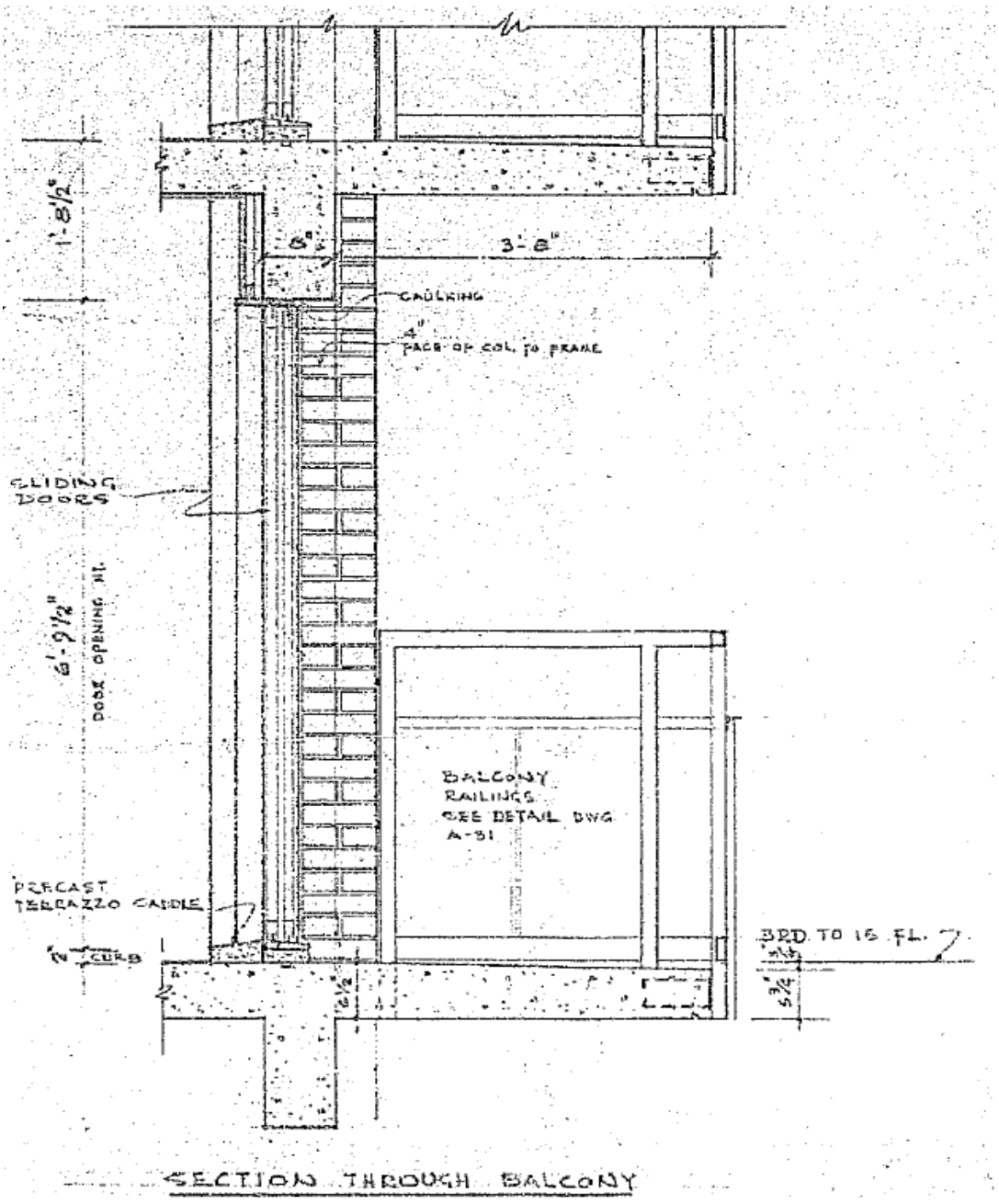

SECTION THROUGH BALCONY

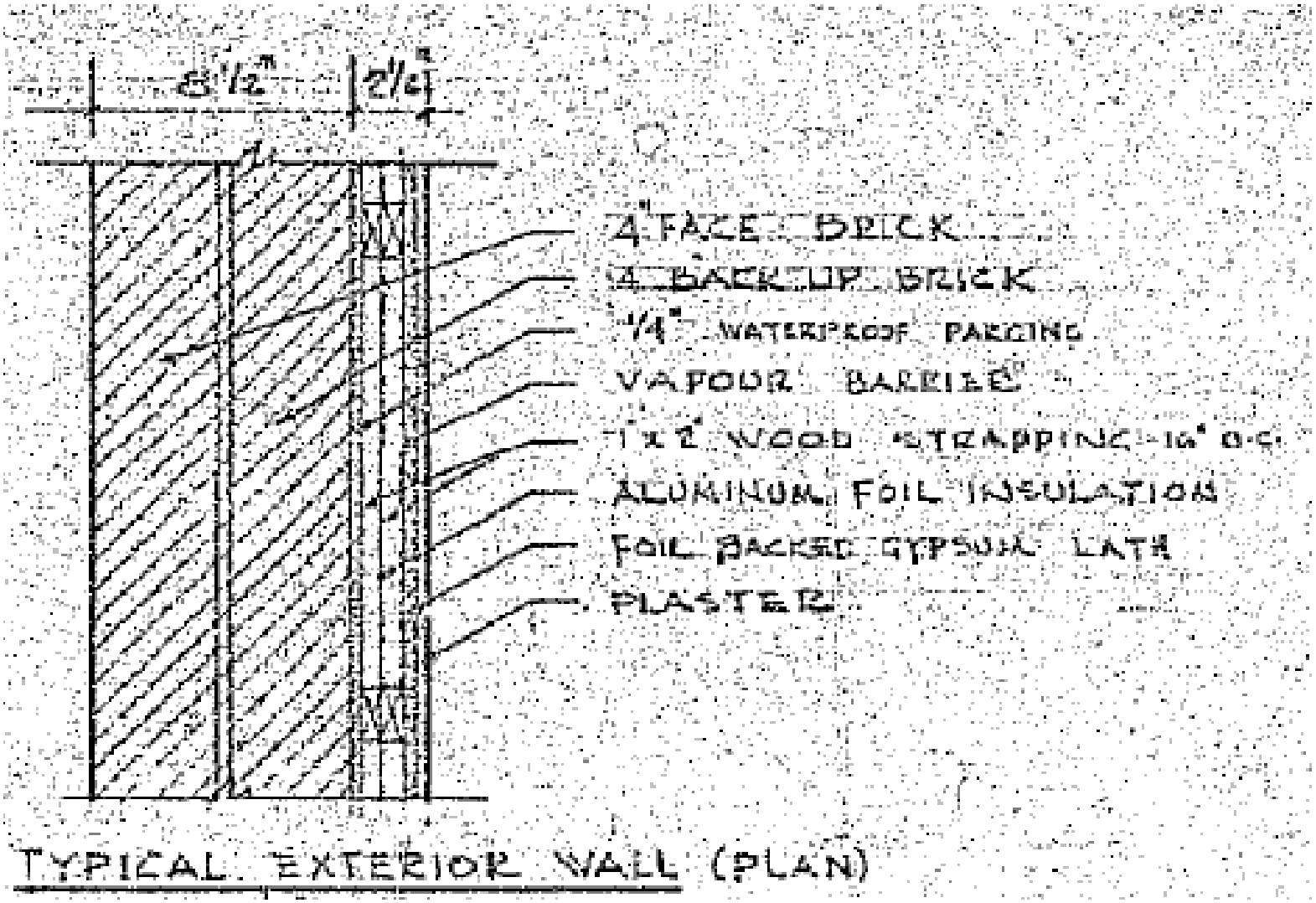

TYPICAL EXTERIOR WALL (PLAN)

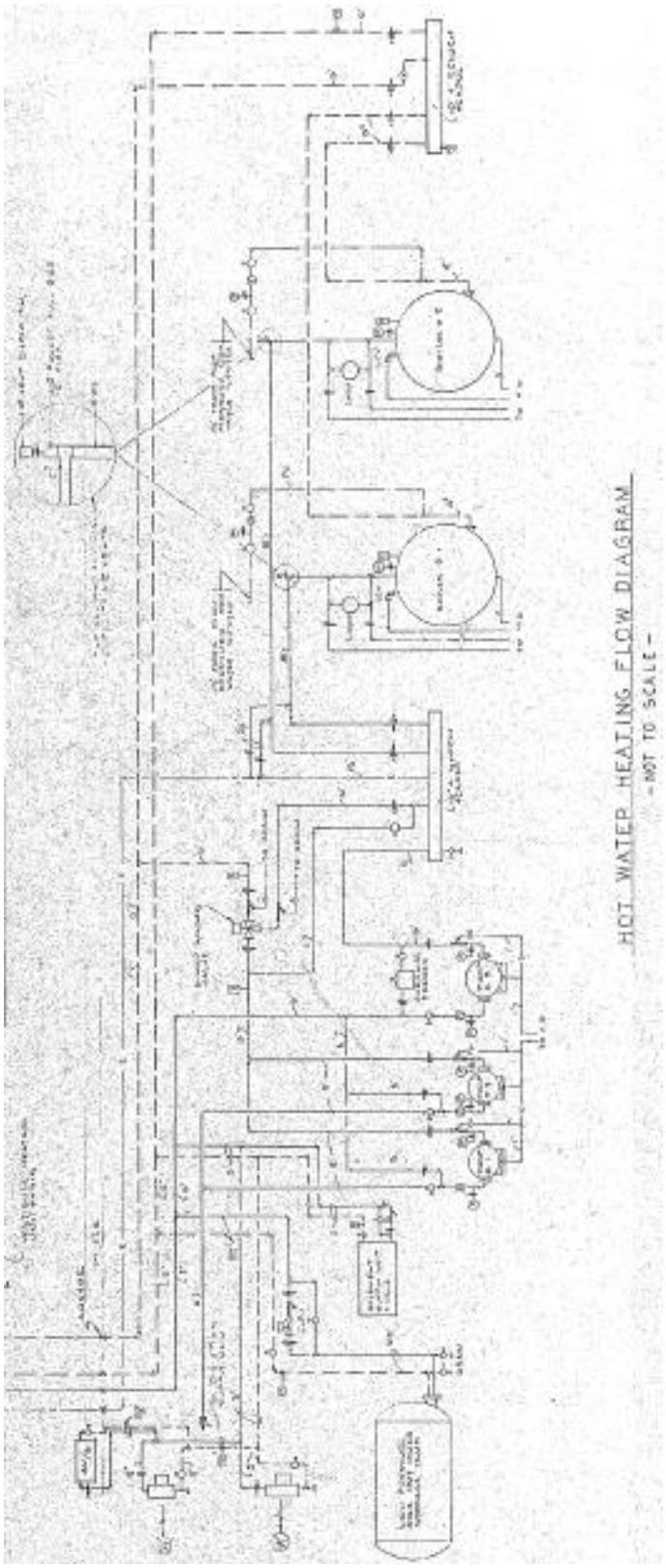

HOT WATER HEATING FLOW DIAGRAM
- NOT TO SCALE -

EXHAUST FAN SCHEDULE

No.	TYPE & SIZE	C.F.M.	R.P.M.	T.S.P.	O.V.	OUTLET VEL.	MOTOR H.P.	LOCATION	FUNCTION	REMARKS
EF-1	[illegible]	[illegible]	[illegible]	[illegible]	[illegible]	[illegible]	[illegible]	[illegible]	[illegible]	[illegible]
EF-2	[illegible]	[illegible]	[illegible]	[illegible]	[illegible]	[illegible]	[illegible]	[illegible]	[illegible]	[illegible]
EF-3	[illegible]	[illegible]	[illegible]	[illegible]	[illegible]	[illegible]	[illegible]	[illegible]	[illegible]	[illegible]
EF-4	[illegible]	[illegible]	[illegible]	[illegible]	[illegible]	[illegible]	[illegible]	[illegible]	[illegible]	[illegible]
EF-5	[illegible]	[illegible]	[illegible]	[illegible]	[illegible]	[illegible]	[illegible]	[illegible]	[illegible]	[illegible]
EF-6	[illegible]	[illegible]	[illegible]	[illegible]	[illegible]	[illegible]	[illegible]	[illegible]	[illegible]	[illegible]
EF-7	[illegible]	[illegible]	[illegible]	[illegible]	[illegible]	[illegible]	[illegible]	[illegible]	[illegible]	[illegible]

CIRCULATING PUMP SCHEDULE

PUMP NO.	LOCATION	FUNCTION	TYPE	SIZE	CAP. IG.P.M.	HEAD FT.	B.H.P.	MOTOR R.P.M.	MOTOR H.P.	REMARKS
1	[illegible]	[illegible]	[illegible]	[illegible]	[illegible]	[illegible]	[illegible]	[illegible]	[illegible]	[illegible]
2	[illegible]	[illegible]	[illegible]	[illegible]	[illegible]	[illegible]	[illegible]	[illegible]	[illegible]	[illegible]
3	[illegible]	[illegible]	[illegible]	[illegible]	[illegible]	[illegible]	[illegible]	[illegible]	[illegible]	[illegible]

VENTILATION SUPPLY UNIT SCHEDULE

[illegible]	[illegible]	[illegible]	[illegible]	[illegible]
FUNCTION	[illegible]	[illegible]	[illegible]	[illegible]
LOCATION	[illegible]	[illegible]	[illegible]	[illegible]
SIZE	[illegible]	[illegible]	[illegible]	[illegible]
TYPE	[illegible]	[illegible]	[illegible]	[illegible]
CAPACITY C.F.M.	[illegible]	[illegible]	[illegible]	[illegible]
E.S.P. (W.G.)	[illegible]	[illegible]	[illegible]	[illegible]
B.H.P.	[illegible]	[illegible]	[illegible]	[illegible]
FAN R.P.M.	[illegible]	[illegible]	[illegible]	[illegible]
OUTLET VEL. F.P.M.	[illegible]	[illegible]	[illegible]	[illegible]
MOTOR H.P.	[illegible]	[illegible]	[illegible]	[illegible]
MOTOR R.P.M.	[illegible]	[illegible]	[illegible]	[illegible]
HEATING MED. & CAPACITY	[illegible]	[illegible]	[illegible]	[illegible]
COILS	[illegible]	[illegible]	[illegible]	[illegible]
TOTAL HEAT REQ'M'T	[illegible]	[illegible]	[illegible]	[illegible]
FACE VEL. F.P.M.	[illegible]	[illegible]	[illegible]	[illegible]
ENTERING D.B.	[illegible]	[illegible]	[illegible]	[illegible]
LEAVING D.B.	[illegible]	[illegible]	[illegible]	[illegible]
WATER RISE	[illegible]	[illegible]	[illegible]	[illegible]
AIR RESISTANCE	[illegible]	[illegible]	[illegible]	[illegible]
[illegible]	[illegible]	[illegible]	[illegible]	[illegible]
FILTERS	[illegible]	[illegible]	[illegible]	[illegible]
NO. & SIZE	[illegible]	[illegible]	[illegible]	[illegible]
	[illegible]			
REMARKS	[illegible]	[illegible]	[illegible]	[illegible]

NOTE - [illegible]

EXHAUST GRILLE SCHEDULE

SYMBOL	SIZE	CFM	TYPE	LOCATION & REMARKS
A	6" Ø	70		WASH ROOMS
B	24"x 5"	75		TOILETS
C	8"x 8"	50		JANITORS ROOM
D	48"x 24"	2500		DRYING ROOM

SUPPLY & RETURN AIR GRILLES REFER TO DRAWINGS

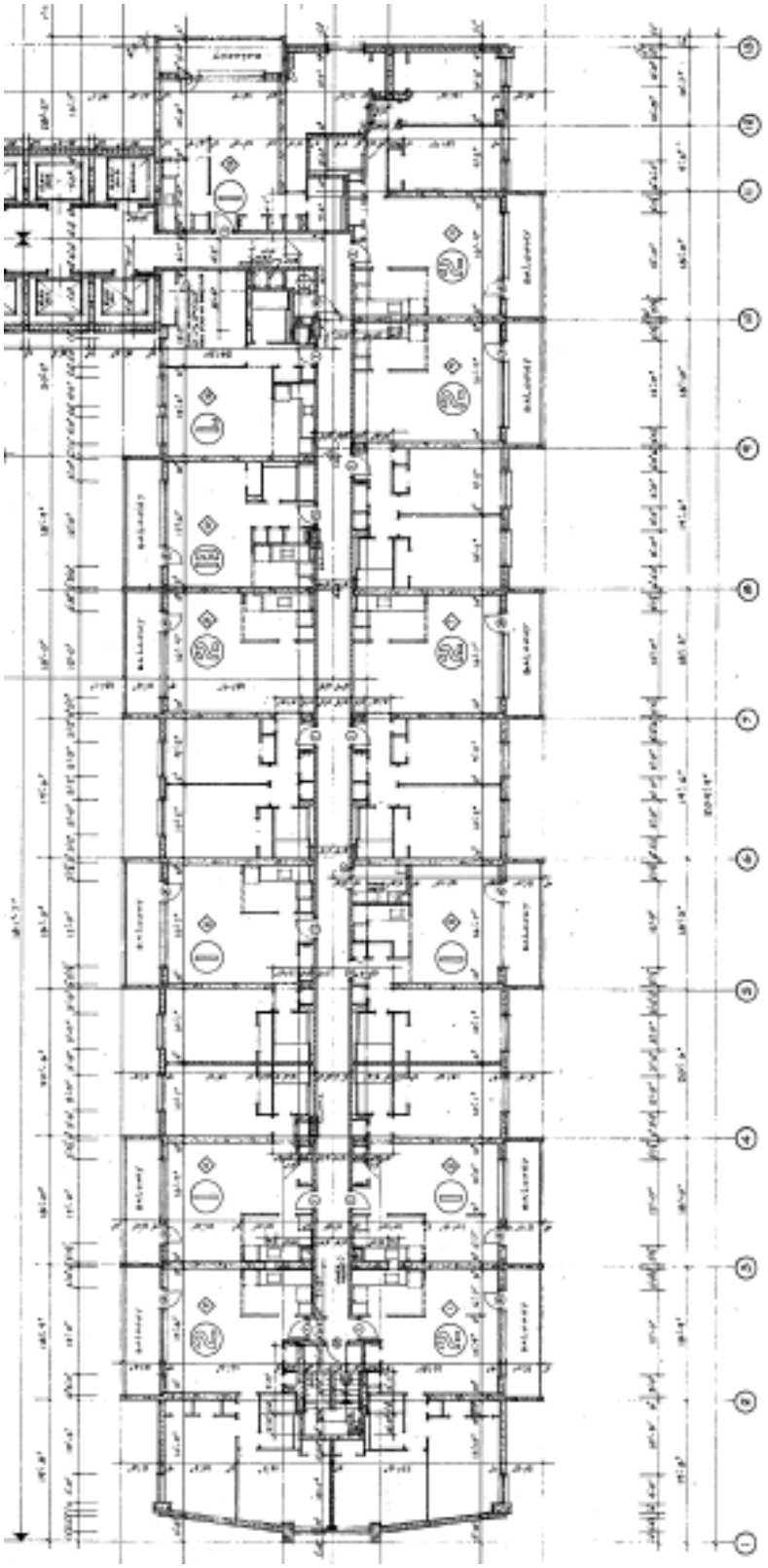

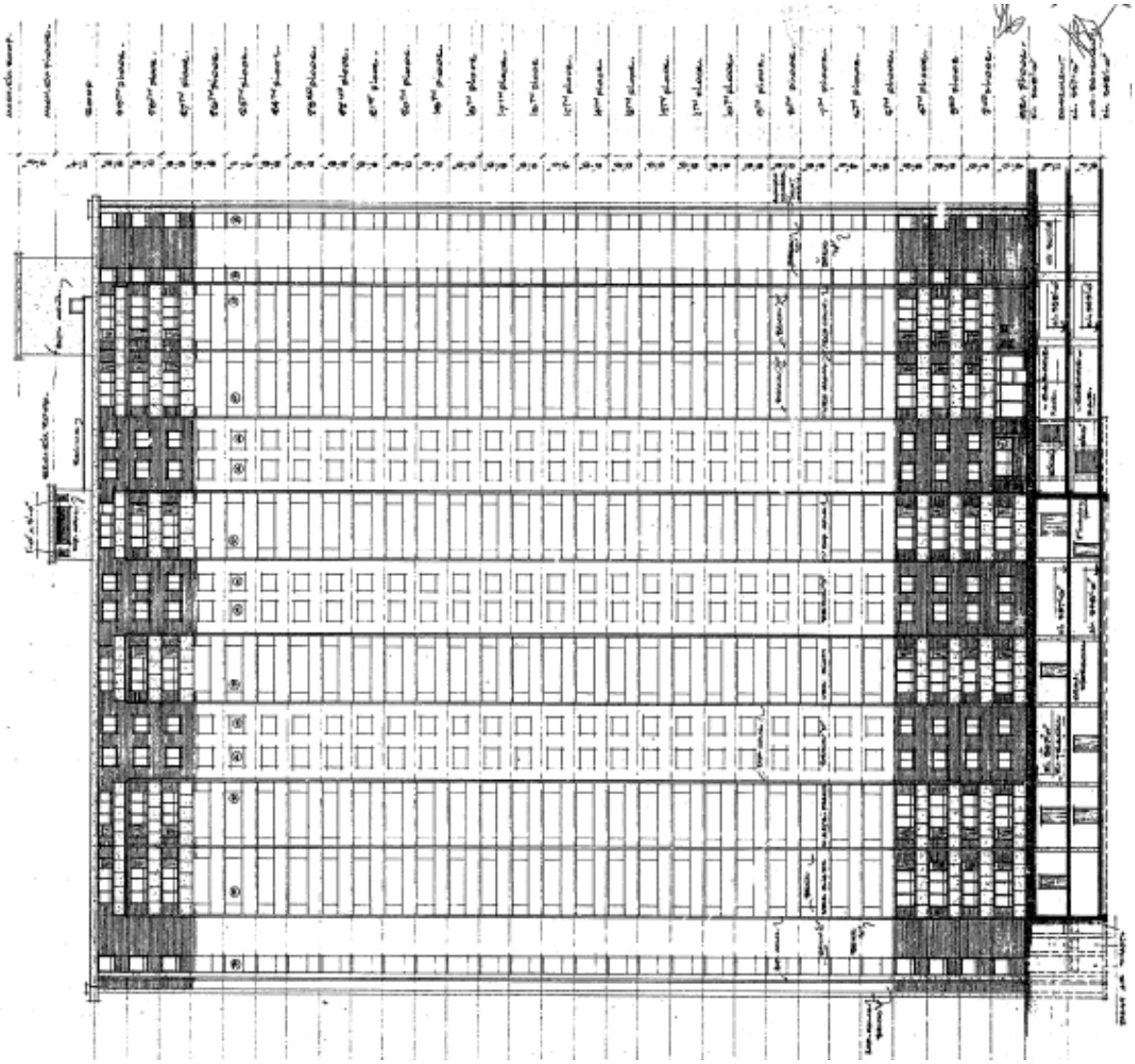

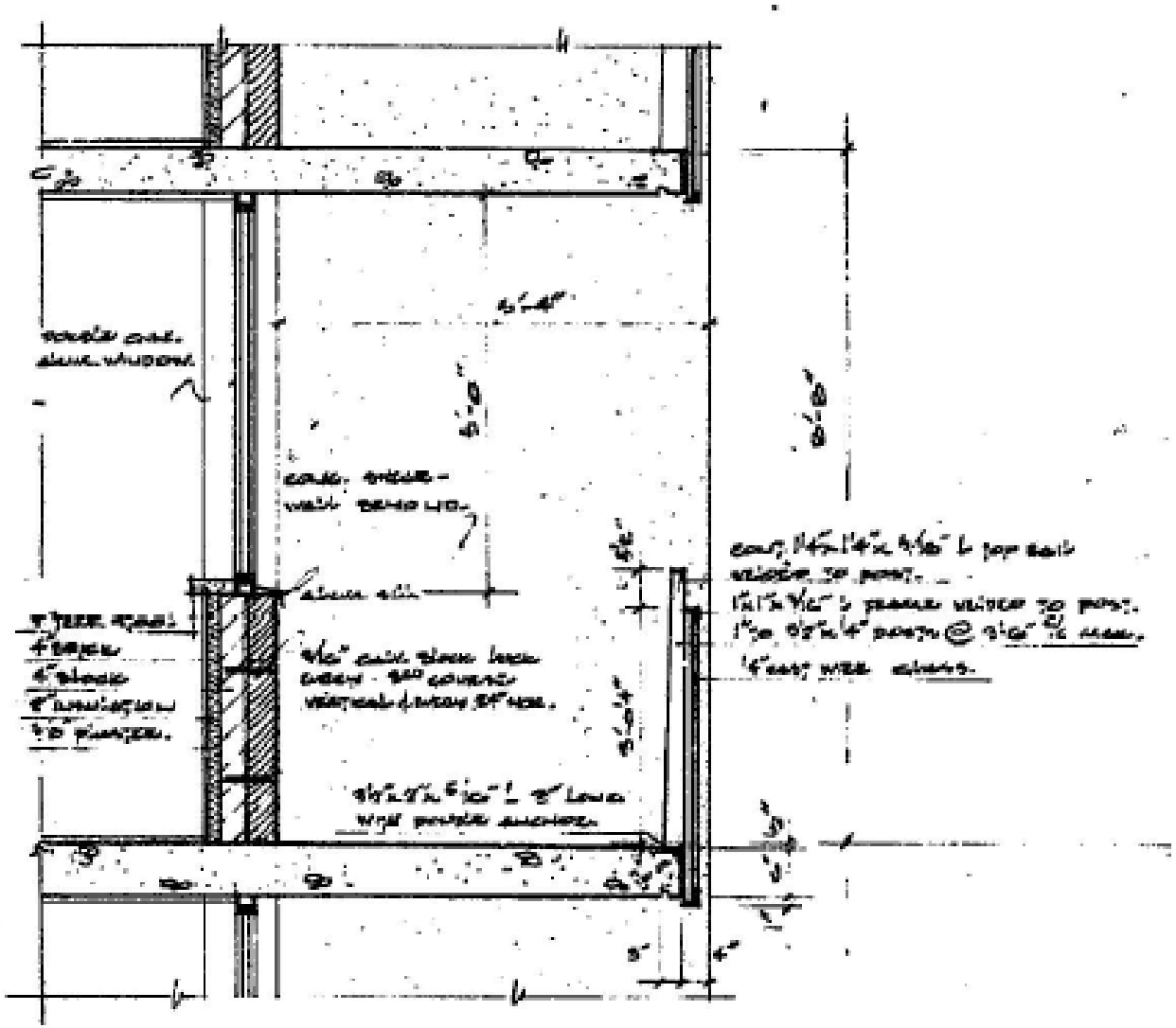

- TYPICAL BALCONY SECTION (14/E)

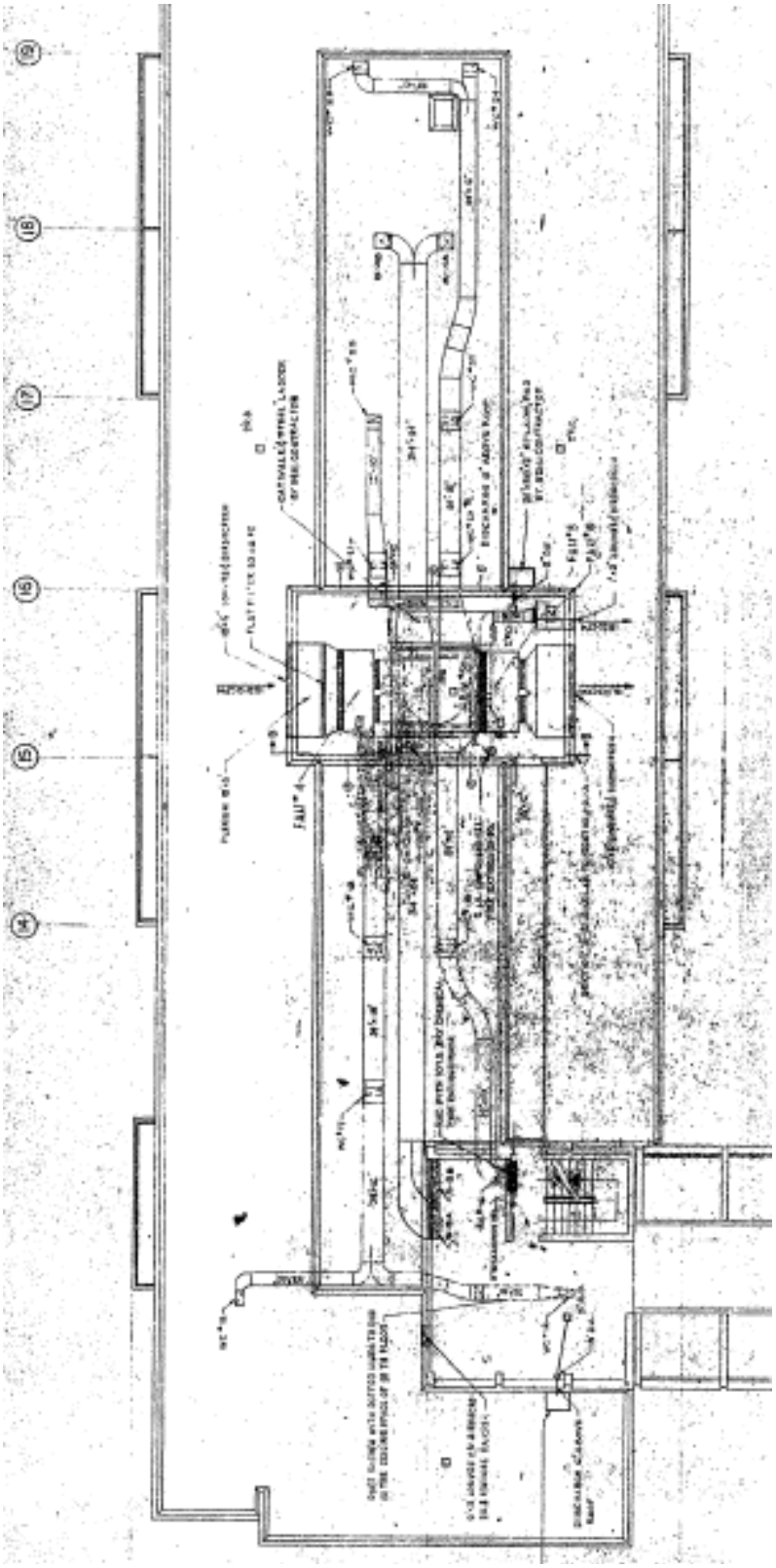

*Appendix C - BELA Screenshots (*Hanam, 2010*)*

BUILDING INPUTS		
Yellow cells = user input		
Blue cells = calculated values		
GENERAL INFO		
Location	Toronto, ON	
Number of Stories	2	
Length, N-S elevations	61	m
Length, E-W elevations	36	m
Floor to Floor Height	3.7	m
Window to Wall Ratio (WWR), North	30%	
WWR, South	30%	
WWR, East	30%	
WWR, West	30%	
Indoor Temperature Winter Low	21	C
Indoor Temperature Summer High	24	C
ENCLOSURE		
Air leakage	0.4	l/s-m2 wall
Wall R-Value	25	hr-ft2-F/Btu
Roof R-Value	20	hr-ft2-F/Btu
Foundation R-Value	10	hr-ft2-F/Btu
Door R-Value	2.0	hr-ft2-F/Btu
# of Doors	5	
Door Height	2.13	m
Door Width	1.83	m
Total Window U-Value	0.347	Btu/hr-ft2-F
Solar Heat Gain Coefficient (SHGC), North	0.4	
SHGC, South	0.4	
SHGC, East	0.4	
SHGC, West	0.4	
Roof Solar Absorptance, α	0.8	
Wall Solar Absorptance, α	0.8	
INTERNAL GAINS		
Lights	8.3	W/m2
Plug loads	12.5	W/m2
People - Sensible	73.2	W/pers
People - Latent	61.9	W/pers
Occupant Density	0.07	people/m2

DAILY SCHEDULE				WEEKLY SCHEDULE (% of Daily)			
Hour	Lighting %	Plug Loads %	Occupancy %	Day	Lighting %	Plug Loads %	Occupancy %
1:00	10%	10%	0%	1	100%	100%	100%
2:00	10%	10%	0%	2	100%	100%	100%
3:00	10%	10%	0%	3	100%	100%	100%
4:00	10%	10%	0%	4	100%	100%	100%
5:00	10%	10%	0%	5	100%	100%	100%
6:00	10%	10%	0%	6	0%	0%	0%
7:00	55%	10%	0%	7	0%	0%	0%
8:00	100%	100%	100%				
9:00	100%	100%	100%				
10:00	100%	100%	100%				
11:00	100%	100%	100%				
12:00	100%	100%	100%				
13:00	100%	100%	100%				
14:00	100%	100%	100%				
15:00	100%	100%	100%				
16:00	100%	100%	100%				
17:00	100%	100%	100%				
18:00	55%	10%	10%				
19:00	10%	10%	0%				
20:00	10%	10%	0%				
21:00	10%	10%	0%				
22:00	10%	10%	0%				
23:00	10%	10%	0%				
0:00	10%	10%	0%				

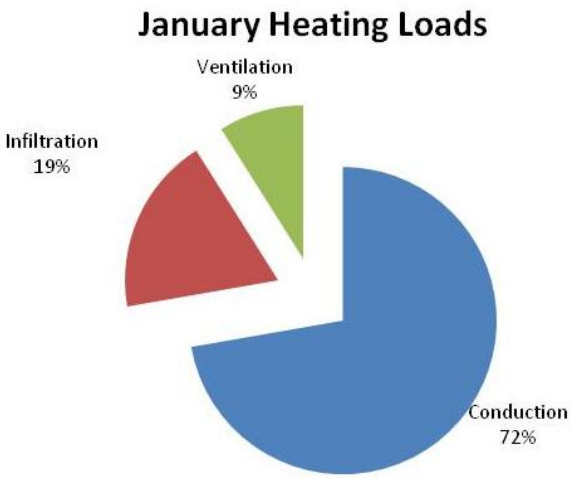
January Heating Loads
Ventilation
9%
Infiltration
19%
Conduction
72%

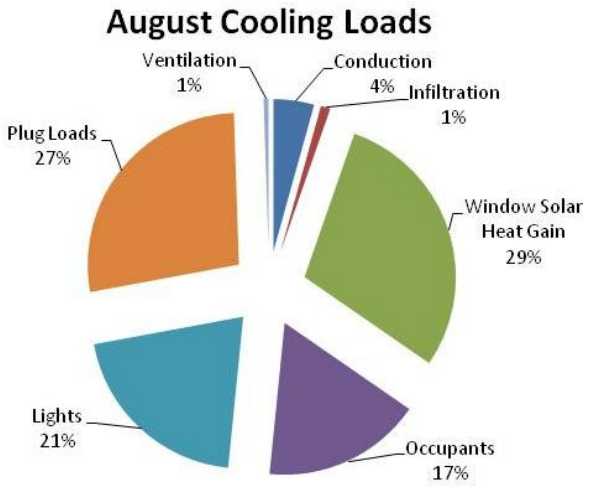
August Cooling Loads
Ventilation
1%
Conduction
4%
Infiltration
1%
Plug Loads
27%
Window Solar
Heat Gain
29%
Lights
21%
Occupants
17%

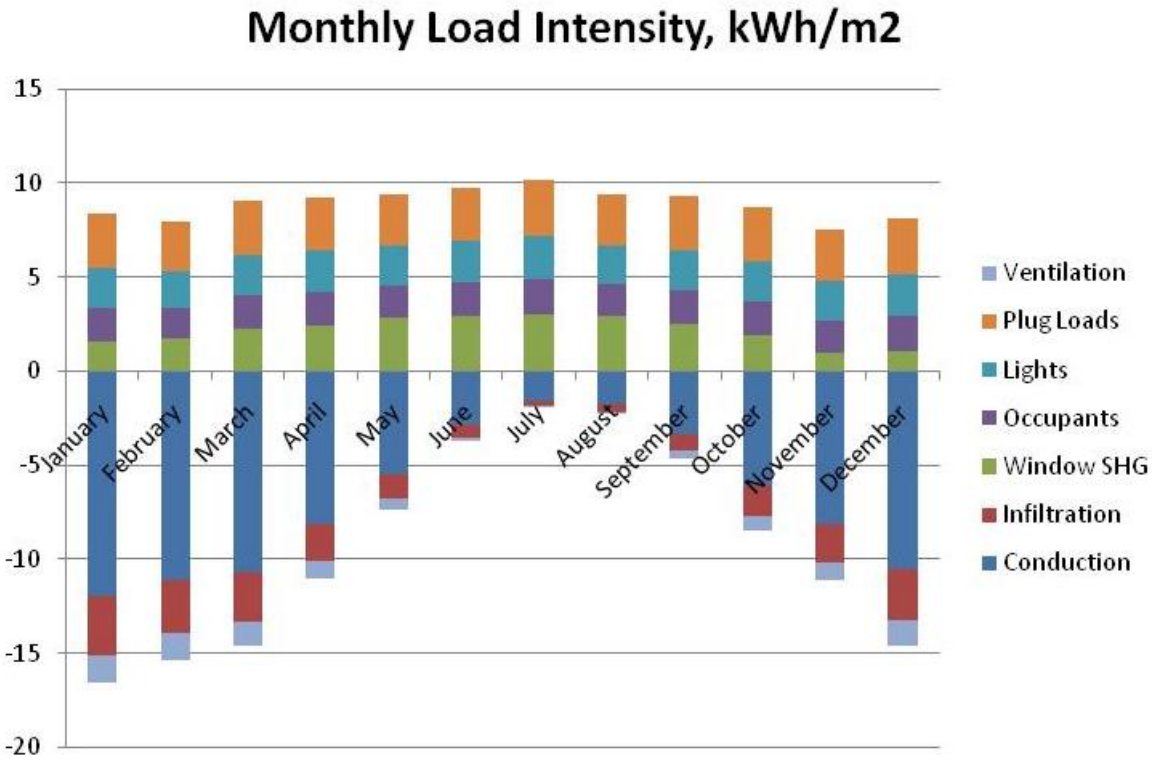
Monthly Load Intensity, kWh/m2
15
10
5
0
-5
-10
-15
-20
January
February
March
April
May
June
July
August
September
October
November
December
Ventilation
Plug Loads
Lights
Occupants
Window SHG
Infiltration
Conduction

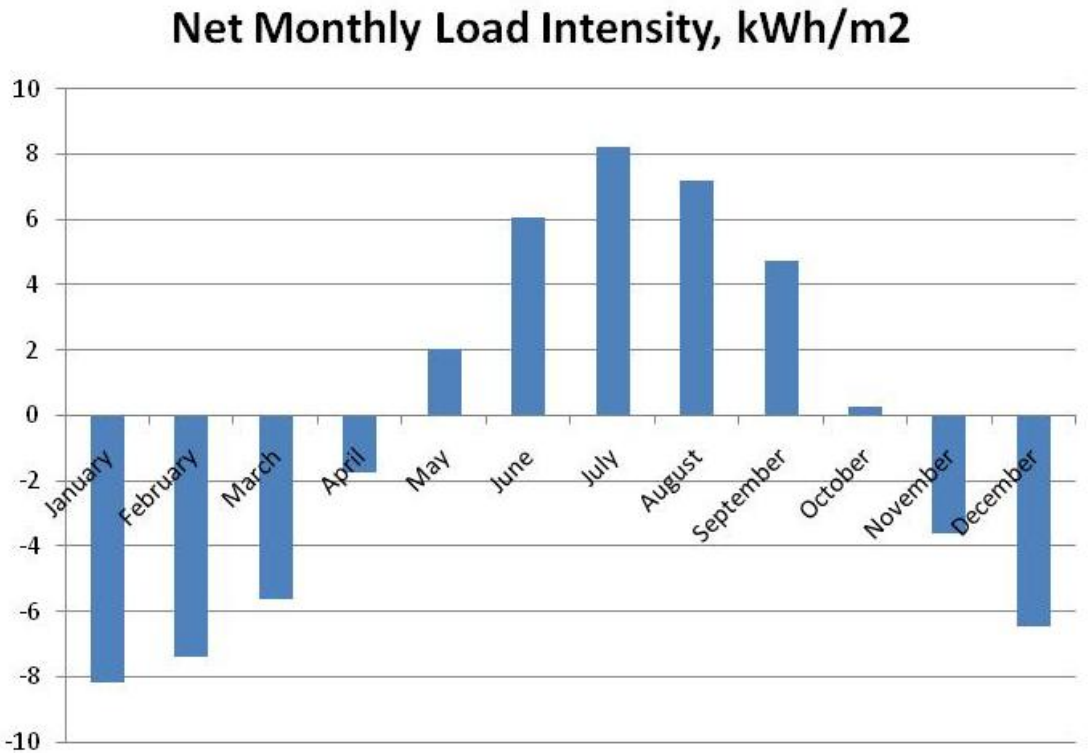
Net Monthly Load Intensity, kWh/m2
10
8
6
4
2
0
-2
-4
-6
-8
-10
January
February
March
April
May
June
July
August
September
October
November
December

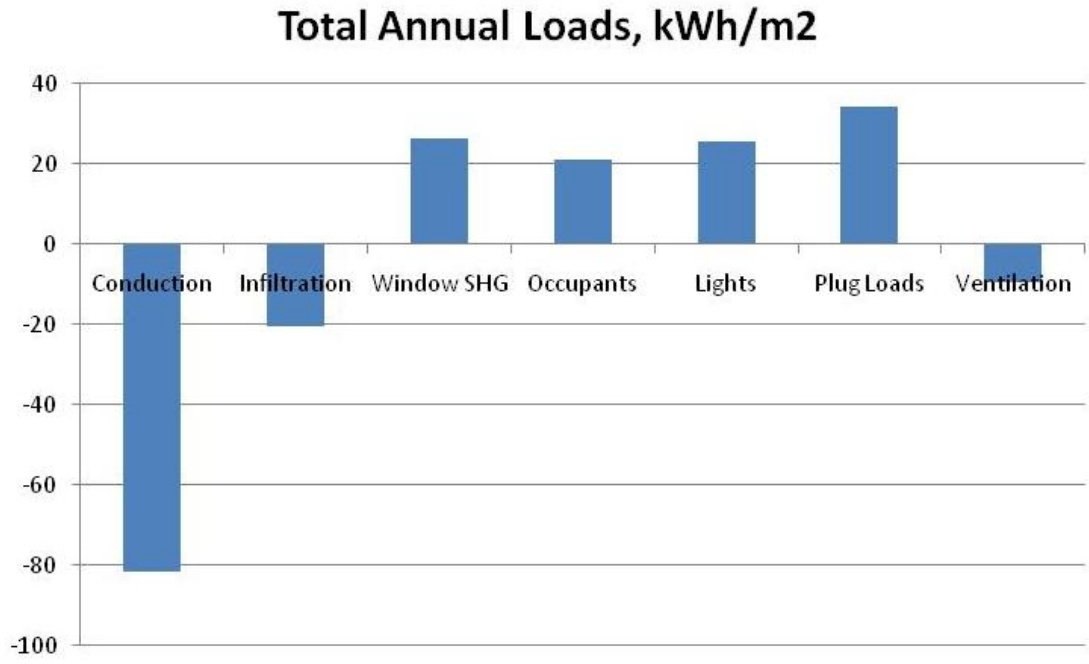
Total Annual Loads, kWh/m2
40
20
0
-20
-40
-60
-80
-100
Conduction
Infiltration
Window SHG
Occupants
Lights
Plug Loads
Ventilation

RADIANT HEATING AND COOLING INPUTS							
Heating Source Efficiency	85%	Cooling Delta T	5	C	Heating Delta T	10	C
Cooling Source COP	3.5	Max Cooling Pump Power	4.23	kW	Max Heating Pump Power	1.03	kW
Pump Efficiency	77%	Design Cooling Flow	12.1	l/s	Design Heating Flow	3.4	l/s
Pump Motor Efficiency	87%	Design Cooling Head	23.8	m	Design Heating Head	20.6	m
Total Pump Efficiency	67%	Cooling to space at max	253.5	kW	Heating to space at max	143.3	kW
		Cooling capacity	57.5	W/m2	Heating capacity	32.5	W/m2

FAN COIL HEATING AND COOLING INPUTS							
		Pumps:			**Fans:**		
Heating source efficiency	85%	Cooling Delta T	15	C	# of fan coil units	15	
Cooling source COP	3.5	Max Cooling Pump Power	1.41	kW	Max Design Fan Flow	50	l/s
Pump Efficiency	77%	Design Cooling Flow	4.0	l/s	Max Design Fan Power	0.127	kW
Pump Motor Efficiency	90%	Design Cooling Head	24.7	m	Design Fan Pressure	1068	Pa
Total Pump Efficiency	69%	Cooling to space at max	253	kW			
Fan Efficiency	60%	Heating Delta T	70	C			
Fan Motor Efficiency	70%	Max Heating Pump Power	0.15	kW			
Total Fan Efficiency	42%	Design Heating Flow	0.5	l/s			
		Design Heating Head	21.3	m			
		Heating to space at max	143	kW			

Radiant with DOAS Energy Intensity

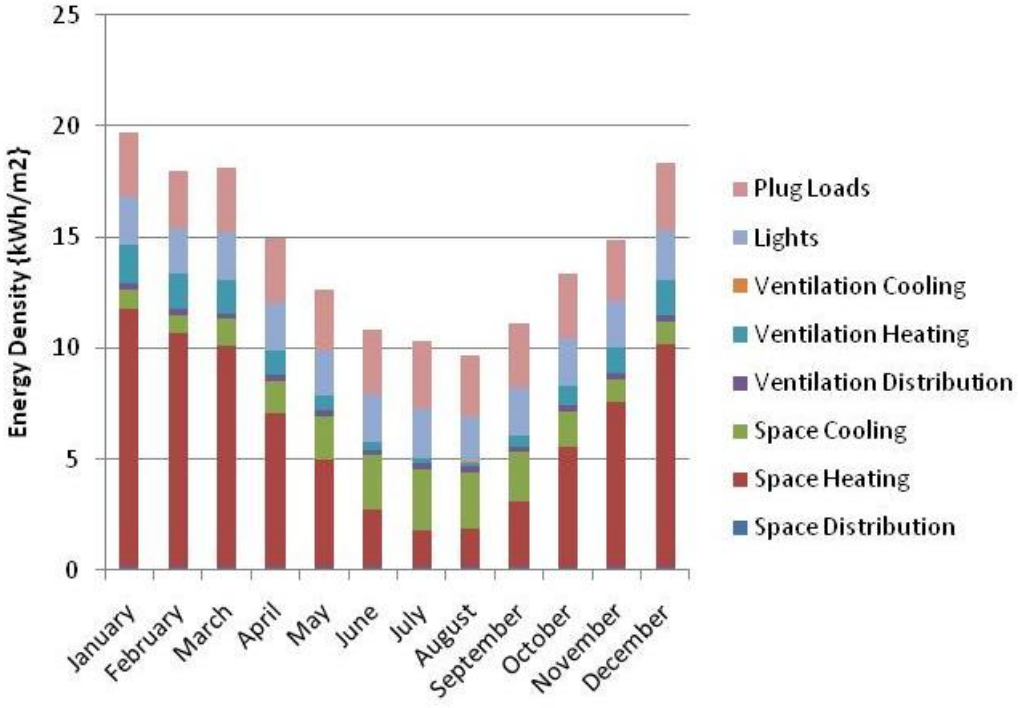

Fan Coils with DOAS Energy Intensity

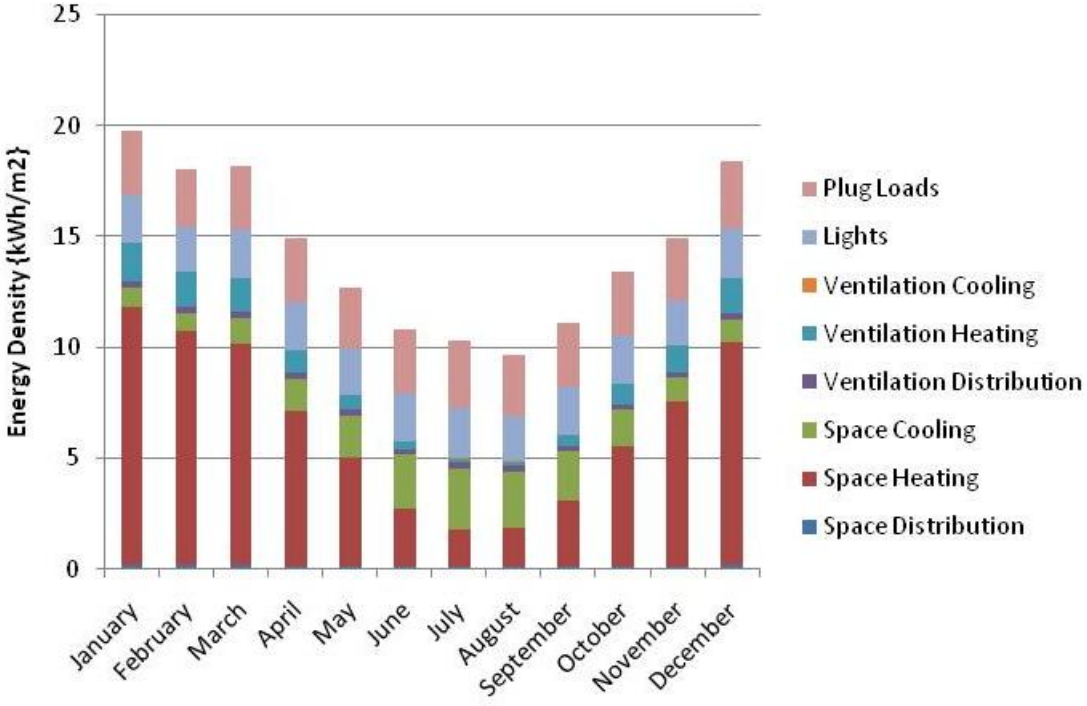

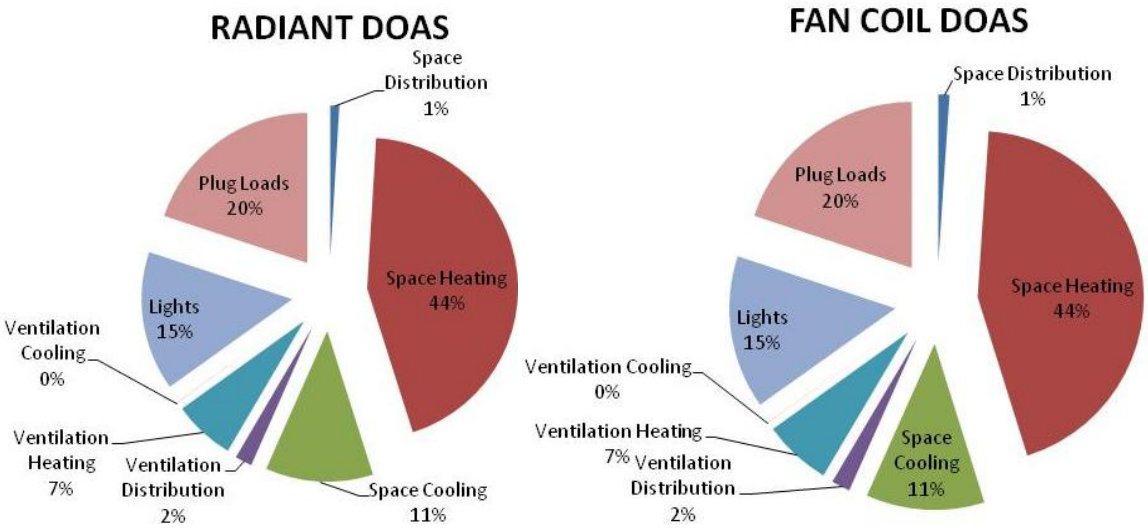
RADIANT DOAS
Space Distribution 1%
Plug Loads 20%
Space Heating 44%
Lights 15%
Ventilation Cooling 0%
Ventilation Heating 7%
Ventilation Distribution 2%
Space Cooling 11%
FAN COIL DOAS
Space Distribution 1%
Plug Loads 20%
Space Heating 44%
Lights 15%
Ventilation Cooling 0%
Ventilation Heating 7%
Ventilation Distribution 2%
Space Cooling 11%

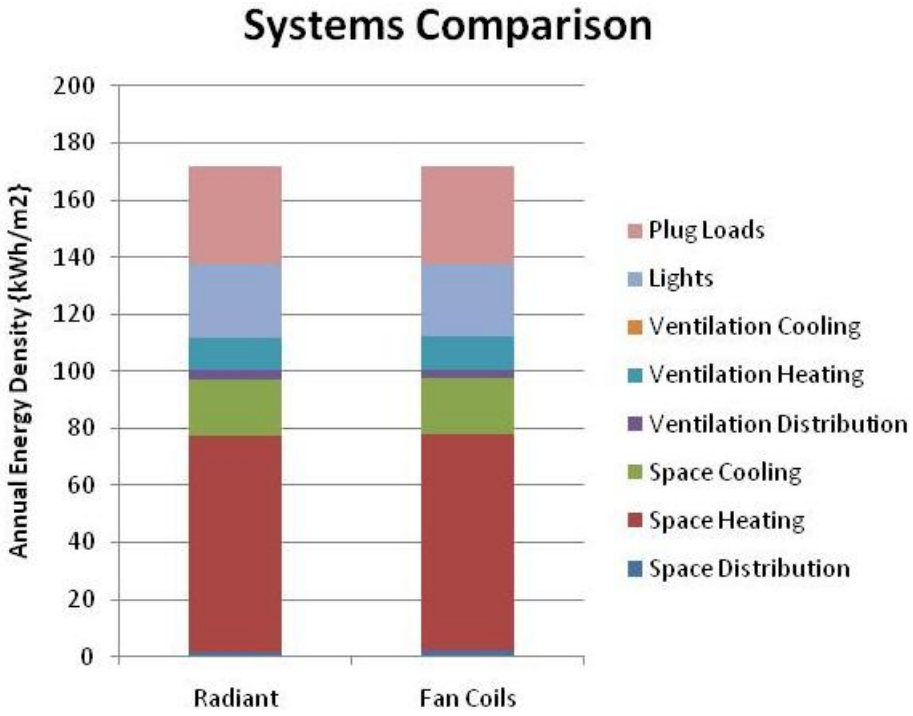
Systems Comparison
Annual Energy Density {kWh/m2}
200
180
160
140
120
100
80
60
40
20
0
Radiant
Fan Coils
Plug Loads
Lights
Ventilation Cooling
Ventilation Heating
Ventilation Distribution
Space Cooling
Space Heating
Space Distribution

Appendix D- Effect of Varying Towers Balcony Geometry on Overall R-Value

Balcony Extension		Slab Thickness		Interior Fibreglass Thickness		Exterior Insulation Thickness on Walls		Exterior Insulation Thickness Around Balcony Slab		U-Factor	R-Value	Average R-Value	Range Percent Difference
(mm)	(feet)	(mm)	(inches)	(mm)	(inches)	(mm)	(inches)	(mm)	(inches)	(W/m^2K)	($hrft^2°F/Btu$)	($hrft^2°F/Btu$)	
1118	3 2/3	165	6 1/2	25	1	76	3	76	3	0.4665	12.17		
1524	5	165	6 1/2	25	1	76	3	76	3	0.4701	12.08		
1118	3 2/3	178	7	25	1	76	3	76	3	0.4736	11.99		
1524	5	178	7	25	1	76	3	76	3	0.4776	11.89	**11.9**	**6%**
2286	7 1/2	178	7	25	1	76	3	76	3	0.4784	11.87		
1524	5	203	8	25	1	76	3	76	3	0.4925	11.53		
2286	7 1/2	203	8	25	1	76	3	76	3	0.4940	11.49		
1118	3 2/3	165	6 1/2	25	1	76	3	0	0	0.6799	8.35		
1524	5	165	6 1/2	25	1	76	3	0	0	0.6822	8.32		
2286	7 1/2	178	7	25	1	76	3	0	0	0.6964	8.15		
1524	5	178	7	25	1	76	3	0	0	0.6988	8.13	**8.1**	**8%**
1118	3 2/3	178	7	25	1	76	3	0	0	0.6997	8.11		
2286	7 1/2	203	8	25	1	76	3	0	0	0.7281	7.80		
1524	5	203	8	25	1	76	3	0	0	0.7347	7.73		
1118	3 2/3	165	6 1/2	25	1	0	0	0	0	1.1757	4.83		
1524	5	165	6 1/2	25	1	0	0	0	0	1.1781	4.82		
1118	3 2/3	178	7	25	1	0	0	0	0	1.1960	4.75		
1524	5	178	7	25	1	0	0	0	0	1.1971	4.74	**4.7**	**5%**
2286	7 1/2	178	7	25	1	0	0	0	0	1.2011	4.73		
1524	5	203	8	25	1	0	0	0	0	1.2343	4.60		
2286	7 1/2	203	8	25	1	0	0	0	0	1.2363	4.59		

Appendix E- Retrofit Results for Electrically Heated Archetype

		Electrically Heated		
		Energy Consumed	Energy Saved	Percent Reduction
		kWh/yr/m^2	kWh/yr/m^2	
Archetype		**351**		
Window	**Retrofit 1**	339	12	3.5%
	Retrofit 2	334	17	5.1%
	Retrofit 3	329	22	6.7%
Wall	**Retrofit 1 - R10**	342	9	2.6%
	Retrofit 1 - R20	339	12	3.5%
	Retrofit 2 - R10	336	15	4.5%
	Retrofit 2 - R20	332	19	5.7%
	Retrofit 3 - R20	331	20	6.0%
Roof	**Retrofit 1**	351	0	0.0%
	Retrofit 2	350.3	0.7	0.2%
	Retrofit 3	350	1	0.3%
HVAC	**Retrofit 1**	301	50	16.6%
	Retrofit 2	276	75	27.2%
Appliance	**Retrofit 1**	348	3	0.9%
	Retrofit 2	344	7	2.0%
Lighting	**Retrofit 1**	349	2	0.6%
	Retrofit 2	348	3	0.9%
Air Leakage	**Retrofit 1**	343	8	2.3%
	Retrofit 2	335	16	4.8%
	Retrofit 3	328	23	7.0%
	Retrofit 4	320	31	9.7%
DHW	**Retrofit 1**	338	13	3.8%
	Retrofit 2	330	21	6.4%

Appendix F- Retrofit Packages Results for Electrically Heated Archetype

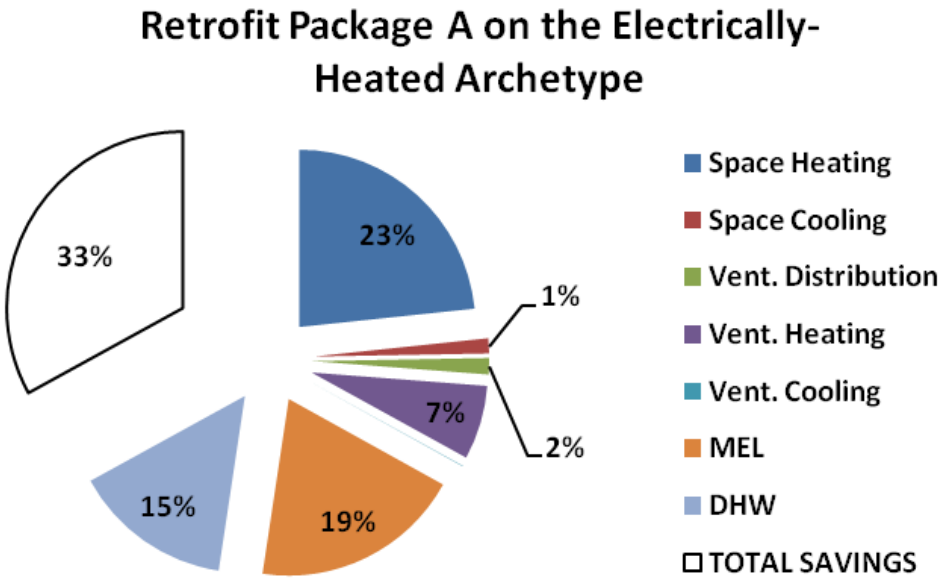

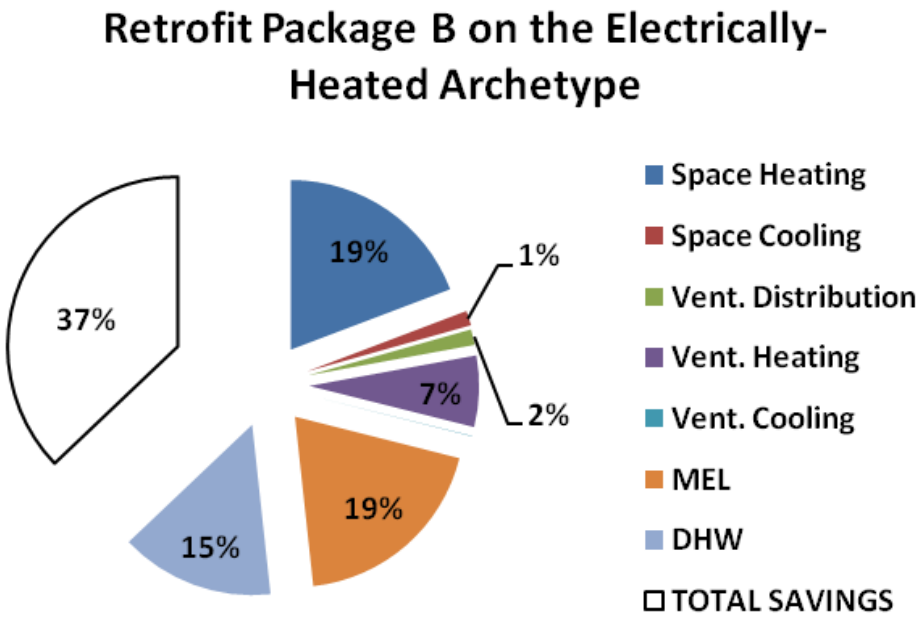

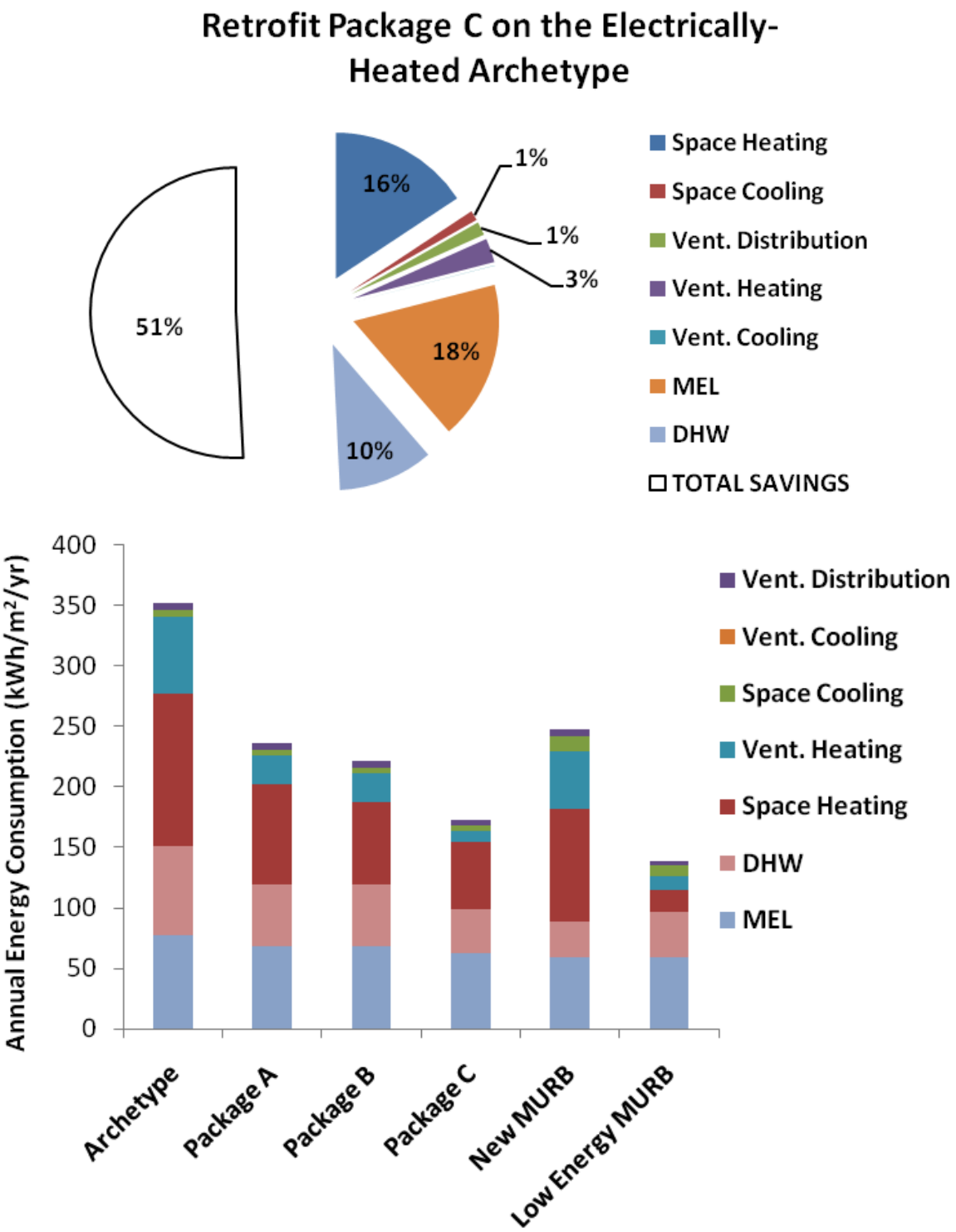
Retrofit Package C on the Electrically-Heated Archetype
16%
1%
1%
3%
51%
18%
10%
Space Heating
Space Cooling
Vent. Distribution
Vent. Heating
Vent. Cooling
MEL
DHW
TOTAL SAVINGS
Annual Energy Consumption (kWh/m²/yr)
400
350
300
250
200
150
100
50
0
Archetype
Package A
Package B
Package C
New MURB
Low Energy MURB
Vent. Distribution
Vent. Cooling
Space Cooling
Vent. Heating
Space Heating
DHW
MEL